UNIVERSITY OF SOUTHAMPTON

FACULTY OF MEDICINE

CLINICAL AND EXPERIMENTAL SCIENCES

INVESTIGATING THE ROLE OF NS5A DOMAIN III IN PROTECTING THE HEPATITIS C VIRUS REPLICATION COMPLEX

BY

EDWARD DAVID KENNETH SULLIVAN

THESIS FOR THE DEGREE OF DOCTOR OF PHILOSOPHY

SEPTEMBER 2017

UNIVERSITY OF SOUTHAMPTON

ABSTRACT

FACULTY OF MEDICINE

Clinical and Experimental Sciences

Doctor of Philosophy

INVESTIGATING THE ROLE OF NS5A DOMAIN III IN PROTECTING THE HEPATITIS C VIRUS REPLICATION COMPLEX

by Edward David Kenneth Sullivan

As a positive sense RNA virus, the Hepatitis C virus makes use of a membrane enclosed replication complex (RC) to replicate its genome in a protected manner. As part of a separate project attempting to visualise the RC, a fluorescent peptide, clover, and a Dihydrofolate reductase (DHFR) destabilizing domain was inserted into the NS5A coding region of a JFH1 replicon. Unexpectedly it was found that the insertion site significantly influenced RNA replication. Under conditions where the DHFR domain was destabilized, insertion within domain III inhibited replication, while insertion at the carboxyl terminus of the protein was better tolerated. However, any difference in replication resulting from the choice of insertion site was lost when transfected cells were treated with trimethoprim to stabilise the DHFR domain. This suggested that rather than causing mis-folding of domain III, insertion into it disrupted an NS5A function that protects the protein from proteolytic degradation. The aim of this work was therefore to further characterise this activity.

In an effort to map the key regions of domain III involved, deletions were introduced into domain III of the replicon construct, within the Clover/DHFR fusion protein linked to the carboxyl terminus. Replication assays identified a 81 amino acid region within domain III of NS5A that seemingly protects these constructs during trimethoprim withdrawal. Further mapping of this region using a series of smaller overlapping deletions further narrowed this to a 61 amino acid sequence.

To confirm that this region of interest is indeed protecting NS5A from degradation, domain III was duplicated to be either full length or truncated. Replication assays with this constructs showed that an intact domain III is capable of protecting replicons from DHFR-mediated degradation. By scrambling domain III it was found that this activity if not dependent on the primary sequence, suggesting that it is due to an intrinsic property of domain III.

The final part of this work was to investigate potential benefits of domain III to the virus lifecycle, specifically investigating the impact of domain III truncation on IFN sensitivity and antigen presentation. However, several experimental issues hindered this work and it was not possible to confirm or deny a role for domain III in modulating these pathways.

CONTENTS

DECLARATION OF AUTHORSHIP

I, Edward Sullivan,

declare that this thesis and the work presented in it are my own and has been generated by me as the result of my own original research.

Investigating the Role of NS5A Domain III In Protecting the Hepatitis C Virus Replication Complex

I confirm that:

1. This work was done wholly while in candidature for a research degree at this University;

2. Where any part of this thesis has previously been submitted for a degree or any other qualification at this University or any other institution, this has been clearly stated;

3. Where I have consulted the published work of others, this is always clearly attributed;

4. Where I have quoted from the work of others, the source is always given. With the exception of such quotations, this thesis is entirely my own work;

5. I have acknowledged all main sources of help;

6. Where the thesis is based on work done by myself jointly with others, I have made clear exactly what was done by others and what I have contributed myself.

7. None of this work has been published before submission.

Signed: ……

Date: ……

ACKNOWLEDGEMENTS

I would like to thank my supervisors, Dr Chris McCormick and Dr Edd James, for giving me the opportunity to undertake this work. The guidance that I have received from them has been invaluable. I would also like to thank Dr Tilman Sanchez-Elsner, Dr Rocio Martinez-Nunez, and Dr Emma Reeves, for all the training and support that they have given me as well.

I am especially grateful to everyone in the Molecular Microbiology department; the community there has really helped me develop as a scientist. Special mention goes to all the residents of LC72 past and present for offering jokes and advice in equal measure.

Finally I would like to thank my family. They have been amazing throughout this entire process, and I would not have been able to make it this far without their love, support, and patience.

Abbreviation	Full form
(-)	Negative sense
(+)	Positive sense
°C	Degrees Celsius
3'	3 prime
5'	5 prime
Å	Angstrom
AP4B	Acetylene-PEG4-Biotin
Apo	Apolipoprotein
APS	Ammonium persulfate
BCA	Bicinchoninic acid
BP	Base pairs
BSA	Bovine serum albumin
C	Core
ccHCV	Cell Culture HCV
CD	Cluster of Differentiation
cfu	Colony forming units
CIAP	Calf Intestinal Alkaline Phosphatase
cLDs	Cytosolic lipid droplets
CNS	Central Nervous System
CO2	Carbon dioxide
CPRG	Chlorophenolred-β-D-galactopyranoside
C-terminus	Carboxyl terminus
Cys	Cysteine
DAAs	Direct Acting Antivirals
DD	Destabilising Domain
DEPC	Diethyl pyrocarbonate
dH2O	Deionised water
DHFR	Dihydrofolate Reductse
DMEM	Dulbecco's modified eagle medium
DMSO	Dimethyl sulphoxide
DNA	Deoxyribonucleic acid
DNAse	Deoxyribonuclease
dNTP(s)	Deoxynucleotide tirphosphate(s)
E. coli	*Escherichia coli*
E1	Ubiquitin activating enzyme
E2	Ubiquitin conjugating enzyme
E3	Ubiquitin ligase
EDTA	Ethylenediaminetetra acetic acid
EGF	Epidermal Growth Factor
eIF	eukaryotic initiation factor

EMCV	Encephalomyocarditis virus
ER	Endoplasmic reticulum
ERK	Extracellular Signal related Kinase
FADD	Fas Associated DEATH Domain protein
FBS	Foetal Bovine Serum
FF luc	Firefly luciferase gene
FKBP12	FK506- and rapamycin-binding protein
Flag	Flag tag (DYKDDDDK)
g	Grams
GAPDH	Glyceraldehyde 3-phosphate dehydrogenase
GFP	Green flourescent protein
Gln	Glutamine
GMP	Guanosine monophosphate
Grb2	Growth factor receptor bound protein
h	Hours
HA	Haemagglutinin
HCC	Hepatocellular carcinoma
HCl	Hydrogen Chloride (Hydrochloric acid)
HCV	Hepatitis C Virus
HEK-293T	Human embryonic kidney 293 T cells
HRP	Horseradish peroxidase
HVR	Hypervariable domain
IDP	Intrinsically Disordered Proteins
IFITM	Interferon Induced Transmembrane Protein
IFN	Interferon
IFNAR	Interferon α receptor
IL	Interleukin
IMP	Inosine 5'-monophosphate
IRES	Internal ribosome entry factor
IRF	Interferon Regulatory Factor
ISDR	Interferon sensitivtiy determining region
ISG	Interferon stimulted genes
ISGF	Interferon Stimulate Gene Factor
ISRE	Interferon Stimulate Response Element
JAK	Janus activated kinase
JFH1	Japanese Fulminatn Hepatitis
JNK	Jun amino-terminal Kinase
kb	Kilobase
kDa	Kilodaltons
l	Litre
L-AHA	L-Azidohomoalanine
LB	Luria Bertani
LCS	Low complexity sequence
LD	Lipid droplets

LDLs	Low density lipoproteins
LEL	Large extracellular loop
M	Molar
mAb	Monoclonal antibody
MAPK	Mitogen-Activated Protein Kinase
MAPKK	MAPK Kinase
MAPKKK	MAPKK Kinase
Met	Methionine
Met-tRNAMet	Methionyl initiator tRNA
mg	Milligram
MHC	Major Histocompatability Complex
miR	MicroRNA
ml	Millilitre
mM	millimolar
MOPS	3-morpholinopropanesulphonic acid
MoRE	Molecular Recognition Elements
mRNA	Messenger ribonucleic acid
MTTP	Microsomal triglyceride transfer proteins
myc	Myc tag (EQKLISEEDL)
NaCl	Sodium chloride
NEAA	Non-essential amino acid
neo	Neomycin resistant
NP40	Nonidet 40
NPC1L1	Niemann-Pick C1-like Chlolesterol Absorption Receptor
NPT	Neomycin Phosphotransferase
NS	Non-structural
N-terminus	Amino terminus
NTPase	Nucelotide triphosphatase
OD	Optical Density
ORF	Open reading frame
PAGE	Polyacrylamide gel electrophoresis
PBMC	Peripheral Blood Mononuclear Cells
PBS	Phosphate buffered saline
PBS-T	PBS+0.1% Tween 20
PCR	Polymerase chain reaction
PEG	Pegylated
PEI	Polyethylenimine
Pen-Strep	Peniciilin-Streptamicin
PI4KA	Phosphatidylinositol 4-kinase IIIa
PKR	Protein Kinase R
PLB	Passive lysis buffer
PVDF	Polyvinylidene flouride
RC	Replication complex
RdRp	RNA-dependent RNA polymerase

RLU	Relative light units
RNA	Ribonucleic Acid
RNAse	Ribonuclease
rNTP	Ribonucleotide triphosphate
RPMI	Roswell Park Memorial Institure medium
SDS	Sodium dodecyl suphate
SEL	Small Extracellular loop
shRNA	Short hairpin RNA
SKP2	S-phase Kinase Associated Protein 2
SL8	SL8 tag (SIINFEKL)
SR-B1	Scavenger Receptor Class B Type 1
STAT	Signal-transducing activators of transcription
SVR	Sustained Virological Response
TAE	Tris- Acetate EDTA buffer
TAP	Transporter associated with Antigen Presentation
TBS	Tris-buffered saline
TBS-T	TBS+0.1% Tween 20
TEMED	N,N,N',N'-tetramethylethylenediamine
TEV	Tabacco etch virus
TFB1, 2	Transformation buffer 1, 2
Th	T-Helper
THPTA	Tris(3-hydroxypropyltriazolylmethyl)amine
TMP	Trimethoprim
TNF	Tumour Necrosis Factor
TNFR	TNF Receptor
TRADD	TNF Receptor type 1 Associated DEATH Domain protein
TRIM	Tripartite motif
U	Units
UHQ	Ultra high quality water
USP	Ubiquitin Specific Peptidase
UTR	Untranslated region
v	Volts
v/v	volume per unit volume
V5	V5 tag GKPIPNPLLGLDST
VLDL	Very low density lipoprotein
w/v	Weight per unit volume
WHO	World Health Organisation
xg	Times gravitational force
µg	Microgram
µl	Microlitre
µM	Micromolar

1 INTRODUCTION

1.1 HEPATITIS C

Hepatitis C Virus (HCV) is a viral infection of human liver hepatocytes. The infection commonly causes chronic inflammation of the liver which can result in a progressive damage and loss of function. Acute infection with HCV is typically asymptomatic, or mild; causing mild fever, abdominal pain, dark urine and jaundice. However, approximately 80% of those infected will fail to clear the infection during the acute phase and will instead go on to develop a chronic infection. Chronic infection is often asymptomatic, but the constant presence of the virus causes chronic inflammation of the liver which is associated with several life threatening sequelae (Lavanchy, 2011); liver disease, liver failure, cirrhosis, hepatocellular carcinoma and eventually death.

1.1.1 TRANSMISSION

HCV is transmitted parenterally, usually through direct blood-to-blood contact. The main routes of transmission are through the shared use of infected needles by injecting drug users, through the reuse of contaminated medical equipment, or the use of infected blood products (Cornberg et al., 2011, Webster et al., 2015). The introduction of universal screening of donated blood by many nations in the 1990s, caused a considerable drop in the risk of transmission by blood transfusion (Selvarajah and Busch, 2012, Donahue et al., 1992), although cost has prevented several countries from implementing this control.

The infection can also be spread sexually (Chan et al., 2016), or from mother to child (Gibb et al., 2000), however these routes are much less common.

1.1.2 EPIDEMIOLOGY

Despite recent advances in HCV therapy (1.7), HCV remains a pathogen of global significance and a major cause of mortality and morbidity worldwide. Due to the majority of acute HCV infections being asymptomatic it is difficult to gauge the incidence of HCV. However, the World Health Organisation estimates that 71 million people are chronically infected with HCV, approximately 1% of the global population, and that this results in 400 thousand deaths each year (W.H.O., 2017). Whilst the quality of epidemiological data varies between nations, there is a clear positive correlation between economic status and HCV infection, with many developed regions, e.g North America and Western Europe reporting a prevalence <2%. In

contrast Central Africa, South East Asia, and the Middle East have a considerably high prevalence.

The highest prevalence is reported in Egypt, where approximately 10% of the population are infected (Petruzziello et al., 2016). This also represents the highest concentration of genotype 4 infections, with oer 90% of those infected with HCV in Egypt being infected with this genotype (Kouyoumjian et al., 2018). The continuing epidemic is due to the wide spread use of infected needles during an earlier health campaign. Between the 1950s and 80s millions of people were injected with tartar emetic in an attempt to control schistosomiasis, a parasitic worm. Lack of knowledge on viral transmission led to re-use of needles and lax sterilization practise, leading to the HCV epidemic that continues to this day (Mohamoud et al., 2013). With the widespread use of therapies such as PEGylated Interferon and the more recent Direct Acting Antivirals, the overall prevalence of HCV infection within Egypt is believed to be falling, however the prevalence of disease stemming from chronic infection continues to rise, and is estimated to continue rising until 2030 (Gomaa et al., 2017). Furthermore several issues still exist including lack of infection control and access to effective treatments (Elgharably et al., 2017), and as such Egypt still faces a considerable challenge.

HCV can be classified into 7 major genotypes, 1-7, based upon phylogenetic and sequence analysis (Messina et al., 2015, Simmonds et al., 1994). These can be further divided into 67 subtypes (Smith et al., 2014) (Figure 1-1), which vary in their prevalence, severity, and treatment response. The most common genotype worldwide is genotype 1, which is estimated to cause 45% of HCV infections (Messina et al., 2015), followed by genotype 3 (30%) and then genotypes 2,4 and 6. Only about 1% of cases are attributed to genotype 5, and these are concentrated in sub-Saharan Africa (Messina et al., 2015). Genotype 7 was first described in 2015 (Murphy et al., 2015), and due to limitations in testing there is little knowledge of its prevalence; Murphy *et al* suggested that isolates identified as genotype 7 could also be mis-characterised as genotype 2, or even not characterised at all.

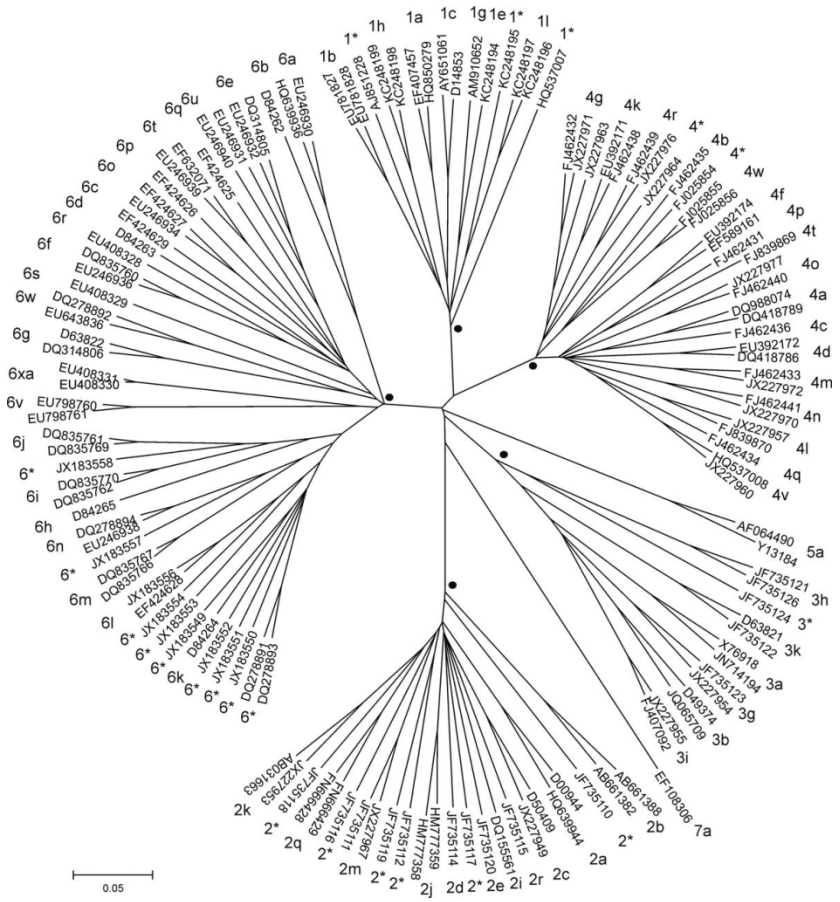

Figure 1-1 **Phylogenetic tree of 129 representative complete coding sequences of HCV isolates.** Taken from (Smith et al., 2014)

1.2 HEPATITIS C VIRUS

The Hepatitis C virus is a member of the *Flaviviridae* family in the *Hepacivirus* genus. The virus exists as spheres of host derived lipid covered in spike like projections of two glycoproteins (E1 and E2) and interspersed with host derived apolipoproteins. These particles demonstrate considerable diversity in both size and density (Catanese et al., 2013) due to the influence of the host lipoprotein pathway during virion formation (Lindenbach, 2013). Multiple studies have shown that this difference in density impacts the infectivity of the virions, with the more infectious virions having lower buoyant densities (Lindenbach, 2013). Within the lipid envelope is a nucleocapsid of core protein (C) that holds within it a single copy of the viral genome (Figure 1-2). It should be noted that the above is a much simplified description; HCV has been found to exist as a range of lipoviral hybrids, varying greatly in size and density (Bartenschlager et al., 2011).

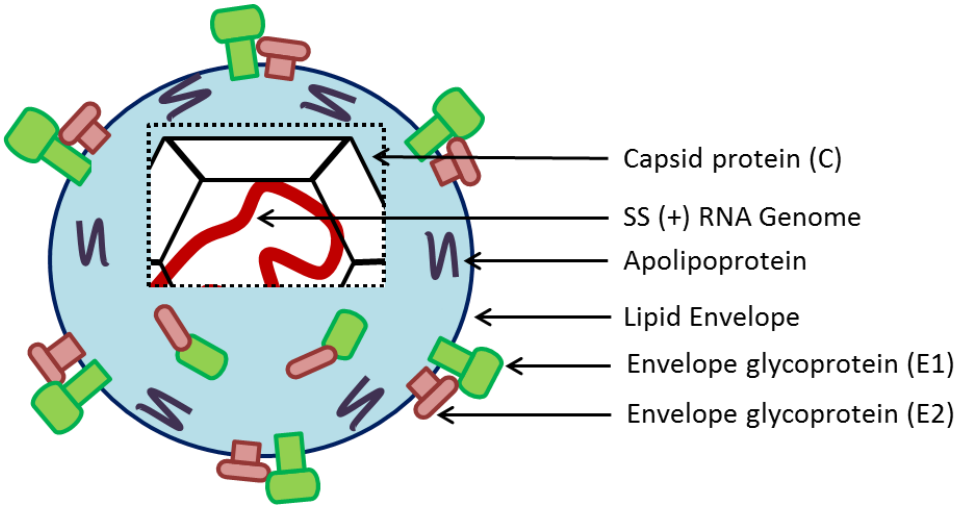

Figure 1-2 **Schematic of the Hepatitis C Virus particle.**

The genome is approximately 9.5 kb in length and contains a single Open Reading Frame (ORF) bordered by Untranslated Regions (UTRs) (Figure 1-3). The 5´ end of the viral genome encodes the 3 structural proteins, C, E1, and E2, while the 3´ contains the sequences of the Non-structural proteins; proteins essential for viral life cycle but not included in the viral particle and which include, p7, NS2, NS3, NS4A, NS4B, NS5A and NS5B. An Internal Ribosome Entry Site (IRES) located in the 5´ UTR drives the expression of a single polyprotein approximately 3000 amino acids in length (Tsukiyama-Kohara et al., 1992). This is then processed by both viral and cellular proteases into individual functional proteins.

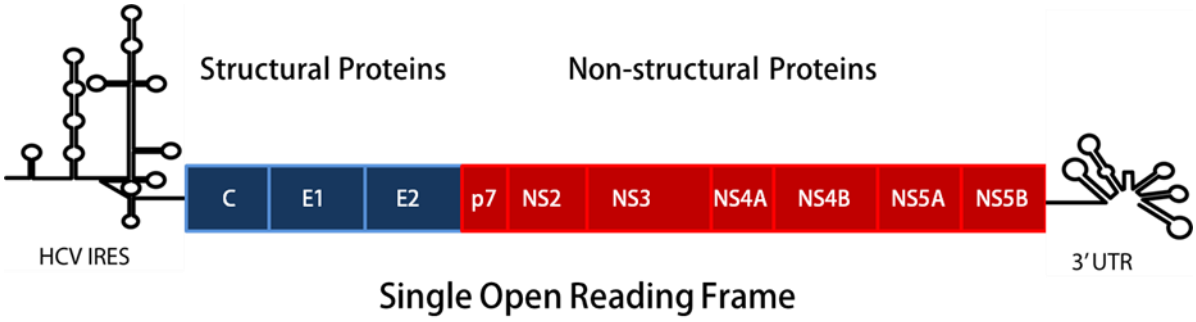

Figure 1-3 **Genome schematic of Hepatitis C Virus showing the structural and non-structural proteins**.

1.3 HCV PROTEINS

1.3.1 CORE

The first protein translated from the HCV genome is the Core protein (C). The protein is responsible for packaging viral RNA during particle formation, leading to the formation of nascent nucleocapsids. Translation initially generates a C protein precursor termed P23, which then undergoes processing to yield P21, the mature C protein, which is then available for particle formation (Ait-Goughoulte et al., 2006).

The P23 form of the C protein is predicted to have 3 distinct domains (Hope and McLauchlan, 2000). Domain I consists of the N-terminal two thirds of the C protein and is highly hydrophilic, carrying numerous positively charged residues. It is this domain that is thought to be responsible for the interaction between the C protein and viral RNA. In addition, motifs within domain I are thought to be the main driving force behind oligomerization (Klein et al., 2004, Klein et al., 2005). In contrast to domain I, domain II, which represents the remaining residues within p21, is highly hydrophobic. This domain is thought to mediate the interaction of the C protein with both lipid droplets (Hope and McLauchlan, 2000, Barba et al., 1997) and the ER membrane (Moradpour et al., 1996), although there is evidence that it also contributes to oligomerisation (Yan et al., 1998) and particle formation (Hourioux et al., 2007). Domain III consists of the C-terminal ~20 amino acids, and serves as a signal peptide for the downstream E1 glycoprotein. However, this domain is cleaved during processing of the C protein, such that it is only present within the P23 form.

In addition to its role in the virus particle the C protein has been shown to have a number of other roles during the virus life cycle (Lai and Ware, 2000, McLauchlan, 2000). Examples include the regulation of apoptosis, regulation of lipid metabolism. The core protein has also been linked to carcinomagenesis within mice(Moriya et al., 1998).

1.3.2 E1 AND E2

The second HCV proteins translated from the genome are the two surface glycoproteins E1, and E2. These extend from the virus particle, and are thought to mediate attachment and entry, discussed below. The C-terminal domains of both proteins consist of 2 transmembrane domains, which form hairpins, allowing anchoring of the glycoproteins to lipid membranes, and therefore the virus' lipid envelope. The N-termini of the membrane proteins project outwards from the envelope and mediate the interaction between the virus and cell surface receptors. Each of these projections contains a number of highly conserved glycosylation sites, up to 5 in E1 and up to 11 in E2, that are important for both structure and function

(Meunier et al., 1999, Goffard et al., 2005). Functionality of the glycoproteins is believed to require the formation of an E1-E2 heterodimer with the key residues for formation of this thought to lie within the transmembrane domains (Op De Beeck et al., 2000).

1.3.3 P7

The p7 protein is 63 amino acids long and hydrophobic. It is believed to cross the ER membrane twice, with both termini facing the ER lumen and a short loop exposed to the cytoplasm (Carrere-Kremer et al., 2002). The mature protein is release from the polyprotein by cleavage of both the E2/p7 and p7/NS2 boundaries by cellular signal peptidases, associated with ER membrane, however, cleavage of these boundaries is inefficient leading to the formation of transient E2-p7 and p7-NS2 intermediates (Lin et al., 1994a, Mizushima et al., 1994, Grakoui et al., 1993). Interestingly one study has shown that if the formation of any of these is disrupted it results in a considerable drop in infectivity (Sakai et al., 2003), suggesting roles for these intermediates in particle formation. However, the importance of these intermediates is called into question by work by Shanmugam and Yi who showed that whilst complete separation of E2 and p7 by insertion of and IRES between them had an inhibitory impact on virus production, the impact was relatively minor (Shanmugam and Yi, 2013).

It has been shown *in vitro* that p7 can oligomerise to form ion channels (Griffin et al., 2003, Pavlovic et al., 2003, Premkumar et al., 2004), consistent with the idea that p7 is a viroporin. Formation of these ion channels has been shown to be essential for infectivity in chimpanzees (Sakai et al., 2003), however the precise role that p7 plays in the viral life cycle is not yet fully understood. Work by Wozniak *et al* has shown that p7 viroporins are able to increase the pH of lysosomes and vesicles, leading to the suggestion that p7 might function as an H+ ion channel, protecting nascent virions from acidification (Wozniak et al., 2010). It has also been suggested that it co-ordinates the envelopment of RNA containing capsids (Gentzsch et al., 2013).

1.3.4 NS2

NS2 is a 23kDa protein, and the first NS protein to be translated. The protein consists of two distinct domains, a hydrophobic region at the N-terminus, and a cytoplasmic domain towards the C-terminus. Crystallography has suggested that NS2 forms a homodimer, with two active protease sites (Lorenz et al., 2006). The activity of these active sites are dependent on a catalytic triad of amino acid residues, with each monomer contributing residues to each site; histidine and glutamate from one, and cysteine from the other (Lorenz et al., 2006). NS2 is

reported to have basal protease activity alone (Schregel et al., 2009), however this is greatly improved by the presence of the Zinc binding domain of NS3, discussed below.

Despite much of it being dispensable for genome replication, the entirety of NS2 is required for particle formation and release (Jones et al., 2007a, Jirasko et al., 2010). Interestingly this does not include the protease activity, which can be deactivated by alanine substitution of the catalytically important cysteine-184, with no impact on particle formation (Jones et al., 2007a). In contrast when another member of catalytic triad, His-143, is substituted it results in a 3-fold drop in core protein release (Jirasko et al., 2010), demonstrating that though the activity is not required, the catalytic structure is. In terms of function, NS2 has been proposed to be responsible for attracting the envelope proteins to the nascent virions (Popescu et al., 2011). NS2 has been observed interacting with almost all HCV proteins, in both a genetic (Yi et al., 2007, Phan et al., 2009) and molecular manner (Popescu et al., 2011), and mutations that impair these have been shown to alter the sub-cellular localisation of NS2, and abolish assembly of nascent virus particles.

In addition to its role in particle formation NS2 also has a role in inhibiting apoptosis (Erdtmann et al., 2003). Specifically NS2 has been shown to be capable of binding to the killing site of the pro-apoptotic CIBE-B protein, inhibiting its activity and interfering with pro-apoptotic signalling. NS2 also demonstrates a broad ability to suppress gene expression (Dumoulin et al., 2003), and so it is likely to perform a number of functions throughout the viral life cycle.

1.3.5 NS3-4A

The NS3 protein is a multifunctional, 70 kDa, protein, and an essential component of the viral replication complex. As with the other NS proteins, NS3 localises to the ER membrane. This is mediated through an amphipathic helix located at the N-terminus, which dictates both localisation and stability (He et al., 2012).

In addition to the amphipathic helix the N-terminal domain of NS3 also contains a serine protease, distinct from that of NS2, which is responsible for all downstream cleavage events. This activity is dependent on binding of a zinc ion by three highly conserved cysteine residues, which stabilises the protease structure (De Francesco et al., 1996). The protease activity is also dependent on the binding of NS4A, a small ~55 amino acid protein that acts as a co-factor for the NS3 protease. As part of the NS3-4A protease complex NS4A contributes to proper positioning of the substrate in relation to the catalytic triad that mediates cleavage (Cicero et al., 1999).

Alongside its role in polyprotein processing, NS3 also plays a direct role in genome replication. Specifically, the C-terminal regions of NS3 demonstrate helicase activity, and this activity has been shown to be essential for replication both *in vitro*(Lam and Frick, 2006) and *in vivo* (Kolykhalov et al., 2000). It has also be shown that NS3 can directly interact with NS5B, the viral RNA dependent RNA polymerase, increasing the production of nascent RNA (Piccininni et al., 2002). It is likely, therefore, that NS3 assists in the removal of transient secondary structures that would otherwise impede the progression of NS5B (Belon and Frick, 2009). Although the helicase resides solely in the C-terminus, its activity is greatly enhanced by the presence of the entirety of NS3 and the NS4A cofactor (Frick et al., 2004, Beran et al., 2007). The role for the protease domain in enhancing helicase activity is further supported by work by Zhang *et al,* showing that the protease domain is required for specific NS3-NS5B interaction (Zhang et al., 2005). Interestingly this work also showed that formation of this interaction enhances NS3 helicase activity, rather than enhancing NS5B.

1.3.6 NS4B

NS4B is a 27kDa membrane protein that is one of the constitutive components of the viral replication complex. It has been shown to localise to the ER membrane with the other members of the replication complex, where it is believe to be anchored to the membrane through the presence of 4 transmembrane domains (Hügle et al., 2001, Lundin et al., 2003). These transmembrane domains fall in the middle of the protein, and are thought to represent the middle of three domains that make up NS4B. The other two, the N- and C- termini are each predicted to consist of two amphipathic helices lying on the cytoplasmic face of the ER membrane (Gouttenoire et al., 2014).

Perhaps the most important function of NS4B is the restructuring of the ER membrane to generate the membranous web, a stack of membrane enclosed vesicles which provide the virus a platform on which to replicate (Gosert et al., 2003), discussed below. The role for NS4B in generating the membranous web was first reported by Egger *et al*, who showed that expression of NS4B was able to cause restructuring of the ER membrane, leading to the generation of a stacks of vesicles within a membranous matrix, both in tetracycline regulated cells (Egger et al., 2002), and replicon infected cells (Gosert et al., 2003). Although NS4B alone was sufficient to generate the membranous web, the expression of the entire polyprotein was shown to greatly enhance this, leading to a much more complex structure. Subsequent work has increased our understanding of this process, and it is now known that the formation of a fully functional membranous web is dependent on a number of other factors (Romero-Brey et al., 2012, Paul et al., 2013). However it remains clear that NS4B is an essential driving force

behind this as mutations within key regions required for NS4B localisation and function have been shown to greatly perturb replication (Gouttenoire et al., 2014)

Alongside its role in membrane restructuring NS4B has a variety of other functions throughout the virus life cycle. One example is its ability to modulate the activity of the viral RNA dependent RNA polymerase (Piccininni et al., 2002); specifically NS4B has been shown to downregulate NS5B polymerase activity. Other functions of NS4B include the regulation of translation, and the interference with a number of host cell signalling pathways (Sklan and Glenn, 2006).

1.3.7 NS5B

NS5B is a 68kDa RNA-dependent RNA polymerase, and is responsible for the replication of the viral RNA (Behrens et al., 1996). It demonstrates the same right hand structure that is typical of all nucleotide polymerases (Penin et al., 2004b). The palm domain contains a unique catalytic site, while the fingers and thumbs surrounding this form a channel to bind the template RNA. Recombinant NS5B is sufficient to generate full length HCV RNA *in vitro* (Behrens et al., 1996, Lohmann et al., 1997, Yamashita et al., 1998). The process occurs in a two-steps; first NS5B uses the positive-sense (+) genome to generate a complementary negative-sense (-) strand, which is then used as a template to generate progeny genomes (Behrens et al., 1996). These genomes can have a variety of fates, including being translated, being used as the template for further genome replication, or being incorporated into virus particles.

The C-terminal 21 amino acids of NS5B have been shown to be dispensable for RNA replication, however their loss greatly impacts the subcellular localisation of the protein as a whole (Yamashita et al., 1998). It is thought that this hydrophobic C-terminal transmembrane domain inserts post-translationally into the ER membrane, thereby anchoring the NS5B protein (Schmidt-Mende et al., 2001).

1.4 HCV LIFE CYCLE

1.4.1 ATTACHMENT AND ENTRY

The first step in the viral life cycle is attachment to a host cell. This is mediated by the HCV glycoproteins E1 and E2, which form a functional heterodimer on the surface of the virus particle necessary for viral entry (Lavie et al., 2007, Dubuisson et al., 1994). Infectivity of the HCV particle however requires the formation of E1 homotrimers, likely resulting in trimeric structures of E1E2 homodimers (Falson et al., 2015).

The earliest proposed receptor of HCV was Cluster of Differentiation 81 (CD81), a tetraspasmin shown to interact with E2 (Pileri et al., 1998); however, subsequent work showed that a more stable interaction is dependent on the formation of the glycoprotein E1-E2 heterodimer (Cocquerel et al., 2003). CD81 is a transmembrane protein, with 4 hydrophobic transmembrane domains, and 2 extracellular loops, the Large Extracellular Loop and the Small Extracellular Loop, of which larger is key for the interaction with the viral glycoproteins (Petracca et al., 2000).

A second potential receptor of HCV is the Human Scavenger Receptor Class B type 1(SR-B1) (Scarselli et al., 2002, Bartosch et al., 2003), which like CD81 was found to interact with glycoprotein E2. SR-B1 is a lipoprotein receptor found on the surface of all eukaryotic cells, and is responsible for the endocytosis of High Density Lipoproteins. Two tight junction proteins, Occludin (Ploss et al., 2009) and Claudin-1 (Evans et al., 2007), were later shown to also contribute to entry. Expression of human occludin by cells non-permissive to HCV infection, was shown to increase uptake of HCV pseudo particles, whilst its silencing in permissive cells led to a marked drop in susceptibility. Likewise expression of Claudin-1 was capable of making non-hepatic cells susceptible to HCV infection, which could then be blocked by antibody binding to Claudin-1. The involvement of these proteins suggests that HCV makes use of the tight junctions of cells to gain entrance into the cytoplasm. More recently it was found that the Niemann-Pick C1-like Cholesterol Absorption Receptor (NPC1L1), located at the apical, canalicular surface of hepatocytes also contributes to entry (Sainz et al., 2012) as antibody blocking of NPC1L1 was capable of inhibiting HCV infection.

Initial attachment of the virus is followed by a coordinated series of events, trafficking the virus to the tight-junctions and eventually leading to the clathrin-mediated endocytosis of the virus particle (Blanchard et al., 2006). The viral envelope then fuses with the membrane of the endocytic vesicle creating a pore through which the virus enters into the cytoplasm (Bartosch and Cosset, 2006), in a pH-dependent manner (Blanchard et al., 2006). It is

believed that the association of the virus glycoproteins with the various cell surface receptors prime them for the conformational changes necessary for membrane fusion and virus entry (Sharma et al., 2011).

An additional method of attachment appears to make use of HCV's association with Low Densitiy Lipoproteins (LDLs). HCV is known to be strongly associated with plasma lipoprotein in the blood (Thomssen et al., 1992, Thomssen et al., 1993), and this has been shown to essential for infectivity (Chang et al., 2007). HCV virus particles have been reported to gain entry to the cell by making use of the LDL-receptor (Agnello et al., 1999, Monazahian et al., 1999), but the precise role of this in HCV infection remains controversial. It has also been suggested that the LDL receptor may contribute to the initial attachment of the virus to the cell surface, but that entry of the virus makes use of a series of other receptors and co-receptors.

Once in the cytoplasm the viral capsid dissociates releasing the viral genome.

1.4.2 TRANSLATION

Within the cytoplasm the HCV genome can be translated directly using a 330nt IRES located within the 5' UTR (Tsukiyama-Kohara et al., 1992). A characteristic of all IRESes, is the presence of complex secondary structure, and HCV is no exception. The 5' UTR is comprised of 4 distinct secondary structures, attributed to extensive base pairing in this region; domains I, II, III and IV(Figure 1-4).

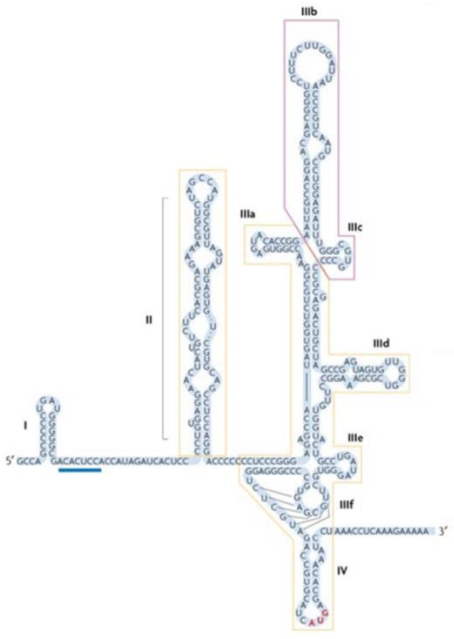

Figure 1-4 **Structure of the HCV IRES.** Taken from Fraser CS, Doudna JA. Structural and mechanistic insights into hepatitis C viral translation initiation. Nature reviews Microbiology. 2007;5(1):29-38.(Fraser and Doudna, 2007)

Domain I forms a basic stem-loop structure consisting of the first 20 nucleotides of the 5' UTR but it is not considered essential for the initiation of translation (Rijnbrand et al., 1995). This region is instead thought to regulate the IRES activity as loss of this hairpin has been seen to increase translation. In contrast to domain I, domains II and III are much more complex, and can be split into two and six subdomains, IIa-b and IIIa-f, respectively (Lukavsky, 2009). Subdomains IIIe and IIIf form a pseudoknot structure, consisting of two helices. The first of these is formed by binding of the region between domains II and III to IIIf, while the second is formed by a sequence upstream of domain IV and subdomain IIIf. Similar to domain I, domain IV, consists of a basic stem and loop structure. This contains the start codon and the start of the open reading frame.

The IRES recruits the 40S subunit of the host cell ribosome directly to the RNA, bypassing the need for a 5' cap as well as eIF4F. The recruitment of the 40S subunit is achieved by domain III, specifically sub domains IIId and IIIe, which are able to form high affinity associations with it(Kieft et al., 2001, Lukavsky, 2009). Once the 40S subunit has bound, the viral IRES recruits a ternary complex (eIF2-Met-tRNA$_i^{Met}$-GTP) and eukaryotic initiation factor 3 (eIF3), forming the pre-initiation complex. This process results in the formation of a 48S with the Methionine tRNA (Met-tRNA$_i^{Met}$) associated with the start codon in the P-site of the ribosome. Hydrolysis of the GTP releases eIF2 and allows the recruitment of the 60S subunit to form the 80S initiation complex. Domain II is not thought to be involved in the recruitment of ribosome, but to contribute to positioning of the RNA within (Spahn et al., 2001). It has been suggested that domain II adopts an elongated form that can probe the RNA binding cleft of the ribosome resulting in a conformational change that may serve to lock the ribosome around the RNA. With the formation of the 80S initiation complex, translation can occur. During periods of stress, or during the interferon response, eIF2 can be deactivated, halting all eIF2 dependent translation within the cell. In these instances it can be replaced in the context of translation of the HCV genome by eIF2A, which interacts with the IIId subdomain to recruit Met-tRNA$_i^{Met}$ (Kim et al., 2011).

Translation of the viral RNA produces a large polyprotein, which is cleaved into individual functional units described above. A signal peptide located between the Core and E1 proteins, targets E1 to the ER lumen, and is co-translationally cleaved by an ER membrane associated Signal Peptidase, releasing the immature core protein. Upon further processing the mature core protein is trafficked to cytosolic lipid droplets (CLDs) (McLauchlan et al., 2002). The core protein remains associated with these ER-membrane associated lipid storage organelles, until required for virus particle formation.

Unlike the Core protein, E1 and E2 both contain ER retention signals, leading to their build-up within the ER lumen. In addition to their role in processing the core/E1 boundary, host signal peptidases are also responsible for the liberation of the rest of the structural proteins, cleaving the polyprotein at the E1/E2, E2/p7 and p7/NS2 boundaries (Hijikata et al., 1991). The glycoproteins then undergo a series of maturation processes including folding, homodimer formation and N-glycosylation, which are aided by chaperone proteins within the ER lumen.

All non-structural proteins are cleaved from the polyprotein by the activity of the viral proteases NS2/3 and NS3/4A. Upon cleavage at the NS2/3 boundary, NS3 is free to form an association with its co-factor NS4A, which allows auto-cleavage of the NS3/4A boundary and *trans*-cleavage of all downstream boundaries. Pulse-chase studies have shown that though liberation of NS3 from NS2 and NS4A is rapid, the subsequent cleavage events occur much slower; cleavage at the NS5A/5B and NS4A/4B boundaries occurs more rapidly that at the NS4B/5B boundary (Lin et al., 1994b, Bartenschlager et al., 1994). Evidence suggests that while NS4A proteinase co-factor enables NS3 to more rapidly cleave the NS4A/4B and NS5A/5B its presence is absolutely required for NS4B/5A cleavage (Lin et al., 1994b). Cleavage hierarchy is thought to be important for assembly of the replication complex as increasing the rate of cleavage at the NS4B/5A boundary has been seen to inhibit replication (Herod et al., 2012). The importance of cleavage kinetics on replication is further supported by work by Wang *et al*, who identified highly conserved threonine residues at the C-terminus of NS3 boundary that inhibited cleavage at the NS3/4A (Wang et al., 2004). These residues are hypothesised to slow cleavage to ensure proper formation of the NS3-4A complex.

All non-structural proteins are anchored to the ER membrane; either through the presence of a transmembrane domain, or through the presence of an amphipathic helix. Initially these proteins are associated with the cytosolic surface of the ER membrane, however formation of the replication complex causes invagination of this membrane, such that these proteins end up in a membrane bound vesicle.

1.4.3 VIRAL REPLICATION

As mentioned previously, replication of the viral genome, and subsequent virus particle formation, is dependent on the formation of a membrane enclosed structure termed the membranous web (Gosert et al., 2003). Within this the non-structural proteins come together to form a membrane associated replication complex, responsible for the generation of new viral RNAs. Within HCV the minimum requirements for this to occur are the non-structural

proteins NS3-5B and the *cis*-acting RNA elements found within the 5' UTR, 3' UTR, and NS5B coding regions.

Although it has been reported that HCV NS5B can make use of both primer dependent and independent initiation *in vitro* (Luo et al., 2000, Zhong et al., 2000, Bressanelli et al., 2002), it is thought likely that HCV makes use of *de novo* initiation *in vivo*. This is supported by the presence of a β-loop close to the catalytic site of NS5B, which is believed would inhibit primer driven elongation (Hong et al., 2001). This loop, alongside a C-terminal arm of NS5B, is believed to control the conformation of NS5B, limiting the formation of RNA duplexes within the catalytic site. It is thought that these structures inhibit primer driven initiation to prevent self-priming that would otherwise lead to truncation of synthesized transcripts. Indeed mutations which disrupt these structures have been shown to greatly impact replication (Cherry et al., 2015, Hong et al., 2001). Despite these arguments, the fact remains that HCV can make use of primer driven initiation, and so the exact method of initiation remains elusive.

Within the genome, replication is driven by sequences within the UTRs, with transcription of the (+) strand to generate the (-) strand intermediate driven by the 3' UTR. The 3' UTR is much less complex, and consists of the 3' variable domain, the poly U/C tract, and the X-region, a series of 3 stem and loop structures. In addition to the 3' UTR, the 5' UTR also has a role in replication. Early studies showed that domain I of the 5' UTR was required for genome replication (Friebe et al., 2001) as its deletion within bicistronic replicons was found to inhibit RNA replication, while having only a moderate impact on translation. In the same study, HCV replicons carrying a HCV-Poliovirus chimeric 5' UTR, were used to demonstrate that the first 125 nucleotides of the HCV UTR are the minimum elements required for RNA replication, although this activity does benefit from the presence of down-stream elements (Friebe et al., 2001, Kim et al., 2002). Part of the role the minimum element within the 5' UTR appears to play is recruitment and binding of miR122 (Jopling et al., 2005), which has been speculated to both modulate translation and protect the 5' UTR from Xrm1 mediated degradation (Thibault et al., 2015). The complementary sequence of the 5' UTR (i.e. the 3' UTR of the (-) RNA strand) has also been shown to play a role in genome replication (Friebe and Bartenschlager, 2009). It is predicted to form a series of seven stem-loop structures, with the minimal requirement for replication falling within the two closest to the 3' end. Consistent with its role in (+) strand synthesis, this same RNA is bound by NS5B and serves as an excellent substrate for *de novo* initiation of RNA synthesis (Simister et al., 2009).

1.4.4 VIRUS PARTICLE FORMATION AND EXIT

Virus particle formation requires the association of the structural proteins with the progeny genome. After translation core protein is trafficked to cytosolic lipid droplets (CLDs) (McLauchlan et al., 2002), which are believed to act as platforms for particle formation. Here the core protein is thought to oligomerise, leading to the formation of the basic capsid structure. RNA recruitment to nascent capsids is also attributed to the core protein; the N-terminal domain of the mature C protein is highly basic and contains an RNA binding motif. In addition this region demonstrates RNA chaperone activity, allowing stable dimerization of the genomic RNA *in vitro* (Cristofari et al., 2004). Dimerization has been demonstrated to be non-essential for genome replication and particle formation, although it has been shown to impact both of these (Shetty et al., 2010). Considering that only a single copy of the viral genome is present within each virion, it has therefore been proposed that this dimerization plays a role in regulating a downstream process, possibly acting as a molecular switch to regulate the transition between different parts of the HCV life cycle.

Two models have been proposed to explain how genomic RNA is recruited to the progeny capsid. In the first the mature core protein is trafficked from the CLDS to the site of genome replication. Here the RNA is transported directly from the RC to the forming capsid. An alternative model proposes that the progeny genomes themselves are trafficked to the CLDs, by the interaction of NS5A with core protein coated lipid droplets (Masaki et al., 2008). Work by Shi *et al* has identified the 3' UTR as a *cis*-acting element that plays a role during genome encapsidation, with mutations abrogating packaging (Shi et al., 2016), possibly lending support to the second model. In both models the core protein is extracted from the CLD membrane, and migrates into the ER membrane, resulting in a luminal lipid droplet, carrying core protein associated with genomic RNA (Bartenschlager et al., 2011). The passage of the capsid through the ER membrane leads to the acquisition of both the lipid envelope and the 2 surface glycoproteins, E1 and E2, both of which are retained on the luminal ER surface post translation.

Acquisition of the lipid envelope and virus egress have both been shown to be dependent on the machinery associated with Very Low density lipid (VLDL) secretion (Huang et al., 2007). It has therefore been suggested that maturation of the virus particle occurs at lipid rich regions of the ER that contribute to the formation of luminal lipid droplets, the starting point of the VLDL pathway (Bartenschlager et al., 2011). Afterwards the viral particles are thought to exit the host cell by exocytosis. This model is supported by the high abundance of proteins involved in VLDL pathway within the membranes of the membranous web, for example

Apolipoprotein B (ApoB), ApoC1, ApoE, and the microsomal triglyceride transfer proteins (MTTP) (Huang et al., 2007). Furthermore ApoE has been found to be essential for the generation of infectious virus particles (Hueging et al., 2014).

Formation of infection virus particles is dependent on the activity of two viral non-structural proteins, p7 and NS2 (Jones et al., 2007a). It is not yet clear the precise role that p7 plays in virus particle formation, but mutational studies have demonstrated the importance of the ion channel activity to the formation of infectious virus particles (Jones et al., 2007a); loss of activity significantly impaired the infectivity of progeny virus, but did not affect the production of virus particles. It has been suggested that p7 facilitates proton permeablisation of intracellular vesicles to generate a pH optimal for virus particle formation.

NS2 is a cysteine protease that acts in conjunction with NS3 to catalyse the cleavage of the two proteins. As with p7, mutation studies were used to demonstrate is role in particle formation (Jones et al., 2007a). It is thought to act to bring together the various components required for the formation of the virus particle (Bartenschlager et al., 2011, Phan et al., 2009, Jirasko et al., 2010); studies have shown that NS2 is capable of forming a variety of protein-protein interactions with both the NS3-NS4A complex and the two glycoproteins, E1 and E2 (Phan et al., 2009). Interestingly NS5A, which is thought to be involved in passing genomic RNA to progeny virions, can be recruited to core protein complexes in an NS2 independent manner (Jirasko et al., 2010), possibly suggesting that recruitment of RNA to the nascent capsid is a distinct event.

1.5 HCV TROPISM

Tissue tropism of HCV is determined by a complex mix of factors impacting all stages of the virus life cycle. Chronologically, the first factors that will impact virus tropisms will be those that affect virus attachment and entry, and so expression of the entry factors discussed above, will form the first determinant of viral tropism. The minimal human factors sufficient to allow HCV entry have been identified as CD81, SR-BI, CLDI and OCLD (Ploss et al., 2009, Ding et al., 2014).

Less is known at the moment about the requirements once the virus gains entry into the host cell. One such requirement that has been identified is the expression of micro-RNA122 (miR-122), which is estimated to constitute up to 70% of the total microRNA population in the liver. Studies have shown that sequestering of miR-122 causes a marked decrease in the level of viral RNA and protein from viral replicons (Jopling et al., 2005), suggesting that miR-122 is essential for efficient genome replication. Replication defective replicons did not show a drop in protein expression however, suggesting that the miRNA impacts genome replication rather than translation. The initial work identified two highly conserved miR-122 binding sites within the HCV, one each in the 3' and 5' UTRS. Subsequent work has since expanded this to include two additional binding sites, a second in the 5' UTR (Jopling et al., 2008) and one in the NS5B coding region. It is the two binding sites within the 5' UTR that appear to be responsible for promoting genome replication; mutation of either site has been shown to inhibit the build-up of HCV RNA, which can in-turn be rescued by making reciprocal mutations within miR-122 (Jopling et al., 2005, Jopling et al., 2008).

Recruitment of miR-122 is thought to protect the viral RNA, promoting stability and replication (Roberts et al., 2011, Machlin et al., 2011). MiR-122 binds to the 5' UTR in association with Argonaute protein 2, forming a complex in which the 5' terminal nucleotides of the HCV genome are masked by a 3' overhang from the miRNA complex. Such is its activity that several groups have demonstrated that expression of exogenous miR-122 enhances the replication of HCV in several non-permissive cell types (Chang et al., 2008, Frentzen et al., 2014, Lin et al., 2010).

In addition to miR-122, efficient replication of the HCV genome is thought to require the presence of SEC14L2 (Saeed et al., 2015). Identified by transduction of a human complementary DNA library into replicon carrying cells, addition of SEC14L2 allowed wild type replicons of various genotypes to replicate at similar levels to those carrying cell culture adaptations. Although the precise mechanism by which SEC14L2 acts is currently unclear it

appears to protect HCV during lipid peroxidation, a factor known to impact activity of the HCV replicase (Yamane et al., 2014), in a vitamin E dependent manner (Saeed et al., 2015).

As discussed previously the generation of infectious virions is closely tied to the synthesis and secretion of lipid proteins. This can be seen by the low buoyant density of HCV particles, as well as the presence of several apolipoproteins within the envelop; a number have been reported to be involved in the production of infectious virus particles including ApoB, MTTP, ApoC1, and ApoE. It stands to reason therefore that factors that affect these systems will impact the ability of the virus to infect, and replicate within, different cell types. Despite the involvement of a number of apolipoproteins current data suggests that only ApoE is essential for the production of infectious virus particles. Work by Hueging *et al* demonstrated that expression of ectopic ApoE along with miR-122 was sufficient to allow production of infectious virus particles in non-permissive cell types, even in the absence of the other apolipoproteins thought to be involved (Hueging et al., 2014), suggesting that ApoE expression may contribute to tissue tropism. This was then shown to impact the virus after acquisition of the capsid, suggesting that ApoE is involved in a late stage of particle formation.

Together these factors control which cell types can support optimum HCV infection.

1.6 EXTRAHEPATIC HCV

While Hepatitis C Virus infection is predominantly associated with the human liver, several cell tissues around the body are capable of supporting HCV infection, albeit to a lesser extent than the hepatocytes. In fact HCV RNA has been detected within cells of the central nervous system(reviewed (Fletcher and McKeating, 2012), the cerebrospinal fluid, as well as the peripheral blood mononuclear cells (PBMCs) (Lerat et al., 1998). Furthermore approximately 75% of HCV patients experience extrahepatic manifestations of HCV, with the most common symptoms being depression, fatigue, joint and muscle pain, itchiness, and loss of sensation. Although many of the reported extrahepatic manifestations of HCV could stem from chronic infection, many do not correlate to liver disease, leading some to suggest that these pathologies stem from secondary populations of virus.

The earliest studies into HCV infection of the central nervous system relied upon the detection of genomic RNA within brain tissue and the CNS(reviewed (Fletcher and McKeating, 2012)); these were sufficient to demonstrate that HCV can infect these tissues, however they were insufficient to determine whether HCV can replicate there. Later works detected negative strand HCV, indicative of replication, providing the first suggestions that these tissues may support HCV replication (Radkowski et al., 2002, Vargas et al., 2002). This is

further supported by the apparent genetic diversity between HCV sequence isolated from the brain and those isolated from the liver, that has been reported by several groups (Forton et al., 2004, Fishman et al., 2008, Radkowski et al., 2002).

Peripheral blood mononuclear cells (PBMCs) represent a second extrahepatic site of HCV replication. The earliest proof that HCV could infect PBMCs was obtained by Lerat *et al,* who were able to detect both positive and negative strand RNA in the PBMCs of HCV infected patients irrespective of genotype or viral load (Lerat et al., 1998). There is some evidence to suggest that presence of HCV in PBMCs impacts treatment outcome; one study showed that patients in whom PBMCs were infected showed a significantly lower response rate to IFN (Gong et al., 2003).

Whilst the clinical symptoms of extrahepatic HCV may be of lesser concern that those associated with liver infection, the possibility of these extrahepatic populations acting as a reservoir does raise some major concerns. HCV related sequelae remain a major cause of liver transplantation, and many of those receiving such transplants often show a drift in the viral quasi-species; the new liver becomes infected with a genetically different strain of virus to the previous liver. This suggests that the virus has evolved elsewhere in the body. Several authors have therefore gone on to suggest that up to 4% of circulating virions originate from extra-hepatic reservoirs (Fletcher and McKeating, 2012, Dahari et al., 2005, Powers et al., 2006).

Outside of the 2 known reservoirs discussed above, epidemiological data suggests that HCV may infect many other tissues. Studies have shown a correlation between HCV infection and cardiovascular disease, renal failure, vasculitis, and B-cell lymphoproliferative diseases. The details of these manifestations will not be explored here, however it is important to note that though HCV is primarily associated with the liver, its influence is felt all around the body.

1.7 TREATMENT

Infection with HCV does not always require treatment; a significant minority of those infected will produce a robust antiviral response that will clear the virus during the acute phase of infection. Additionally not all cases of chronic infection require treatment as most patients don't experience severe liver disease, and the side effects of treatment can be severe. However, the problem remains that it is not yet possible to predict who will develop the disease. The aim of therapy is to induce a Sustained Virological Response (SVR), defined as the absence of detectable viral RNA in the serum, 6 months after completion of treatment. HCV infection is cured in 99% of those who achieve SVR (Swain et al., 2010).

Until 2011 the approved therapy for HCV infection relied on a combination of a weekly injection of Pegylated Interferon (peg-IFN) and a daily oral dose of Ribavirin. However, the efficacy of this is limited, with only approximately 50% of those infected with genotype 1 HCV achieving SVR; this figure rising to 80% for those infected with genotypes, 2, 3, 5, and 6 (Manns et al., 2006). In addition to the low efficacy the combination of peg-IFN and ribavirin causes a variety of side effects, e.g. headache, rash, depression, nausea, fatigue, anaemia, and myalgia (Manns et al., 2006).

Due to the considerable short comings of peg-IFN and ribavirin much research was undertaken to develop new therapies for the treatment of HCV, culminating in 2011 in the licencing in the EU of the first of a number of Directly Acting Antivirals (DAAs), telaprevir and boceprevir. Specifically targeted at genotype 1, these drugs improved SVR rates approximately 20%. Since then several others have been licensed, with even more in the pipeline. These DAAs come in a number of varieties, targeting a number of HCV proteins, and these will be discussed in detail below.

1.7.1 INTERFERON

Interferon-α (IFN-α) is a member of the type I interferons, alongside IFN-β. These are released by cells in response to a viral infection and induce an antiviral response in surrounding cells. The interferon receptor, a heterodimer of Interferon-α receptors (IFNAR) 1 and 2 on the cell detects extracellular interferon and trigger a signalling cascade through Janus activated kinase 1 (JAK1) and Tyrosine kinase 2. These then activate signal-transducing activators of transcription (STAT) 1 and 2 which enter the nucleus and induce the expression of a number of proteins with antiviral effects. Examples of IFN stimulated genes (ISG) include Protein Kinase R (PKR), which phosphorylates eIF2α to inhibit translation, and the 2'-5'-oligoadenylate synthetases, which activates endoribonuclease that degrade viral RNA. Over

300 individual ISGs have been identified, many of which have been shown to impact HCV replication (Metz et al., 2013), e.g. Tripartite motif containing 14 (TRIM14) (Metz et al., 2012), TRIM22 (Yang et al., 2016), and Tetherin (Dafa-Berger et al., 2012).

Exogenous IFN-α is a widely used antiviral. Its historic use in the treatment Hepatitis B infections first led to its use against Hepatitis C, then known as Non-A, Non-B, hepatitis. The efficacy of this treatment was limited however, with only 50% of genotype 2 and 3 infected patients responding, and only 20% of genotype 1 infected individuals. One change that improved response rates was the addition polyethylene glycol chains to the interferon. Pegylated Interferon (pegIFN) demonstrates a lower elimination rate, reduced distribution, and slower absorption, such that the drug remains in the system longer. This reduced the frequency of injections from three a week down to one.

1.7.2 RIBAVIRIN

Ribarivin is a broad spectrum antiviral that is used to treat a variety of RNA and DNA viruses. A guanosine analogue, ribavirin is processed by cellular phosphate kinases into mono-, di- and tri-phosphorylated forms. Although widely used the precise mode of action of ribavirin remains unclear, although several have been proposed (Te et al., 2007). One proposed mechanism is that ribavirin can be incorporated into RNA strands by RNA polymerases in place of guanosine, and inhibit viral replication in one of two ways. If successfully incorporated into the viral genome it may cause mutation pushing the virus towards error catastrophe. Alternatively binding of ribavirin to the polymerase can block the binding of the correct nucleosides, thereby inhibiting replication. Additionally ribavirin may block replication in another way, by depleting GTP. Ribavirin is capable of mimicking inosine 5'-monophosphate (IMP), a regulator of GMP phosphorylation. Both IMP and ribavirin competitively bind to, and inhibit Inosine-5'-monophosphate dehydrogenase, an essential enzyme for the generation of GTP, thus ribavirin could block replication by depleting the host cell of GTP. Finally ribavirin has been seen to have immunomodulatory activity, diverting the immune response away from a Th2 response towards a Th1 response. In HCV infection this may shift the immune response away from an ineffectual humoral response towards a more effective cytotoxic T-lymphocyte response.

The current recommended therapy still relies on the combination of peg-IFN and ribavirin, but now also includes one of several direct antiviral agents, which are more effective, and have fewer side effects. The introduction of these has dramatically improved the response rate to 90% of all cases, and has cut length of treatment to just 12 weeks. Such agents include: NS3-4A protease inhibitors, to inhibit the production of mature viral proteins; nucleotide

analogue inhibitors, to inhibit the viral RNA-dependent RNA polymerase; non-nucleoside inhibitors of the RNA-dependent RNA polymerase; and inhibitors of the viral NS5A protein. Newer therapies have recently been licensed that lack IFN, however their use by healthcare providers such as the NHS is still restricted because of cost. This is especially true in the developing world; in these regions the high cost of the newer therapies is prohibitive, such that the bulk of people in need of therapy remain reliant on peg-IFN and ribavirin.

1.7.3 NS3/NS4A PROTEASE INHIBITORS

Both telaprevir and boceprevir, the first 2 DAAs licenced for treatment against HCV, are examples of HCV protease inhibitors. These drugs block the activity of the NS3/4A protease, inhibiting the maturation of functional non-structural proteins from the HCV polyprotein. Both telaprevir and boceprevir function by binding to the active site of the NS3/4A complex, thereby inhibiting the protease activity.

Early telaprevir precursors were first developed in 2000 by Eli Lilly and Vertex (Kwong et al., 2011). Early development was kick started by the molecular characterisation of the NS3/4A complex and subsequent identification of the protease active site as a potential target for inhibitors. Early precursors to Telaprevir were developed based on the NS5A-5B substrate (Kwong et al., 2011, Chen and Tan, 2005), and the understanding that natural substrates of NS3 can have an inhibitory effect on the protease (Steinkuhler et al., 1998). Subsequent optimisation led to the eventual development of telaprevir. This carries a keto-carbonyl group which forms a covalent bond with the catalytic serine residue within the protease's binding site (Lin et al., 2006a), allowing it to compete with the NS5A/5B substrate, and therefore inhibit the protease activity. During early clinical trials patients treated with telaprevir alone demonstrated a robust drop in HCV plasma RNA and liver damage markers (Kwong et al., 2011, Reesink et al., 2006). However, when telaprevir was used alone, it was shown to lead to the emergence of resistance mutants in a high proportion of patients (Gentile et al., 2009, Sarrazin et al., 2007). As such telapravir was used in combination with IFN and ribavirin. It was initially license by the US FDA in May 2011, but was withdrawn from the market in 2014 due to the emergence of newer more effective therapies. Telaprevir is only indicated for used against genotype 1 infections.

Similarly to telaprevir, boceprevir competes with the NS substrates to bind to the active site of the NS3 protease, specifically Ser139 (Malcolm et al., 2006). As with telaprevir, boceprevir was limited to being used in genotype 1 infections and it has since been removed from the market due to the availability of superior DAAs.

Other examples of NS3 inhibitors include paritaprevir and sovaprevir.

1.7.4 NS5A INHIBITORS

The second class of DAAs available against HCV, target the NS5A phosphoprotein. NS5A is an essential component of the replication complex, and as such represents a prime target for drug development. Due to the versatility of NS5A, it is likely that inhibitors of this protein will impact multiple points in the HCV life cycle. Despite the efficacy of many of these drugs, they have a low barrier to resistance, and so are not used in isolation. Commonly these are given in conjunction with pegIFN and another DAA, as NS5A resistant mutants generally remain sensitive to these (Fridell et al., 2010).

Daclatasvir is an NS5A inhibitor that binds to the N-terminus of the NS5A protein, preventing it from associating with the membranes of the cell, and thereby altering its subcellular localisation (Lee et al., 2011). This prevents the formation of the replication complex, inhibiting RNA replication and virion formation. The precursors to daclatasvir were originally developed by Bristol-Myers Squibb, as part of a library of compounds prepared for general screening campaigns (Lemm et al., 2010). These were then screened for their ability to inhibit the replicon of both genotype 1b HCV and Bovine viral diarrhoea virus. A class of compounds with a thiazolidinone core, were found to be highly effective, and non-toxic, inhibitors of HCV. Further screening identified that these early precursors interacted with NS5A by a novel mechanism targeting domain I, and thus served as an attractive focus for further development (Belema and Meanwell, 2014, Lemm et al., 2010). From these initial screens the thiazolidinone core compounds went through extensive modification to generate what is now called daclatasvir (Figure 1-5). The first clinical trials for daclatasvir were published in 2010, and it was approved under the name Daklinza in 2014 in the EU, and 2015 in the US. Daclatasvir is only used in the treatment of genotype 1, 3, or 4 infections and is used in combination with sofosbuvir, ribavirin, and IFN, although the precise combination depends on the genotype and the scale of liver damage (FDA, 2016).

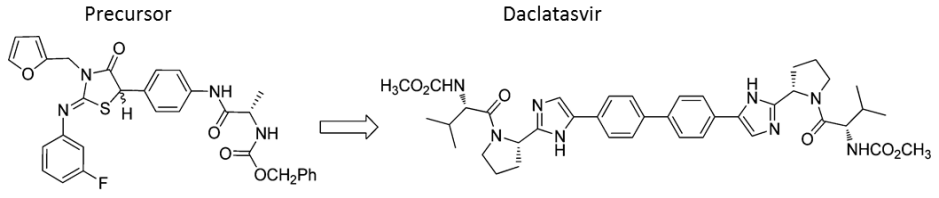

Figure 1-5 **Structure of Daclatasvir and its precursor.** Modified from Belema and Meanwell, Discovery of Daclatasvir, a Pan-Genotypic Hepatitis C Virus NS5A Replication Complex Inhibitor with Potent Clinical Effect, J. Med. Chem., 2014, 57 (12), 5057–5071(Belema and Meanwell, 2014).

Another example of an NS5A inhibitor is Ledipasvir, developed by Gilead (Link et al., 2014). The drug consists of a an unsymmetrical benzimidazole-difluorofluorene-imidazole core and distal [2.2.1]azabicyclic ring. It is known to bind directly to the NS5A protein, inhibiting one or more of the functions of the protein, however, the precise binding site and activity of the drug remains unknown. In early clinical trials ledipasvir monotherapy was found to be capable of causing an average three-log decrease in viral load (Link et al., 2014), and in phase 2 trials in which ledipasvir was paired with sofosbuvir, with or without ribavirin, combination therapy achieved 100% SVR after 12 weeks, in prior non responders. Ledipasvir, in combination with sofosbuvir was then licensed by the FDA in October 2014 (FDA, 2015).

Other examples include ombitasvir, ravidasvir, elbasvir, and velpatasvir.

1.7.5 NS5B INHIBITORS

The final class of DAAs available against HCV target the viral RNA dependent RNA polymerase, NS5B, inhibiting the ability of the virus to replicates its genome. NS5B is an attractive therapeutic target as the host cell has no equivalent system that may suffer an off target effect. There are two types of NS5B inhibitor, the nucleoside inhibitors, and non-nucleoside inhibitors.

Nucleoside inhibitors are analogues of ribonucleotide triphosphate, and are able to enter the active site of the polymerase. Once within the active site the inhibitor either stalls the polymerase activity or causes premature termination. One example of this type of inhibitor is sofosbuvir, which was developed by Pharmasset (Lam et al., 2010), and later licensed by Gilead. Taken as a prodrug, sofosbuvir is metabolised to an active form, which can be incorporated into nascent RNA molecules. Once incorporated a 2' methyl group is thought to cause a steric clash resulting in premature chain termination (Ma et al., 2007, Appleby et al., 2015). Sofosbuvir has been used in genotypes 1-6 (Gentile et al., 2013), however co-therapy is tailored differently between genotypes. For genotypes 2 and 3, sofosbuvir is given in combination with both ribavirin and interferon, however with genotypes 1, 4, 5, and 6 the recommended therapy includes ledipasvir, an NS5A inhibitor. There is also limited data the sofosbuvir can be used in the treatment of genotype 7 infections (Schreiber et al., 2016).

In contrast to the other classes of DAAs, nucleoside inhibitors display a high threshold to resistance (McCown et al., 2008), most likely due to the inability of the virus to distinguish between inhibitors and true NTPs.

The second type of NS5B inhibitors are the non-nucleoside inhibitors. These are able to bind to sites other than the active site and inhibit polymerase activity in a non-competitive manner.

These are possibly the most diverse of the DAAs, and they target large number of different sites of the NS5B protein, however only one has so far been approved, Dasabuvir. Dasabuvir binds to NS5B outside of the active site, inducing a conformational change that inhibits the elongation of nascent viral genomes (Gentile et al., 2014). Due to variation within NS5B between genotypes dasabuvir is only used in the treatment of genotype 1a and 1b infections.

1.7.6 RECENT ADVANCES IN HCV THERAPY

The last few years have seen the emergence of a number of pangenotypic therapies for the treatment of HCV infections. These show increased efficacy and have largely replaced the earlier DAAs.

Mavyret/Maviret is one such example. Developed by AbbVie, it combines an NS3 protease inhibitor, Glecaprevir, with an NS5A inhibitor, pibrentasvir (Lawitz et al., 2015). Early clinical trials have shown that this combination is highly effective across all major genotypes and is capable of SVR in a shorter period (Lawitz et al., 2015, Zeuzem et al., 2018). It was licensed in the US and EU in August 2017, and, as of January 2018, is recommended by the National Institute for Health and Care Excellence for the treatment of all genotypes in the UK (NICE, 2018).

Another pan genotypic therapy is marketed under the name Vosevi. This is a combination of the NS5B inhibitor sofosbuvir, the NS5A inhibitor velpatasvir, and the NS3/4A inhibitor voxilaprevir, and is the first triple DAA therapy licensed in the US and EU (Heo and Deeks, 2018). Although it has been shown to cause high levels of SVR in genotypes 1-6, the combination of sofosbuvir and veltapasvir without voxilaprevir is superior. As such Vosevi is instead recommended as a retreatment option for those for whom previous DAA based therapies have failed (Bourliere et al., 2017).

1.7.7 HOST FACTORS IMPACTING TREATMENT

Although the infecting genotype is the main determinant in the success of treatment, host factors also play an essential role determining outcome. The most basic factors that impact outcome include; age, gender, co-infection, and alcohol consumption. Additionally there is strong evidence to support a genetic element as well, with several polymorphisms being identified that impact treatment outcome. Several genome association studies have identified a link between polymorphisms in the *IL28* locus and the outcome of interferon treatment (Abe et al., 2010, Ge et al., 2009, Suppiah et al., 2009, Tanaka et al., 2009). The major polymorphism present in Asian, European, and American populations for example, has been

linked to both successfully treatment, and spontaneous clearance of the virus. It has been proposed that the different allele types result in different cytokine profiles, and that the major allele, promotes a stronger inflammatory response (Abe et al., 2010). Other genes linked to treatment outcome include; *MxA* (Hijikata et al., 2000, Knapp et al., 2003), *OAS-1* (Knapp et al., 2003), *PKR* (Knapp et al., 2003), *IFNRA1* (Matsuyama et al., 2003) and *MAPKAPK3* (Tsukada et al., 2009).

In addition to directly impacting the success of therapy, several human genes have been implicated in the development and severity of side effect. Examples of this include *ITPA* and *SLC28A2* both of which are thought to impact the development of anaemia in patients undergoing treatment including a protease inhibitor (Ampuero et al., 2015). Factors such as these contribute to the success of therapy indirectly, by impacting the quality of life during treatment, and therefore adherence.

Cell-based work on HCV replication initially relied on the infection of cell culture or primary cell lines with whole virus. These systems were hindered however, due to the very low levels of replication that could be achieved and the difficulty in obtaining primary hepatocytes. A major breakthrough occurred in 1999 with the development of a selectable replicon system by Lohman *et al* derived from the consensus sequence of a genotype 1b isolate designated con1 *(*Lohmann et al., 1999*)*. This system relies upon a bicistronic RNA molecule carrying a G418 resistance marker (*Neo*) which expresses Neomycin phospotransferase (NPT), and the viral non-structural proteins NS3-5B; NS2 was found to be non-essential for the replication of the replicon, whilst its inclusion yielded markedly lower amounts of replication. As such it was discarded. The *Neo* gene was expressed using the HCV IRES, while expression of the replicase was controlled by a second IRES derived from Encephalomyocarditis virus (EMCV)(Figure 1-6). The *Neo* gene is often replaced with a Firefly luciferase gene (*luc),* allowing RNA replication to be monitored using a simple assay in which luciferase activity equates to replication (Lohmann et al., 2003).

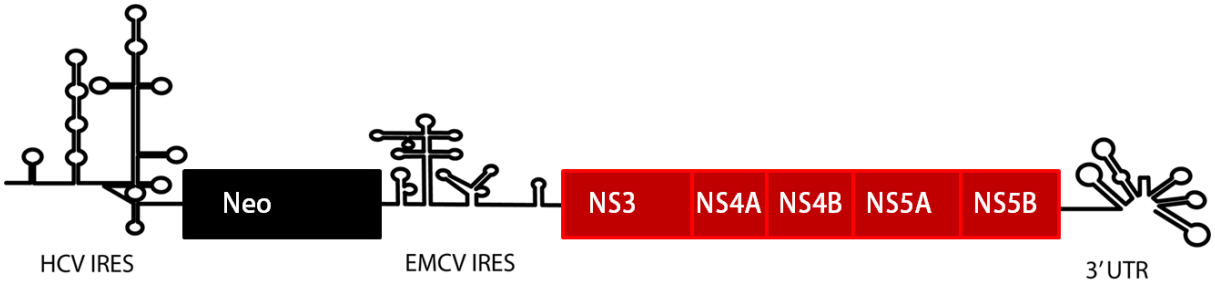

Figure 1-6 **Hepatitis C Virus replicon.**

During the initial work with the replicon system, stable cells lines showed high levels of both viral protein and RNA, confirming the ability of the replicons to replicate. However, selection using G418 yielded few colonies, leading to the suggestion that either only a minority of the transfected cells were capable of supporting replication, or that the replicon had acquired mutations that allowed it to replicate in cell culture (Lohmann et al., 1999). Work has since been published that provides support to both theories.

The presence and impact of cell culture adaptive mutations within the HCV replicons is now well known and has been the subject of much research. These mutations likely occur from errors made during *in vitro* transcription and/or from errors made during the initial period after transfection as the replicons undertake a limited degree of replication. Upon introduction of selective pressure, those replicons carrying beneficial mutations convey G418

resistance to the cell and can be selected out. Mutations can then be introduced back into the parental replicons, resulting in a marked improvement in colony formation.

Several groups have published work on culture adaptation and have identifying an array of mutations (Blight et al., 2000, Krieger et al., 2001, Lohmann et al., 2001, Lohmann et al., 2003). All cell culture adaptive mutations identified in this way have been located within the viral replicase as opposed to the UTRs of the replicon. Of these, the most effective individual mutations have been located within NS5B, NS5A, and NS4B. Interestingly, whilst several culture adaptive mutations have been identified within the NS3 protease (Lohmann et al., 2003, Krieger et al., 2001), these provide little benefit alone. However, in combination with mutations elsewhere these had a synergistic effect greatly increasing replication. Inversely those mutations elsewhere in the replicase are often incompatible with each other as replicons carrying multiple mutations that individually greatly increase replication became non-viable (Lohmann et al., 2003).

Although culture adaptation of the replicon appears to be the main driving force behind increased replication, it is possible for replicons to replicate without these as sub-clones of Huh7 cells are able to support replication of replicon RNAs that lack culture adapted mutations (Blight et al., 2002). These sub clones can be 'cured' by extended use of IFN-α, to generate a cell line that is highly permissive to HCV replication (Blight et al., 2002).

Another major breakthrough in the field of HCV research was the discovery of Japanese Fulminant Hepatitis 1 (JFH1), a genotype 2a isolate of HCV (Kato et al., 2001). Prior to this the low efficiency of replication limited the study of the complete HCV life cycle. Replicons derived from JFH1 do not have this problem however, and replicate efficiently in Huh7 cells without the need for culture adaptive mutations. Because of this JFH1 has been widely adopted as the standard isolate to be used, such that it is widely considered the 'work horse' of HCV research.

The discovery of JFH1 eventually led to the development of cell culture HCV systems (ccHCV). Transfection of *in vitro* transcribed JFH1 RNA was found to be capable of generating infectious virus particles, allowing the study of the entire life cycle with a single isolate (Lindenbach et al., 2005, Wakita et al., 2005, Zhong et al., 2005).

Unfortunately, JFH1 allowed insight into only a single genotype. Work by Pietschmann *et al* expanded this by both forming intragenotypic and intergenotypic chimeras of HCV expressing the structural proteins of genotype 1a, 1b, and 2a, and the non-structural proteins of JFH1 (Pietschmann et al., 2006). The non-structural proteins from JFH1, fused by a site

within NS2 immediate downstream of the first transmembrane domain, allowed robust replication of the chimeras, leading to the production of infectious particles.

Since the development of these chimeras the expansion of the ccHCV system has been championed by Jens Bukh. This work has led to the development of systems that allow the study of genotype 1a, 1b, 3a, 4a, 2a, and 2b strains of HCV (Li et al., 2015, Ramirez et al., 2014, Gottwein et al., 2010).

Prior to the establishment of the replicon and cell culture systems, the ability to study HCV was limited by the absence of suitable models. As such many early studies relied on the use of surrogates of HCV, most commonly Bovine Viral Diarrhoea Virus (BVDV) models (Buckwold et al., 2003). BVDV is a pestivirus with a high degree of genetic similarity to HCV (Miller and Purcell, 1990). Similarly to HCV, it generally causes long term, chronic infections in its natural host. In addition it shares several molecular similarities with HCV, including IRES structure, NS3 helicase/NPTase activity, and NS5B structure. Before the use of the HCV replicon based models became widespread, BVDV was used due to the ease of culturing it *in vivo*. Even with the advent of early replicon systems, BVDV had the advantage of simulating the entire viral life cycle, though the development of ccHCV systems means that this is no longer the case.

1.9 NS5A

1.9.1 STRUCTURE

NS5A, is a multifunctional viral phosphoprotein which is approximately 450 amino acids in length, although the size varies between genotypes, and which co-localises with the other non-structural proteins, in the HCV RC (Mottola et al., 2002, El-Hage and Luo, 2003). At its N-terminus NS5A has a 33 amino acid amphipathic α-helix which anchors the protein to the ER membrane (Elazar et al., 2003, Brass et al., 2002). This α-helix is believed to be embedded within the ER membrane, such that it lies parallel to the lipid bilayer, with the hydrophobic face aimed towards the membrane (Brass et al., 2002).

Extending into the cytosol from the amphipathic helix are three functional domains (Figure 1-7), domains I-III, responsible for the activities of NS5A, separated by Low Complexity Sequences (LCS) I and II. The presence of the three domains and inter-domain LCS regions was first suggested based on observations from limited protease treatment of NS5A originating from a genotype 1b isolate of HCV. This identified two trypsin sensitive regions within NS5A that fall at residues 215 and 355 (Tellinghuisen et al., 2004). Domain I corresponds to the 180 amino acids immediately downstream of the amphipathic helix, and can be separated into two sub-domains (Tellinghuisen et al., 2005). Sub-domain I consists of 3 antiparallel β-sheets and an α-helix, while domain II encompasses a series of 6 antiparallel β-sheets. Cysteine residues present in sub-domain I form a zinc binding motif, such that a single zinc atom is bound to each protein molecule (Tellinghuisen et al., 2004). This, in conjunction with a disulphide bond in sub-domain II, maintains the structure and functionality of domain I. An initial study into domain I structure showed that domain I was able to form homodimers, with 2 domain I monomers linked via interactions located close to the N-terminus. The homodimer formed a basic groove which was predicted to be capable of binding to RNA, an activity that has since been confirmed (Huang et al., 2005), although the location within domain I where RNA binds has yet to be experimentally verified. The formation of the homodimer has also been suggested in several subsequent studies that have determined the structure of domain I (Love et al., 2009, Tellinghuisen et al., 2005, Lambert et al., 2014), however these structures differ in the orientation of the two monomers relative to each other. There is also some limited data suggesting the formation of a dimeric structure *in vitro* (Hwang et al., 2010). All of NS5A upstream of LCS I is essential for RNA replication; mutations which disrupt either domain I or the amphipathic helix are lethal to RNA replication (Tellinghuisen et al., 2004, Brass et al., 2002, Penin et al., 2004a).

Domains II and III, which are essential for RNA replication and virus particle formation respectively, are much less well structured (Hanoulle et al., 2010, Hanoulle et al., 2009, Liang et al., 2007), and are thought to be similar to a class of proteins called Intrinsically Disordered Proteins (IDPs). These proteins have little or no structure alone, but undergo conformational change in association with a ligand (Penin et al., 2004b, Wright and Dyson, 1999). Often these proteins form small, transient, amphipathic secondary structures to facilitate binding of the target ligand (Wright and Dyson, 1999, Wright and Dyson, 2009), termed Molecular Recognition Elements (MoREs). Several MoREs have been identified within NS5A including; a Proline-Tryptophan turn essential for RNA-replication (Dujardin et al., 2015), two α-helices in domain III thought to allow interaction with Cyclophilin A (Verdegem et al., 2011), and 2 further α-helices that form a SH3 binding motif (Feuerstein et al., 2012). Two models have been put forward to explain the interaction of IDPs with their ligands, Induced Folding and Conformational Selection. The Induced Folding model proposes that IDPs remain completely unstructured in the absence of a ligand; binding then induces folding of the IDPs into the necessary structures. Alternatively the Conformational Selection model suggests that IDPs undergo some folding in isolation, and that the ligand then preferentially binds proteins that are folded more closely to the active form (Wright and Dyson, 2009). In actuality it is likely that a hybrid of the two mechanisms is used; some degree of folding being essential to allow the initial interaction which then induces further conformational changes. This can be seen in NS5A, with the α-helices that form the SH3-binding motif forming even in the absence of a ligand, but the protein remaining mostly unstructured (Feuerstein et al., 2012). A common feature of IDPs is the ability to form multiple protein-protein interactions, folding into various structures in association with different ligands, and NS5A is no exception, having been shown to associate with a large number of proteins (Macdonald and Harris, 2004). The lack of structure contributes to this promiscuous nature by providing the flexibility necessary to form these myriad interactions.

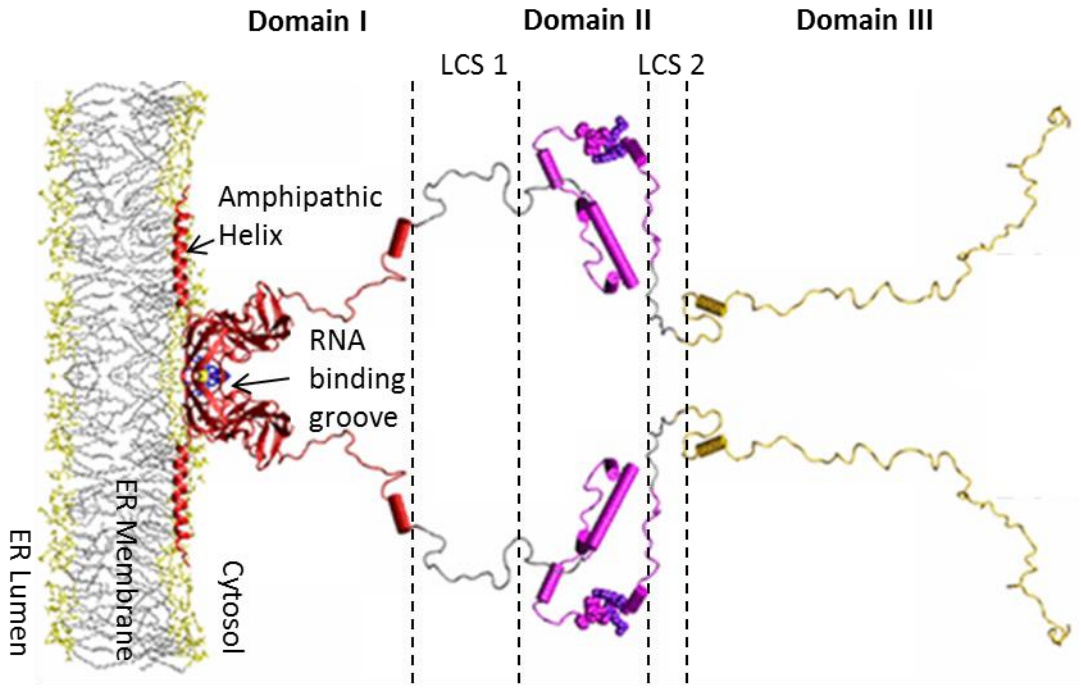

Figure 1-7 **Structure of the HCV NS5A protein.** An amphipathic helix at the N-terminus anchors NS5A to the ER membrane, with three functional domains extending outwards into the cytosol. Interactions within domain I allow the formation of a homodimer, and support the formation of and RNA binding groove. Modified from Badillo *et al,* Overall Structural Model of NS5A Protein from Hepatitis C Virus and Modulation by Mutations Confering Resistance of Virus Replication to Cyclosporin A, Biochemistry, 2017, 56 (24), 3029–3048 (Badillo et al., 2017).

1.9.2 PHOSPHORYLATION

As previously stated NS5A is a phosphoprotein, with the key sites of phosphorylation being serine and threonine residues located with, LCSI, LCSII and domain III (Figure 1-8). It exists in two forms, the basal state, p56, and a hyperphosphorylated form, p58, that produce distinct bands when analysed by sodium dodecylsulphate polyacrylamide gel electrophoresis (SDS-PAGE) (Kaneko et al., 1994). Several host protein kinases have been identified as having an impact on NS5A phosphorylation including: casein kinase 2, casein kinase 1α, Protein Kinase A, serine/threonine-protein kinase 1 (Ross-Thriepland and Harris, 2015, Macdonald and Harris, 2004) and phosphatidylinositol 4-kinase IIIa (PI4KA) (Reiss et al., 2011). Cellular factors such as these appear to be sufficient for the generation of the hypophosphorylated p56, however hyperphosphorylation of this, to the p58 form, appears to be dependent on the presence of other non-structural proteins (Macdonald and Harris, 2004). Work with genotype 1b isolates has suggested a requirement for upstream non-structural proteins, NS3 to NS4B (Kaneko et al., 1994, Liu et al., 1999, Neddermann et al., 1999), however some data

suggests that only NS4A is required, as a shift from p56 to p58 can be triggered with the co-expression of NS4A alone (Asabe et al., 1997).

Phosphorylation appears to have a regulatory function, modulating the involvement of NS5A in genome replication and the formation of the virus particle. The precise role that hyperphosphorylation plays, however, remains unclear. Early studies in genotype 1b isolate con1 suggested that hyperphosphorylation of NS5A inhibited genome replication (Evans et al., 2004). Indeed it has been shown for the con1 isolate that substituting serine residues key for hyperphosphorylation typically promotes RNA replication (Appel et al., 2005). Conversely, studies in the Harris group on genome 2a isolate JFH1, have suggested that hyperphosphorylation of NS5A promotes replication. In these studies it was seen that inhibiting hyperphosphorylation of certain residues within LCSI was lethal to replication (Ross-Thriepland and Harris, 2014). In this study however it was noted that phosphorylation state is not the universal control, as substitution of some serine residues with aspartic acid, which can also be phosphorylated, was found to be lethal. Interestingly several studies have shown that other non-structural proteins are capable of modulating NS5A phosphorylation state, e.g. mutations in NS4B to boost replication were shown to down-regulate NS5A phosphorylation (Appel et al., 2005), while an electrostatic switch mechanism is proposed to allow NS4A regulation of NS5A phosphorylation (Lindenbach et al., 2007).

Phosphatidylinositol 4-kinase IIIa (PI4KA) is a cellular kinases that has been linked to the generation and maintenance of a microenvironment essential for replication (Reiss et al., 2011). It is thought that enhanced PI4KA activity is required to generate an enriched membrane microenvironment, in which the virus may replicate. It was noted that enhanced PI4KA activity was driven by NS5A. In contrast however, work by Harak *et al* showed that replication within the much more permissive Huh7 cell line, cells that already express high levels of PI4KA, required culture adaptive mutations that reduced PI4KA activity (Harak et al., 2016). Importantly several of the NS5A culture adaptive mutations associated with PI4KA activity, targeted serine residues within LCSI which have previously been linked to phosphorylation, suggesting a link between NS5A phosphorylation state, PI4KA recruitment, and replication. Together these data demonstrate that a delicate balance between p56 and p58 is required for optimal replication.

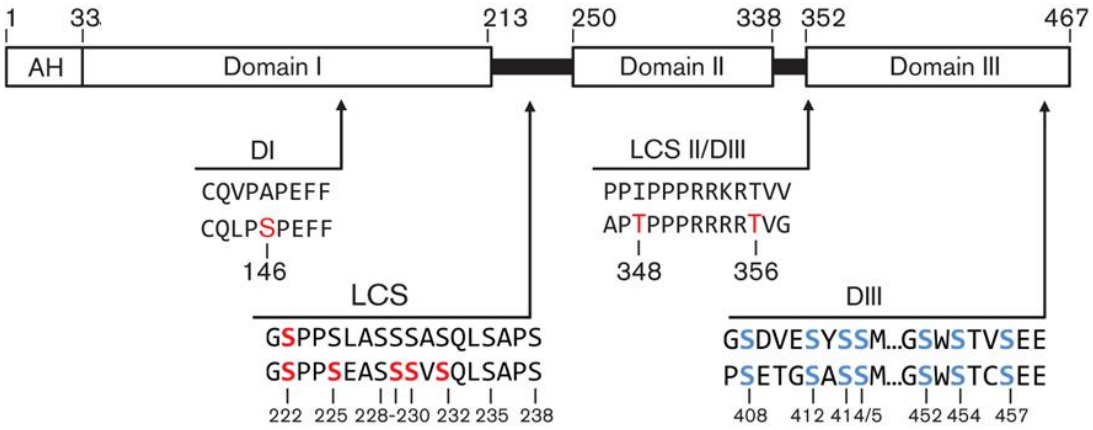

Figure 1-8 **Organisation of NS5A showing the key phosphorylation sites**. Sites in red have been confirmed by mass spectrometry, while sites in blue have been proposed by genetic analysis but lack biochemical data. The sequences presented are from genotype 1b (J4 isolate, GenBank accession number AF054250, upper sequence) and genotype 2a (JFH-1 isolate, GenBank accession number AB047639, lower sequence). Figure modified from Ross-Thriepland D, Harris M. Hepatitis C virus NS5A: enigmatic but still promiscuous 10 years on! The Journal of general virology. 2015;96(Pt 4):727-38(Ross-Thriepland and Harris, 2015).

1.9.3 FUNCTION

NS5A has a variety of functions within the virus life cycle, including promoting the activity of the RNA-dependent RNA polymerase, NS5B (Shirota et al., 2002, Tellinghuisen et al., 2004), and aiding in the maintenance of the RC (Reiss et al., 2011). NS5A is also known to have an essential role in virion formation, and is believed to be involved in the connection between the sites of this and the sites of RNA replication. Additionally NS5A has shown the ability to interact with and regulate the host cell cycle, promoting cell proliferation (Ghosh et al., 1999). Much of the focus on NS5A is due to its importance in the viral response to the immune system; NS5A has been shown to inhibit both apoptosis (Ghosh et al., 2000) and the interferon response(Tan and Katze, 2001, Song et al., 1999, Paterson et al., 1999). Much work has therefore been performed to understand the physiological and clinical importance of this protein. Interestingly NS5A is considered to lack any enzymatic activity, and instead is thought to mediate its myriad functions through interaction with a vast array of proteins.

1.9.3.1 RNA REPLICATION

Evidence that NS5A has a role in viral replication was first brought to light by the development of the replicon system, as many mutations that improved colony formation mapped to NS5A (Lohmann et al., 2001, Blight et al., 2000). A direct link between NS5A and replication was then shown by Krieger *et al,* who observed RNA replication in transiently transfected cells using a luciferase reporter. It was found that mutations within both NS5A and NS5B increased RNA replication (Krieger et al., 2001). This was further supported by the

observation that loss of the N-terminal amphipathic helix from NS5A impairs RNA replication (Elazar et al., 2003).

Though the precise role that NS5A plays in replication remains elusive, it is clear that the process involves direct interaction with NS5B; NS5A is known to bind NS5B, and this has been shown to modulate NS5B activity (Shirota et al., 2002, Quezada and Kane, 2009). Furthermore this association has been shown to be essential for replication; if this interaction is lost replication is inhibited (Shimakami et al., 2004, Elazar et al., 2003). NS5A also has indirect roles in regulating genome replication. As mentioned previously NS5A has been shown to recruit, and enhance the activity of, PI4KA, an activity that is essential for replication (Reiss et al., 2011). The functional interaction site for this interaction lies within the C-terminal region of domain I.

It is important to note that not all of NS5A is essential for replication. Whilst both domains I and II are thought to be involved in some capacity, domain III is widely considered dispensable for replication as replicons with both large scale deletions (Appel et al., 2005) and insertions (Moradpour et al., 2004) within domain III remain functional. What is essential for replication is the entirety of domain I, and the C-terminus of domain II and typically mutations targeted at either of these regions result in a lethal drop in replication (Ross-Thriepland and Harris, 2015, Arumugaswami et al., 2008, Tellinghuisen et al., 2008, Ross-Thriepland et al., 2013).

Interestingly, the contribution to replication of the amphipathic helix at the N-terminus of domain I extends beyond its ability to anchor NS5A to membranes. Work by Brass *et al* examined the interchangeability of amphipathic helices from NS5As from HCV and related members of the *Flaviviridae* (Brass et al., 2007). Despite having similar propensities for membrane anchoring, only a very small number of residue exchanges were tolerated in the context of HCV RNA replication. This suggests a role for the amphipathic helix in replication complex formation, possibly through the formation of essential interactions with other components of the replication complex. One such interaction that has been proposed, is with NS4B. Work in the Tellinghuisen group has identified key residues on the charged face of the amphipathic helix, that form an interaction with the NS4B protein, and which are essential for replication (Biswas et al., 2016).

1.9.3.2 VIRION FORMATION

NS5A plays an essential role during virion formation, specifically during the association of the progeny genomes with the core protein. NS5A is thought to bind to progeny genomes and contribute to the transport of these to lipid droplets allowing them to become encapsidated

with core protein (Masaki et al., 2008). In support of this model, NS5A has been found to exist in two populations within both replicon and virus infected cells (Wolk et al., 2008, Eyre et al., 2014); large non-motile structures that were suggested to exist in the membranous web, and smaller, fast moving structures, thus demonstrating motile potential for NS5A and its binding partners. Both Domain I and III are thought to contribute to this function of NS5A, having been shown to interact with lipid droplets (Miyanari et al., 2007) and core protein respectively (Appel et al., 2008). Although traditionally the entirety of domain III is considered necessary for virion formation, some evidence now suggests that this process is dependent only on the N-terminus and the C-terminal 15 amino acids (Zayas et al., 2016)

1.9.3.3 IFN RESISTANCE

Much of the research into NS5A has been driven by its proposed role in protecting the virus during the immune response, specifically by providing resistance to interferon-α (IFN-α), which remains part of the recommended therapy for HCV infection. This hypothesis originates from the observation that mutation within a 40 amino acid long region of domain II, termed the Interferon Sensitivity Determining Region (ISDR), appeared to have an impact on the effectiveness of IFN-α therapy in chronically infected patients (Enomoto et al., 1996, Murakami et al., 1999). This hypothesis remains controversial however, as several studies have found little or no correlation between mutation within this region and treatment outcome (Paterson et al., 1999, Aizaki et al., 2000). These observations do not contradict the idea that NS5A plays a role in IFN resistance, but instead question the importance of the ISDR. Further studies have suggested that the C-terminal region of NS5A plays a more important role in mediating IFN resistance, with the so-called V3 region in domain III being implicated (Nousbaum et al., 2000); more mutations associated with IFN resistance and sensitivity were found within this region, than within the ISDR. The question still remains however, how does NS5A mediate this apparent resistance?

One potential mode of action is through the repression of Protein Kinase R (PKR). PKR is activated in the presence of double-stranded RNA, which is only present during viral infection, and causes the phosphorylation of eIF2α, an essential factor in eukaryotic translation. Phosphorylation of eIF2α universally inhibits translation, preventing the production of viral proteins. PKR was first reported to be a target of NS5A by Gale *et al* (Gale et al., 1997), who demonstrated that NS5A was able to bind to, and inhibit, PKR. Binding to PKR was later shown to be dependent on the ISDR (Gale et al., 1998), supporting its involvement in mediating IFN resistance. NS5A was found to bind to PKR at the same site as a known PKR inhibitor, $P58^{IPK}$, within a region of PKR responsible for dimerization; suggesting that inhibition occurs by preventing the formation of the active dimer.

Another target of NS5A appears to be the IFN-induced JAK-STAT signalling pathway. The first evidence that HCV interfered with JAK-STAT signalling was provided by Heim *et al,* who showed that expression of the HCV genome was capable of inhibiting ISGF3 induction (Heim et al., 1999), and this was later shown *in vivo,* in mice (Blindenbacher et al., 2003). Multiple subsequent studies have since shown the involvement of NS5A in this process (Gong et al., 2007, Kumthip et al., 2012, Lan et al., 2007, Polyak et al., 2001), likely by blocking or reversing the phosphorylation of the STAT proteins, thereby preventing the induction of the ISRE controlled genes.

1.9.3.4 NS5A AND THE CELL CYCLE

HCV NS5A has been shown to effect a wide variety of host cell mechanisms other than just blocking IFN signalling (Macdonald and Harris, 2004, He et al., 2006). Another key role of the NS5A protein is to modulate the host cell's growth and proliferation. In eukaryotic cells the cell cycle is controlled by multi-layered signalling pathways which detect both internal and external stimuli and modulate cell growth, proliferation, differentiation, gene expression and cell death. Key to these signalling cascades are the Mitogen-Activated Protein Kinases (MAPKs) a diverse family of proteins present in all eukaryotic cells (Chang and Karin, 2001). In their basal forms MAPKs are catalytically inactive, however dual threonine/tyrosine phosphorylation causes conformational change, allowing the MAPKs to bind to downstream targets and elicit a cellular response. Phosphorylation, and therefore activation, of MAPKs is the responsibility of a diverse group of proteins called MAPK Kinases (MAPKKs), which are in turn regulated by an even more diverse group of proteins called the MAPKKKs. Specific MAPKKKs can be activated by a wide variety of stimuli, both intra- and extra-cellular resulting in a vastly complex signalling pathway. Despite the vast array of MAPKKs and MAPKKKs, only relatively few classes of MAPKs exist in eukaryotic cells; extracellular signal related kinases (ERKs), Jun amino-terminal kinases (JNKs), p38 proteins, and ERK5 (Chang and Karin, 2001).

HCV, and NS5A specifically has been shown to be capable of inhibiting all MAPK signalling pathways (Macdonald and Harris, 2004). Growth factor receptor-bound protein 2 (Grb2) is a cellular growth factor essential for proliferation of many cell types, and a member of the ERK signalling cascade, involved in the cells response to Epidermal Growth Factor (EGF). NS5A has been seen to interact with this Grb2 via a highly conserved proline rich motif, inhibiting the activation of the ERK signalling cascade (Tan et al., 1999, He et al., 2002). Consistent with NS5A inhibiting EGF signalling, it has been reported that in multiple cell types cells expressing NS5A became resistant to the addition of exogenous EGR (Macdonald et al., 2005, Tan et al., 1999). Interestingly work has shown that the poly protein motif of NS5A is capable

of interacting with many other Src-homology 3 domain containing proteins (Macdonald et al., 2004). One example of this is the Phosphoinositide 3 kinase (PI3K) cell survival pathway (Macdonald et al., 2005), which is linked to regulation of apoptosis. NS5A has been shown to interact with the p85 regulatory subunit of PI3K, and stimulation of this pathway by NS5A has been shown to inhibit apoptosis (Street et al., 2004, He et al., 2002).

NS5A has also been demonstrated to modulate the p38 MAPK pathway (He et al., 2001, Wu et al., 2008). For example NS5A has been shown to inhibit activation of the p38 pathway inhibiting the phosphorylation of eIF4E. This has been proposed to limit cap-dependent translation, potentially generating a cellular environment during late stage infections that favours HCV's cap-independent translation (Macdonald and Harris, 2004, He et al., 2001). However, inhibition of translation is not the only function impacted by NS5A modulating the p38 pathway. NS5A has also been shown to inhibit the activation of the Abnormal Spindle-like microephal associated protein, leading to cell cycle arrest (Wu et al., 2008).

Finally NS5A interacts with JNK MAPK (Park et al., 2003). NS5A has been shown to interact with the TNF receptor associated factor 2, inhibiting the downstream activation of nuclear factor kappa-light-chain-enhancer of activated B cells (NF-κB). As NF-κB plays an important role in the regulation of apoptosis, its deactivation was proposed to sensitize cells to apoptosis. However, more recent data proposes that it may in fact have the opposite effect (Xie et al., 2017).

These various data clearly show that NS5A is capable of modulating cell signalling pathways linking to cell growth, proliferation, and survival. Although the precise role that this modulation plays in the viral life cycle has been the source of much speculation, the models formulated are varied and complex, and so will not be discussed in detail.

1.9.3.5 APOPTOSIS INHIBITION

Essential to any virus that causes chronic infection is the inhibition of apoptosis, and HCV is no exception. Numerous studies have shown impaired apoptosis in cell expressing various HCV proteins, and many of these have suggested a role for NS5A in this process (Ross-Thriepland and Harris, 2015). Apoptosis is a highly regulated process and can be induced either by internal signals, via the intrinsic pathway, or by external stimuli, through the extrinsic pathway. Evidence suggests that NS5A may modulate both pathways to block apoptosis.

Mitochondrial health is one of the key regulators of the intrinsic apoptotic pathway; proper mitochondrial activity, morphogenesis, and dynamics are essential to the health of the cell

and to the host as a whole, and dysregulation of this delicate system can have devastating outcomes (Liesa et al., 2009). As such mitochondrial fission, fusion, and mitophagy are tightly regulated, and have a major role in regulating apoptosis (Suen et al., 2008). HCV infection is well known to cause membrane restructuring, principally during the formation of the membranous web, and the mitochondrial membrane is not exempt from this, showing considerable impairment during infections. Changes observed during HCV infection include altered membrane potential and impaired oxidative phosphorylation (Piccoli et al., 2007), both of which lead to an overall shift in cellular metabolic activity towards glycolysis. This damage should induce cell death, however HCV has been shown to modulate mitochondrial dynamics to block apoptosis and to promote virus replication (Kim et al., 2014, Siu et al., 2016, Kim et al., 2013). NS5A, alongside the Core protein, has been shown to promote mitochondrial fission and breakdown, thereby attenuating the pro-apoptotic signal caused by infection.

DNA damage is also a major pro-apoptotic pathway. In response to DNA damage activated p53 binds to DNA and induces the expression of proteins involved in cell cycle arrest, DNA repair, and apoptosis. NS5A has been shown to bind p53 and sequester this is in the cytoplasm, limiting the expression of downstream factors (Majumder et al., 2001), and potentially inhibiting the induction of apoptosis (Lan et al., 2002).

Extrinsic apoptosis is regulated by death receptors, cell surface receptors that induce apoptosis in response to the binding of extracellular ligands. These death receptors have a cytoplasmic death domain which activates a signal cascade to induce apoptosis. The two most well understood death receptors are the TNFR-I receptor, that recognises Tumour Necrosis Factor α, and Fas, which binds the FasL. In both systems binding of the ligand to the death receptor causes trimerisation of the receptor, causing clustering of the cytoplasmic death domains, allowing the recruitment of one of the two adaptor protein, either TRADD or FADD. In the Fas pathway a death effector domain in the FADD protein then activates pro-caspase 8, causing a pro-apoptotic cascade. The TNFα pathway has two potential outcome. If TRADD is recruited alone it will recruit a serine/threonine kinase, RIP, and an adaptor, TRAF-2, which will activate a signalling cascade, generating and antiviral response. Alternatively TRADD can recruit FADD and trigger apoptosis through pro-caspase 8. NS5A has been found to bind to TRADD and inhibit TNF-α induced signalling, blocking both the induction of apoptosis (Majumder et al., 2002, Ghosh et al., 2000) and the expression of antiviral effectors (Park et al., 2003, Park et al., 2002). This activity is specific to TRADD however, as NS5A is not capable of inhibiting FasL induced apoptosis (Majumder et al., 2002).

1.10 PROTEIN DEGRADATION

One of the key methods the cells utilise to combat invasive pathogens is to break down pathogen derived protein. This relies on the systems already in place to degrade cellular proteins.

Eukaryotic cells have a variety of mechanisms to allow them to breakdown protein, both endogenous, and exogenous. Of these the two best characterised are the lysosome and the proteasome, and these will be discussed in detail below.

1.10.1 THE PROTEASOME

Proteasomes are large protein complexes that are responsible for the breakdown of the majority of cytosolic proteins. The 20S proteasome is made up of 4 stacked heptameric protein rings, consisting of structural α-subunits and hydrolytic β-subunits. The 2 outer most rings are predominately made of α-subunits, and act as a scaffold for regulatory factors. The N-termini of these residues form a 13Å gate that regulates entry into the catalytic chamber; only unfolded proteins are allowed access to the catalytic inner rings. The two central rings each contain seven β-subunits, forming the catalytic core. This core is relatively large, 53Å, and has no intrinsic regulatory activity; any protein present will be degraded. 3 distinct protease activities are present in the proteasome, trypsin-like, chymotrypsin-like, and peptidylglutamyl-peptide hydrolysing. Hydrolysis of proteins by the proteasome yields short peptide fragments, approximately 20 amino acids in length, that are able to exit the catalytic chamber. Once in the cytoplasm these are rapidly degraded by resident proteases, converting them back into individual amino acid residues to be reused.

While the 20S proteasome can exist alone it has no ability to cause unfolding of target proteins, and so is predominately involved in the break-down of proteins with little or no complex structure. Higher order proteins are targeted instead to the 26S proteasome, a complex of a 20S proteasome and a 19S regulatory subunit. The 19S subunit can be divided into 2 subdomains, a 9 subunit ring that mediates association with the 20S complex, and a 10 subunit lid domain. 6 of the 9 subunits of the ring structure are ATPases, which drive the unfolding of target proteins. These ATPases associate with the 20S complex via coils at their C-termini, while coils at the N-termini allows dimerization, ultimately forming a ring of 3 dimers aligned to the lumen of the 20S complex. This interaction requires the binding, but not the hydrolysis, of ATP by the ATPases. Binding of these ATPase subunits causes conformational changes in the 20S enlarging the lumen.

The activity of the 26S proteasome is tightly controlled, such that only proteins carrying appropriate degradation signals are broken down. This is the role of the lid domain of the 19S particle. Canonically control is mediated by modification of a lysine residue of the targeted protein, specifically by addition of Ubiquitin, a 76 amino acid peptide. The covalent binding of ubiquitin to the target protein involves 3 enzymes, a ubiquitin activating enzyme (E1), and ubiquitin-conjugating enzyme (E2), and a ubiquitin ligase (E3). E1 enzymes recruit ubiquitin in an ATP dependent manner, and then transfer this to E2s. E3 ligases then catalyse the transfer of the bound ubiquitin to the NH_2 side chain of a lysine residue of the target protein. The specificity for this process is determined by the E3 ligases, a highly diverse protein family. Targeting of a protein to the proteasome requires polyubiquitination, the presence of at least 4 bound ubiquitin residues. Ubiquitin itself contains seven lysine residues that can be targeted by E3 ligases, allowing the formation of a diverse array of ubiquitin chains on the target protein. Due to the highly complex nature of ubiquitination, impacted by the diversity of enzymes involved and linkages that can be made, polyubiquitination can play a variety of roles. The main polyubiquitin chain associated with protein degradation involves the linkage of subsequent ubiquitin molecules to Lys48, and this will be discussed further.

Upon polyubiquitination target proteins are trafficked to the proteasome to be degraded. The precise method by which this achieved is yet to be elucidated but is known to involve Ubiquitin receptors. These have both a Ubiquitin associating domain, to bind the target protein, and a ubiquitin like domain, that mediates recruitment to the 19S subunit of the 26S proteasome. Upon being trafficked to the proteasome, the polyubiquitinated protein is bound by a ubiquitin receptor of the 19S subunit in an ATP-dependent manner. Target proteins are then unfolded by the activity of the 19S ATPases, while ubiquitin is cleaved by the activity of a deubiquitinase located within the lumen of the 6 ATPases. The order in which these processes occur is unclear, however both must occur before the protein can be translocated into the catalytic core.

The proteasome has an important role in defence against viruses; involved in both the detection, and attack of viral infections. An essential part in detecting infected cells is the presentation of viral epitopes in the context of Major Histocompatibility Complex (MHC) class I. After translation MHC molecules are retained in the ER, in association with a Transporter Associated with Antigen Processing (TAP) (Suh et al., 1994). Peptide fragments released by the proteasome are transported into the ER by the TAP translocon, where they associate with empty MHC class I complexes. Loading of an appropriate peptide fragment stabilizes the MHC complex, and this is then transported to the cell surface, through the Golgi apparatus. CD8+ Cytotoxic T lymphocytes continually scan peptides presented on the cell surface. If these

detect antigenic peptide they trigger apoptosis in the infected cell in an attempt to limit pathogen spread.

1.10.2 THE LYSOSOME

Lysosomes are spherical organelles within the cell cytoplasm that contain a diverse range of approximately 50 hydrolytic enzymes, involved in the breakdown of both intracellular and extracellular debris. The pH of the lysosome is roughly 4.5, with the acidity both contributing to the breakdown of waste and promoting the activity of lysosomal enzymes, all of which show optimal activity at lower pH. The acidic pH is maintained by chloride ion channels and proton pumps, which continually transport H^+ ions from the cytoplasm into the lysosome.

Lysosomal enzymes are co-translationally translocated into the lumen of the rough-ER, where they undergo modification and maturation. Each is given a mannose-6-phosphate tag, which marks the protein for passage to the lysosome. These pass into the Golgi, bind mannose-6-phosphate receptors, and are packaged into vesicles that are then transported to, and fuse with, late endosomes. The relatively low pH of the late endosomes, roughly 5.5, causes the lysosomal proteins to dissociate from the receptors, which are then recycled. The receipt of a full complement of hydrolases allows late endosome to mature into lysosomes. In this way the formation of lysosomes can be considered to intersect with endocytosis.

Lysosomes are predominately associated with 3 cellular processes: endocytosis, the uptake and breakdown or extracellular material; phagocytosis, the uptake and breakdown of large extracellular material e.g. bacteria and viruses; and autophagy, the engulfment and breakdown of cellular derived material. In each of the three processes the material to be degraded is surrounded by a cellular derived membrane, which then fuses with a lysosome ultimately resulting in the degradation of the enclosed material. The most relevant to this work is autophagy, which itself can be split into 4 types: macroautophagy, which is the pathway used to breakdown organelles or proteins; microautophagy, which is used to breakdown small cytoplasmic material; mitophagy, which is the breakdown of mitochondria; and chaperone-mediated autophagy, an extremely selective form of autophagy in which proteins carrying a specific sequence are transported to the lysosome by heat shock protein 70. The machinery of autophagy has been found to be capable of being highly specific, identifying tagged substrates to be degraded and targeting them to lysosome (Kraft et al., 2010). In this way autophagy functions to recycle cytoplasmic material.

As with the proteasome, lysosomes play an important role in protecting cells during viral infection; principally by intercepting pathogenic material that enters the cell by endocytosis.

Lysosomes fuse with virus carrying endosomes, exposing the virus to the potent hydrolases within. Lysosomes are also essential to apoptosis, allowing controlled death of the host cell to limit viral spread.

1.10.3 VIRUSES AND PROTEIN DEGRADATION

It is well known the protein degradation pathways play key roles in protecting cells during viral infection, be it the increased turnover of protein during the IFN response, or the generation of antigenic peptides to be displayed by MHC. It is also clear that viruses have evolved myriad mechanisms to interfere with these processes, either blocking then or co-opting them for their own benefit. One example of this is the Influenza A neuraminidase that has been shown to induce rupture of lysosomes (Ju et al., 2015), an activity essential for the virus life cycle and cell death. Additionally Influenza A has been shown to inhibit autophagy, allowing it to control the death of the host cell and optimise conditions for viral replication (Gannage et al., 2009).

Another example of a virus that inhibits cellular protein degradation is in the Epstein-Barr virus (EVB). The viral nuclear antigen 1 protein is the sole protein required to replicate the viral genome during latent infections, and as such is an important marker in the detection of infected cells. This protein however contains a long and repetitive sequence composed only of alanine and glycine residues, a factor that has previously been shown to inhibit protein unfolding and progression into the catalytic core of the proteasome (Hoyt et al., 2006). In this way EVB can inhibit the degradation of the nuclear antigen 1 protein (Zhang and Coffino, 2004, Levitskaya et al., 1997), limiting the peptide fragments available to be presented by MHC, and thereby delay detection of virally infected cells.

Of course viruses can also protect cellular proteins from degradation. NS5A for example has been shown to inhibit the degradation of the epidermal growth factor receptor 2 (Igloi et al., 2015). This protein is thought to be important for viral entry (Diao et al., 2012, Lupberger et al., 2011) and HCV replication during the IFN response (Lupberger et al., 2013), and therefore protection of it by the virus would support both re-infection and IFN resistance.

The above examples all demonstrate viruses' abilities to protect proteins from degradation, but the reverse is also possible; many viruses have evolved to target cellular proteins for degradation. NS5A itself for example has been shown to bind to the Nucleosome Assembly Protein (NAP1L1), a chaperone protein involved in chromatin remodelling during transcription, and targeting it for proteasome-mediated degradation (Cevik et al., 2017). This

impairs a variety of signalling pathways necessary for an effective antiviral response, and HCV can therefore co-opt the proteasome into inhibiting the immune response.

Together these examples show the myriad interactions between viruses and the protein degradation machinery. This work focuses on the possible ability of NS5A to block targeted degradation. A similar activity has been demonstrated in Turnip yellow mosaic virus. The RNA dependent RNA polymerase of this virus was found to be susceptible to polyubiquitination and decay, causing a reduction in viral infectivity (Camborde et al., 2010). The virus was later found to produce a protein capable of countering this activity, causing deubiquitination of the viral protein and promoting infectivity (Chenon et al., 2012). It is possible that NS5A performs a similar function during HCV infections, however as yet this remains unclear.

1.11 HYPOTHESIS

Preliminary work has identified a novel activity within domain III of NS5A that was capable of protecting the protein from artificially-mediated targeted degradation. The hypothesis of this thesis is that the NS5A protein of HCV also counteracts a biologically relevant degradation process, promoting both the stability of itself and other viral proteins from targeted degradation.

1.12 AIMS

To identify the region of NS5A required to allow the protein to persist in the face of a destabilizing event.

To characterise the protective nature of NS5A; identifying which degradation pathways are affected and what cellular factors may be involved.

To determine the physiological benefit of this activity during the viral life cycle; specifically how NS5A's protective potential may impact on the interaction between HCV and the host immune response.

2 MATERIALS AND METHODS

2.1 WATER

Deionised water (dH_2O) was used for most solutions including those for gel electrophoresis and SDS-PAGE. Ultra High Quality water (UHQ) was used in nucleic acid solutions, and all solutions involved in the manipulation of RNA.

2.2 CHEMICALS AND REAGENTS

Unless stated otherwise all plastic and reagents were purchased from Thermo Fisher Scientific. Enzymes were purchased from either New England Biolabs of Thermo Fisher Scientific.

Reagent	Supplier
100X Non-essential Amino Acids	Gibco
100X PenStrep (5000units/ml penicillin, 5mg/ml streptomycin)	Gibco
30% Acrylamide Solution	Thermo Fisher Scientific
30% Formaldehyde Solution	Thermo Fisher Scientific
30% Hydrogen Peroxide	Thermo Fisher Scientific
5X Passive Lysis Buffer	Biotium
Acetic Acid	Thermo Fisher Scientific
Acetylene-PEG4-Biotin	Jena Bioscience
Agarose	Thermo Fisher Scientific
Ammonium Persulfate (APS)	Sigma Aldrich
Ampicillin sodium salt	Sigma Aldrich
ATP	Sigma Aldrich
Bovine serum albumin	Sigma Aldrich
Bromophenol blue	Sigma Aldrich
Calcium chlorate	Sigma Aldrich
Calf Intestinal Alkaline Phosphatase (CIAP)	Fermentas
Chloroform	Thermo Fisher Scientific
Co-Enzyme A	Sigma Aldrich
cOmplete Protease Inhibitor	Sigmal Aldrich
Coomasie blue	Sigma Aldrich
Copper sulphate	Sigma Aldrich
Coumaric acid	Sigma Aldrich
Diethyl pyrocarbonate (DEPC)	Sigma Aldrich
Dimethyl Sulfoxide	Thermo Fisher Scientific
DNase 1	New England Biolabs
DNTPs (Deoxynucleotides triphosphates)	Thermo Fisher Scientific
Dulbecco's Modified Eagle Medium (DMEM)	Gibco
Dulbecco's Phosphate Buffered Saline	Gibco

Ethanol, absolute	Thermo Fisher Scientific
Ethidium bromide	Sigma Aldrich
Ethylenediaminetetraacetic acid (EDTA)	Sigma Aldrich
Film	
Formaldehyde	Thermo Fisher Scientific
Formanide	Sigma Aldrich
G418	Melford Laboratories Ltd
GeneRuler 1 kb DNA Ladder	Thermo Fisher Scientific
Glo Lysis Buffer	Biotium
Glycerol	Thermo Fisher Scientific
Glycine	Sigma Aldrich
Heat Inactivated FBS	Gibco
HEPES	Sigma Aldrich
HEPES (Tissue culture	Gibco
HyClone Trypsin 0.25% (1x)	GE Healthcare Life Sciences
Hydrochloric acid (HCl)	Thermo Fisher Scientific
Hydrogen peroxide	Sigma Aldrich
Kanamycin sulphate salt	Sigma Aldrich
L-Azidohomoalanine	Jena Bioscience
L-Cysteine	Sigma Aldrich
Luciferin	Sigma Aldrich
Luminol	Sigma Aldrich
Magnesium chlorate	Sigma Aldrich
Methanol	Thermo Fisher Scientific
Minimum Essential Medium Non-Essential Amino Acids	Gibco
MOPS	Sigma Aldrich
NP-40 (Nonidet-P40)	Thermo Fisher Scientific
Opti-MEM	Thermo Fisher Scientific
Phenol:Chloroform:Isoamyl Alcohol (25:24:1)	Thermo Fisher Scientific
Polyethylenimine (PEI)	Sigma Aldrich
Potassium acetate	Sigma Aldrich
Potassium hydroxide	Sigma Aldrich
Rely+On Virkon	DuPont
RiboLock RNase Inhibitor	Thermo Fisher Scientific
RNA secure	Thermo Fisher Scientific
RNTPs (Ribonucleotide triphosphates)	Thermo Fisher Scientific
Rubidium chloride	Sigma Aldrich
Sodium acetate 3 hydrate	Sigma Aldrich
Sodium ascorbate	Sigma Aldrich
Sodium chloride (NaCl)	Thermo Fisher Scientific
Sodium deoxycholate	Sigma Aldrich
Sodium hydroxide	Sigma Aldrich
Superfect transfection reagent	Qiagen
SYBR Safe	Invitrogen

SYBR® Safe DNA gel stain	Invitrogen
TEMED (Tetramethylethylenediamine)	Thermo Fisher Scientific
Trimethoprim	Sigma Aldrich
Tris Base	Thermo Fisher Scientific
Tris(3-hydroxypropyltriazolmethyl)amin	Jena Bioscience
Triton X-100	Thermo Fisher Scientific
Tryptone	Thermo Fisher Scientific
Tween 20	Thermo Fisher Scientific
Yeast Extract	Melford Laboratories Ltd
β-Mercaptoethanol	Thermo Fisher Scientific

Table 2-1 **Reagents and manufacturers.**

Enzyme	Supplier
BamHI	New England Biolabs
BglII	Thermo Fisher Scientific
ClaI	Thermo Fisher Scientific
CpoI (RsrII)	Thermo Fisher Scientific
EcoRI	Thermo Fisher Scientific
HindIII	New England Biolabs
Mfe1	Thermo Fisher Scientific
MluI	Thermo Fisher Scientific
Mung Bean Nuclease	New England Biolabs
Phusion - HF	Thermo Fisher Scientific
PmeI	New England Biolabs
PvuI	New England Biolabs
SpeI	Thermo Fisher Scientific
T4 DNA ligase	Thermo Fisher Scientific
T7 DNA polymerase	Thermo Fisher Scientific
Taq DNA polymerase	New England Biolabs
XbaI	Thermo Fisher Scientific
XhoI	Thermo Fisher Scientific

Table 2-2 **Restriction enzymes and manufacturers.**

2.3 PLASTIC WARE

All plastic ware was purchased from Thermo Fisher Scientific, with the exception of 1.5 ml microfuge tubes, which were purchased from Sarstedt.

2.4 PLASMIDS USED IN THIS STUDY

G418 resistant pSGRJFH1 replicon constructs were kindly donated by Takaji Wakita (Date et al., 2004), while pSGRJFH1luc replicon constructs were originally donated by John McLauchlan (Targett-Adams and McLauchlan, 2005). These replicons express a HCV sub-

genomic replicon based upon the Japanese Fulminate Hepatitis (JFH1) isolate. All pFK5.1 based constructs were generated from ones previously generated in the group but which originate as a gift from Ralf Bartenschlager (Herod et al., 2012). These plasmids express a sub-genomic replicon derived from the Con1 isolate of HCV. pCDNA3.1 (Invitrogen) and pSuper (Oligoengine) are commercial vectors. pLVTHM, psPAX2, and pMD2.G, originally generated by the Trono Lab (Naldini et al., 1996), were purchased through Addgene.

2.5 BACTERIAL CULTURE

2.5.1 LURIA BERTANI (LB) MEDIUM

Escherichia coli (E. coli) were gown in Luria Bertami (LB) media prepared by dissolving 10 g/l Trypton, 5 g/l Yeast Extract and 5 g/l Sodium Chloride in distilled water. This was autoclaved for 15 minutes at 121°C and stored at room temperature. An appropriate antibiotic was added immediately prior to use.

2.5.2 LB-GLYCEROL STOCKS

For long term storage glycerol stocks of bacteria were produced by adding 500 µl of 30% (v/v) Glycerol to 500 µl of overnight culture, to a final concentration of 15% glycerol (v/v). Glycerol stocks were then stored at -70°C.

2.5.3 LB AGAR

LB Agar plates were used to isolate single *E. coli* colonies. To produce these 15 g/l Agar was added to LB media and autoclaved. The agar was cooled to 40°C and appropriate antibiotic added. The cooled agar was then poured into plastic Petri dishes. The plates were transferred to a laminar flow hood to solidify and dry. Plates were stored upside down at 4°C until needed.

2.5.4 AMPICILLIN

Ampicillin (Sodium salt) was dissolved in dH_2O at 50 mg/ml and filter sterilized using a 0.2 micron filter. Aliquots were then stored at -20°C. The working concentration was 100 µg/ml.

2.5.5 KANAMYCIN

Kanamycin (Sulphate salt) was dissolved in dH_2O at 10 mg/ml and filter sterilized using a 0.2 micron filter. Aliquots were then stored at -20°C. The working concentration was 50 µg/ml.

2.6 ESCHERICHIA COLI (E. COLI)

Escherichia coli (E. coli) used in this study are listed below, alongside their genetic background(Table 2-3).

Strain	Genetic Markers
DH5α	F-, endA1, glnV44, thi-1, recA1, relA1, gyrA96, deoR, nupG, ϕ80d*lacZ*ΔM15,Δ(*lacZY* A-ArgF)U169, hsdR17(rK- mK+), λ-
STBL 2	F-, endA1, glnV44, thi-1, recA1, gyrA96, relA1 Δ(lac-proAB), mcrA, Δ(mcrBC-hsdRMS-mrr), λ-

Table 2-3 **Strains of *E. coli* used in this work and their genetic background**.

2.7 GROWTH OF E. COLI

Liquid cultures of both STBL2 and DH5α strains of *E. coli* were typically grown in LB media, supplemented with appropriate antibiotic, at 37°C, shaking at 200 rpm, for 18 hours. However, cells transformed with either pSGR JFH1 or pFK5.1 plasmids, were instead grown for 24 hours at 30°C to overcome plasmid stability issues.

Single colonies were produced by streaking onto LB-Agar plates supplemented with an appropriate antibiotic. Plates were then incubated at 37°C for 18 hours.

2.8 COMPETENT CELLS

Competent cells were prepared by inoculating 1.2 ml of an overnight culture of naïve *E. coli* into 120 ml of LB media in a 1 l conical flask and growing with agitation at 37°C until it reached an Optical Density (OD) $_{600}$ of 0.38. The culture was incubated on ice for 15 minutes before being centrifuged at 3000 g for 10 minutes at 4°C. Pelleted cells were re-suspended in 40 mls of ice cold Transformation Buffer 1 (Table 2-4) and re-centrifuged at 3000 g for 10 minutes at 4°C. The pellet was then re-suspended in 4 ml Transformation Buffer 2 (Table 2-4) and stored as 100 µl aliquot at -80°C until required.

Buffer	Content
Transformation Buffer 1	30 mM Potassium Acetate, 10 mM Calcium Chlorate, 50 mM Magnesium Chlorate, 100 nM Rubidium Chloride, 15% Glycerol, pH 5.6 using acetic acid
Transformation Buffer 2	10 mM MOPS, 75 mM Calcium Chlorate, 10mM Rubidium Chloride, 15% Glycerol, pH 6.5 using Potassium Hydroxide

Table 2-4 **Buffers used in the generation of competent cells.**

2.9 TRANSFORMATION

To transform competent *E. coli* 2 µl of DNA solution was added to 50 µl of competent cells in a 1.5ml microfuge tube on ice, and incubated for 20 minutes. The transformation was then heat shocked at 42°C for 50 seconds, before being returned to the ice for a further 10 minutes. The transformed bacterial were transferred to 450 µl of LB media and incubated at 37°C for 1 hour to allow recovery. 150 µl of this was then plated on LB Agar supplemented with appropriate antibiotic, and grown as above.

2.10 ISOLATION OF PLASMID DNA

Plasmid DNA was extraction from bacterial culture using a Miniprep kit (Thermo Fisher Scientific) following the manufacturers recommendations. Briefly, bacteria from an overnight culture were pelleted by centrifuging at 5000 g for 15 minutes and re-suspended in 250 µl re-suspension buffer before being transferred to a 1.5 ml microfuge tube. A volume of 250 µl of lysis buffer was added and the solution mixed by gentle inversion, followed by the addition of 350 µl of neutralising buffer and further inversion. The resulting cell debris was pelleted by centrifuging at 16,000 g for 10 minutes. The DNA containing solution was passed through a spin column which was then washed twice with 500 µl of wash buffer; centrifuging at 16,000 g for 2 minutes between each step. Residual ethanol was removed by centrifuging the column a further time before it was transferred to a fresh microfuge tube. Bound DNA was eluted by adding 50 µl elution buffer, and centrifuging at 16,000 g for 2 minutes. DNA concentration

was determined using a Thermo Fisher Scientific Nanodrop 100 Spectrophotometer. DNA was stored at -20°C until used.

2.11 RESTRICTION DIGESTION OF DNA

DNA digestion was performed with between 500 ng and 5 µg of DNA, in reactions ranging from 10-100 µl. Each digestion was performed in a buffer appropriate to the restriction enzyme used, such that a minimum of 50% enzyme activity was maintained. A 2:1 ratio of enzyme (units of activity) to DNA (µg) was used during overnight digestions, while a 3:1 ratio was used for digestions between 1-4 hours.

2.12 DNA LIGATION

All DNA ligation was performed in 10 µl reactions using 1 x T4 Ligase Buffer. In a typical 10 µl reaction, 5-10 femtomoles of vector DNA was combined with a 5-fold excess of insert, 1 µl of 10 x T4 Ligase Buffer, and 10 units T4 DNA. This was then incubated at room temperature overnight.

2.13 PHENOL CHLOROFORM EXTRACTION

Phenol Chloroform was used to remove protein from DNA samples. An equal volume of Phenol Chloroform was added to the DNA, and the two phases mixed by vortex, before being centrifuged at 16,000 g for 10 minutes. The upper aqueous phase, containing the DNA, was carefully transferred to a clean microfuge tube, where an equal volume of chloroform was added; once again being mixed thoroughly by vortex. The tube was then centrifuged at 13,000 g for 10 minutes. The DNA containing aqueous phase was extracted and transferred to a fresh microfuge tube.

2.14 ETHANOL PRECIPITATION

To purify DNA, 1/10th volume of 3M Sodium acetate and 2 volumes of 100% ethanol was added to the DNA sample. This was vortexed to mix thoroughly and incubated at -70°C for 30 minutes before the DNA was pelleted by centrifugation at 16,000 g for 30 minutes. The supernatant was extracted and the pellet washed in 50 µl of 70% ethanol. The pellet was then dried and re-suspended in UHQ.

2.15 POLYMERASE CHAIN REACTION

Amplification of DNA by Polymerase Chain Reaction (PCR) was achieved using Phusion polymerase (Thermo Fischer Scientific). All PCR reactions, unless stated otherwise, contained 1-5 ng of each template, 1 x Phusion High Fidelity Buffer, 0.5 Units Phusion Enzyme, 0.5 µM primers, and 0.8 mM dNTPs, in a 50 µl reaction. Each step of the reaction was performed at specific temperatures as described in Table 2-5. Prior to heating PCR mixtures were stored on ice and the thermocycler pre-heated to 98°C. Initial denaturation of the template DNA was achieved by heating to 98°C for 2 minutes. At the start of each cycle this was repeated for 15 seconds to once again denature the template. To allow annealing of the primers to the template the temperature was lowered to 54°C for 30 seconds. The elongation temperature for all reactions was 72°C, although the length of this step varied depending on the length of template to be replicated, typically 1 minute per kb. Typically 20 cycles of denaturation, annealing, and elongation were performed followed by a final 10 minute elongation at 72°C.

Step	Temperature / °C	Time / seconds
Initial Melting	98	120
Template Denaturation	98	15
Primer Annealing	54	30
Primer Elongation	72	60 per kb
Final Elongation	72	600

Table 2-5 **Standard conditions used for PCR using Phusion HF.**

2.16 GEL ELECTROPHORESIS

Gel electrophoresis was used to separate DNA fragments, determine purity, and assess recovery of DNA. Agarose was added to 1 x Tris-Acetate EDTA buffer (TAE) (Table 2-6) typically to a concentration of 0.7% (w/v), and heated to boiling point in a microwave. This was cooled to approximately 50°C before 0.5 x SYBR Safe (Invitrogen) was added. The agarose was then poured into a gel casting tray, prepared with an appropriate comb, and allowed to cool and solidify. Once solidified, the gel was overlaid with TAE buffer (Table 2-6) and the comb removed. Samples to be run were mixed with 1 x Loading Buffer (Table 2-6) and loaded into the wells alongside Generuler 1 kb ladder (Fisher). A potential difference of 40 V was applied across the gel until the loading buffer had migrated approximately two thirds of the way down the gel. The gel was then visualised using a BioDoc-IT™ 2UV Transilluminator (UVP), set at a wavelength of 302 nm.

Buffer	Content
50 X TAE	242 g/l Tris-base, 18.6 g/l Ethylenediaminetetraacetic acid, 5.7% Acetic Acid
6 X Agarose Gel Loading Buffer (diluted in UHQ)	305 mM Glycerol, 25 mM Ethylenediaminetetraacetic acid, 0.01% bromophenol blue

Table 2-6 **Buffers used in DNA gel electrophoresis.**

2.17 PURIFICATION OF DNA FROM AGAROSE

DNA was retrieved from agarose gels using a Thermo Fisher Scientific GeneJet Gel Extraction Kit (Thermo Fisher Scientific). If DNA was to be extracted from the gel, it was run for no more than 1.5 hours, and a blue light filter was used during visualisation to prevent Ultra Violet induced mutation. The desired DNA bands, made visible by the use of a Dark Reader™ (Clare Chemical Research), were excised from the gel using a scalpel, and transferred to a 1.5 ml microfuge tube. The excised agarose slice was weighed and a volume of DNA binding buffer equal to the mass of the agarose was added (100 µl of DNA binding buffer was added to a 100 µg slice of agarose). To melt the agarose fragment, it was heated to 65°C for 10 minutes. Once melted the agarose and binding buffer were transferred to a spin column, bound, and washed with 700 µl of wash buffer, centrifuging at 16,000 g for 2 minutes after each step. Residual ethanol was removed by centrifuging the column dry for 2 minutes. The spin column was transferred to a fresh microfuge tube and the DNA eluted into 25 µl of elution buffer.

In cases low of DNA yield, an alternative method was utilised to purify DNA from agarose using phenol. As above DNA to be extracted was excised from the gel and transferred to a 1.5 ml microfuge tube. This was then frozen at -70°C for a minimum of 10 minutes. The gel slice was macerated using a clean pestle, and frozen once more. The maceration process was repeated until a fine slurry was produced. This was weighed and an equal volume of phenol solution added. The microfuge tube was vortexed to mix and centrifuged at 13,000 g for 10 minutes. The aqueous layer, containing the DNA, was then transferred to a fresh microfuge tube and an equal volume of chloroform added. This was once again vortex and centrifuged at 13,000 g for 10 minutes. The purified DNA, located in the top aqueous was extracted and purified by ethanol precipitation. Typically the DNA was eluted into 20 µl DNAse free water.

2.18 T7 TRANSCRIPTION REACTIONS

To generate an excess of template DNA 5 µg of plasmid was linearized using an appropriate restriction digestion and any overhangs left by digestion were removed using mung bean nuclease (New England Biolabs). Linear DNA was then purified by Phenol Chloroform extraction and ethanol precipitation, and eluted into 20 µl UHQ. To confirm recovery and

purity of the DNA 1 µl of this was analysed by gel electrophoresis. RNA was produced in a 50 µl reaction using a T7 polymerase (Thermo Fisher Scientific) in 1 x T7 Polymerase Buffer (Thermo Fisher Scientific). The remaining 19 µl of DNA recovered from the ethanol precipitation, 10 µl 5 x T7 Polymerase Buffer, 2 µl RNA Secure and 11.75 µl DEPC H_2O were heated to 60°C for 10 minutes before 40 units of T7 polymerase, 50 units RiboLock RNase inhibitor (Thermo Fisher Scientific) and 8mM rNTPs were added, and the reaction incubated at 28°C for between 10 and 24 hours (overnight). To degrade the remaining DNA, 2 µl (4 units) of DNAse I (New England Biolabs) was added, and the reaction incubated at 37°C for 30mins.

2.19 RNA CLEAN UP

After the transcription reaction, RNA was purified using an RNA Clean & Concentrator Kit (Zymo Research) by following the general procedure provided by the manufacturer. 104 µl of buffer was added to each 52 µl transcription reaction, and pipetted up and down to mix, followed by 156 µl 100% ethanol. The sample was transferred to a Zymo-Spin™ column and centrifuged at 16,000 g for 2 minutes, and 400 µl RNA prep buffer was passed through the column. The bound RNA was then washed in, first 700 µl, then 400 µl, RNA wash buffer, centrifuging between each step. The RNA was eluted into 2 x 30 µl RNAse free UHQ, transferred to a clean RNAse free screw cap tube, and stored at -70°C.

The concentration of the recovered RNA was determined using a Thermo Fisher Scientific Nanodrop 1000 Spectrophotometer.

2.20 RNA GEL ELECTROPHORESIS

To determine the quality of RNA recovered after a transcription reaction it was run on a 3-morpholinopropane-1-sulfonic acid (MOPS) formaldehyde gel. 0.32 g of agarose was added to 3.5ml 10 x MOPS buffer (Table 2-7) and 29.5 ml DEPC treated water, and heated in a microwave to melt the agarose. This was transferred to a fume hood and cooled to roughly 50 °C before 2 ml of formaldehyde was added into the solution mix. The resulting MOPS-formaldehyde gel was poured into a gel casting unit prepared with a comb, and allowed to set in the fume hood. Once the gel had set it was overlaid with 1 x MOPS buffer. 2.5 µl of each sample to be run was added to 7.5 µl RNA loading buffer (Table 2-7) and heated to 85°C for 5 minutes, before being loaded into the gel. A potential difference of 40V was applied across the gel for a period of 2 hours. The results were visualized using a BioDoc-IT™ 2UV Transilluminator (UVP), set at a wavelength of 302nm.

Buffer	Content
10 X MOPS Buffer	5.86 g/l EDTA, 41.8 g/l MOPS, 6.8 g Sodium acetate 3 hydrate, pH 7.0 using Sodium Hydroxide
MOPS-formaldehyde Loading Buffer	240 µl Formamide, 50 µl 10 X MOPS Buffer, 87 µl Formaldehyde, 15 µl 0.1% Bromophenol blue, 25 µl glycerol, 1 µl 5 mg/ml Ethidium Bromide

Table 2-7 **Buffers used in RNA gel electrophoresis.**

2.21 EXTRACTION OF PROTEIN FROM ADHERENT EUKARYOTIC CELLS

To extract protein, cells were washed with sterile PBS and trypsinised. The cells were transferred to a 1.5 ml microfuge tube and pelleted by centrifuge at 2500 g at 4°C for 5 minutes. The cell pellet was washed in ice cold PBS and the cells re-suspended in 50-100 µl of RIPA buffer (Table 2-8) supplemented with 2 x Complete Protease Inhibitor. To pellet the nuclei and cell debris the lysates were centrifuged at 16,000 g at room temperature for 1 minute. The supernatant containing the cytoplasmic protein was collected and stored at -20°C.

Buffer	Content
RIPA Buffer	25 mM Tris Base pH8, 150 mM Sodium Chloride. 0.1% SDS, 1 % Sodium deoxycholate, 1% NP40,

Table 2-8 **Composition of RIPA buffer.**

2.22 BCA ASSAY

A Bicinchoninic Assay (BCA) was performed using a kit from Pierce (Pierce) to determine to concentration of protein within cell lysates. A 2 µl sample from each lysate was mixed with 8 µl of sterile PBS in one well of a 96 well plate, alongside known albumin standards ranging from 5 µg/ml to 0.25 µg/ml. 100 µl of a 50:1 mixture of BCA Reagent A and BCA Reagent B was added to each well, and the plate rocked for 30 seconds to mix. The plate was then incubated at 37°C for 30 minutes, before being read at 570 nm using a BIO-RAD iMark™ Microplate Reader. The absorption readings of the albumin samples were used to generate a standard curve and the absorption of the protein samples compared to this to determine concentration.

2.23 SDS PAGE

Protein was separated based on size by (Sodium dodecyl sulphate Polyacrylamide gel electrophoresis (SDS-PAGE), using a 10% separating gel and 3% stacking gel. The separating layer was produced first (Table 2-9), poured, overlaid with 0.1% SDS, and allowed to polymerize. Once the separating layer had polymerized, the 0.1% SDS was removed and the stacking layer (Table 2-9) poured on top. Wells were produced by inserting a 15 µl well comb into the still liquid stacking layer and allowing it to polymerize. Once both gels had polymerized the gel unit was inserted into an SDS-PAGE tank, and both the top and bottom reservoirs filled with running buffer (Table 2-9). Equal amounts of protein, alongside 5 µl PageRuler Prestained Protein Ladder (Fermentas), were boiled in 1 x SDS Page Loading Buffer (Table 2-9) and loaded onto the gel. A potential difference of 180 V was applied across the gels until the bromophenol blue dye had reached the end of the gel.

Buffer	Content
4 X Stacking Gel Buffer	0.5 M Tris Base, 0.46 M Hydrogen Chloride, pH 6.8
4 X Separating Gel Buffer	1.5 M Tris Base, 0.25 M Hydrogen Chloride, pH 8.8
1 X Stacking Gel (5ml)	3.2 ml dH2O, 1.25 ml 4 X Stacking Gel Buffer, 50 µl 10% SDS, 0.5 ml 30% acrylamide, 25 µl APS, 5 µl TEMED
1 X Separating Gel (5ml)	2.03 ml dH2O, 1.25 ml 4 X Separating Gel Buffer, 50 µl 10% SDS, 1.65 ml 30% acrylamide, 25 µl APS, 5 µl TEMED
2X SDS Page Loading Buffer	250 µl dH2O, 250 µl 4 X Stacking Gel Buffer, 200 µl 10 % SDS, 200 µl Glycerol, 100 µl β-mercaptoethanol, 50 µl 0.1% Bromophenol blue
Running Buffer	3 g/l Tris Base, 14.4 g/l Glycine, 0.1% SDS

Table 2-9 **Buffers used in SDS Page.**

2.24 WESTERN BLOTTING

For immunoblotting, protein was transferred from an SDS-PAGE gel onto Polyvinylidene Fluoride (PVDF) membranes, using a Thermo Scientific Owl HEP-1 Semi-dry transfer unit. A membrane of appropriate size was briefly wet in 100% Methanol, and then incubated for 2 minutes in Transfer buffer (Table 2-10). Meanwhile, the polyacrylamide gel was removed from the SDS-PAGE apparatus and the stacking layer removed, and incubated in Transfer buffer for 2 minutes. 2 sheets of extra thick blotting paper (Biorad) were pre-wetted with Transfer buffer. The membrane was placed on one sheet of blotting paper, and the gel place on top of this, with the second piece of blotting paper over this. Air bubbles were removed by gently compressing using a 10 ml pipette. The transfer was then arranged into the transfer unit with the membrane positioned toward the anode, with relation to the gel, and the anode plate was secured. A potential difference of 15 V was then applied to the transfer unit for between 45-90 minutes.

Post transfer the PVDF membrane was incubated in Tris Buffered Saline (TBS) (Table 2-10) supplemented with 0.1% (v/v) Tween 20 (TBS-T) for 2 minutes. To block non-specific binding, the membrane was then incubated, rocking, for 1 hour, in TBS-T supplemented with 10% (w/v) powdered milk. The membrane was then washed 4 x 5 minutes in TBS-T, and sealed within a plastic bag containing 2 ml TBS-T + 5% (w/v) milk powder and appropriate primary antibody (Table 2-11). This was incubated rocking at room temperature for 1 hour, or at 4°C overnight. The membrane was once again washed for 4 x 5 minutes in TBS-T, and then incubated in TBS-T + 5% milk powder and an appropriate secondary antibody conjugated to horseradish peroxidase (HRP) (Table 2-11), rocking for 1 hour at room temperature. The membrane was washed 4 x 5 minutes in TBS-T, and exposed to a 50:50 solution of enhance chemiluminescence 1 and 2 (ECL1 and ECL2), (Table 2-10), for 1 minute. Excess ECL was removed and the membrane sealed in plastic.

To visualize the blot, film was exposed to the membrane in the dark. After an appropriate exposure time the film was developed and fixed.

Buffer	Content
Transfer Buffer	3 g/l Tris Base, 14.4 g/l Glycine, 0.1 % SDS, 15 % Methanol
20 X TBS	24.2 g/l Tris Base, 87.7 g/l Sodium Chloride, pH 7.5
Blocking Buffer	1 x TBS, 0.1% Tween 20, 10% Milk powder
ECL 1	17.7 ml dH_2O, 200 µl 250 mM luminol in DMSO, 88 µl Coumaric Acid in DMSO, 2 ml 1 M Tris HCl (pH 8.5)
ECL 2	18 ml dH_2O, 12 µl 30 % Hydrogen peroxide, 2 ml 1 M Tris HCl (pH 8.5)

Table 2-10 **Buffers used in western blotting.**

Antibody	Supplier	Dilutions
Goat αGFP	Serotec	1/2000
Mouse αGAPDH	Chemicon International	1/2000
Mouse αHA	Biolegend	1/2000
Mouse αMyc	New England Biolabs	1/2000
Mouse αNS3	Biofront	1/1000
Mouse αNS5A	Gift from Dr. Tim Tellinghuissen	1/2000
Rabbit αUSP19	Abcam	1/1000
Rat αFlag	Biolegend	1/1000
Rat αV5-protein	Gift from Prof. Rick Randall	1/1000
Sheep αNS5A	Gift from Prof. Mark Harris	1/5000
Streptavadin HRP	Thermo Fisher Scientific	1/2000
αMouse HRP	Sigma Aldrich	1/2000
αRabbit HRP	Sigma Aldrich	1/2000
αSheep HRP	Sigma Aldrich	1/5000

Table 2-11 **Antibodies, manufacturers, and dilutions used in western blotting**.

2.25 CELL CULTURE

All HCV replicon work was conducted using Huh7.5 and Huh7 cell lines. Huh7 cells are an immortalised endothelial cell line derived from a cellular carcinoma tumour. These cells are widely used for the ability to support HCV replicon infection as first shown by Lohmann *et al* (Lohmann et al., 1999). Huh7.5 cells are derived from Huh7 and demonstrate improved ability to support HCV replicon infection (Blight et al., 2002). This cell line was generated by curing a HCV replicon transfected Huh7 cells by prolonged exposure to IFNα. One such cured cell line was shown to be highly permissive to subsequent replicon transfections, supporting higher levels of RNA replication without the need for additional selection. This improvement is thought to be due to a single point mutation within the Retinoic acid-inducible gene I, which detects dsRNA (Sumpter et al., 2005). Together with the low level of Toll-like receptor

3 expression reported in Huh 7 cells (Li et al., 2005), it has been suggested that this limits the activation of innate antiviral processes thereby promoting replicon replication.

Human embryonic kidney-293 T cells (HEK-293T) are a human kidney cell line that has been transformed to express the large T-antigen. These cells were used when large amounts of protein was required, as they have been shown to support high levels of expression of heterologous protein expression.

B3Z cells are a T-cell hybridoma cell line generated in the Edd James group. These cells are able to detect a mouse albumin peptide SL8 when presented by a mouse Major Histocompatability Complex (MHC) class 1 molecule (H2K). Detection of SL8 activates the expression of a lacZ gene, leading to the expression of β-galactosidase. This can then be detected by the addition of chlorophenolred-ß-D-galactopyranoside (CPRG), and monitoring the colour change at 595 nm.

All cells were grown at 37°C in 5% CO_2. Huh7.5 and Huh7 derived cell lines were grown in Dulbecco's Modified Eagle Medium (DMEM) (Gibco) supplemented with 10% Foetal Bovine Serum (Gibco), 1 x Non-essential Amino acids (Gibco), 50 units/ml penicillin and 50 µg/ml streptomycin (Gibco). HEK293T cells were maintained Dulbecco's Modified Eagle Serum additionally supplemented with 25 mM HEPES.

B3Z cells were maintained in Roswell Park Memorial Institute medium (RPMI) supplemented with 10% Foetal Bovine Serum (Gibco), 1xNon-essential Amino acids (Gibco), 50 U/ml penicillin 50 µg/ml streptomycin (Gibco), 25 mM HEPES, and 100 µM 2-mercaptoethanol.

2.26 TRANSFECTION OF PLASMID DNA INTO EUKARYOTIC CELLS

Polyethylenimine (PEI) was used to introduce plasmid DNA into both Huh7.5 and HEK293T cells. At least 24 hours prior to transfection 4 x 10^5 cells were seeded into 6 well plates. On the day of transfection these were washed with sterile PBS and each well was given 2 mls of media. To sterilize the DNA for transfection it was pasteurized by incubating at 65°C for 20 minutes. For each transfection, 2 µg of plasmid was mixed with an appropriate volume of PEI, and made up to 200 µl in 15 0mM NaCl. In HEK293T cells 3 µl of PEI was used for each 1 µg of DNA while in Huh7.5 cells 3.5 µl of PEI was used for each 1 µg of DNA. The resulting mixture was vortexed and incubated at room temperature for 20 minutes before being added to the cells in the 6 well plates. To prevent toxicity from PEI, 48 hours post transfection the transfected cells were given fresh media.

2.27 ELECTROPORATION

RNA transcripts were introduced into Huh7.5 cells using a Bio-Rad Gene Pulser set at 270 V and 960 µF. Huh7.5 cells were detached from the flask using trypsin, washed twice in ice-cold Diethyl Pyrocarbonate (DEPC)-treated Phosphate Buffered Saline (PBS), and re-suspended in DEPC-PBS at a concentration of 1 x 10^7 cells per ml. 400 µl of this was then added to 2 µg of appropriate RNA, pipetted up and down to mix and transferred to a pre-chilled electroporation cuvette. Cells were electroporated and re-suspended in 6ml of appropriate media.

2.28 REPLICON REPLICATION ASSAYS

Replication assays were carried out to determine the impact of modifications to NS5A on the replication of HCV replicons. Replicon RNA was electroporated into Huh7.5 cells as described above and the re-suspended into multi well plates; either 500 µl of re-suspension into 6-well plates, or 150 µl of re-suspension into 12-well plates. The cells were then incubated under standard conditions. After 4, 24, 48, or 72 hours the cells were washed in PBS and lysed in either Passive Lysis Buffer, or Glo Lysis Buffer (Promega). Cells in a 12-well plate were lysed in 150 µl of buffer, while cells in a 6-well plate were lysed in 300 µl.

Replication was determined by luciferase assay, to detect the activity of the Firefly luciferase marker present in the replicon RNA. 40 µl of lysate was combined with 100 µl of Luciferase Assay Reagent (Table 2-12) and the activity read using a Luminometer. Readings were taken twice and the mean calculated. These were then made relative to the 4 hour reading.

To provide a comparison each replication assay also included a positive replication control (luc), in which no modification had been made, and a negative replication control (lucGND), in which the GDD motif of the viral polymerase, NS5B, is mutated to knock-out function.

Buffer	Content
Luciferase Assay Reagent	530 µM ATP, 470 µM Luciferin, 270 µM Co-Enzyme A
(4 X) Luciferase Assay Buffer	80 mM Tris, 15 mM $MgSO^4$, 0.4 mM EDTA, 133.2 mM DTT. (p H 7.8)

Table 2-12 **Composition of luciferase assay buffer.**

2.29 COLONY FORMATION ASSAY

Colony forming assays were performed to allow both the observation of replicon replication, and the selection of stable replicon containing cells for further work. Replicons carrying a Neomycin Phosphotransferase gene (Neo), were electroporated into Huh7.5 cells as

described above, and a viable cell count performed. 10^3, 10^4, or 10^5 viable cells were then seeded into the wells of a 6 well plate, with each well supplemented with untransfected cells to a final concentration of 2 x 10^5 cells per well. 48 hrs post transfection the media was supplemented with 650 µg/ml G418 to begin selection. This was replaced every 3 days until visible colonies had formed.

In the case of replication assays, colonies were washed in sterile PBS and fixed in 100 µl of 100% methanol incubated at -20°C for 20 minutes. Fixed colonies were then stained with Coomassie blue prior to counting.

To generate stable cell lines colonies were trypsinised and re-suspended in fresh media, and seeded at an appropriate cell density. Transfected cells were selected by inclusion of 650 µg/ml G418 until colonies were formed, after which the colonies were harvested and expanded. These cell lines were maintained under selective pressure by the inclusion of 250 µg/ml G418 in the growth media.

Buffer	Content
Coomassie blue	0.1% Coomassie blue, 30% Methanol, 10% Acetic acid

Table 2-13 **Composition of Coomassie Blue Stain**

2.30 B3Z ASSAY

Antigen presentation was monitored by use of a B3Z assay, developed in house by the James group. SL8 is an 8 amino acid peptide which can be presented by a mouse MHC class I molecule (H2K). A T-cell hybridoma cell line called B3Z, generated in house, is capable of recognising presented SL8 bound to H2K on the cell surface of co-cultured cells. Recognition of SL8 by B3Z cells leads to the expression of the l*acZ* gene, resulting in the generation of β-galactosidase. This can be detected by the addition of chlorophenolred-β-D-galactopyranoside (CPRG) and measuring the colour change at 595 nm.

Huh7.5 cells being tested were plated into 96 wells plates forming a 1/2 dilution series from 10^5 cells per well to 7.812 5x 10^2 cells per well and incubated for 4 hours in 100 µl of appropriate media to allow attachment. Each dilution series was produced twice, and an additional well seeded at 10^5 as a control. Once the Huh7.5 cells had attached, 10^5 B3Z cells were added to each well, apart from the control, and the plates incubated under standard conditions for 12 hours. The plates were then centrifuged at 500 x g and the media aspirated. 100 µl CPRG was added to each well and the plates incubated at room temperature for 24 hours before being analysed using a plate reader to measure light absorption at 595 nm.

2.31 LENTIVIRAL TRANSDUCTION

Stable expression of genes in Huh7.5 cells was achieved using Lentiviral transduction as described by Didier Trono's group (Naldini et al., 1996) (Figure 2-1). Oligonucleotides encoding USP19 targeting shRNAs were cloned into the lentiviral vector (Addgene), which overexpresses the shRNA and GFP in an inducible manner. Expression is regulated by KRAB repression system controlled by tetracycline/doxycycline (Figure 2-2).

2 x 10^6 HEK293T cells were plated onto 10 cm^2 plates and incubated overnight to allow adherence. 5 µg of pLVTHM carrying the desired gene was then transfected into these alongside 3.75 µg psPAX2 (Addgene) and 1.5 µg pMD2.G (Addgene), using Superfect transfection reagent (Qiagen), following manufacturer's instructions. Briefly, the 3 plasmids were combined into a total 300 µl of Opti-MEM (Thermofisher), mixed by vortexing, and 60 µl of Superfect transfection reagent added. DNA:Superfect complexes were mixed gently by pipetting and incubated at room temperature for 20 minutes. The reaction was quenched with 2 ml DMEM+10% (v/v)FBS which was pipetted onto freshly washed HEK293T cells. The HEK293T cells were incubated at 37°C and 5% CO_2 for 3 hours in the transfection media before replacing this with 6ml fresh media. Cells were then incubated for 48 hours under standard conditions.

24 hours after the transfection of the HEK293T cells, 2 x 10^5 Huh7.5 cells were seeded into 3 wells of a 6 well plate, in 3 ml, in preparation for transduction.

48 hours post transfection the media containing the lentiviral particles was removed from the transfected HEK293T cells and replaced with 6 ml fresh media. The media was centrifuged at 2000 g for 15 minutes to pellet any cells or cell debris, and the supernatant containing the lentiviral particles extracted. This was added to the media of the Huh7.5 cells, in a 1/2 dilution; 4.5 mls of lentiviral media was added to the 4.5 ml of media remaining on the Huh7.5 cells. Huh7.5 cells were then centrifuged at 2200 rpm, 37°C for 90 minutes, and incubated under standard conditions. 24 hours later the transduction was repeated.

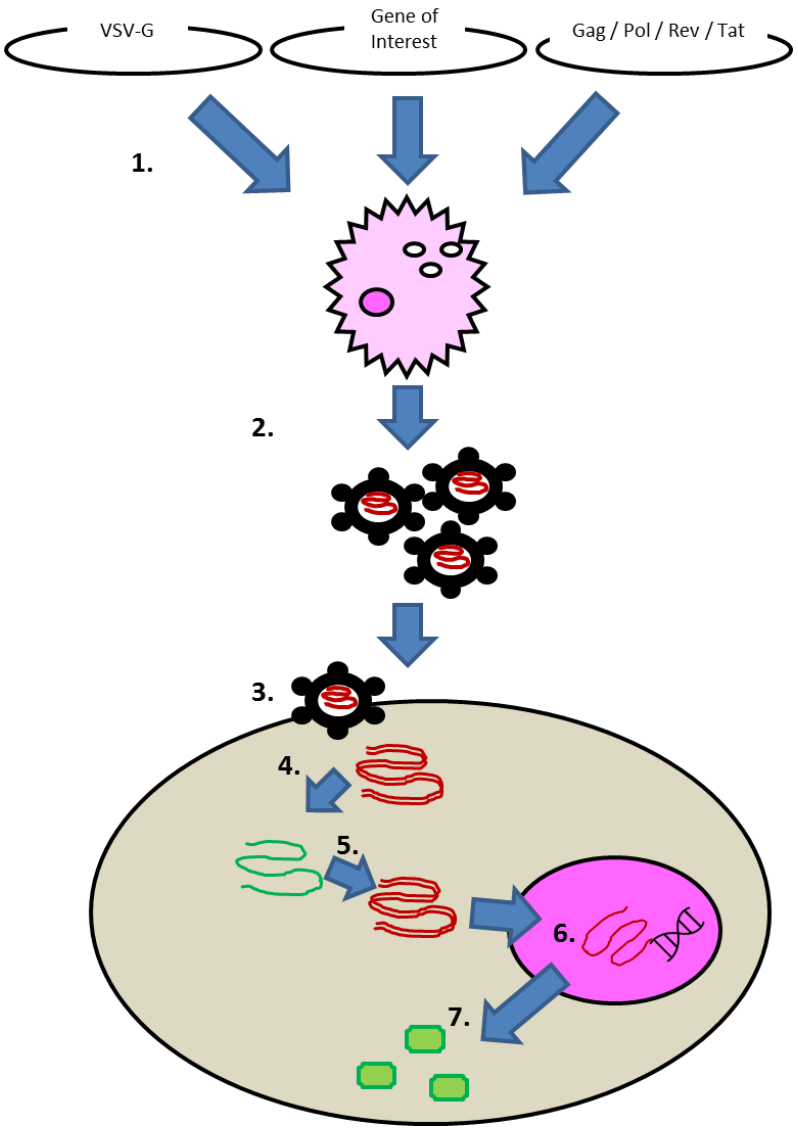

Figure 2-1 **Schematic of the lentiviral transduction protocol.** (1) Transfection of plasmids expressing the Vesicular stomatitis virus envelope protein (VSVG), gene of interest, and the lentiviral packaging and integration genes (Gag, Pol, Rev/ Tat) into HEK293T packaging cells. (2) Formation of lentiviral particles carrying a lentiviral plasmid expressing the gene of interest. (3) Transduction of the Huh7.5 cells with lentiviral particles. (4) Transcription of lentiviral particle DNA, expressing the gene of interest into RNA. (5) Reverse transcription of lentiviral ssRNA into dsDNA. (6) Integration of lentiviral DNA carrying the gene of interest into chromosomal DNA. (7) Expression of gene of interest.

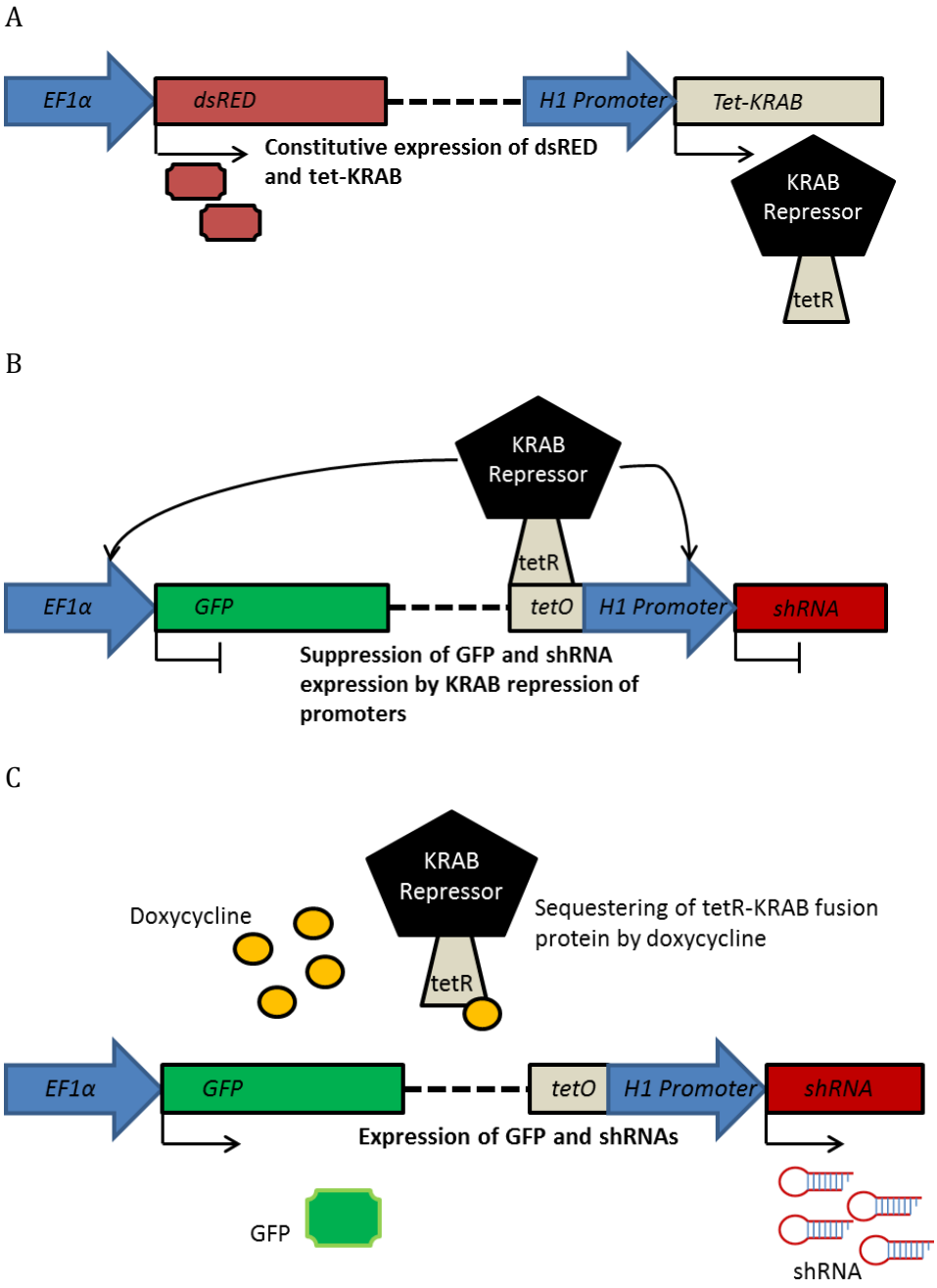

Figure 2-2 **Schematic of the KRAB repression system.** (A) The tet-KRAB fusion protein and the dsRed fluorochrome, introduced during a separate lentiviral transduction, are constitutively expressed. (B) In the absence of doxycycline the tetR-KRAB fusion protein binds to the *tetO* gene upstream of the H1 promoter. This causes epigenetic silencing of promoters within approximately 3kb, including both the H1 promoter that regulates expression of the gene of interest (shRNA), as well as the EF1α promoter regulating the marker gene (*GFP*). (C) In the presence of tetracycline tetR is prevented from binding to the *tetO* gene. This sequesters the KRAB repressor away from the DNA, allowing expression of both the gene of interest and the maker.

2.32 FLOW CYTOMETRY AND CELL SORTING

Sorting and analysis of cells expressing fluorescent proteins was achieved using a FACS Aria. Cells were washed in PBS before being detached from the flask by trypsin. They were then washed in ice cold PBS and re-suspended in PBS + 10% (v/v) FBS to be used for analysis. Viable Huh7.5 cells were selected using Forward (FSC-A) and Side (SSC-A) scatter, and from this population 100,000 cells were acquired that expressed the desired fluorescent marker. Sorted cells were collected in Dulbecco's Modified Eagle Serum (Gibco) supplemented with 10% Foetal Bovine Serum (Gibco).

2.33 VIABLE CELL COUNT

A haemocytometer was used to determine the viable cell density of cells held in suspension; 50 µl of cell suspension was added to 50 µl of trypan blue and mixed by pipetting up and down. The haemocytometer was loaded with 10 µl of stained cell mixture and observed under a microscope. Unstained cells were considered viable, and were counted. In each count two 1 mm^2 grid were counted with the total multiplied by 10^4 to calculate the cell density per ml.

2.34 PULSE CHASE

Huh7.5 cells carrying JFH1 replicons were pulse chased to study the impact of domain III truncation on the stability of NS5A. The cells were labelled with L-Azidohomoalanine (L-AHA), a nucleotide analogue that can be incorporated into protein in place of methionine. L-AHA carries an azido moiety that can be detected by click chemistry, described below.

Prior to the pulse chase, Huh7.5 stably transfected with HCV replicons were seeded into 6-well plates and incubated until they reached a confluence of approximately 80%. These were briefly washed in a starvation medium termed DMEM A (Table 2-14), lacking methionine, and then incubated in fresh DMEM A. After 30 minutes DMEM A was removed and replaced with DMEM B (Table 2-14), a starvation media supplemented with L-AHA for labelling purposes. The cells were then incubated in DMEM B for 4 hours. After labelling DMEM B was replaced with complete DMEM and the cells were chased for 0, 1, 2, 3, 4, or 8 hours. To harvest the protein, the cells were washed in sterile PBS and detached using 150 µl of trypsin per well. The cells were then re-suspend in 850 µl of complete media, before being centrifuged at 2500 g, for 3 minutes at 4°C. The cell pellet was washed in ice cold PBS and centrifuged again for at 2500 g, for 3 minutes at 4°C. To lyse the cells the pellet was suspended in 100 µl of Click lysis

buffer, (Table 2-14), and centrifuged at 16,000 g for 2 minutes at 4°C. The supernatant was collected and stored at -70°C.

Buffer	Content
DMEM A	DMEM(-Cys-Met), 48 mg/l Cysteine
DMEM B	DMEM(-Cys-Met), 48 mg/l Cysteine, 0.7 mg/ml L-AHA
Click Lysis Buffer	50 mM HEPES (pH 7.4), 150 mM NaCl, 1% (v/v) Triton X100

Table 2-14 **Buffers used in Click Chemistry**

2.35 CLICK CHEMISTRY

To visualised proteins which had been labelled for pulse, the incorporated L-AHA was biotinylated by click chemistry. Click chemistry reagents were added sequentially, with the reaction vortexed briefly between. To each 1 ml of lysate was added freshly made stock solutions of; 10 µl of 2.3 mg/ml Acetylene-PEG_4-Biotin (AP4B), 10 µl of 86.9 mg/ml Tris(3-hydroxypropyltriazolylmethyl)amine (THPTA), 20 µl of 12.5 mg/ml Copper Sulphate ($CuSO_4$), and 20 µl of 9.9 mg/ml Sodium Ascorbate (NaAsc). Reactions were then incubated on a rotator at 4°C overnight.

2.36 METHANOL PRECIPITATION

Prior to pulldown protein was purified by methanol precipitation. 400 µl of 100% methanol was added to each 100 µl of protein sample, vortexed and centrifuged to a maximum of 1000 g for 5 seconds. Then 100 µl of chloroform and 300 µl dH_2O was added, vortexing and pulsing in between. Afterwards samples were centrifuged at 9000 g for 1 minute to bring the precipitated protein down on the interface between the two solutions that had formed. The upper phase was extracted, and a further 300 µl of 100% methanol added. Samples were gently mixed, being careful to avoid breaking up the sheet of precipitated protein, and centrifuged at 9000 g for 2 minutes. The supernatant was extracted and the protein pellet re-suspended in 40 µl of 50 mM Tris (pH7.5) 4% (w/v) SDS. Once the pellet had successfully bee re-suspend 760 µl of lysis buffer was added to dilute the SDS to 0.1% (w/v).

2.37 PULL DOWN

Pulldown was achieved by two methods, one using magnetic beads, SureBeads™ (Biorad), and one using agarose beads, Streptavadin Sepharose High Performance (GE Healthcare).

When using magnetic beads 50 µl of re-suspended beads was used in each pulldown. Prior to use the beads were washed three times in 1ml PBS supplemented with 0.1% (v/v)Tween 20

(PBS-T), magnetising and discarding the supernatant between each wash. The beads were then re-suspended in 200 µl PBS-T alongside 1 µg of antibody, and rotated at room temperature for 30 minutes. The beads were washed three times in PBS-T and re-suspended in 250 µl of protein sample, before being incubated rotating at room temperature for 2 hours or at 4°C overnight. The supernatant was extracted and the beads washed thrice in PBS-T. To elute the bound protein the beads were re-suspended in 40 µl 1 x SDS PAGE Loading Buffer (Table 2-9) and incubated at 70°C for 10 minutes. The beads were then magnetised and the Loading Buffer collected. Results were visualised by western blot.

When pulling down protein using biotin Streptavadin Sepharose High Performance (GE Healthcare) beads were used. Beads were stored in a 80% slurry with 20% ethanol, and 10 µl of beads were required for each pulldown. Prior to pulldown the beads were washed twice in 500 µl of Click lysis buffer (Table 2-14), and re-suspended as a 50% slurry. 20 µl of this was added to each 200 µl of protein sample which were then incubated on a rotator at room temperature for 2 hours. To pellet the beads, samples were centrifuged at 16,000 g for 2 minutes, and the supernatant extracted. The beads were washed a further two times in click lysis buffer and re-suspend in 40 µl 1 x SDS PAGE Loading Buffer (Table 2-9), before being boiled for 10 minutes. The tubes were then centrifuged at 16,000 g for 2 minutes and the supernatant carrying the protein harvested. Results were visualised by Western blot.

2.38 STATISTICAL ANALYSIS

Luciferase assay data from individual experimental groups within a single experiment was normalised to the signal obtained 4 hour post transfection. Subsequently, these data were used to calculate mean +/- SEM values for graphical display. Different replicons were compared by unpaired T-test on the mean of the normalised 48 hour time point. Significance was determined using a P value of 0.05

3 RESULTS CHAPTER 1 - MAPPING THE ACTIVITY OF DOMAIN III RESPONSIBLE FOR RESCUING NS5A FROM DESTABLISATION DOMAIN INDUCED DEGRADATION.

3.1 INTRODUCTION

The work detailed below will examine a novel role for domain III in protecting NS5A from targeted degradation.

3.1.1 DESTABILISING DOMAINS

Experimentally controllable protein degradation has recently been made possible through the development of destabilizing domain (DD) fusion partners. Destabilising domains, generally consist of a protein that has been mutated to be unstable, and which can convey this instability to a conjoined protein. This instability typically results in an unfolding event within the DD triggering degradation of the DD and the conjoined protein by cellular processes. Importantly however, the instability can be reversed by the presence of a suitable ligand, which will bind to and stabilise the DD (Banaszynski et al., 2006).

The earliest used DDs are those based upon the human FK506- and rapamycin-binding protein (FKBP12) (Banaszynski et al., 2006). Prior to the development of the DD system, FKBP12 had been widely studied and a phenylalanine to valine mutation had been identified that destabilised it through the formation of a destabilising cavity (Clackson et al., 1998). This mutation, however, could be stabilised by the presence of a ligand carrying complementary 'bumps', but which importantly, was both specific to the mutant and non-toxic. A library of FKBP mutants were cloned into Yellow Fluorescent Protein (YFP), and tested to identify those which showed reduced YFP in the absence of a ligand. Further testing of these was then used to identify those that displayed a dynamic response to the addition of the stabilising ligand, Shield1 (Banaszynski et al., 2006). This system was shown to be usable both *in vitro,* and *in vivo.*

The same researchers went on to develop an alternative DD, one based upon a mutant form of *E. coli* derived dihydrofolate reductase (DHFR) (Iwamoto et al., 2010). DHFR was selected for screening due to the existence of a number of highly specific inhibitors. One of these, trimethoprim was known to be biologically silent within human cells, as it had previously be shown to preferentially target *E. coli* DHFR (Matthews et al., 1985). Similar to the FKBP approach, error prone PCR was used to generate a library of DHFR mutants that were expressed as YFP proteins. These were then analysed to identify variants which exhibited low

protein levels in the absence of TMP, large dynamic range, robust and predictable does-response behaviour, and rapid kinetics of degradation (Iwamoto et al., 2010). One key benefit of DHFR over FKBP is ready availability of the TMP ligand, making the system cheaper to use.

Other reported destabilising domains include: one based on UnaG, that in the presence of bilirubin is both stabilised and fluorescent (Navarro et al., 2016); and one based on the oestrogen receptor (Miyazaki et al., 2012).

3.2 PREVIOUS WORK

Previous work done within the group had attempted to visualise the replication complex (RC) formed by genotype 2a JFH1 replicons using a novel strategy. Replicon constructs were modified such that a mutant, Dihydrofolate Reductase (DHFR) destabilising domain and a green fluorescent (Clover) tag fusion protein were introduced into domain III of NS5A (Figure 3-1). The expectation was that in the presence of a ligand, Trimethoprim (TMP), the DHFR domain would fold into a tight, stable conformation, allowing its conjugated NS5A partner to be available for incorporation into the replication complex. In the absence of TMP, however, the DHFR domain would sample a mis-folded state, and become ubiquintinated, resulting in the proteasomal degradation of itself as well as any other protein domain attached to it. It was predicted that the restricted access host proteins have to pre-existing replication complexes would prevent degradation of NS5A-DHFR-Clover within them upon TMP withdrawal, thus allowing these compartments to be selectively visualised.

In initial experiments the DHFR-Clover cassette was introduced into two locations within NS5A expressed from a standard bicistronic replicon. One position was internal to domain III of NS5A (pSGRJFH1*lucNS3-5B(DHFRClover@2394)) a location well documented to be suitable for foreign insertions(Jones et al., 2007b, Moradpour et al., 2004, McCormick et al., 2006). The second location was at the carboxyl terminus of NS5A (pSGRJFH1*lucNS3-5B(DHFRClover@2442)) (Figure 3-1). The impact that the DHFR-clover domain had on viral replication was then tested in the presence and absence of 10μM TMP.

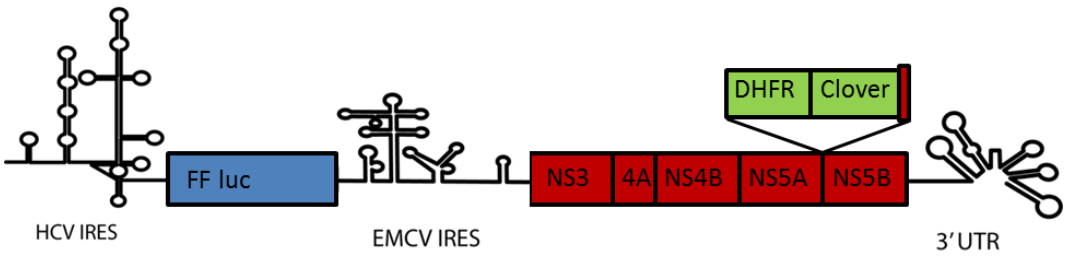

Figure 3-1 **Schematic of subgenomic JFH1-based replicons expressing a NS5A-DHFR-Clover fusion Protein**. The HCV IRES within the 5' UTR drives translation of the firefly luciferase reporter while an EMCV IRES directs translation of the N3-5B replicase. Positioning of the DHFR-clover coding region is either within domain III of NS5A (pSGRJFH1*lucNS3-5B(DHFRClover@2394)) or at the carboxyl terminus (pSGRJFH1*lucNS3-5B(DHFRClover@2442)). For this latter construct the DHFR-clover cassette is flanked either side by the last 8 carboxyl terminal residues of NS5A in such a way so as to enable cleavage away from NS5B but prevent cleavage of DHFR-clover away from NS5A.

When stabilised by the presence of TMP both DHFR carrying replicons resulted in identical increases in luciferase activity over the first 48 hours, with levels of luciferase activity decreasing slightly after this. In contrast, the luciferase activity in cells transfected with a polymerase defective control construct (lucGND) diminished from 4 hours onwards. This is consistent with both constructs being capable of robust replication, albeit at a slightly reduced level compared to a comparable control replicon lacking the DHFR-Clover insert. In the absence of TMP however, it was evident that the positioning of the DHFR-Clover insert dramatically influenced the results. Whilst both replicons demonstrated impaired replication when TMP was withdrawn, the 2442 replicon demonstrated a degree of recovery after 48 hours not seen for the 2394 replicon. This experiment was subsequently repeated as part of the work done for this thesis (Figure 3-2), the results being identical to those described above.

The different replication profiles the two replicons exhibited upon the withdrawal of TMP suggested that NS5A domain III might harbour a novel activity; one that conveyed stability to the polyprotein under conditions where protein turnover was enhanced. It was hypothesized that insertion at the 2394 site had disrupted this activity, hence the failure of the construct to replicate upon TMP withdrawal. The purpose of the rest of the experiments in this chapter was to confirm the existence of this activity and map key residues within domain III responsible for this protective phenotype.

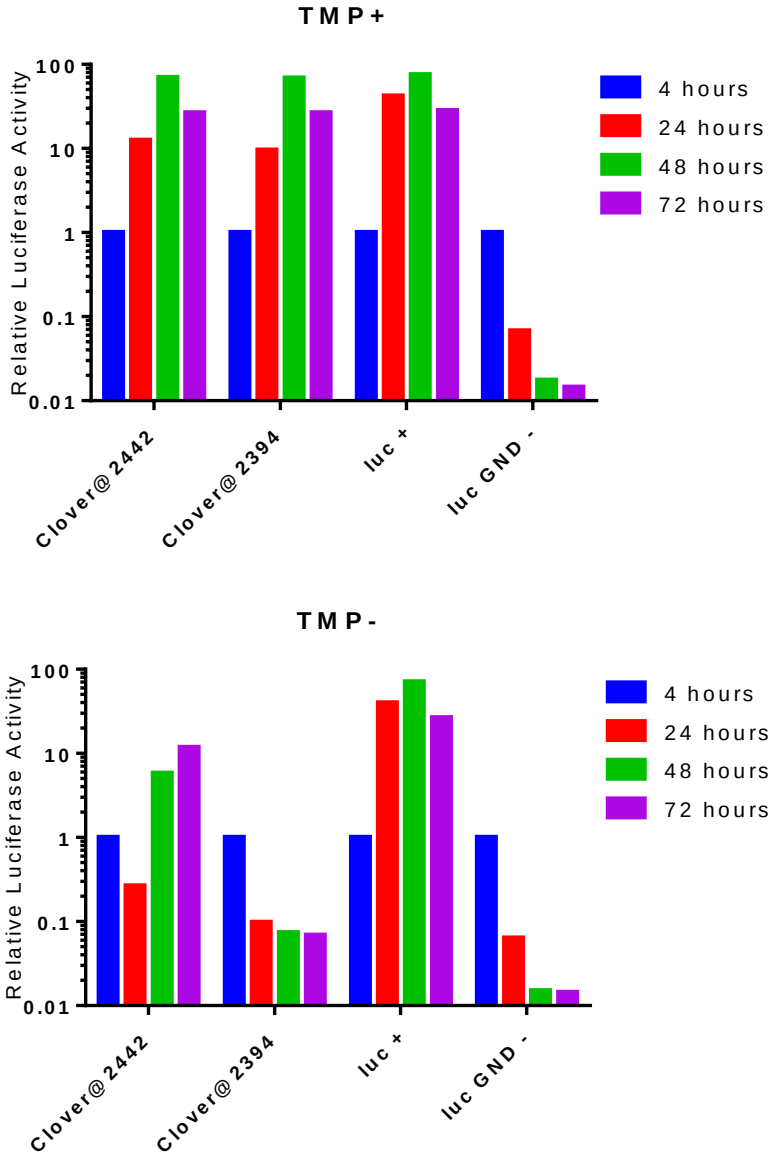

Figure 3-2 **Replication of pSGRJFH1*luc replicons carrying a DHFR-clover cassette either internally (@2394) or at the carboxyl-terminus (@2442).** Huh7.5 cells were transfected with the JFH1 replicons carrying the appropriate insertion alongside a positive replication control (luc) or a replication deficient control (luc GND). Cells were then incubated in the presence (A) or absence (B) of 10 μM TMP, lysed 4, 24, 48, or 72 hours post transfection and replicon replication monitored by luciferase assay. Results represent mean values from a single assay, but which are consistent with those observed in identical assays carried out before the start of this project.

3.3 LARGE SCALE DELETION OF DOMAIN III

To investigate further this potential role for domain III in counteracting the effect that TMP withdrawal had on replication, pre-existing bicistronic luciferase replicons, previously generated by Dr Chris McCormick, were used that contained deletions within domain III, centred on the initial 2394 insertion site (positions relative to the JFH1 genome –accession number AB047639(Kato et al., 2001)). These deletions were between residues 2328-2354, 2354-2404, and 2404-2435 (Figure 3-3), their positioning chosen because a prior study had shown that these deletions were tolerated and the resulting NS5A proteins exhibited differential binding to Ubiquitin Specific Protease 19 (USP19), an interaction that was of potential relevance to the current observations(Pichlmair et al., 2012, Appel et al., 2008)(see results chapter 2). Each deletion was introduced in the replicon carrying the DHFR-clover insert at position 2442, to allow artificial regulation of NS5A stability using TMP.

To determine the effect that these deletions had on viral replication, these constructs were transfected into Huh7.5 cells alongside a replicon carrying the DHFR cassette at the same position but with no deletion. Additional controls included the polymerase functional (luc) and dysfunctional (lucGND) replicons expressing luciferase but lacking the DHFR-Clover insertion in NS5A. Replication was monitored over 72 hours in the presence and absence of 10 μM TMP (Figure 3-4). In the presence of TMP all DHFR-Clover replicons, including those with deletions in NS5A, exhibit enhanced luciferase activity compared to the polymerase defective control at 24 hours post transfection and onward. This is consistent with them being able to replicate. In two of the deletion constructs however, Δ2354-2404 and Δ2404-2435, there was a minor drop in activity relative to the DHFR@2442 construct, suggesting that the deletions are having a negative impact on replication. This effect became more evident in the absence of TMP; while the Δ2328 replicon showed high levels of replication, similar of the full length construct, the other 2 deletion replicons showed a significant drop after 48 hours. The fact that the latter two deletions inhibited recovery from DHFR destabilisation is consistent with a role for these regions of NS5A in protecting viral proteins from degradation.

To characterize further the effect that these deletions have on the stability of the virus, the above transcripts were transfected into Huh7.5 cells which were then exposed to concentrations of TMP ranging from 10 μM to 0.001 μM. After 48 hours the cells were lysed and a luciferase assay performed to monitor replication (Figure 3-2C). As before, deletion of the 2328-2353 region of domain III appeared to have little impact on replication as the Δ2328-2353 replicon was able to generate peak luciferase activity with only 1μM TMP, similar to the wild type control. Conversely the Δ2354-2404 replicon showed increased

sensitivity to TMP withdrawal, showing levels of replication lower than the control at all times and not reaching peak levels below the maximum dosage of TMP. While the previous data had suggested that deletion of amino acids 2404-2435 caused a negative impact on replication, it demonstrated increased resistance to TMP withdrawal; the Δ2404-2435 replicon reaching peak replication at the same TMP dosage as both the control and the Δ2328 replicon. Together these data suggest that the key amino acids or structures of interest spans these two deletions but that the 2354-2404 region is more influential.

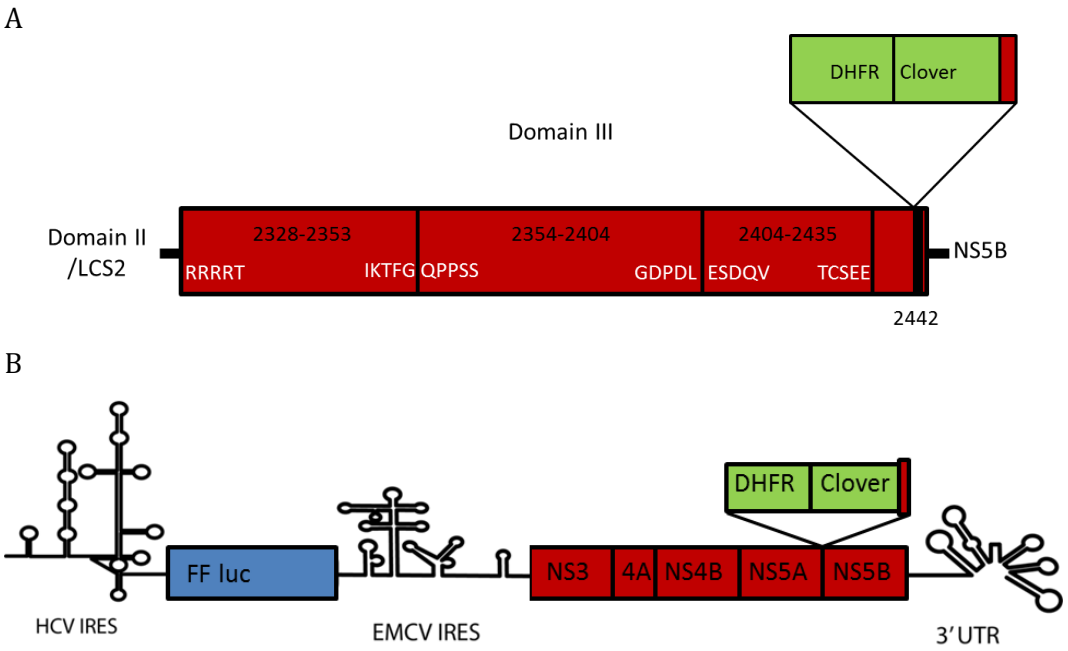

Figure 3-3 **Schematic of the pSGRJFH1luc constructs carrying the 3 large deletions in NS5A Domain III**. (A) The distribution of the 3 large scale deletions within domain III. (B) The pSGRJFH1*luc(DHFRClover@2442) Replicon construct. In white are the 5 amino acid residues surrounding these deletions.

A

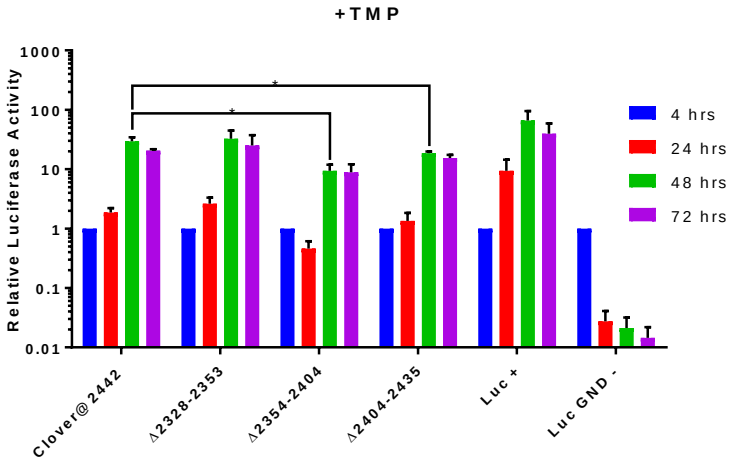

B

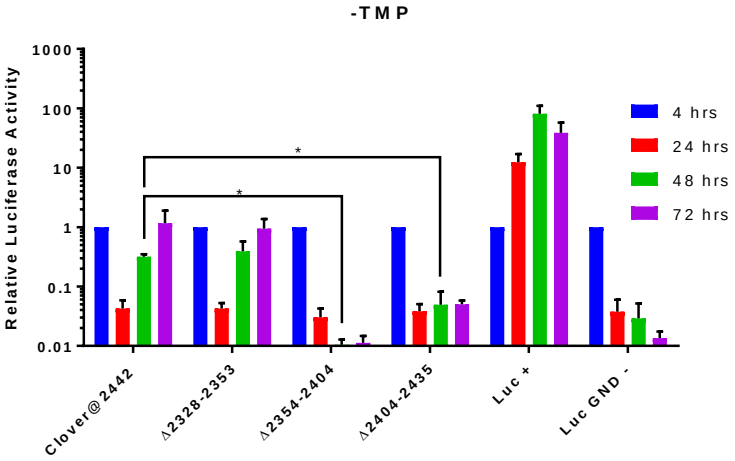

C

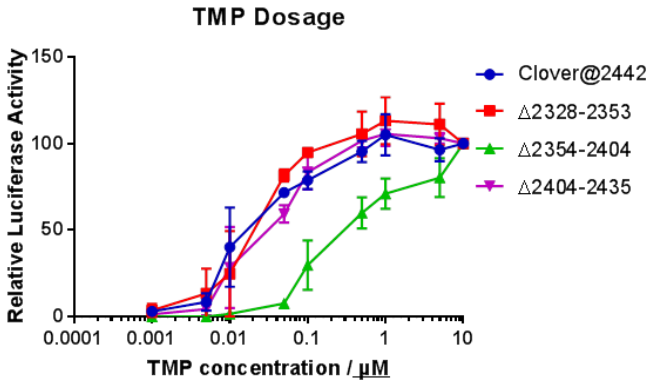

Figure 3-4 **Replication of pSGRJFH1*lucNS35B (DHFR-Clover@2442) replicons**. Huh7.5 cells transfected with JFH1 replicons containing deletion of between 25 to 50 amino acids within domain III were grow in the presence (A) or absence (B) of 10 µM TMP and analysed for luciferase activity 4, 24, 48, and 72 hours post transfection. (c) Huh7.5 cells transfected with the JFH1 replicons were incubated for 48 hours in media supplemented with between 10 and 0.001 µM TMP before Replication was monitored by luciferase assay. Data represents the mean +/- standard error of 3

experiments. * Represents a significant difference ($p \leq 0.05$) as determined by unpaired T-test.

3.4 20AA DELETION REPLICATION ASSAYS

Having demonstrated that intact NS5A domain III is capable of protecting viral replicons from presumed DHFR-directed degradation of this protein, and identified 2 large regions of domain III that are seemingly involved, smaller deletions were introduced into domain III to allow finer mapping of this activity. Seven overlapping 20 amino acid deletions were introduced into NS5A, spanning residues 2354 and2435 within the JFH1 polyprotein (Figure 3-5). These deletions were introduced into a pSGRJFH1*lucNS3-5B(DHFRClover@2442) template, as described in the appendix (8.1) Using the newly generated, constructs replication assays were performed in the presence and absence of TMP to determine the impact each of the 20 amino acid deletions had on replication (Figure 3-6).

Based on the luciferase activities seen all 7 constructs replicated at a similar level to the control DHFR-clover construct lacking deletions, confirming their ability to replicate. In the absence of TMP, however, six of the seven replicons, covering residues 2354 to 2415, demonstrate a drop in replication compared to the WT control, although this was slight and far more modest than that seen using the larger NS5A domain III deletion constructs. Of these, one shows a significant difference to the control, whilst the other 5 trend towards significance. Overall these results suggest that none of the six regions deleted plays a greater role than the others, and it is likely that the protection conveyed by NS5A is a product of a larger region of the protein, such that the 20 amino acid deletions introduced are not severe enough to impact replication when the DHFR-NS5A fusion protein is destabilised. The deletion which had no impact on replication during TMP withdrawal lies towards the c-terminus, spanning residues 2414-2435. This is consistent with the previous data, which suggested that the 2404-2435 region is less involved that the 2534-2404 (Figure 3-4). Although it is not possible to determine key residues from these data, it was possible to further narrow the region of interest to residues spanning positions 2354-2415.

A

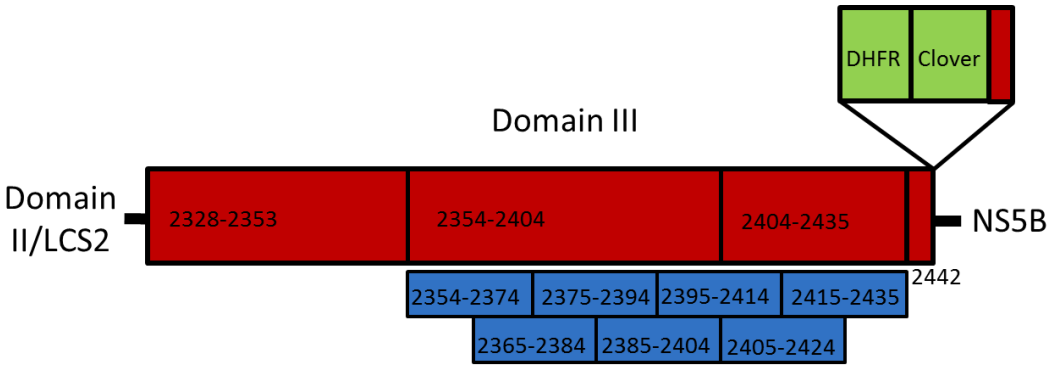

B

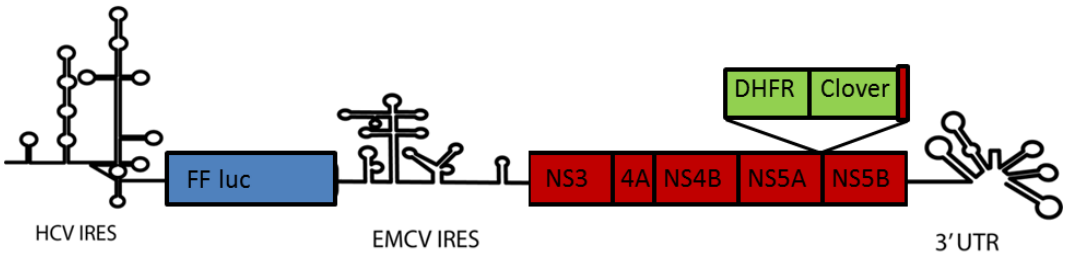

Figure 3-5 **Distribution of the 20 amino acid deletions introduced into NS5A Domain III (A) of the pSGRJFH1*luc(DHFRClover@2442) replicon (B).**

A

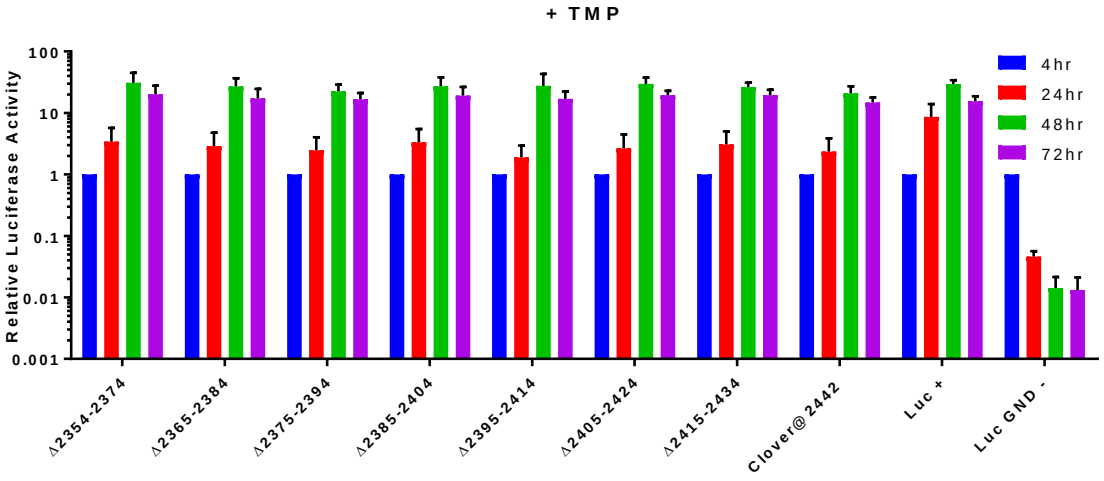

B

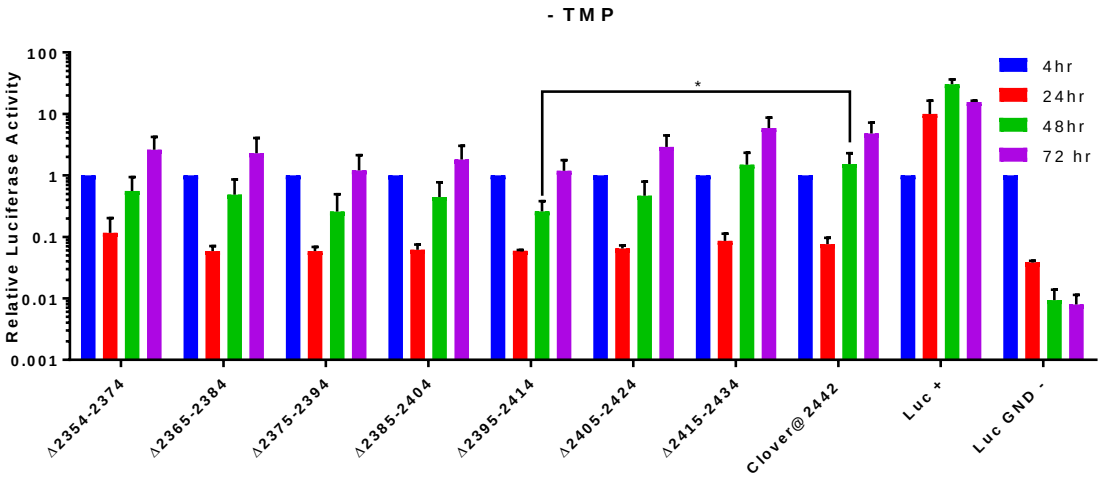

Figure 3-6 **Replication of pSGRJFH1*lucNS35B (DHFR-Clover@2442) replicons containing 20 amino acid deletions in Domain III**. Huh7.5 cells were transfected with JFH1 replicons containing 20 Amino acid deletions spanning residues 2354 to 2435, and grown in the presence (A) or absence (B) of 10 μM Trimethoprim. Data represent the mean + standard error of 3 experiments. * Represents a significant difference ($p \leq 0.05$) as determined by unpaired T-test.

3.5 INVESTIGATING WHETHER THE PROPOSED ROLE FOR DOMAIN III EXTENDS TO GENOTYPE 1

All previous experiments had been performed in replicons derived from JFH1, a genotype 2a strain of HCV, selected due to its high level of replication. However, HCV exists in 7 distinct genotypes, demonstrating a high degree of diversity within NS5A domain III (Figure 3-7). This raised the interesting question of whether or not the protection afforded by domain III being observed in JFH1 may be genotype specific. Particularly due to the presence of an approximately 20 amino acid insertion within domain III in genotype 2 sequences. These additional amino acids consist of residues 2406-2425 and thus partially overlap with the sequence previously determined to be involved in countering DHFR induced degradation.

To answer this question the equivalent of the Δ2354-2404 deletion was introduced into pFK5.1 a culture adapted replicon based on the genotype 1b strain Con1 (accession number AJ238799 (Lohmann et al., 1999)). Based on an alignment of 20 strains, representing genotypes 1-6, the equivalent deletion was considered to represent residues 2354-2400 of the Con1 sequence (Figure 3-7), and this was therefore introduced into pFK5.1Con1neo, see appendix 8.2.

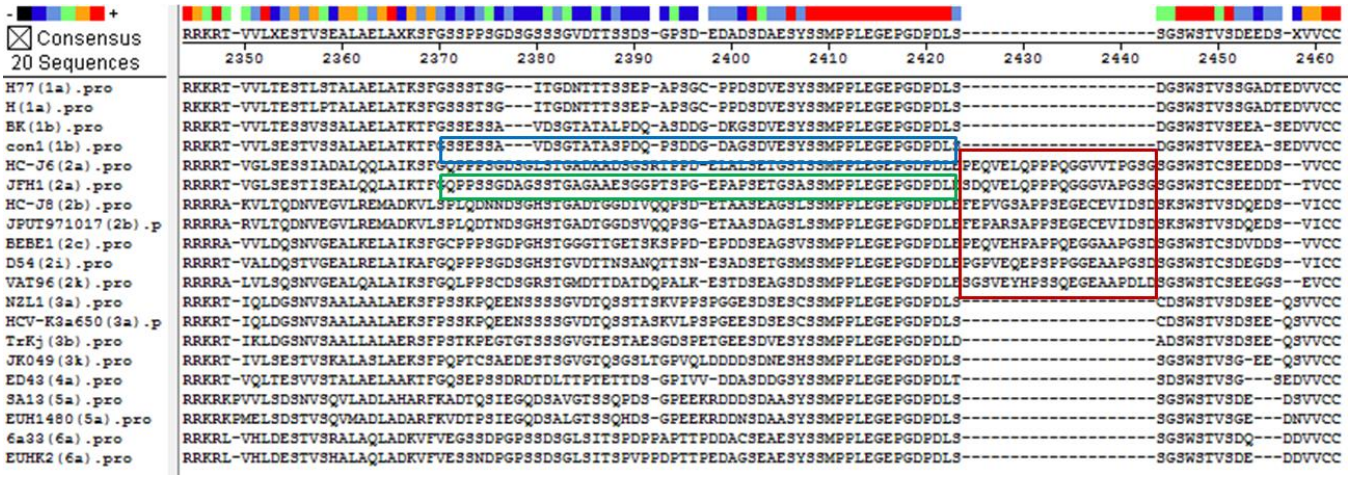

Figure 3-7 **Sequence alignment of NS5A Domain III.** The green box represents the Δ2354-2404 truncation in JFH1 whilst the Blue box represents the equivalent Δ2354-2400 truncation in con1. The red box indicates the 20 additional amino acids present in genotype 2 isolates.

3.6 CON1 NS4B/5A BOUNDARY MUTANT REPLICATION ASSAYS

The inclusion of the Con1 replicon in the study opened up the possibility of targeting NS5A for degradation via two different means. The first was use of DHFR, as had been employed in the JFH1 replicon, but the second derived from a study looking at how cleavage rate at the NS4B/5A boundary impacted on genome replication. Importantly for the purpose of this investigation, it was found that artificial NS4B/5A boundaries could be engineered into the Con1 genome that maintained replication while changing the amino-terminal end of NS5A to including ones that would be expected to destabilize the protein due to the N-end rule (Herod et al., 2012). The N-end rule states that the stability of a protein is a product of its N-terminal amino acid(Gonda et al., 1989). Therefore, as an alternative to the inclusion of a DHFR domain, Con1 based constructs were employed that made use of NS4B/5A boundary mutations to destabilise NS5A. These constructs carried either a wild type (PG/SGS) or mutated boundary predicted to increase NS5A degradation (SV/QGG), in the context of either a full length (WT) or truncated (Δ2354-2400) domain III (Figure 3-8). The boundary mutant constructs were generated by cloning the NS5A, from pFK5.1Con1neo and pFK5.1Con1neoΔ2354-2400 into a pFK5.1Con1luc and pFK5.1Con1LucSV/QGG vectors (Herod et al., 2012)(Appendix 8.3).

To determine the impact of domain III status on the replication of NS4B/5B boundary mutants, RNA transcripts generated from the plasmid clones described above were transfected into Huh7.5 cells, alongside GND negative control, and incubated for up to 72 hours (Figure 3-9). The pFK5.1Con1Luc construct served as the positive control.

In replicons expressing full length NS5A, mutation of the 4B/5A boundary had no impact on replication, with both the pFK5.1Con1luc and pFK5.1Con1luc(SV/QGG) constructs replicating to a similar level as the control. This confirmed that the mutation in combination with an intact domain III is tolerated, as had been reported previously. Conversely mutation of NS5A domain III proved to be lethal, resulting in a drop in luciferase activity irrespective of the status of the NS4B/5A boundary and comparable to that seen for the polymerase defective control construct included in the assay. It is not clear why truncation is tolerated by JFH1 replicons but not Con1. One possibility however, could be due to variations in replication between the two isolates. Con1 replicons replicated far less robustly than their JFH1 counterparts, which when coupled with the truncation, could cause a fatal drop in replication.

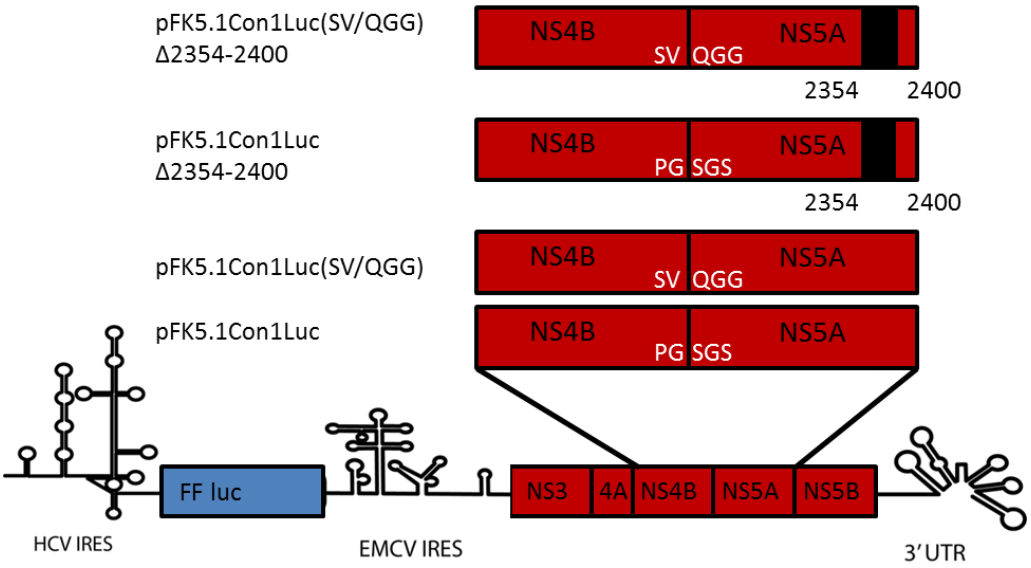

Figure 3-8 **Schematic of the pFK5.1Con1Luc constructs carrying either a wild type or destabilising NS4B/5A boundary and either a full length of truncated NS5A Domain III.** . In white are the amino acid residues surrounding the NS4B/5A boundary, with PG/SGS representing the wild type boundary and SV/QGG representing the destabilising boundary.

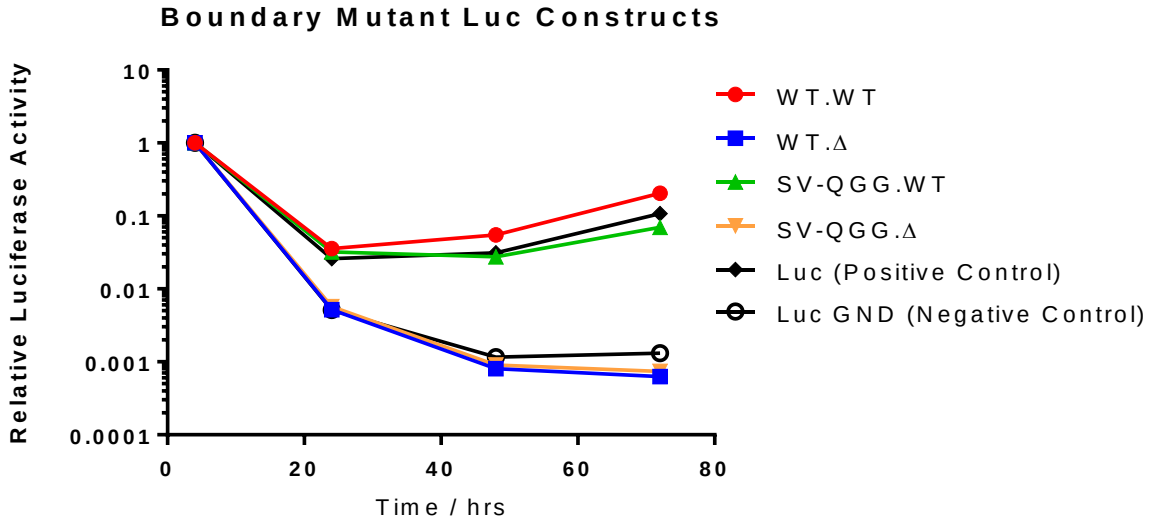

Figure 3-9 **Replication of pFK5.1luc replicons carrying either a wild type or mutant NS4B/5A boundary and either a full length or truncated NS5A Domain III**. pFK5.1Con1luc, pFK5.1Con1lucΔ2354-2400, pFK5.1Con1luc(SV/QGG) and pFK5.1Con1luc(SV/QGG)Δ2354-2400 transcripts were electroporated into Huh7.5 cells. After 4, 24, 48, or 72 hours these were lysed in 1 x Passive lysis buffer. A luciferase assay was used to detect replication of the replicons. Data represents the mean of 2 experiments.

3.7 CON1 DHFRCLOVER COLONY FORMING ASSAYS

To allow artificial control of NS5A stability, pFK5.1 constructs were also generated carrying the DHFR-Clover insert, from pSGRJFH1*lucNS3-5B(DHFRClover@2442), introduced at the equivalent position, @2419. To block cleavage of the DHFR-Clover insert from the mutant NS5A, the final cysteine of NS5A was converted into a proline. As in the JFH1 replicons cleavage of NS5B away from the NS5A fusion protein was facilitated by placing a duplicated copy of the final 8 residues of NS5A after DHFR-Clover.

Initial plans had been to use luciferase based constructs similar to the JFH1 assays described previously, as cloning of the DHFR-containing Con1 replicons had been undertaken alongside the generation of the NS4B/5A boundary mutant constructs. However, because preliminary data from the NS4B/5A boundary mutant constructs indicated that Con1 replicons were intolerant of domain III mutations, such that no signal was visible during transient transfection, it was decided to instead use a more sensitive colony forming assay for the DHFRClover experiments. As such the DHFR-clover insert was cloned into pFK5.1 constructs expressing Neomycin phosphotransferase from the upstream ORF in place of the firefly luciferase (Figure 3-10) (Appendix 8.4).

These pFK5.1Con1neo constructs containing the DHFR insert were then used in a colony forming assay to determine the impact of domain III truncation on the replication of pFK5.1Con1 replicons. Transcripts of pFK5.1Con1neo(DHFRclover@2419) and pFK5.1Con1neo(DHFRclover@2419)Δ2354-2400 were transfected into Huh7.5 cells and seeded into 6 well plates. These transfected cells were then placed under selective pressure using 650 μg/ml G418 to allow colony formation.

Although both replicons formed colonies in the presence of TMP (Figure 3-11), the DHFRclover@2419 construct showed an approximate 10-fold increase in colony numbers compared to the Δ2354-2400, indicating that the deletion is having an impact on replication. When incubated in the absence of TMP, neither replicon yielded colonies at a higher rate than the polymerase knock-out control, suggesting a lack of replication. It is therefore possible that the combined effect of inserting of the DHFR-clover cassette and destabilising it by withdrawal of TMP was sufficient to fully inhibit replication.

This increased susceptibility to TMP withdrawal is most likely due to the decreased replicative potential shown by Con1. As mentioned previously Con1 is known to be less permissible to growth in cell culture than JFH1 and this decreased fitness likely limits what modifications can be supported. Whatever the reason, it was felt that the dramatic difference

in colony formation between pFK5.1Con1neo(DHFRclover@2419) and pFK5.1Con1neo(DHFRclover@2419)Δ2354-2400 in the presence of TMP would complicate further investigations trying to see whether the Δ2354-2400 showed a greater susceptibility to enhance rates of targeted protein degradation through decreasing TMP concentrations.

A

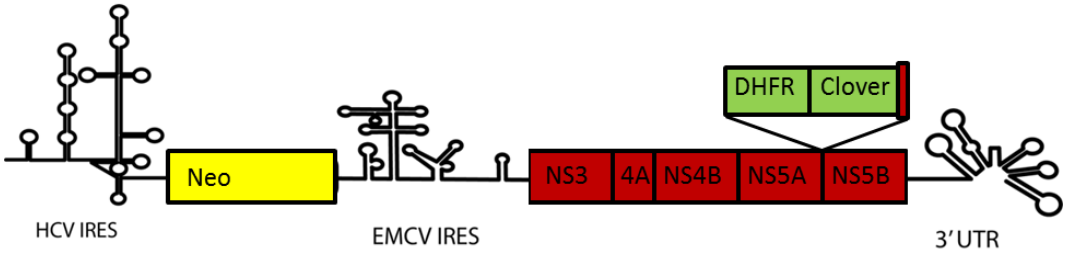

B

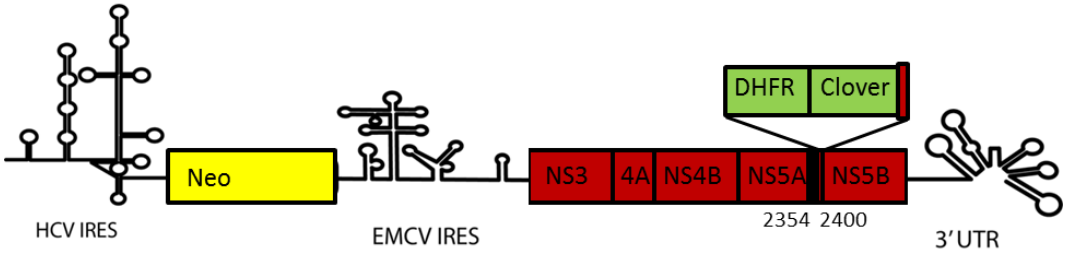

Figure 3-10 **Schematic of the pFK5.1Con1 replicon constructs carrying the DHFR-clover insert @ the C-terminus**. (A) pFKCon1neo(DHFRClover@2419). (B)pFK5.1Con1neo(DHFRClover@2419)Δ2354-2400

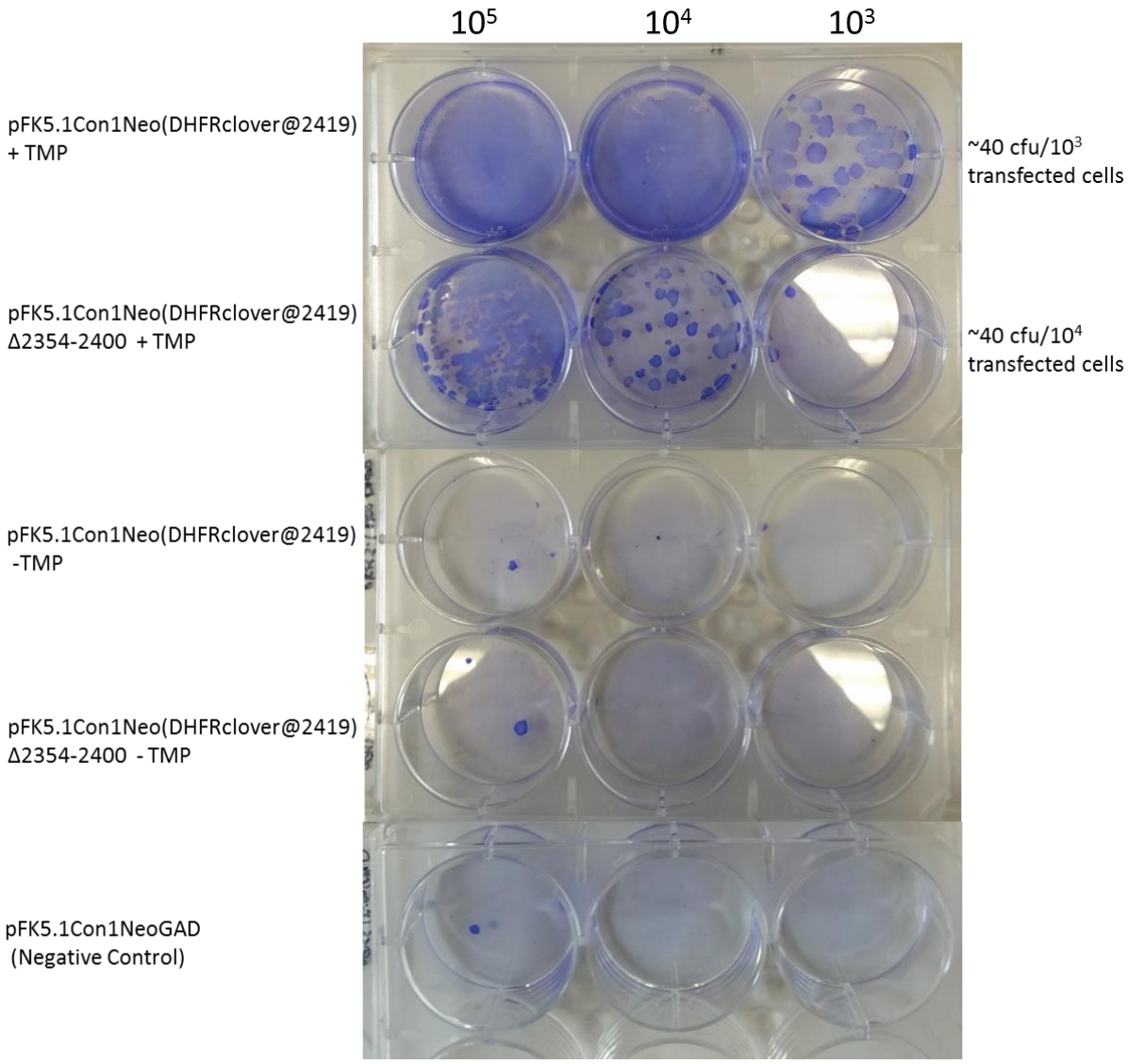

Figure 3-11 **Colony formation by pFK5.1Con1 replicons carrying a DHFR-clover cassette.** pFK5.1Con1neo(DHFRclover@2419) and pFK5.1Con1neo(DHFRclover@2419)Δ2354-2400 transcripts were electroporated into Huh7.5 cells in the presence or absence of 10 μM TMP. Transfected cells were then seeded at 10^5, 10^4, or 10^3, cells per well. 48 hrs post transfection the cells were put under selective pressure using 650 μg/ml G418. After 3 weeks colonies were stained with Coomassie blue and counted. Data represents a single assay

3.8 SUMMARY

NS5A remains a focus of much research, and in recent years has become an attractive target for HCV drug development. This is down to the myriad of functions that NS5A serves during an infection including being involved in genome replication, virion formation, and evading the immune response. It makes sense therefore that HCV would invest in protecting this protein.

Whilst it had been expected that destabilising the fused DHFR would lead to rapid degradation of NS5A, and therefore a complete lack of replication, as in the case of the pSGRJFH1*lucNS3-5B(DHFRclover@2394) replicon , the ability of the pSGRJFH1*lucNS3-5B(DHFRclover@2442) to recover provided an interesting avenue of research. The differential response to TMP withdrawal that the two replicons show, suggests that domain III carries within it an activity that can counter the DHFR mediated destabilisation, one that was interrupted by the 2394 insertion. Had the internal insertion been acting to destabilise NS5A, one would expect this to impact replication even in the absence of TMP.

Having seen that domain III can counter the destabilising effect of a fused DHFR, further work was undertaken to map which parts of domain III are involved. As such 3 large mutations were introduced into the domain, centred around the original 2394 insertion site. The idea was to determine which deletions inhibited the recovery of NS5A from DHFR mediated destabilisation, and as such narrow down amino acids residues that might be involved. The three deletions introduced were selected based on work from the Bartenschlager group (Pichlmair et al., 2012), and so were known to be tolerated under stable conditions. Under destabilised conditions two of these deletions had a similar impact on replication as the 2394 insertion, in that they inhibited the recovery of the replicon upon TMP withdrawal. Using this information it was possible to map the activity of interest to lying between residues 2354-2435.

Having identified this relatively large region, smaller 20 amino acid deletions were introduced into domain III, with the aim of mapping the activity better and ultimately identify key residues involved. As domain III most likely lacks enzymatic activity, because it is unstructured, initial thoughts were that if key residues could be identified these would probably represent contact points on domain III involved in recruiting a ‘protective’ host protein. However, the fine mapping experiments met with little success. Although it was possible to narrow down the region of interest to residues 2354-2415, any hope of identifying key residues through this method was quickly lost as each 20 amino acid deletion

made into this region had only a slight detrimental impact on replication. Several scenarios exist that could explain this finding.

Firstly, it remains possible that the protection conveyed by domain III is due to the recruitment of another protein, but that this is mediated by multiple contact sites spread throughout the domain, rather than one major contact site. Those six 20 amino acid deletions that did cause an impact may partially disrupt one of these contact sites, explaining the minor drop in replication, but that this can be compensated for elsewhere. Secondly, it may be that the insertion and subsequent deletions were causing domain III to be perceived by the cell as partially misfolded, an activity that alone is of little consequence, but when combined with DHFR-destabilisation impacts on replication. The smaller deletions would cause less disruption to the domain, explaining why those constructs carrying the 20 amino acid deletions caused only a minor drop in replication. Alternatively there is a possibility that domain III is protective but functions without the need for host protein recruitment and that the activity observed is due to an intrinsic property of the sequence. The large deletions may disrupt this essential sequence, explaining the correlation between the size of the deletion and the drop in replication. In those replicons carrying the 20 amino acid deletions however, sufficient sequence homology remains to allow recovery, although with a small drop in replication across the board.

These proposed models will be discussed in greater detail later.

Although finer mapping proved unsuccessful, the continued impact that modification of domain III had on replication during destabilisation is clear. In an effort to determine whether or not the protective ability seen in JFH1 extends to other isolates and genotypes, the equivalent of the 2354-2404 deletion was introduced into a Con1 replicon. This was then destabilised by mutation of the NS4B/5A boundary, to avoid the use of DHFR. Presence of the deletion proved lethal however, irrespective of the status of the NS4B/5A boundary. Although previous data from the JFH1 replicons had shown evidence that deletions in NS5A domain III had a negative impact on replication, even under stabilising conditions this was relatively mild. In the Con1 replicons this was not the case, suggesting that domain III may be more involved in replication than previously thought. It is perhaps worth noting that published work looking at the role of domain III in genotype 1b replication has only ever employed relatively small deletions (Tellinghuisen et al., 2008) or targeted relatively few residues for alanine scanning mutagenesis in any one construct (Shimakami et al., 2004). This situation is notably different for genotype 2 studies in which the whole of domain III can be deleted with only a minor impact on replication.

Having observed that Con1 was more sensitive to truncation than JFH1, it was decided to revert to use of DHFR to destabilize NS5A and employ colony formation assays to gauge replication. In the presence of TMP both full length and Δ2350-2400 replicons yielded colonies during the colony formation. Disappointingly however, neither Con1 replicon yielded colonies when TMP was withdrawn, showing that neither was able to overcome the impact of DHFR destabilisation. This is most likely due to the reduced rate at which Con1 replicons replicate.

Interestingly, despite domain III being widely considered to be dispensable for genome replicon in both JFH1 and Con1, the equivalent of the 2354-2404 truncation resulted in a drop in replication, even under stable conditions. Whilst this does not indicate that domain III is directly involved in genome replication, it may indicate that domain III is more important for genome replication than previously thought, perhaps by maintaining NS5A stability even under steady state conditions.

An important caveat to note is that all of these observations are based on luciferase assays, measuring the activity of firefly luciferase expressed from a separate open reading frame of the replicons. As such this does not detect NS5A stability or turnover directly, but rather luciferase values serve as an indirect marker for both viral protein expression and viral genome replication.

One alternative method that could have been implemented would be the use of Quantitative Reverse Transcription Polymerase Chain Reaction (Q RT PCR). This would allow direct monitoring and quantification of replicon RNA replication. However the set-up to allow this made it unfeasible, requiring the purchase of a Q PCR machine and reagents.

A more direct method of detection would be to detect NS5A by Western blot, similar to that described in Results Chapter 3. This would provide a semi quantitative method to monitor NS5A stability. Unfortunately early attempts to detect various NS5A from the various replicons were unsuccessful. Difficulties arose with the detection of both NS5A itself and the inserted Clover peptide by antibodies. Two antibodies were tested, a mouse monoclonal, and a sheep anti-NS5A antisera. Unfortunately both appeared to recognise an immunodominant epitope in domain III of NS5A, and as such were incapable of recognising NS5A carrying various truncations. While this could had been overcome by blotting for the Clover fusion partner, it would be insufficient to detect NS5A lacking this insertion. Furthermore there remained a slight possibility that due to internal proteolytic cleave, the fusion partner could be degraded during DHFR-mediated destabilisation while sufficient NS5A remained to fulfil a replicative function.

Another alternative would be to detect clover fluorescence by flow cytometry. GFP, of which clover is a modified variant, has been shown to be a quantitative reporter of gene expression(Soboleski et al., 2005), and, as with western blotting, would therefore allow the direct monitoring of NS5A turnover. However, several barriers prevented this. As with western blotting, monitoring of clover could be hindered by the possible cleavage of the DHFRclover domain. In addition, although flow cytometry apparatus was available during the course of this work, the use of this includes a not inconsiderable cost, making extensive use prohibitively expensive. Finally there are issues with practicality. Cells and fluorochromes can suffer from deterioration post fixing. The replication assays covered a 72 hour period, and it is possible therefore that fluorescence of early time point samples could have deteriorated somewhat before analysis.

4 RESULTS CHAPTER 2 – INVESTIGATING POSSIBLE MECHANISMS BEHIND THE RESCUE OF NS5A FROM DHFR MEDIATED DEGRADATION

4.1 INTRODUCTION

Previously discussed work has identified residues 2354-2415 of the JFH1strain as being capable of rescuing replication when NS5A is targeted for destabilisation. This chapter will look at potential mechanisms that might contribute to this activity, as well as whether or not this protection can extend outside of NS5A.

4.1.1 USP19

Work by Pichlmair *et al* has previously demonstrated that NS5A domain III forms an interaction with human Ubiquitin Specific Protease 19 (USP19) (Pichlmair et al., 2012). Within NS5A this interaction was mapped to residues 2354-2404, and as such represents a considerable portion of the region identified in this work as being capable of rescuing NS5A.

USP19 is a 145 kDa deubiquitinase. As a deubiquitinase USP19 is a cysteine protease that specifically cleaves ubiquitin from ubiquitin-conjugated protein substrates. Two major isoforms of USP19 are known to exist, differing solely in the C-terminus. One isoform has a transmembrane domain that has been reported to allowi it to be anchored to the ER membrane, facing into the cytoplasm (Hassink et al., 2009). The other isoform instead carries an EEVD extension allowing it to interaction with tetratricopeptide repeats. Upstream of the C-terminus is the deubiquitinase domain, which constitutes the majority of USP19. The precise structure of this domain is not yet fully understood, but it is known to also carry myeloid translocation proteins 8, Nervy and Deaf1 motif (Hassink et al., 2009), that are believed to mediate protein-protein interactions (Gross and McGinnis, 1996). The N-terminal region of USP19 carries two CHORD and SGT1 domains (Hassink et al., 2009), which are thought to mimic p23, a co-chaperone that operates in conjunction of Heat-shock protein 90. The presence of these domains has led to the suggestion that USP19 might have some chaperone ability itself, either alone or in complex with HSP90 (Hassink et al., 2009).

Known roles for USP19 include the regulation of apoptosis (Mei et al., 2011), promoting cell proliferation (Lu et al., 2009), recovery from hypoxia (Altun et al., 2012) and the regulation of muscle myogenesis and atrophy (Wing, 2013). USP19 has also been shown to play a regulatory role in type I interferon signalling (Gu et al., 2017). Of particular interest to this work however is the ability of USP19 to rescue proteins from proteasomal degradation and

Endoplasmic Reticulum Associated Decay (ERAD) first investigated by Hassink *et al* (Hassink et al., 2009). In this work USP19 was observed to be capable of rescuing both cytosolic and ER bound proteins, leading to increased abundance of proteins that would otherwise be rapidly degraded. Furthermore USP19 expression was shown to be greatly enhanced during ER stress, a state that HCV infection is known to cause (Joyce et al., 2009). The previous findings that USP19, a deubiquitinase, can interact with NS5A domain III, a protein known to be natively unstructured, and that it is capable of rescuing proteins from proteasomal degradation provided an attractive model for the role of domain III in rescuing NS5A. USP19 may be recruited to domain III to promote deubiquitination of NS5A as a whole. In the context of the DHFR constructs, the presence of USP19 is capable of counteracting the degradation induced by the destabilising domain. In the absence of artificial destabilisation the recruitment of USP19 by domain III may serve to promote stability in response to other factors, for example in response to increased protein turnover during the IFN response. Some of these potential benefits will be explored in a later chapter.

4.2 USP19 SHRNA KNOCKDOWN

To investigate this potential role for USP19 in NS5A rescue, short hairpin RNAs (shRNAs) were generated that targeted at USP19 and the impact on both full length and truncated replicons observed. ShRNAs are an artificial form of RNA interference, similar to microRNAs. Once expressed by either RNA polymerase II or III, shRNA molecules self-hybridise forming a hairpin structure. This is processed by Droscha and Dicer enzymes forming a small dsRNA molecule. The antisense portion of this can then associate with an Argonaut protein, as part of the RISC complex, allowing it to interact with complementary mRNA sequences and suppressing translation in one of two ways. In the case of perfect complementarity between the shRNA and mRNA, the RISC complex cleaves the mRNA, or in the case of imperfect complementarity, the RISC complex represses translation of the mRNA. Both result in the knockdown of gene expression and are examples of post transcriptional gene regulation. ShRNAs are capable of targeting both endogenous and exogenous genes in this way, and as such represent a versatile tool for transient gene silencing.

USP19 targeting shRNAs were designed using Invitrogen Block-iT (Table 8-4), and introduced into pSuper, a mammalian expression vector. Initial attempts to confirm the activity of these vectors to knockdown USP19 expression were hampered, however, by difficulties detecting native USP19 by Western blot due to a low transfection efficiency; any knockdown was masked by those cells not successfully transfected with an shRNA. To circumvent this issue a plasmid was generated expressing an N-terminal V5 tagged USP19 by cloning V5-USP19 from an in-house pCRBlunt construct (itself generated by others in the lab from a USP19 expression vector (Addgene)) into pCDN3.1 (Appendix 8.5).

To test knockdown the pSuper plasmids carrying all 5 shRNAs, were transfected into Hek293T cells alongside pCDNA3.1-V5-USP19. A flag-tagged pFBM-TEV construct was also included to detect any difference in transfection efficiency that might occur between experimental groups. After 48 hours the levels or V5-USP19 and Flag-tagged TEV were detected by Western blot (Figure 4-1). All cells transfected with a functional shRNA demonstrated a drop in V5 expression relative to the pSuper control, indicating successful knock down of USP19. No noticeable difference was seen in TEV expression, confirming that what was being observed was indeed knock-down rather than a reduction in transfection efficiency. Reduced expression of V5-USP19 was most evident in those cells expressing shRNAs 1, 2, and 3, and therefore it was these shRNA constructs that were selected for further experimentation.

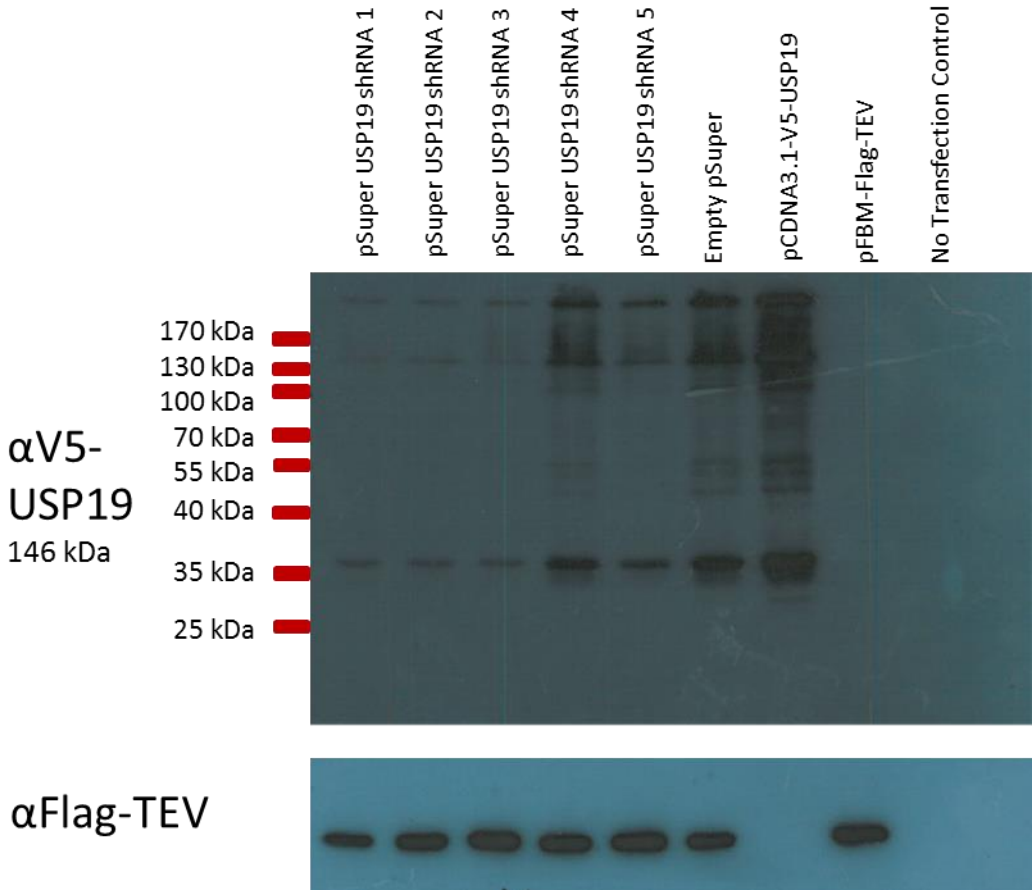

Figure 4-1 **Knockdown of USP19 by shRNAs.** 4.5 x 10^5 HEK293T cells were transfected with 660 ng each of an shRNA expressing pSuper, pCDNA3.1-VS-USP19, and a Flag-TEV expression plasmid. An empty pSuper was included as a knockdown control, and pCDNA3.1-V5-USP19 and the FLAG-TEV were also transfected alone. 48 hours later the cells were lysed in 100 µl RIPA buffer with 1 x Complete Protease Inhibitor. Expression of USP19 was detected by Western blot using an αV5 antibody to detect the N-terminal V5 tag and the Flag-TEV control was detected using an αFlag antibody.

Whilst transient transfection of the USP19 shRNAs using pSuper expression constructs had proved effective it was not a viable vehicle for subsequent assays involving replicon transcripts; sequential transfection of cells with both the shRNA vector and replicon RNA would result in only a low percentage of double positive cells. As such lentiviral transduction was used to generate Huh7.5 cell lines which would express the 3 most functional shRNAs in an inducible manner, which could subsequently be transfected with HCV replicons. USP19 shRNAs 1, 2, and 3, were first cloned into pLVTHM using BglII and MluI, alongside a control shRNA (shC) kindly donated by Dr Tilman Sanchez-Elsner. This control is regulated in the same manner as the USP19 shRNAs but does not cause knockdown of any cellular proteins, thus acting as a control for the impact of Lentiviral transduction.

Cells were transduced sequentially with two different lentiviral constructs. The first introduced a plasmid carrying the gene for a tet-Krab repressor, to suppress the subsequently introduced shRNAs alongside a ds-Red fluorochrome to monitor transduction efficiency. Fluorescence Activated Cell Sorting (FACS) was used to confirm transduction success and select those cells expressing the highest levels of ds-Red and therefore the Krab Repressor (Figure 4-2). These cells were propagated and used in the second transduction. This second transduction introduced the USP19 targeting shRNAs, or the control shC, and a GFP reporter gene; expression of GFP indicates successful integration of the lentiviral plasmid, and therefore of the shRNA/shC. After the second transduction the cells were incubated in media supplemented with 2.5 μg/ml doxycycline, to induce the expression of both the shRNA genes and the GFP reporter. These were then re-sorted to select out a population of cells expressing both fluorescent markers, and therefore transduced with both the Tet-KRAB repressor and shRNA genes (Figure 4-2). The cells (Huh7.5 Krab shUSP19 C, 1, 2 and 3) were then maintained under standard conditions.

To confirm the ability of the shUSP19 cell lines to knock down endogenous USP19, the cell lines were induced for between 1 and 5 days in the presence of 2.5 μg/ml doxycycline, and the impact on USP19 observed by western blot (Figure 4-3). To provide a control for direct detection of USP19, Huh7.5 cells were also transfected with pCDNA3.1-V5-USP19, and incubated alongside the shRNA cell lines.

Over the course of the induction both the naïve Huh7.5 and shC cells showed a slight increase in the expression of USP19. This could indicate that doxycycline was inducing expression of USP19, possibly due to a stress response. Irrespective of this all three cell lines expressing a USP19 targeted shRNA demonstrated some level of knock down, although this varied in intensity between cell lines. The most effective shRNA proved once again to be USP19

shRNA3 which demonstrated the most dramatic and rapid drop in detectable USP19. Sh2 demonstrated a more gradual effect, while sh1 caused only a slight knockdown after the full 5 days. For this reason only the sh2 and sh3 cell lines were maintained.

Also during the induction the cells were visually monitored to look for signs of cytotoxicity. None of the cell lines demonstrated dramatic change in morphology or cell death suggesting a tolerance to both the shRNAs and doxycycline.

Note that the predicted band size of USP19 is approximately 146 kDa, however, all of the blots show several bands with there being no clear major band of the expected size. Whether these are post-translationally modified USP19 or degradation products is unclear. However, discussion with the manufacturer of the USP19 specific monoclonal antibody used in the blots([EPR14816]) (Abcam) confirmed that they knew it detected multiple species by Western blot, but considered most of these to be USP19 specific based on analysis using a parental and USP19 knock-out cell line. Consistent with this viewpoint many of these bands showed a visible reduction in their abundance upon anti-USP19 shRNA induction.

A

Untransfected Huh7.5 cells

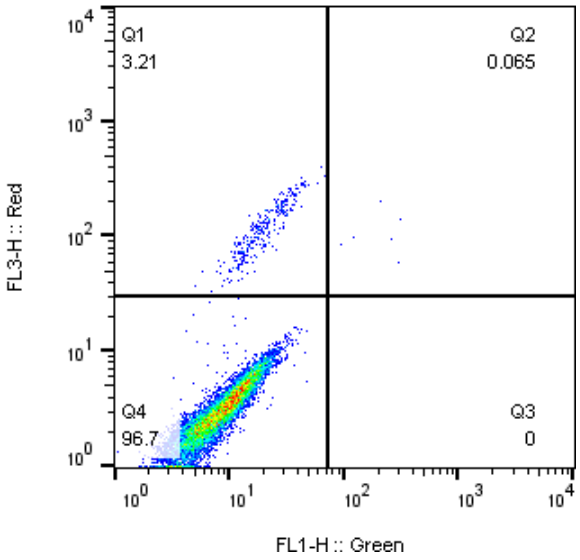

B

Huh7.5 cells expressing the KRAB repressor

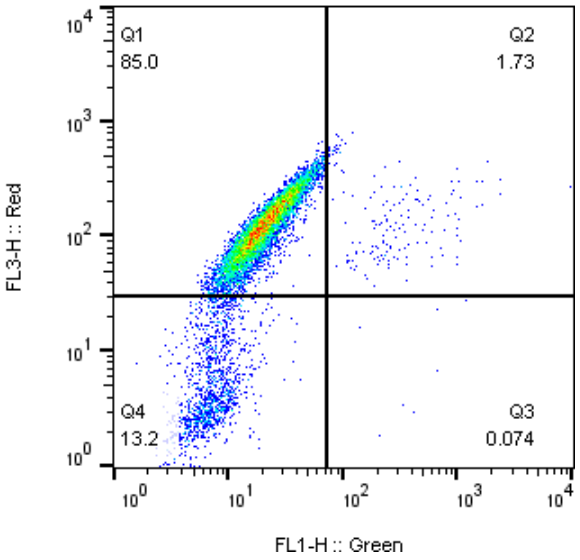

C

Huh7.5 cells expressing both the KRAB repressor and USP19 shRNA 3

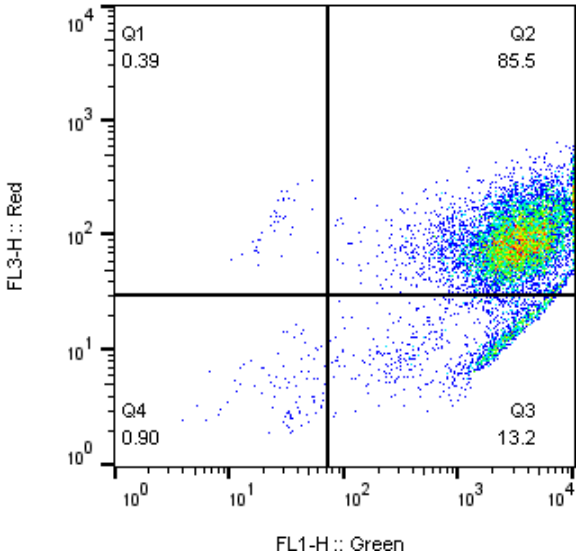

D

Shift in florescence resulting from lentiviral transduction

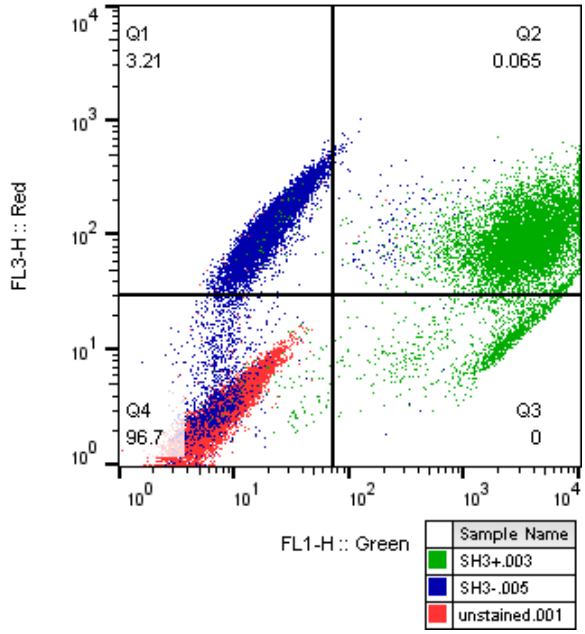

Figure 4-2 **Expression of the fluorescent reporter genes introduced during lentiviral transduction**. Samples were gated using forward and side scatter to select out only average sized Huh7.5s, excluding outliers and cell debris. These gated cells were sorted by detection of GFP and ds red using appropriate light channels. (A) naïve HuH7.5 cells. (B) Huh7.5-Krab Cells. (C) Huh7.5-Krab-sh3 cells. (D) Shift in fluorescence profile.

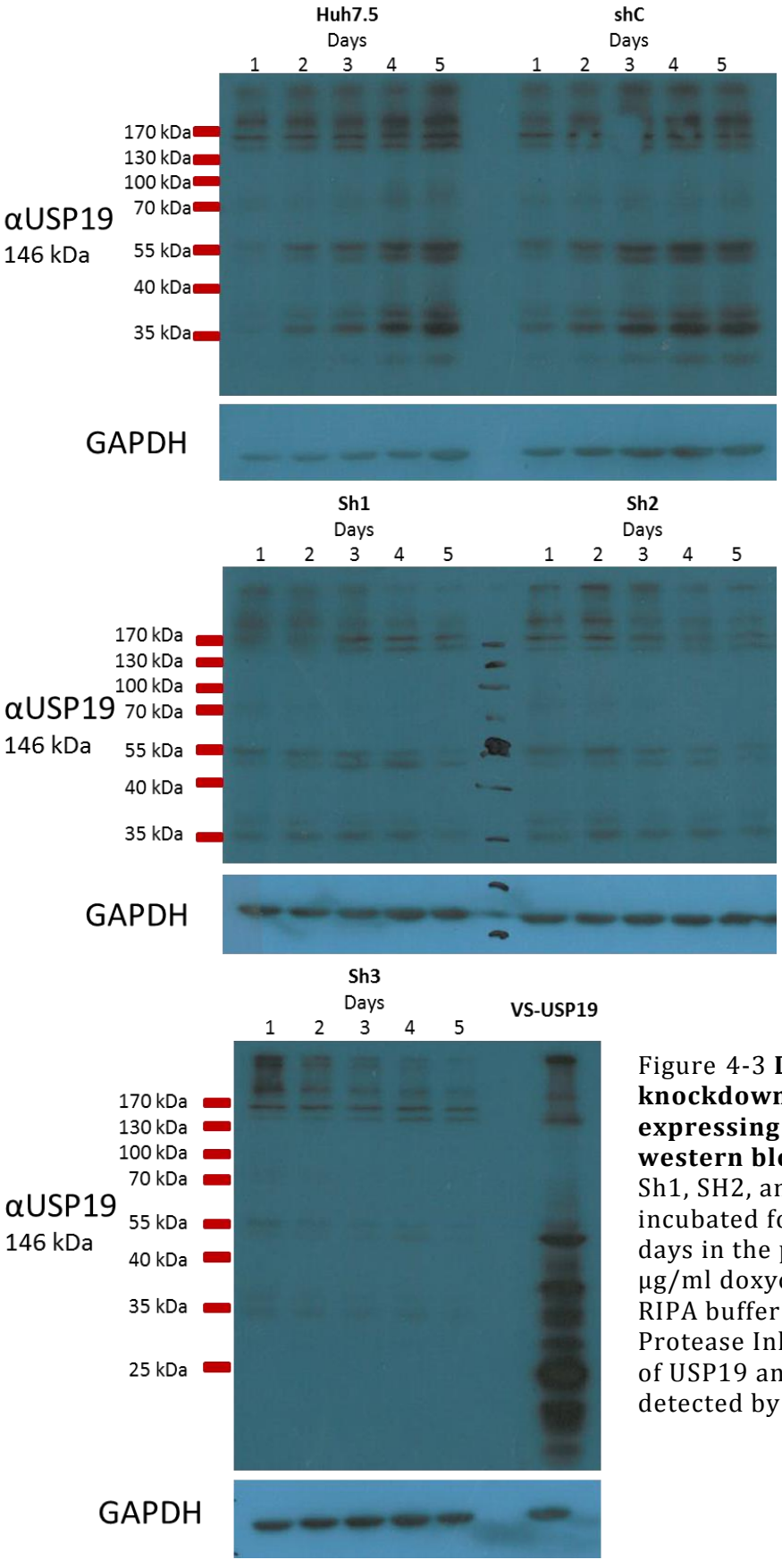

Figure 4-3 **Detection of USP19 knockdown in SHRNA expressing cell lines using western blot**. Huh7.5, shC, Sh1, SH2, and sh3 cells were incubated for between 1 and 5 days in the presence of 2.5 µg/ml doxycycline and lysed in RIPA buffer + 2 x Complete Protease Inhibitor. Expression of USP19 and GAPDH was detected by western blot.

4.3 USP19 KNOCKDOWN REPLICATION ASSAYS

To investigate the possible role of USP19 in the activity of NS5A domain III, a replication assay was performed in induced shC, shUSP19 2, and shUSP19 3 cells. pSGRJFH1*lucNS3-5B(DHFRClover@2442) and pSGRJFH1*lucNS3-5B(DHFRClover@2442)Δ2354-2404 replicons were transfected into shC, sh2, or sh3 cells which had previously been treated for 5 days with 2.5 μg/ml doxycycline. The resulting cells were then incubated in the presence or absence of 10 μM TMP, and replication of each replicon monitored over a 72 hour period (Figure 4-4)(Figure 4-5). If USP19 was indeed playing a role it was expected that its knockdown by the shRNAs would lead to sensitization of the full length NS5A to TMP withdrawal, and that replication of full length replicons would be inhibited similarly to the truncated mutant.

In the absence of doxycycline, under conditions where USP19 should be expressed, both replicons behaved in the manner observed previously. Irrespective of cell type the full length replicon showed robust replication in both the presence and absence of trimethoprim demonstrating the same resistance to DHFR mediated destabilisation described previously. Similarly the Δ2354-2404 replicon once again proved to be sensitive to TMP withdrawal, failing to replicate in the absence of TMP.

In both the shC and sh2 expressing cells, the wild type replicon displayed a very similar replication profile in the presence of doxycycline as they do its absence, suggesting that induction of the shRNAs is having no impact on the replicons' ability to replicate(Figure 4-4). However, there is some evidence in the sh3 expressing cells that knockdown of USP19 is having an effect. In particular USP19 knockdown did appear to cause a slight drop in the replication of the pSGRJFH1*lucNS35B(DHFRclover@2442) replicon after 72 hours. This is most evident during TMP withdrawal, although there is also a very slight drop when stabilised. As in the shC and sh2 cells however, the Δ2354-2404 truncated replicon demonstrates a similar replication profile as observed previously. Any impact that USP19 knockdown may be having is masked by the low overall replication of this replicon.

The ability of the full length replicon to recover from DHFR induced destabilisation even when USP19 is knocked down suggests that USP19 is not the key mediator of resistance; however, the slight drop seen may indicate that it does play a more minor role.

A

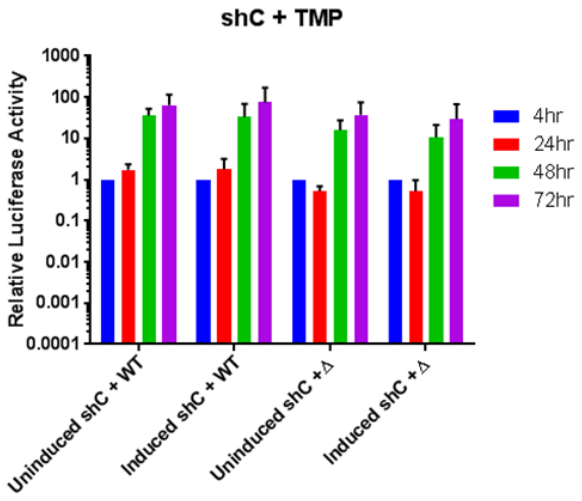
shC + TMP
Relative Luciferase Activity
1000
100
10
1
0.1
0.01
0.001
0.0001
4hr
24hr
48hr
72hr
Uninduced shC + WT
Induced shC + WT
Uninduced shC +Δ
Induced shC +Δ

B

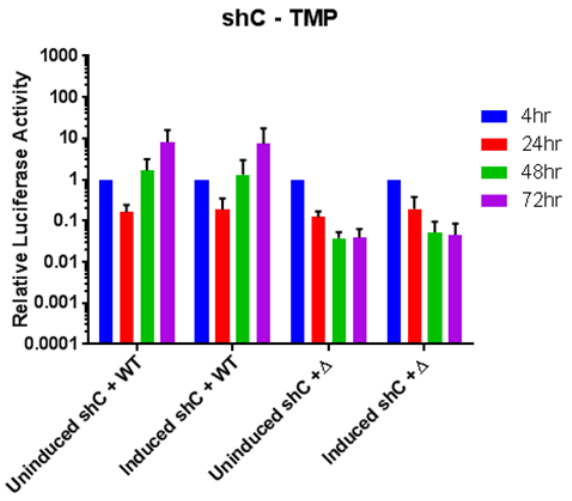
shC - TMP
Relative Luciferase Activity
1000
100
10
1
0.1
0.01
0.001
0.0001
4hr
24hr
48hr
72hr
Uninduced shC + WT
Induced shC + WT
Uninduced shC +Δ
Induced shC +Δ

C

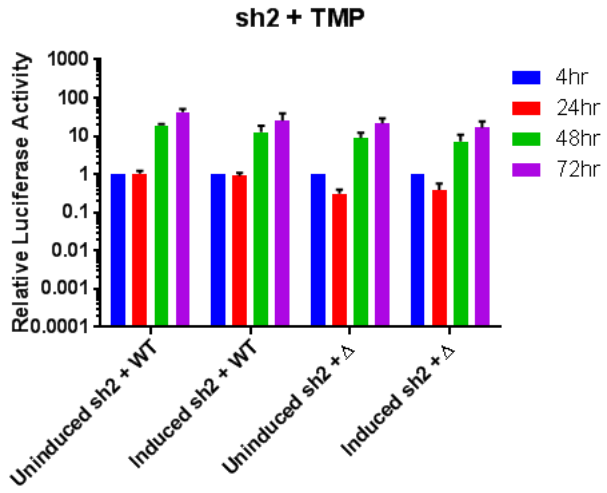
sh2 + TMP
Relative Luciferase Activity
1000
100
10
1
0.1
0.01
0.001
0.0001
4hr
24hr
48hr
72hr
Uninduced sh2 + WT
Induced sh2 + WT
Uninduced sh2 +Δ
Induced sh2 +Δ

D

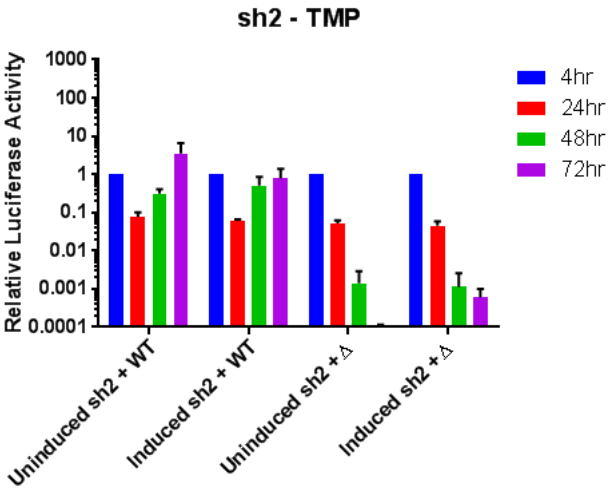
sh2 - TMP
Relative Luciferase Activity
1000
100
10
1
0.1
0.01
0.001
0.0001
4hr
24hr
48hr
72hr
Uninduced sh2 + WT
Induced sh2 + WT
Uninduced sh2 +Δ
Induced sh2 +Δ

E

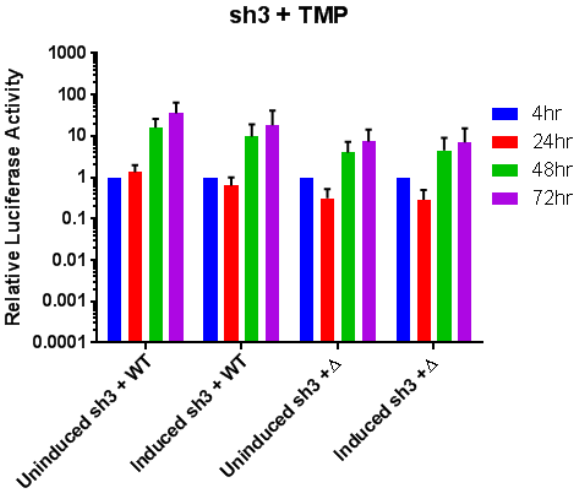
sh3 + TMP
Relative Luciferase Activity
1000
100
10
1
0.1
0.01
0.001
0.0001
4hr
24hr
48hr
72hr
Uninduced sh3 + WT
Induced sh3 + WT
Uninduced sh3 +Δ
Induced sh3 +Δ

F

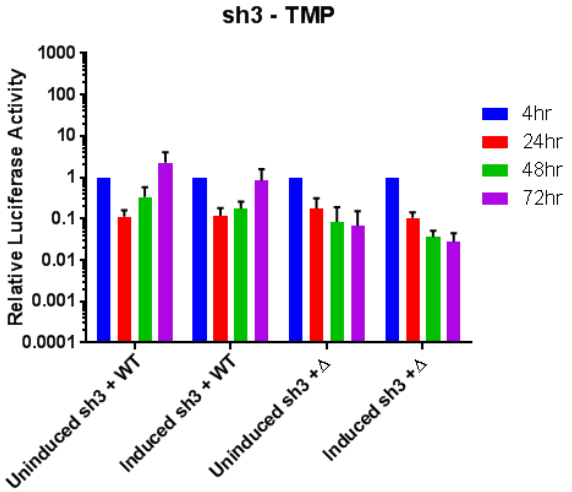
sh3 - TMP
Relative Luciferase Activity
1000
100
10
1
0.1
0.01
0.001
0.0001
4hr
24hr
48hr
72hr
Uninduced sh3 + WT
Induced sh3 + WT
Uninduced sh3 +Δ
Induced sh3 +Δ

Figure 4-4 **Replicative ability of pSGRJFH1*lucNS35B (DHFR-Clover@2442) replicons in cells expressing USP19 targeted shRNAs**. pSGRJFH1*lucNS3-5B(DHFRClover@2442) and pSGRJFH1*lucNS3-5B(DHFRClover@2442)Δ2354-2404 replicons were transfected into shC, sh2, or sh3 cells which had previously been treated for 5 days with 2.5 μg/ml doxycycline. The resulting cells were then incubated in the presence or absence of 10 μM TMP, and replication of each replicon monitored over a 72 hour period. Data for shC and sh3 represents the mean +/- standard error of 3 experiments. Data for sh2 represents the mean +/- standard error of 2 experiments. No significant difference was found in the replication of pSGRJFH1*luc replicons in induced and uninduced shUSP19 expressing cells.

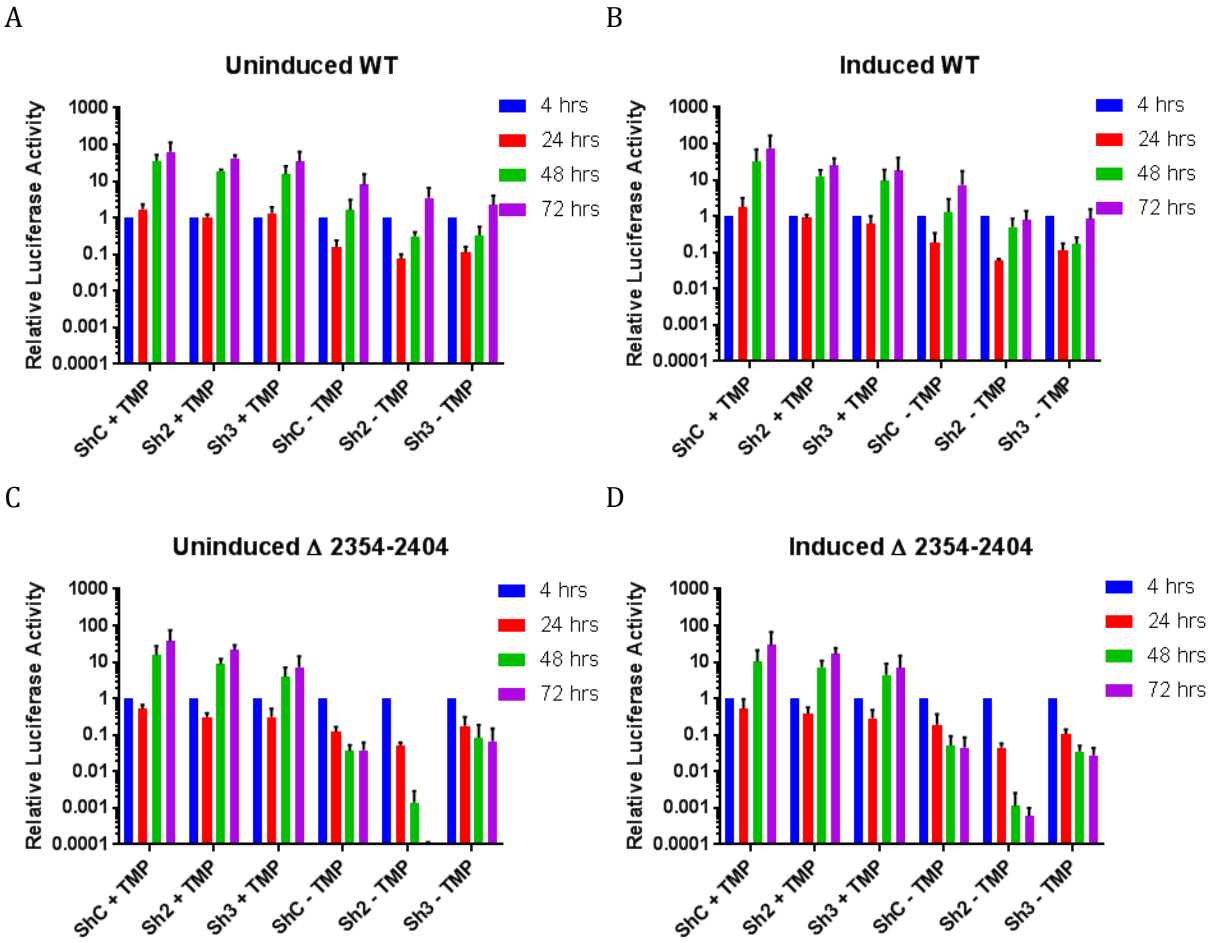

Figure 4-5 **Replicative ability of pSGRJFH1*lucNS35B (DHFR-Clover@2442) replicons in USP19 knockdown Huh7.5 cell lines**.. Rearrangement of the data from Figure 3-4 showing each replicon in Uninduced of Induced shC, shUSP19 2, and shUSP19 3 expressing Huh7.5 cells. Data for shC and sh3 represents the mean +/- standard error of 3 experiments. Data for sh2 represents the mean +/- standard error of 2 experiments. No significant difference was found in the replication of pSGRJFH1*luc replicons in shC, sh2 , and sh3 cells.

4.4 DOMAIN III DUPLICATION REPLICATION ASSAYS

Assuming that the difference in NS5A degradation rates are the underlying reason behind the differential response to TMP between the various DHFR-Clover containing replicons, the results can be explained in two ways. Either, the modifications made into domain III are blocking an intrinsic activity capable of rescuing viral proteins from DHFR induced instability, or they act as cryptic degradation signals, promoting the turnover of the tagged proteins, but to the extent that this only manifests itself as a reduction in replication when NS5A is already destabilised by mis-folded DHFR. To determine which of these mechanisms was likely, JFH1 derived replicons were generated that expressed two fused copies of domain III as part of the viral polyprotein, either full length or containing the Δ2354-2404 deletion (Figure 4-6). Should domain III play an active role in protecting viral proteins from degradation it was hypothesised that a single functional copy should be sufficient to allow recovery from destabilisation. Alternatively, if the modifications introduced into domain III acted as degrons then a single mutant copy should be sufficient to promote protein turnover and prevent recovery during TMP withdrawal.

To limit the possibility of recombination the sequence encoding the second copy of domain III was derived from a synthetic, divergent replicase (DVR), which has 100% amino acid similarity to JFH1, but only 66% nucleotide similarity(Accession Number KR140016 (Gomes et al., 2016)). Domain III from this DVR construct, either full length of carrying the Δ2354-2404 deletion, was cloned into either pSGRJFH1*lucNS3-5B(DHFRClover@2442) or pSGRJFH1*lucNS3-5B(DHFRClover@2442)Δ2354-2404 (Appendix 8.6). The resulting constructs are referred to as pSGRJFH1*lucWT/WT(DHFRClover@2442), pSGRJFH1*lucWT/Δ(DHFRClover@2442), pSGRJFH1*lucΔ/WT(DHFRClover@2442) and pSGRJFH1*lucΔ/Δ(DHFRClover@2442), depending on whether the DVR/JFH1 domain III is full length (WT) or carries the 2354-2404 deletion (Δ).

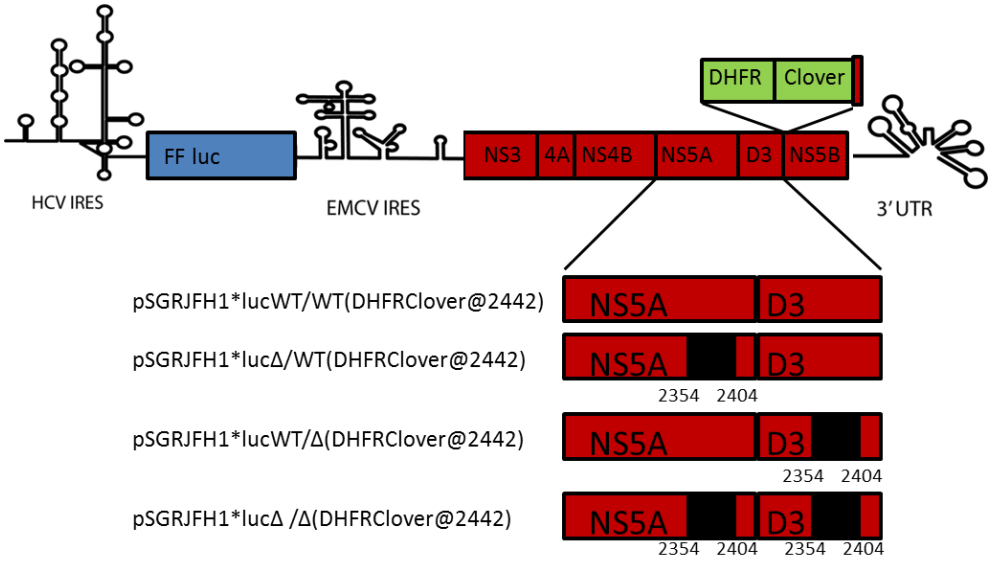

Figure 4-6 **Schematic of the pSGRJFH1*luc(DHFRClover@2442) replicons carrying two fused copies of NS5A Domain III.**

Transcripts of these constructs were transfected into Huh7.5 cells, and replication assays performed in the presence or absence of TMP (Figure 4-7). Cells were also transfected with a positive replication control (pSGRJFH1luc), and a negative replication control (pSGRJFH1lucGND), alongside DHFRClover based replicons carrying only a single copy of domain III (pSGRJFH1*lucNS3-5B(DHFRClover@2442) and pSGRJFH1*lucNS3-5B(DHFRClover@2442)Δ2354-2404).

In the presence of TMP, all replicon constructs carrying duplicated domain III showed robust levels of replication that were comparable to the replicon carrying only a single copy of intact domain III, consistent with the notion that duplicated domain III in NS5A was well tolerated. However, in the absence of TMP replication between these constructs varied. Both the WT-WT as well as the WT-Δ and Δ-WT replicons demonstrated levels of replication at least equal to that of the control construct with a single intact domain III. In fact the WT-WT construct appeared to replicate significantly more robustly that its single domain III counterpart, consistent with the idea that two copies of domain III might counteract the effect of destabilised DHFR more effectively than a single copy. In contrast, the replicon carrying two disrupted copies of domain III, Δ-Δ, exhibited significantly lower resistance to TMP withdrawal, although some evidence of recovery was observed after 72 hours. None-the-less the principle finding that replicons carrying a single full length and single disrupted copy of domain III (WT-Δ and Δ-WT) both showed recovery of replication in the absence of TMP, provides clear evidence that a single full length copy of domain III is protective rather than it being the case that a deleted version of domain III acts as a degron. That the Δ-Δ construct exhibited partial recovery of replication in the absence of TMP re-enforces this conclusion.

A

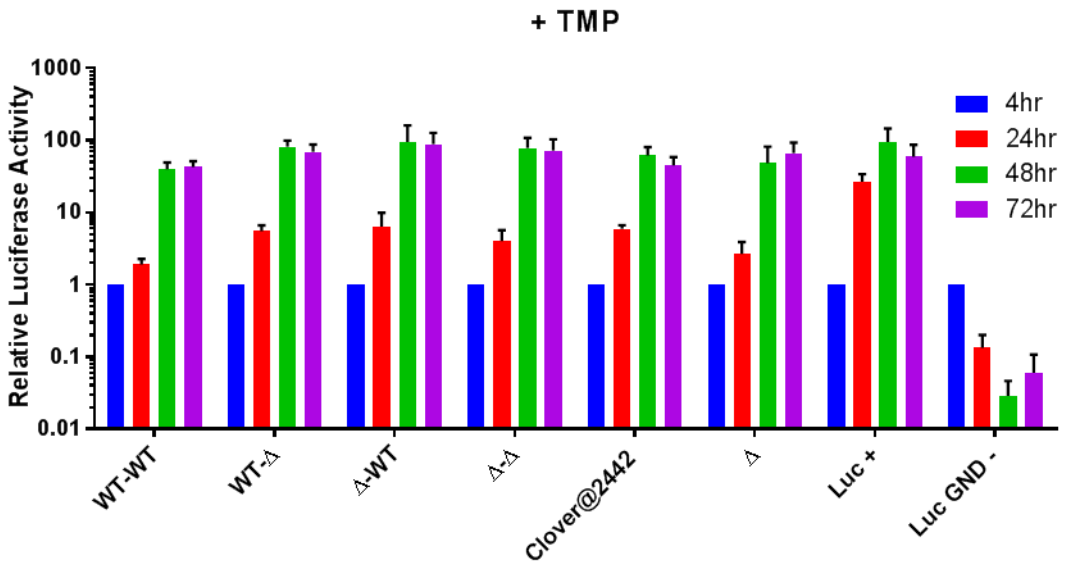

B

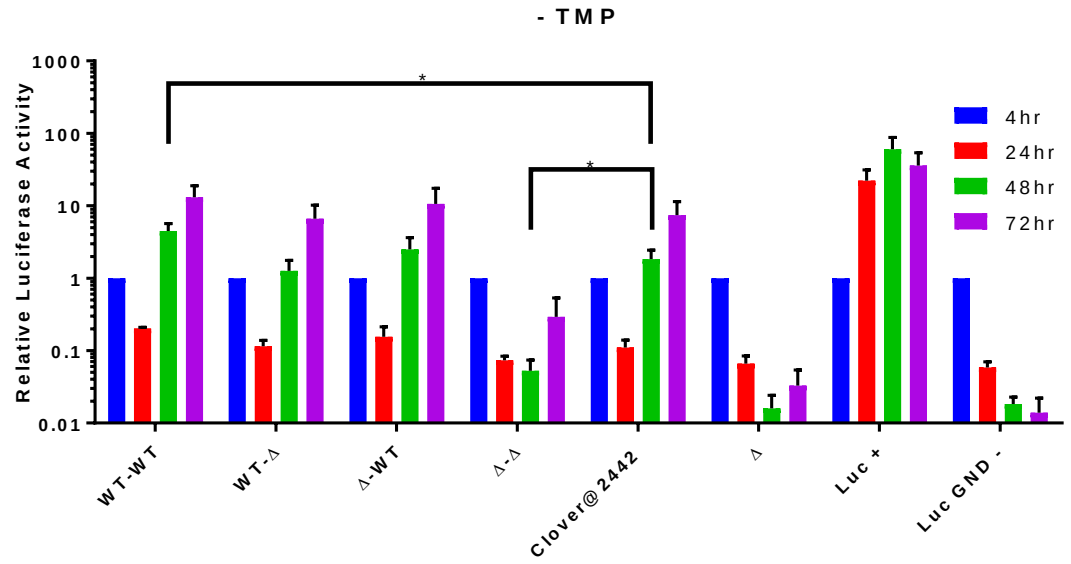

Figure 4-7 **Replication assay of pSGRJFH1*lucNS35B (DHFR-Clover@2442) replicons carrying two fused copies of Domain II**I. Huh7.5 cells were transfected with JFH1 replicons containing two fused copies of domain III, and grown in the presence (A) or absence (B) of 10 μM Trimethoprim. Replication was monitored by luciferase assay 4, 24, 48, and 72 hours post transfection. data represents the mean +/- standard error of 3 experiments. * Represents a significant difference ($p \leq 0.05$) as determined by unpaired T-test.

4.5 SCRAMBLED DOMAIN III

Attempts to map the region of domain III responsible for the proposed protection showed that a relatively large region contributes to rescue, however replication assays with smaller deletions did not suggest that any specific residues within the sequence were vital. This raised the possibility that a characteristic of the region may be responsible for rescue, rather than a specific amino acid sequence. This hypothesis is supported by the variability of this region between isolates; this region carries both highly conserved sequences and a hyper variable domain.

To investigate this possibility a JFH1 replicon was generated in which the 2354-2404 region was randomised (Table 4-1). To ensure that no new motifs or secondary structure was introduced into the protein the randomised sequence was analysed using five prediction programmes, Interpro (Finn et al., 2017), ScanProsite (de Castro et al., 2006), MotifScan (Pagni et al., 2007), NCBI CDD (Marchler-Bauer et al., 2013), and JPRED 4 (Drozdetskiy et al., 2015). None of these identified any motifs of note or suggested that the region would be anything but unstructured (i.e. similar in secondary structure to the sequence being replaced). Scrambling was achieved at the amino acid level and the DNA sequence generated using Invitrogen GeneArt portal. The scrambled amino acid sequence was reverse transcribed for optimal human expression, and flanked by 50 bps of border sequence. The scrambled sequence was purchased as a synthetic DNA String (Thermo Scientific)(Table 8-6), and introduced into a pSGRJFH1*lucNS3-5B(DHFRClover@2442) plasmid by two-step PCR (Appendix 8.7). The resulting construct is referred to as pSGRJFH1*luc(DHFRClover@2442)Scr.

	Amino Acid sequence
WT Sequence	QPPSSGDAGSSTGAGAAESGGPTSPGEPAPSETGSASSMPPLEGEPGDPD
Scrambled Sequence	MSESSATSGGPGEEPADAPPGPASGPTEGPGSGDQSGETAPSTPGASPDS

Table 4-1 **Amino acid sequence of wild type JFH1 NS5A residues 2354-2404 and the scrambled sequence introduced into pSGRJFH1*lucNS3-5B(DHFRClover@2442).**

As in previous experiments a replicon carrying a scrambled domain III and DHFR insert, was introduced into Huh7.5 cells by electroporation which were then incubated in the presence or absence of 10μM TMP. To provide a comparison both full length replicons (pSGRJFH1*lucNS3-5B(DHFRClover@2442) and (pSGRJFH1*lucNS3-5B(DHFRClover@2394)) and a truncated replicons (pSGRJFH1*lucNS3-5B(DHFRClover@2442)Δ2354-2404) were included, alongside a positive (pSGRJFH1*luc) and negative control (pSGRJFH1lucGND).

In the presence of TMP the scrambled replicon demonstrated similar levels of replication as the wild type, confirming that, as with the previous mutations, the modification is well tolerated by the replicon. A similar pattern was observed in the absence of TMP, with the scrambled replicon replicating robustly, albeit with a minor drop relative to the wild type. This indicates that the scrambled domain III retains the ability to protect NS5A from DHFR mediated degradation, possibly suggesting that the protection observed in previous experiments may not be a result of a specific sequence, but rather an intrinsic property of the domain. These will be explored more in Section 4.7.

A

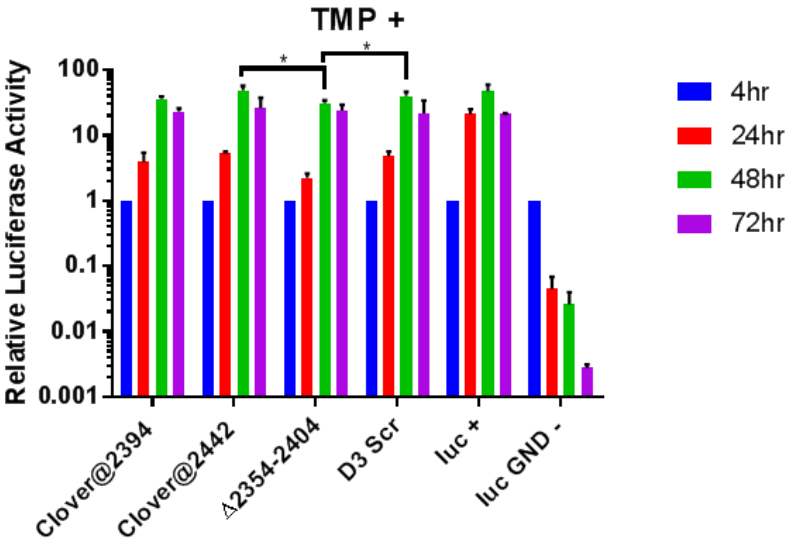

B

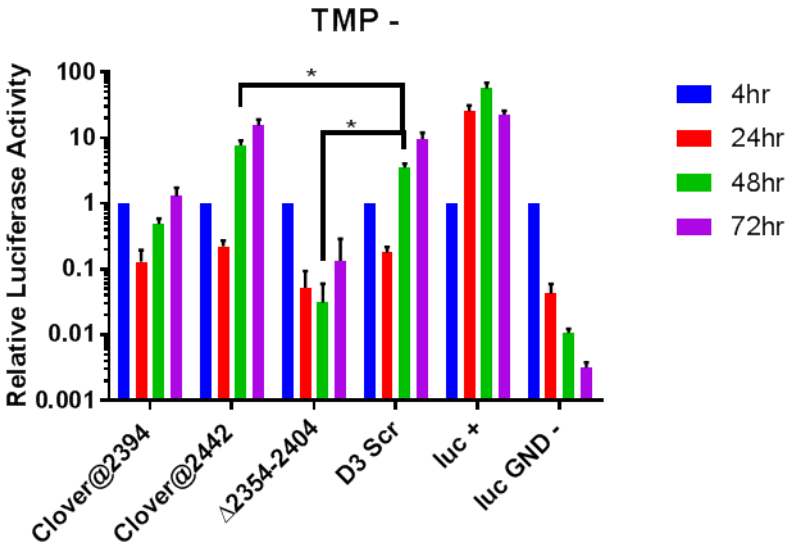

Figure 4-8 **Replication assay of pSGRJFH1*lucNS35B (DHFR-Clover@2442) replicons carrying a Scrambled NS5A domain III.** Huh7.5 cells were transfected with JFH1 replicons containing a scrambled domain III, and grown in the presence (A) or absence (B) of 10 µM Trimethoprim. Replication was monitored by luciferase assay 4, 24, 48, and 72 hours post transfection. Data represents the mean +/- standard error of 3 experiments * Represents a significant difference ($p \leq 0.05$) as determined by unpaired T-test.

4.6 NS3 MUTATION

Up until now all of the work described has been focused on NS5A, however this is but one component of the replication machinery; as discussed above it comes together with the other non-structural proteins to form the replication complex. Due to this close, intertwined relationship that the NS proteins share, it is possible that the activity of domain III may allow NS5A to compensate when other NS proteins are destabilised, preserving the RC as a whole. To investigate this possibility, NS3 was mutated by modification of the N-terminus such that it would be destabilised by the N-end rule; the N-end rule stating that the stability and half-life of a protein are products of its N-terminal amino acid (Gonda et al., 1989). For this work pSGRJFH1*luc constructs were generated carrying an additional amino acid at the N-terminus, connected downstream of a 76 amino acid ubiquitin coding region (Figure 4-9); the principle being that the ubiquitin would be cleaved away from the N-terminus by a cellular hydrolase leaving only the additional amino acid residue (Gonda et al., 1989). This approach was chosen due to the absence of appropriate insertion sites within the other components of the HCV replication complex. Outside of NS5A domain III, no other site within the RC would tolerate the insertion of the DHFR-clover cassette, or similar destabilising domain, without drastically impacting replication. In addition only NS3 was suitable for modification of the N-terminus in such a way as introducing ubiquitin within the polyprotein would affect the cleavage of the individual NS proteins, and therefore impacting replication.

The amino acids added included, a stabilising Alanine residue, a destabilising Glutamine, or an intermediate Tyrosine residue. Two constructs were generated with each residue, one which had a full length NS5A, and one carrying the Δ2354-2404 truncation. The constructs generated carrying these mutations were referred to as pSGRJFH1*lucUbiAla, pSGRJFH1*lucUbiTyr, pSGRJFH1*lucUbiGln, pSGRJFH1*lucUbiAla Δ2354-2404, pSGRJFH1*lucUbiTyr Δ2354-2404, and pSGRJFH1*lucUbiGln Δ2354-2404. Each of these was generated by multi-step PCR (Appendix 8.8).

Replication of these was examined by luciferase assay alongside equivalent control constructs where NS3-5B was expressed without an NS3 extension (Figure 4-10).

Interestingly, replication of the control constructs expressing a truncated NS5A domain III was noticeably reduced compared to the one expressing intact NS5A, a difference that appeared more marked than had been seen when NS5A was expressed as a DHFR-Clover fusion protein, particularly after 24 hours. More perplexing however, were the results obtained from the constructs expressing the NS3-5B replicase as a ubiquitin-fusion product. Firstly, the presence of ubiquitin appeared to suppress replication across all 3 constructions,

something that had not been expected and which frustrated the side-by-side analysis that had been planned. Secondly, it was the constructs which expressed NS3 with the most destabilizing of amino acids that replicated the most effectively, the replicative fitness of the different constructs being Gln>Tyr>Ala. As had been observed with the control constructs, the absence of a full length domain III in NS5A further suppressed replication on top of that already seen from introduction of ubiquitin upstream of NS3.

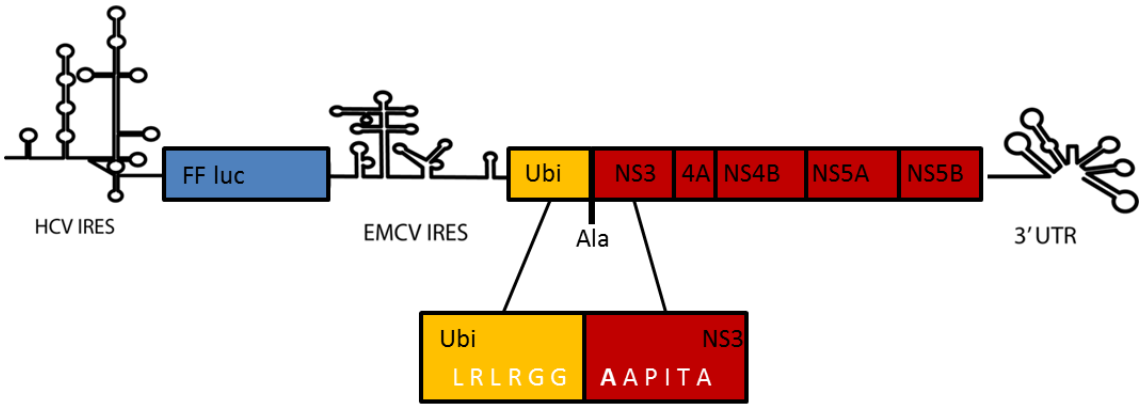

Figure 4-9 **Schematic of the pSGRJFH1*lucUbiAla replicon construct.** In white are the amino acid residues surrounding the Ubiquitin/NS3 boundary, including the additional alanine.

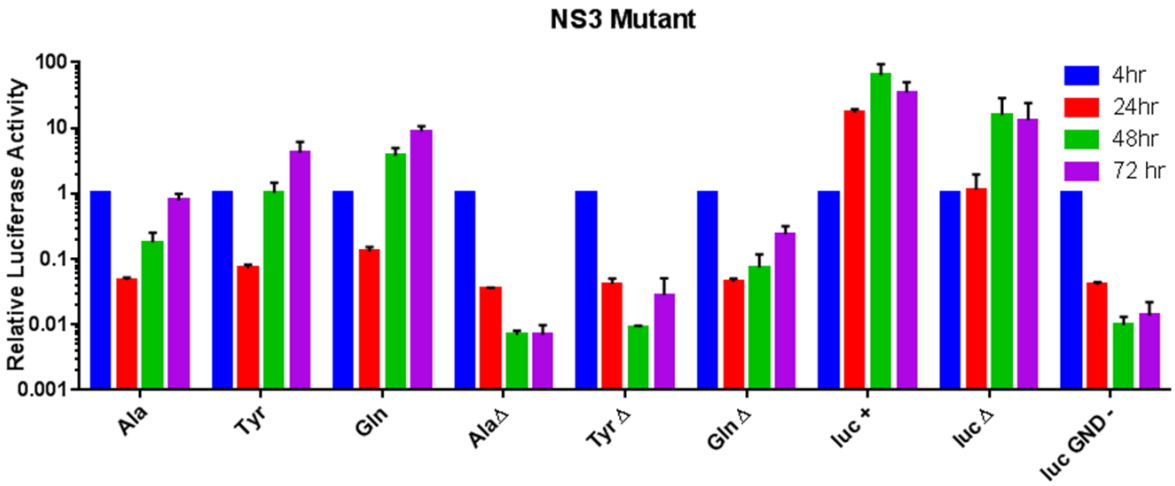

Figure 4-10 **Replication assay of pSGRJFH1*lucUBI NS3 replicons.** Huh7.5 cells were transfected with JFH1 replicons containing a mutant NS3, and/or a truncated NS5A domain III and replication was monitored by luciferase assay 4, 24, 48, and 72 hours post transfection. Data represents the mean +/- standard error of 3 experiments. Due to issues with this assay (discussed in the text) no statistical analysis was performed.

4.7 SUMMARY

This chapter's work focused on attempts to understand the role that domain III plays in rescuing NS5A from DHFR-mediated destabilisation, and to investigate how this may occur.

An early hypothesis was that domain III may recruit another protein that is responsible for this activity. This scenario would fit with the known activity of both domains II and III, which have been shown to form a multitude of protein-protein interactions. In support of this theory was the finding by *Pichlmair et al.* that part of the same region that has been identified in this work is able to form a protein-protein interaction with USP19 (Pichlmair et al., 2012), a protein with deubiquitinase activity. The data here fails to support this relationship however; knockdown of USP19 failed to sensitize full length NS5A to DHFR-mediated degradation. Although this would suggest that USP19 is not involved, there does remain the possibility that another protein may be, or that NS5A can recruit a selection of proteins to achieve the same function. If this were the case then down regulation of USP19 alone might not be sufficient to inhibit recovery.

All of the work described in the previous chapter relied on the assumption that domain III contributes to recovery; however the finding that USP19 was not involved meant that there was no obvious mechanism for this to be the case. This raised the possibility that this early assumption was incorrect. There remained the possibility that the internal insertion (@2394), and the subsequent deletions in domain III, were merely acting as degrons rather than interrupting a novel activity. In certain respects some of the findings in results chapter 1 supported this idea, such as the fact that the 20 amino acids deletions failed to identify key binding sites for an alternative binding partner. To address this possibility JFH1 replicons were generated that carried two fused copies of domain III, either full length or carrying the Δ2354-2404 truncation. Had the deletion been acting as a degron it was expected that a single copy of domain III carrying the truncation should block replication. Replication data from these replicons supports the initial hypothesis, with a single functional domain III being sufficient to allow replication under destabilising conditions. Additionally even the replicon carrying two Δ2354-2404 truncations proved able to replicate upon TMP withdrawal, albeit to a far lesser degree, suggesting that enough of the activity was being retained within the 2405-2415 region for partial recovery.

Although the activity of domain III had been confirmed, the lack of a binding partner, or even a binding site, meant that the mechanism by which domain III functions remained elusive. This was further compounded by the earlier finding that domain III may play a role in

preserving NS5A in other genotypes. Whilst the proposed active region of domain III, 2354-2415 in JFH1, carries some highly conserved motifs, the majority consists of highly variable sequence, including both the hypervariable V3 domain and half of the 20 amino acid sequence present in only genotype 2 isolates. One similarity shared by the two genotypes however is lack of structure and complexity. Could these factors contribute to the activity of domain III? To further explore this, the 2354-2404 region of JFH1 was scrambled, randomising the sequence, but maintaining the same amino acid composition. Remarkably, scrambled replicons retained the ability to survive DHFR-mediated destabilisation, showing that scrambling had had little impact on the protective activity of domain III. This suggests that it is not the primary structure of the protein that is important and that rather than functioning through a protein-protein interaction or enzymatic activity, both of which would be ablated by scrambling, domain III may function through an intrinsic property.

One property that may impact domain III is the amino acid composition. When compared to the surrounding sequence the 2354-2415 region of domain III shows considerably lower complexity, with 7 amino acids (A, D, E, G, P, S, T) representing 87% of the residues present in JFH1, and 85% in Con1. This low complexity is made further apparent by the lack of both aromatic and positively charged amino acids within JFH1. Several other isolates do carry positively charged or aromatic residues, however these are rare, and fall outside of the highly conserved sequence. In contrast both non-polar and negatively charged residues are relatively common, with both hydrophilic and hydrophobic residues spread throughout the sequence of interest.

Furthermore when run through a SEG analysis, to analyse the complexity of the amino acid sequence, the consensus sequence of the 2354-2415 sequence comes back as low complexity (Wootton, 1994), and the same is true of both JFH1 and Con1 sequences. Low complexity is known to inhibit proteasomal degradation, by hindering the entry of peptides into the 20S catalytic core (Aufderheide et al., 2015). Could this explain the activity observed? It is possible. Within this work the destabilisation has been achieved by destabilising the conjugated DHFR which is likely to result in proteasomal degradation. It is possible that the lack of complexity within domain III acts to delay progression of NS5A into the proteasome. Proteasomal degradation is widely reported to start at unstructured proteins, and so domain III may function as a shield, inhibiting the progression of the proteasome and protecting the functions of the upstream domains. A number of possible outcomes exist as to how this may ultimately allow rescue. The simplest is that by delaying progress into the proteasome, domain III extends the half-life, and therefore functionality of NS5A. An alternative is that the

delay provides NS5A sufficient time to form complexes with either cellular or viral proteins, sufficient to allow it to escape degradation.

Unfortunately it has not been possible to determine whether or not NS5A domain III can rescue replication when other NS proteins are being destabilised. Whilst addition of additional amino acids at the N-terminus of NS3 successfully resulted in variations in replication, the impacts that the mutations had was opposite to that which was expected. Due to this it was not possible to distinguish the impact of the NS3 mutation and the impact of the NS5A truncation.

Why the replicons expressing NS3 as a ubiquitin fusion product behaved in the manner they did is unclear as the fusion of ubiquitin upstream of proteins to generate an altered N-terminal residue is common practise. For example initial studies into the impact of N-terminal amino acid on protein stability by Gonda *et al* made use of this method to generate β-galactosidase samples carrying each of the 20 amino acids, and only reported problems with Ubi-Pro (Gonda et al., 1989). Furthermore ubiquitin has previously been successfully fused to NS3, albeit in the context of a hygromycin-ubiquitin fusion peptide. More recent studies have shown however that in some cases the presence of ubiquitin at the N-terminus can be recognised by an E3 ligase, leading to polyubiquitination and proteasomal degradation rather than hydrolysis of the ubiquitin tag (Kravtsova-Ivantsiv and Ciechanover, 2012). This may explain the unexpected results achieved using the ubiquitin-NS3 mutants; it is possible that Ubiquitin in the context of NS3 is recognised as a degron, with the Ala and Tyr sequences being recognised more readily that Gln.

As to why the impact of NS3 mutation varies between those replicons carrying a WT NS5A and those carrying the 2354-2404 truncation, no definitive answer is clear. The most likely explanation is that while each of the two types of mutations alone impair replication, in combination these changes to NS3 and NS5A cause a catastrophic loss of function that the RC cannot overcome.

5 RESULTS CHAPTER 3 – INVESTIGATING THE MECHANISM BEHIND DOMAIN III RESCUE OF NS5A FROM DHFR MEDIATED DEGRADATION

5.1 INTRODUCTION

This chapter will focus on my attempts to understand the potential benefits that domain III may convey to NS5A, and HCV as a whole. Potential benefits that were considered included interferon resistance and a possible reduction in antigen presentation. In addition, work described in this chapter sought to establish any role domain III might play in enhancing NS5A stability.

5.1.1 INTERFERON

Interferons are a group of signalling proteins so named for their ability to interfere with viral infections. IFNα was the first therapy introduced for the treatment of HCV infections, and although it has since been replaced as the principal component of treatment by the more effective DAAs (1.7), it remains an important part of the immune response to HCV infection and in the treatment of many of those most at risk.

The release of IFNs mainly occurs as a result of pathogen detection through recognition of Pathogen Associated Molecular Pattern (PAMP) or Damage Associated Molecular Pattern (DAMP) molecules by Pattern Recognition Receptors (PRRs). A large number of PRRs exist which recognise many different PAMPs and DAMPs, making the induction of IFNs highly complex (reviewed (Haller et al., 2006)). Regardless of the PRR that is activated, a signal pathway is triggered leading to the activation of a transcription factor such as Interferon Regulatory Factors 3 and 7, or Nuclear factor kappa-light-chain-enhancer of activated B cells. Once activated, these are transported to the nucleus where they bind upstream of the IFN genes, triggering their expression. Analagous systems exist to control the expression of the different IFNs, however slight variation does exist in the molecules involved and their feedback (Levy et al., 2011). When released by host cells, interferons induce an antiviral response in neighbouring cells, with the ultimate aim to contain the infection.

In the case of type I interferons such as IFNα and IFNβ, these bind to the IFN-receptor on the cell surface, a heterodimer of IFNα Receptor1 and 2, triggering a signal cascade (reviewed (Ivashkiv and Donlin, 2014)). Binding of IFNα to the receptors triggers activation of the associated Janus Kinases (JAKs), JAK1 and TYK2, leading to the phosphorylation of the cytoplasmic domains of the receptor complexes. This phosphorylation generates a binding

site for the Signal Transducer and Activator of Transcription (STAT) 1 and 2 proteins, which are then recruited and themselves phosphorylated by the activity of the JAK protein. The phosphorylated STAT proteins form a heterodimer which then associates with the Interferon Regulatory Factor 9 (IRF-9), forming the Interferon-stimulated gene factor 3 (ISGF3) transcription factor. This enters the nucleus of the cell and binds to the Interferon Stimulated Response Element (ISRE), driving the expression of a host of IFN stimulated genes (ISG). ISGs have a vast array of functions, and many have been shown to directly interact with HCV (reviewed(Metz et al., 2013)). A few examples will be discussed below.

Proteins Kinase R (PKR) is a cytosolic detector of dsRNA, a product only present during viral infections. Binding of PKR to dsRNA causes it to homodimerize activating the kinase domain. This phosphorylates eukaryotic initiation factor 2 α (eIF2α), inhibiting all cap dependent translation within the cell. *In vitro* studies have shown that during HCV infection PKR is capable of binding to RNA elements within the 5' UTR of the genome (Shimoike et al., 2009). The precise role that PKR plays in inhibiting HCV replication is controversial, as although some studies have shown activated PKR to have an inhibitory effect (Wang et al., 2003, Pflugheber et al., 2002, Tokumoto et al., 2007), others have suggested that PKR actually promotes HCV replication (Garaigorta and Chisari, 2009, Arnaud et al., 2010), potentially by inhibiting the translation of other ISGs without impacting eIF2α independent translation of HCV proteins.

The Interferon Induced Transmembrane Proteins (IFITM) 1, 2, and 3 have also been demonstrated to have inhibitory effects on both viral entry and replication (Narayana et al., 2015). IFITM1 has shown been to bind to two HCV co-receptors, CD81 and Occludin, and it has therefore been proposed that IFITM1 may block the interaction of the two, inhibiting a crucial step in HCV entry (Wilkins et al., 2013). In contrast IFITM2 and 3 both localise to late endosomes, suggesting that these inhibit late stage viral entry, possibly by targeting the virion for degradation (Narayana et al., 2015). There is also some evidence to suggest that IFITM1 and 3 are capable of inhibiting HCV translation and replication (Yao et al., 2011, Raychoudhuri et al., 2011), however the precise mechanisms behind this is unclear.

Another ISG shown to impact HCV infection is the RNase L pathway (Han and Barton, 2002). RNase L is an endonuclease that cleaves single stranded RNA, both viral and cellular. Initially inactive, RNase L is activated by 2´,5´-oligoadenylate generated by the IFN inducible 2´,5´ oligoadenylate synthetases. RNase L cleavage mainly occurs after UU or UA dinucleotides. These occur with a higher frequency within the genomes of IFN sensitive genotypes and IFN

resistant genotypes (Han and Barton, 2002), supporting a role for RNase L in controlling HCV infection (Metz et al., 2013).

As well as having direct antiviral effects, IFN signalling also modulates the expression of PRRs. These are normally present in cells at low levels, however, IFN signalling greatly enhances their expression, thereby priming the cell to detect invading pathogens. One example is the RIG-I protein, which detects double stranded RNA within the cytoplasm. A number of studies have shown that RIG-I is an effective detector of HCV infection both *in vitro* and *in vivo* (Saito et al., 2008, Schnell et al., 2012, Zhang et al., 2009). Interestingly it has been reported that at least one product of RNase L cleavage of the HCV genome is a potent activator of RIG-I (Malathi et al., 2010), demonstrating the synergism between ISGs.

A number of ISGs have also been linked to degradation of NS5A, possibly explaining its need to develop a protective activity. One example that has been found to target NS5A is TRIM22. This has been found to cause ubiquitination of NS5A, leading to its degradation by the proteasome (Yang et al., 2016). Another is the S-phase Kinase Associated Protein 2 (SKP2). As with TRIM22, SKP2 is an E3 ubiquitin ligase, that has been linked to polyubiquitination of NS5A (Xue et al., 2016). Importantly for this work, it was found that mutation in domain III was capable of inhibiting this activity.

These examples are just some of the ISGs that have been shown to have an impact on HCV infection, and this interaction between IFN and HCV remains an important avenue for research. IFNα is still an important component of anti-HCV therapy, particularly for those for whom the Direct Acting Antivirals are too expensive. Furthermore one of the key determinates of successful therapy or spontaneous clearance is associated with the *IL28* locus (Abe et al., 2010, Ge et al., 2009, Suppiah et al., 2009, Tanaka et al., 2009), which encodes IFN λ, a type III interferon.

As mentioned previously NS5A has been widely studied due to its role in IFN resistance. Work later in this chapter details attempts to expand upon this by studying the impact of domain III truncation on the sensitivity of JFH1 replicons to IFNs.

5.1.2 ANTIGEN PRESENTATION

In contrast to the IFNs, which can be stimulated by the detection of basic signals such as the presence of double stranded RNA, the adaptive immune response requires a more specific activation. In the case of T-cells, these require the detection of antigenic peptide on the surface of infected cells. This depends on the Major Histocompatibility Complexes (MHCs), which are essential to the presentation of antigenic peptide in the correct context to be

recognised by T-cells (reviewed (Vyas et al., 2008, van de Weijer et al., 2015)). MHC class II is mostly restricted to the professional antigen presenting cell such as the dendritic cells. These cells take up extracellular material and present it to stimulate naïve T-cells. More important to this work, however, is MHC class I.

MHC class I is expressed by all nucleated cells within the human body and is responsible for presenting peptide on the cell surface, such that it can be detected by CD8+ cytotoxic T cells. This allows the immune system to monitor events within the cells, and therefore to respond accordingly. As viruses co-opt the cells own machinery, their proteins are also presented by MHC, and as such this represents an important method by which viral infections are detected.

MHC Class I complexes are heterodimers, formed from an α subunit bound non-covalently to a β2-microglobulin. The α subunit consists of three domains numbered 1, 2, and 3, with domains 1 and 2 folding to form the peptide binding groove. A transmembrane domain located within the α subunit binds the entire complex to the cell surface.

The MHC subunits are co-translationally translocated into the ER, where chaperone proteins including calnexin, calreticulin, tapasin and Erp57 (Sadasivan et al., 1996), stabilize the complex, and aid it in folding into the correct conformation. Within the ER calnexin binds to the α subunit, stabilizing it until it is able to bind to the β2-microglobulin, at which point calnexin dissociates. Unloaded MHC is inherently unstable and is therefore stabilised within the ER by binding of Erp57 and calreticulin chaperone proteins. Once stabilised the complex is ready for peptide loading.

The bulk of peptides presented by MHC Class I are generated by proteasomal degradation of cytoplasmic proteins (Rock and Goldberg, 1999). These are cleaved into small peptide fragments, approximately 8-16 amino acids in length, which are then released back into the cytoplasm. To bring these fragments into contact with MHC they must first be transported into the ER lumen. This is achieved by the Transported Associated with Antigen Processing (TAP), which interacts with MHC class I via tapasin, a chaperone essential for efficient loading of the MHC complex. Once cytosolic peptide has bound to a peptide binding pocket TAP undergoes a conformation change, driven by ATP hydrolysis, leading to the translocation of peptide fragments into the ER lumen.

Once an appropriate peptide fragment has bound to MHC, the chaperone proteins dissociate, and the complex is released from the ER. It is transported from the ER to the cell surface, where the presented peptide is exposed to CD+ T cells.

Should the scanning T cells detect an abnormality they become activated, almost always leading to the induction of apoptosis within the presenting cell. Alongside the CD8+ cells the peptide profile of cells is also monitored by Natural Killer (NK) cells, however rather than being activated by MHC, NK cells are deactivated. In this way NK cells are able to detect cells in which MHC is being suppressed, and therefore preserve the ability to mount an immune response.

Many viruses have been found to interfere with this process to delay their detection, and therefore inhibit the immune response. Approaches used by viruses include, inhibiting the activity of TAP thereby limiting the availability of peptide for presentation, inhibiting the transport of MHC to the cell surface, and even inducing the return of loaded MHC from the cell surface back to the ER. There have only been a limited number of studies into the ability of HCV to inhibit antigen presentation, and there is little consensus within them. Work by Tardif and Siddiqui has shown that expression of MHC is downregulated in replicon infected cells lines (Tardif and Siddiqui, 2003), whilst Herzer *et al* has demonstrated upregulation of the MHC class I expression by core protein(Herzer et al., 2003). In addition, work by Moradpour *et al* showed that antigen processing and presentation was not impacted by overexpression of HCV proteins (Moradpour et al., 2001). More recently however Kang *et al* have shown that MHC expression is inhibited in HCV infected cells using the HCV cell culture system (Kang et al., 2014). The conflicting nature of these data means that the precise interaction between HCV and antigen presentation remains enigmatic, however it does appear that one exists. One aspect of the work in this chapter examined a potential role for NS5A domain III in limiting antigen presentation.

5.2 PRODUCTION OF STABLY TRANSFECTED CELL LINES

All previously described work has focused on the impact of NS5A on replication, the implication being that domain III is involved in promoting the stability of the protein. It was therefore important to verify this. As direct observation of protein stability ideally required cell lines where NS5A expression was at a steady state, G418 resistant replicons were made. To achieve this the neomycin resistance gene NPTII from pSGRJFH1Neo (Wakita et al., 2005) was cloned into the pSGRJFH1*, pSGRJFH1*NS3-5B(DHFRclover@2394), pSGRJFH1*NS3-5B(DHFRclover@2442), pSGRJFH1*NS3-5B(DHFRclover@2442)Δ2328-2353, pSGRJFH1*NS3-5B(DHFRclover@2442)Δ2354-2404, and pSGRJFH1*NS3-5B(DHFRclover@2442)Δ2404-2435 constructs (Appendix 8.9).

Transcripts of these were electroporated into Huh7.5 cells and 48hr post transfection the cells were placed under G418 selection at 650 μg/ml, in the presence of 10 mM TMP, to allow the emergence of resistant colonies. Three weeks post transfection the cells were harvested to yield stably transfected cell lines and Western blotting was used to confirm the expression of Neomycin phosphotransferase (NPT), NS3, and NS5A (Figure 5-1). Initial attempts to blot for NS5A directly using a polyclonal anti-NS5A antibody failed to detect NS5A carrying the Δ2354-2404 truncation, a result later concluded to be due to the antibody preferentially recognising the region of domain III deleted in the Δ2354-2404 and Δ2404-2435 replicons. Instead indirect detection of NS5A was achieved using a polyclonal anti-GFP that can recognise the Clover antigen present in the DHFR-clover cassette and which is in turn fused to NS5A. Generation of these cells lines proved problematic with the cell lines demonstrating minor variance in the expression of detectable NS5A, NPT, and NS3. Subsequent repetitions of the selection yielded similar results, indicating that this variance is a factor of the replicons themselves; it appears that the fusion proteins carrying the various deletions and insertions may differ inherently in stability.

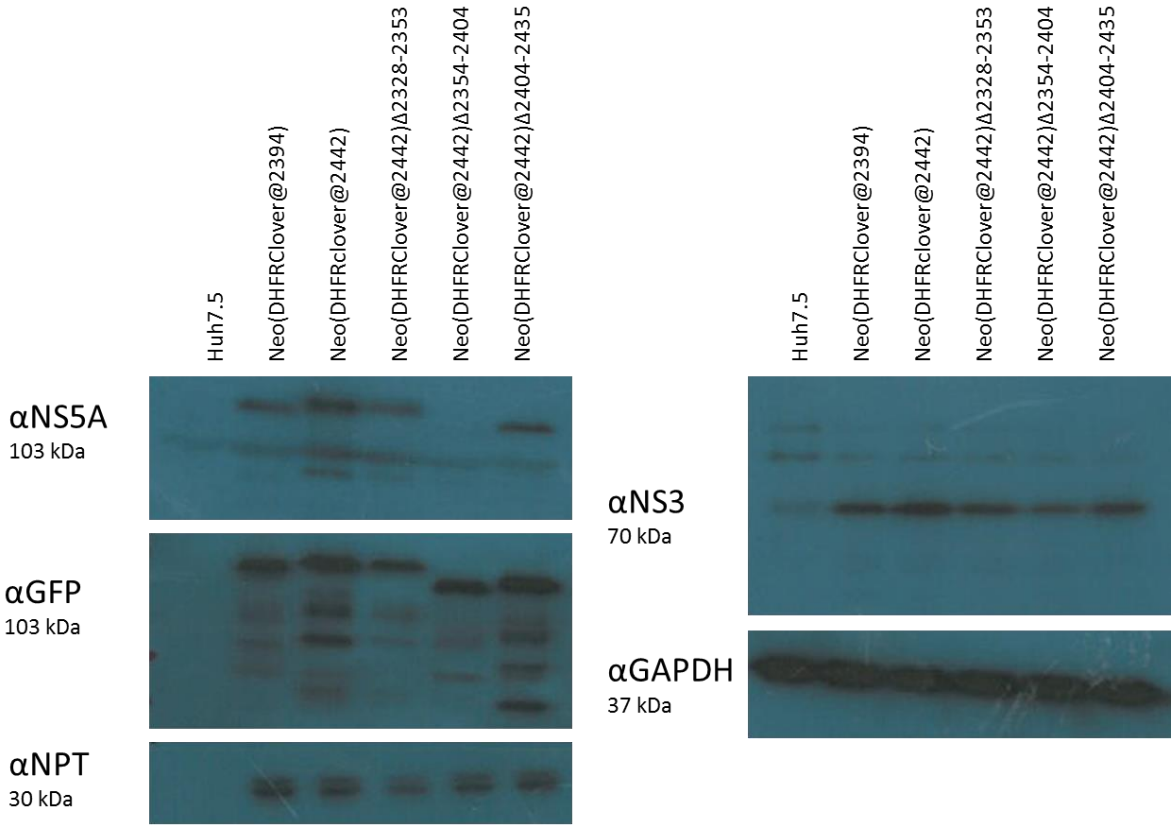

Figure 5-1 **Expression of NS5A, NPT and NS3, by Huh7.5 cells stably transfected with JFH1 replicons**. Stably transfected cells were lysed in RIPA buffer + 2 x complete protease inhibitor. Expression of NS5A, NPT, NS3, and GAPDH was determined by western blot. The NS3 antibody displayed some cross-reactivity to a host protein of a similar molecular size.

5.3 DETERMINING THE PATHWAY OF NS5A BREAKDOWN

Within cells, protein can be degraded by the activity of either the proteasome or the lysosome, with both activities being partially enhanced by polyubiquitination of protein substrates. Assessment of which route of degradation is occurring can be achieved by treatment of cells with either Carbobenzoxy-Leu-Leu-Leucinal (MG132) and Chloroquine (CQ) which block proteasome and lysosome activity respectively. MG132 is a peptide-aldehyde which covalently binds to the active site of the β-subunits of the 20S proteasome thereby blocking its proteolytic activity. CQ is a lysosomotropic agent that accumulates in lysosome and endosomes. It raises the pH within the lysosome inhibiting the activity of lysosomal enzyme that function at lower pH, and also inhibits the fusion of lysosomes with autophagosomes.

A preliminary experiment was first performed to determine the ideal concentrations of MG132 and CQ to use to maximise inhibition of these degradation pathways while minimising cytotoxic effects. In the case of chloroquine inhibition of the lysosome was determined by monitoring the ratio of the LC3-I and LC3-II forms of the microtubule-associated protein 1A/1B-light chain 3 (LC3) protein. During autophagy LC3-I becomes conjugated to phosphatidylethanolamine to form LC3-II, which is recruited to the membrane of autophagosomes, where it is eventually internalised and recycled. Inhibition of the lysosome prevents the recycling of LC3, resulting in a build-up of LC3-II on the cytoplasmic face of autophagosome. The shift in LC3-I into LC3-II can therefore be used as a method to detect the activity of lysosomes. To ascertain the ideal concentration of chloroquine to use, Huh7.5 cells were transfected with a plasmid expressing GFP-conjugated to LC3 (a gift from Prof. Mark Harris), and treated with between 100 μM and 12.5 μM chloroquine for 24 hours. Toxicity was determined by observing morphological changes, whilst inhibition of lysosomal activity was detected by western blotting for GFP-LC3.

Treatment with chloroquine proved toxic across all concentration, resulting in a visible change in morphology, and inhibition of growth within 12 hours (Figure 5-2), although this was most visible in those cells treated with 100 μM. Toxicity proved so severe in this initial experiment that the planned 24 hour incubation was cut short and reduced to 20 hours. Against the increased toxicity, treatment of cells with 100 μM CQ resulted in the most dramatic of LC3-I to LC3-II, which suggested that an even higher concentration may be more effective. Despite this possibility it was essential to balance effect the inhibitory effect with toxicity and the decision was made to use a concentration of 100 μM during subsequent work, with the cells being left for a maximum of 12 hours.

Optimisation of MG132 was achieved using a similar method as that described for Chloroquine. Huh7.5 cells were transfected with pCDNA3.1 expressing a HA-tagged Ubiquitin, and treated with MG132 at concentrations ranging from 5 μM to 20 μM, over a 24 hour period. After 24 hours the cells were lysed and a Western blot was performed to observe the build-up of HA-Ubiquitin tagged products. Concurrently the treated cells were observed for morphological changes to determine toxicity.

As with Chloroquine, MG132 treatment led to cytotoxicity such that at 24 hours cells were rounding up and developing large numbers of inclusion bodies (Figure 5-3). Unsurprisingly this proved concentration dependent, with higher levels of cytotoxic effects observed at higher concentrations of MG132. This toxicity correlates to the inhibition of the proteasome, with a build-up of larger tagged products evident at all 3 concentrations. Whilst treatment with 10 μM resulted in considerable cell death, it also demonstrated increased inhibition of the proteasome compared to 5 μM, and more importantly didn't trigger the most noticeable cytotoxic effect until quite close to the 24 hour time point. It was therefore decided that for future experiments, as with CQ, cells would be treated with MG132 for 12 hours, thus achieving an acceptable balance between toxicity and length of time that protein stability could be monitored.

As the stability experiments planned benefitted from being able to block new protein synthesis to better monitor pre-existing protein degradation, Huh7.5 cells were also incubated in media supplemented with cycloheximide, at 10 μg/ml for 24 hours, to assess whether blocking protein synthesis would be possible. Huh7.5 cells appeared to be tolerant to cycloheximide; showing little if any morphological change (Figure 5-4). It was therefore decided to include cycloheximide in future experiments

With optimal conditions determined, it was possible to use cycloheximide, chloroquine and MG132, to observe the stability of mutant NS5A. Stably transfected cells were treated with cycloheximide and either chloroquine or MG132, in either the presence or absence of 10 μM TMP and incubated for 12 hours. Lysates from these cells were then used to observe the change in detectable NS5A over the 12 hour incubation.

Preliminary observations provided evidence that modification of NS5A might have a detrimental impact on protein stability. Both the Δ2354-2404 and Δ24045-2435 cell lines showed a drop in detectable NS5A upon TMP withdrawal (compare lanes 2 and 5), not present in either the Clover@2442, or Δ2328-2353 cell lines. Interestingly, although the Clover@2394 cell line did show evidence of a drop in protein stability, this was far less apparent than in the two deletion carrying replicons, indicating that insertions into domain

III were much better tolerated than deletions. However, further interpretation of the data was hindered by some of the unexpected results from when cells were treated with either MG132 or CQ. In the case of the Δ2354-2404 construct, both drugs appeared to increase the amount of NS5A present when the protein had been 'destabilised' by TMP withdrawal (compare lane 5 to lanes 6 and 7), although MG12 had the more prominent effect. In contrast, CQ seemed to further reduce the amount of NS5A present in the Δ2404-2435 cells, while MG132 caused a heightened level of NS5A to appear. Taken at face value, this data is consistent with the hypothesis that NS5A domain III does counteract an endogenous degradation pathway in the cell, and given the use of DHFR to drive degradation, poly-ubiquitination is almost certainly involved. Furthermore, while the data does not exclude a role for both degradation pathways in the disappearance of NS5A-DHFR-Clover, the evidence favours the proteasome playing a more prominent role.

Unfortunately, numerous repeats of this experiment generated variable results; for example in one such repeat the major band was all but invisible, replaced with multiple degradation bands. As such it was decided that an alternative approach was required to better elucidate the interaction between NS5A and protein degradation.

A

Untransfected control

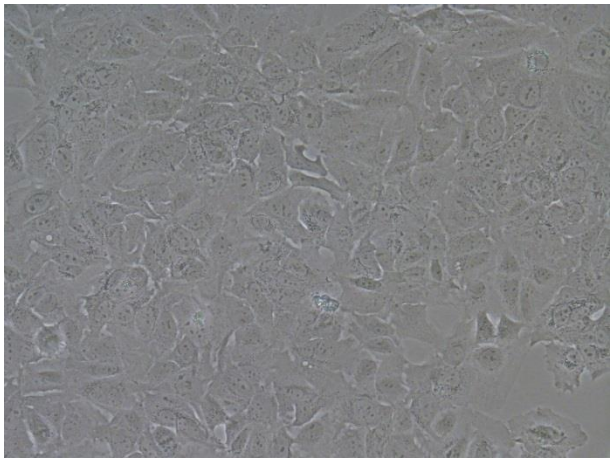

0 µM Chloroquine (Mock treated)

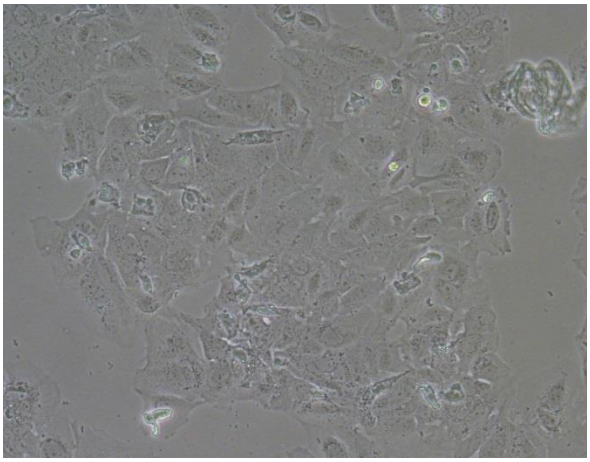

12.5 µM Chloroquine

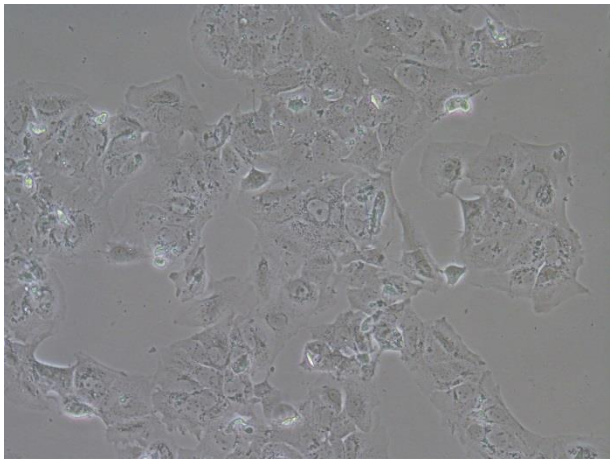

100 µM Chloroquine

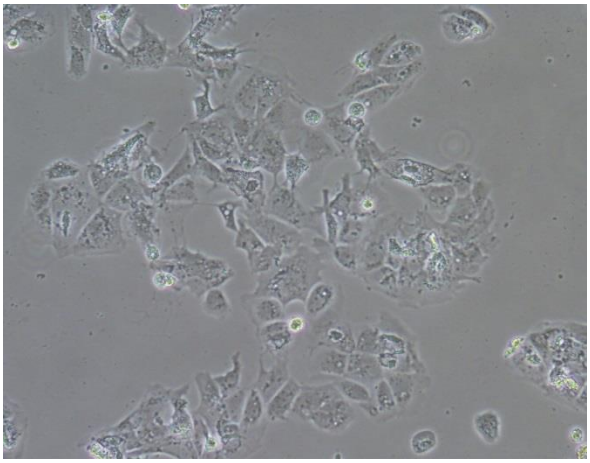

B

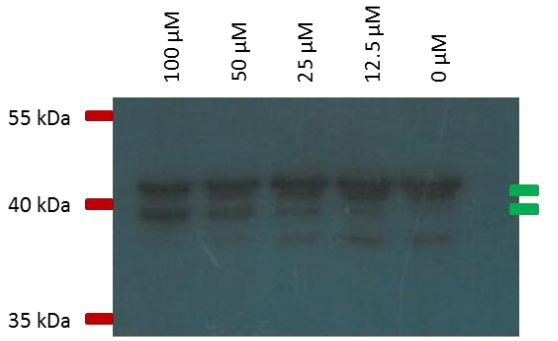

Figure 5-2 **Determining the optimal concentration of chloroquine to use with Huh7.5 cells.** Huh7.5 cells were transfected with pEGFP-LC3, expressing a GFP tagged LC3 peptide. These were incubated in the presence of 12.5, 25, 50, or 100 µM chloroquine for 24 hours, or mock treated with DMSO. (A) Toxicity was monitored by light microscopy to observe morphological changes. (Images captured at 12 hours) (B) Inhibition of the lysosome was determined by the shift of LC3-I to LC3-II. This was detected by western blot.

A

Untransfected control

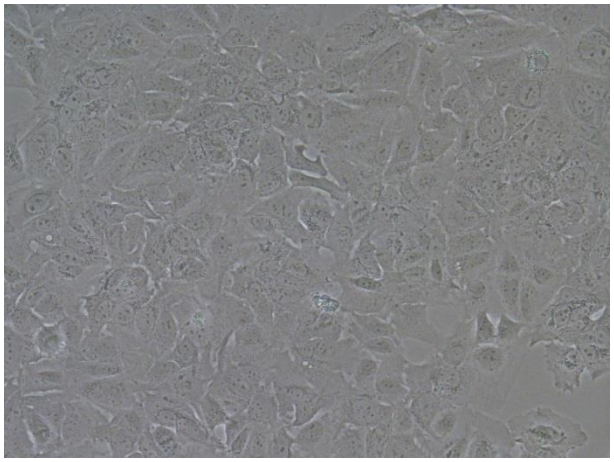

0 µM MG132 (Mock Treated)

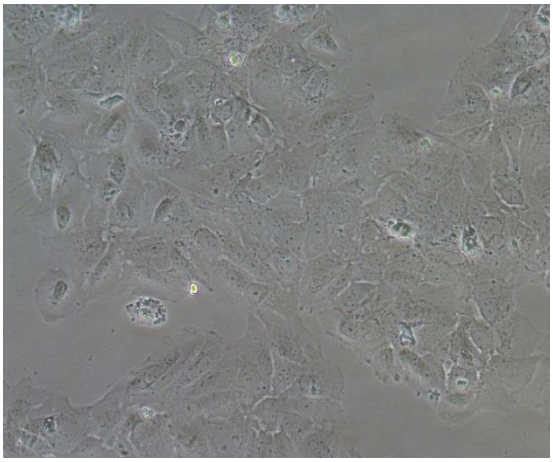

5 µM MG132

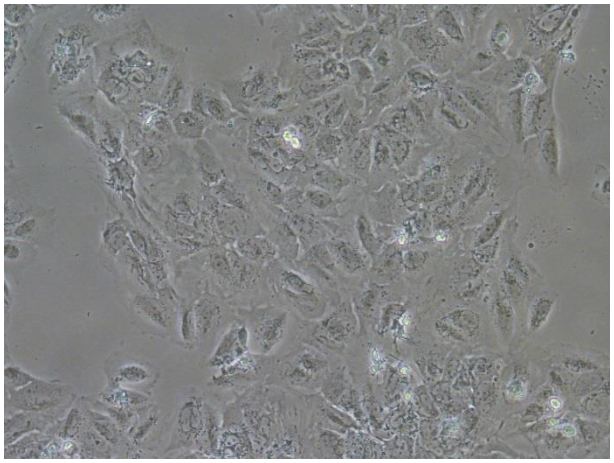

20 µM MG132

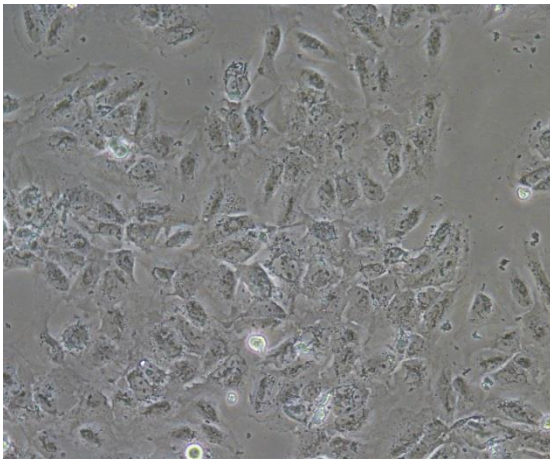

B

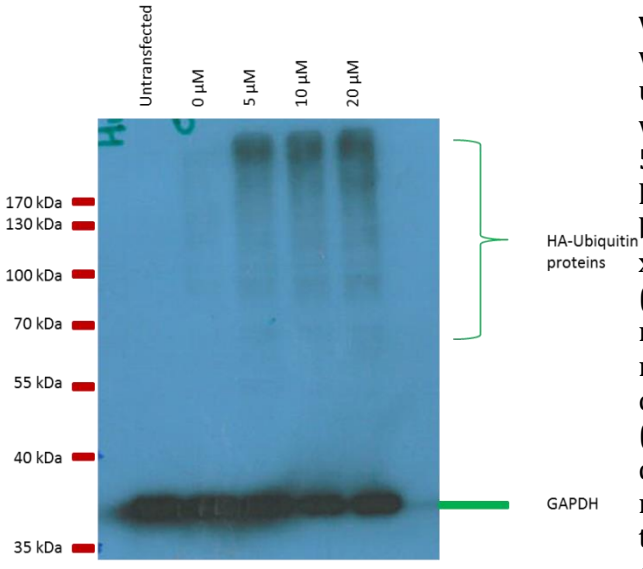

Figure 5-3 **Determining the optimal concentration of MG132 to use with Huh7.5 cells**. Huh7.5 cells were transfected with pCDNA3.1-ha-ubi, expressing ha ubiquitin. These were incubated in the presence of 5,10, or 20 µM chloroquine for 24 hours, or mock treated with DMSO, before being lysed in RIPA buffer + 2 x Complete Protease Inhibitor.
(A) Toxicity was monitored by light microscopy to observe morphological changes.(Images captured at 12 hours)
(B) Inhibition of the proteasome was determined by the build-up of High molecular weight waste proteins tagged with HA-Ubiquitin. This was detected by western blot.

0 µg/ml Cycloheximide 10 µg/ml Cycloheximide

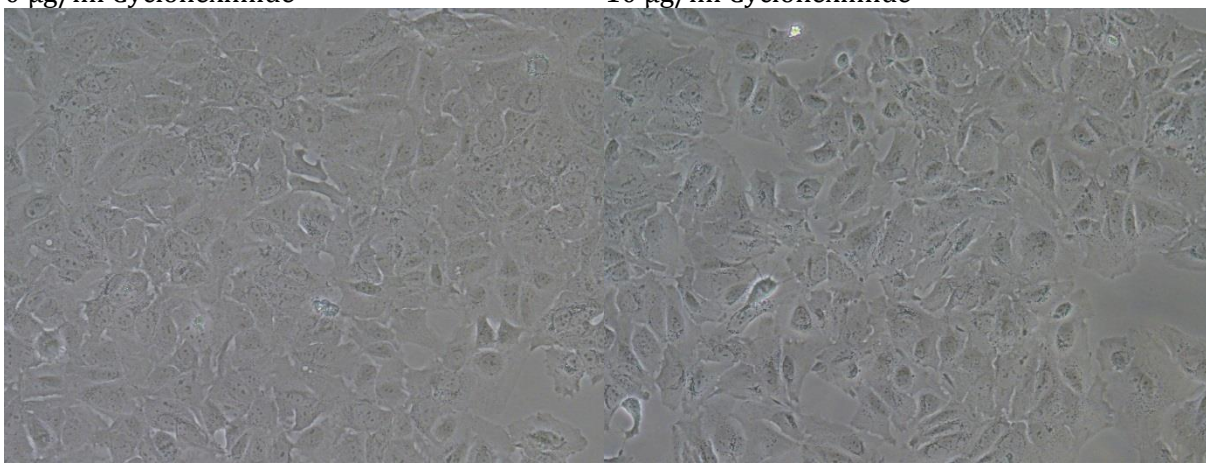

Figure 5-4 **Determining the sensitivity of Huh7.5 cells to cycloheximide concentrations sufficient to inhibit translation**. Huh7.5 cells were incubated for 24 hours in the presence of 0 or 10 µg/ml cycloheximide for 24 hours. Toxicity was monitored by light microscope. (Images captured at 12 hours)

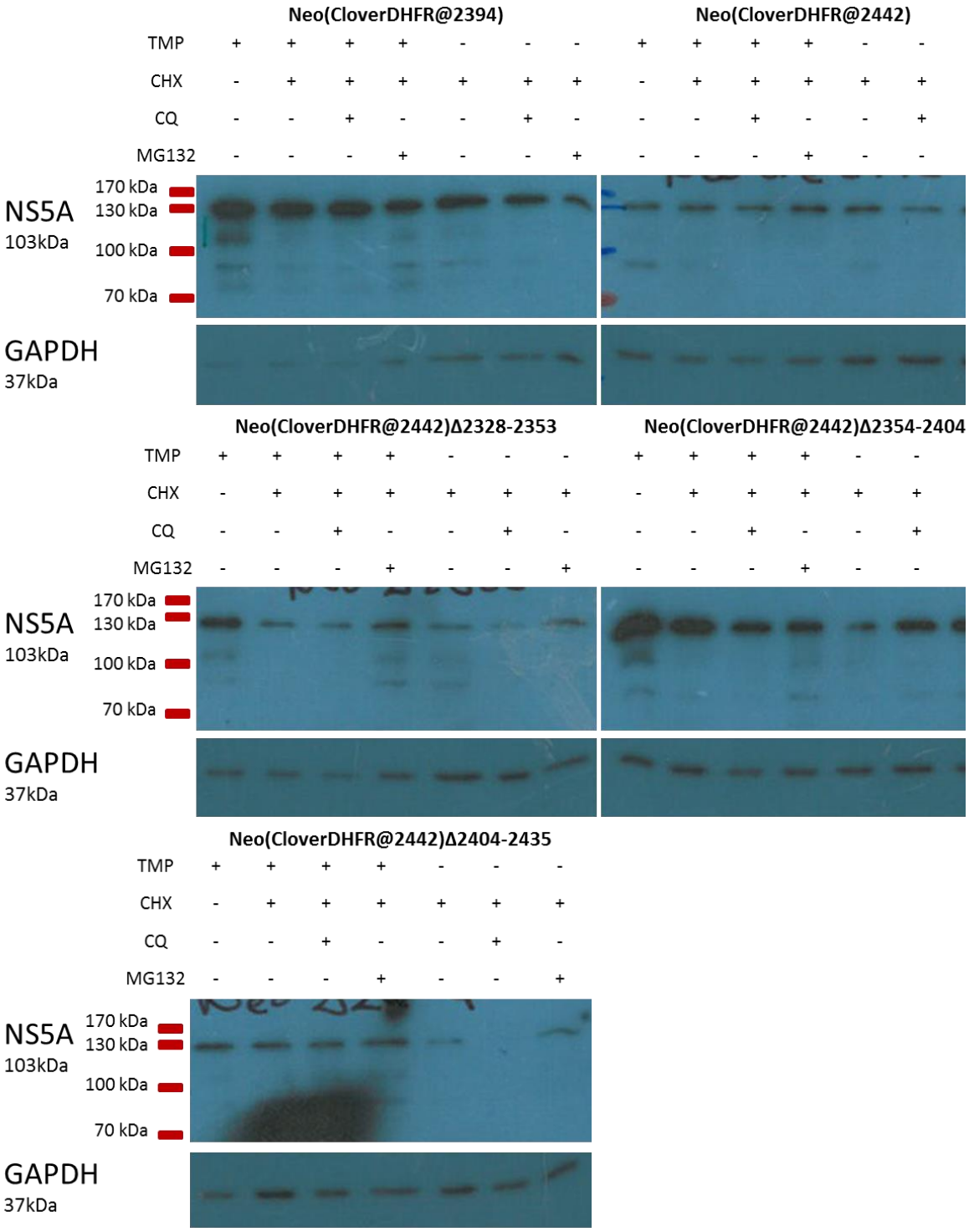

Figure 5-5 **Stability of the NS5A protein in stably transfected cell lines in which either the proteasome or lysosome is inhibited**. Huh7.5 cells stably transfected with G418 resistant JFH1 replicons were incubated in the presence or absence of 10 μM TMP and treated with 100 μg/ml Cycloheximide (CHX). To inhibit the proteasome or lysosome the cells were also treated with either 10 μM MG132 or 100 μM Chloroquine (CQ). After 12 hours the cells were lysed in Ripa buffer + 2 x Complete protease inhibitor. NS5A stability was determined by western blot using a Goat αGFP polyclonal to detect Clover as part of the DHFR-Clover cassette. GAPDH was detected as a control using a mouse αGAPDH monoclonal.

5.4 INTRODUCTION OF A MYC TAG INTO NS5A DOMAIN III

Treatment of stably transfected cell lines with cycloheximide, MG132, and chloroquine provided the first direct evidence that modification of domain III may have a negative impact on the stability of NS5A. However, during the performance of these experiments several limitations became evident. One of these was the toxic nature of cycloheximide, which made it unsuitable for carrying out prolonged time course experiments and increased the risk of off-target effects. Another was the lack of a suitable anti-NS5A antibody, with both the 9E10 mouse monoclonal and sheep anti-NS5A antisera appearing to recognise an immunodominant epitope in domain III of NS5A. While this had been overcome by blotting for the Clover fusion partner in various replicon constructs there remained a slight possibility that due to internal proteolytic cleavage, the fusion partner could be degraded during DHFR-mediated destabilisation while sufficient NS5A remained to fulfil a replicative function. To get around needing to use cycloheximide, it was decided a pulse chase would be performed. However, to avoid the problem of using anti-GFP to detect NS5A and instead have a reliable means of detecting 'functional' NS5A, it was decided to insert a Myc tag epitope into domain II, between residues 2279 and 2280, a site known to tolerate such insertions(Remenyi et al., 2014), but which lies between two regions of NS5A essential for replication. Thus loss of anti-myc reactivity should equate to loss of functional NS5A.

To retain the ability to artificially control stability, the Myc tag was introduced into pSGRJFH1*neoNS3-5B(DHFRClover@2442) and pSGRJFH1*neoNS3-5B(DHFRClover@2442) Δ2354-2404 plasmids, and the resulting plasmids called pSGRJFH1*neo (DHFRClover@2442) Myc and pSGRJFH1*neo (DHFRClover@2442)Δ2354-2404Myc (Appendix8.10). Transcripts of these were introduced into Huh7.5 cells by electroporation, and stably transfected cells were selected for by growth in media supplemented with 650 μg/ml G418 and 10 μM TMP. Interestingly, those cells transfected with the truncated replicon produced approximately 10 times more colonies than those carrying the full length. Three weeks post transfection cells were harvested and the cell lines named Huh7.5 NeoMyc and Huh7.5 NeoMycΔ2354-2404. Expression of NS3, and the Myc tagged NS5A was confirmed by Western blot, showing that both cell lines were supporting the replicons (Figure 5-6).

A

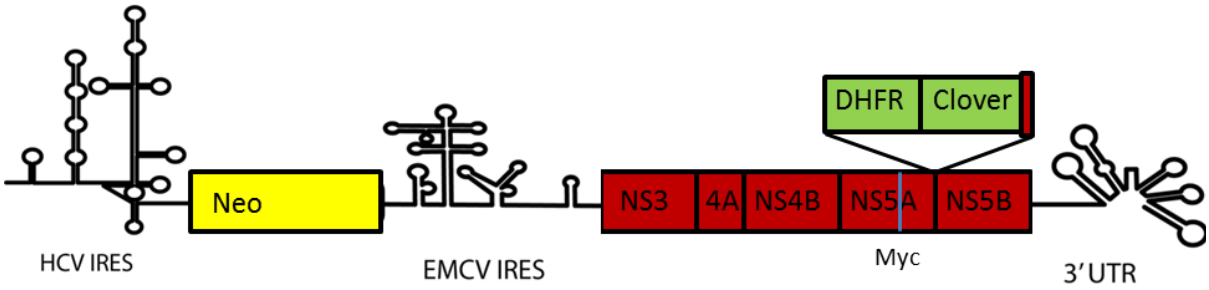

B

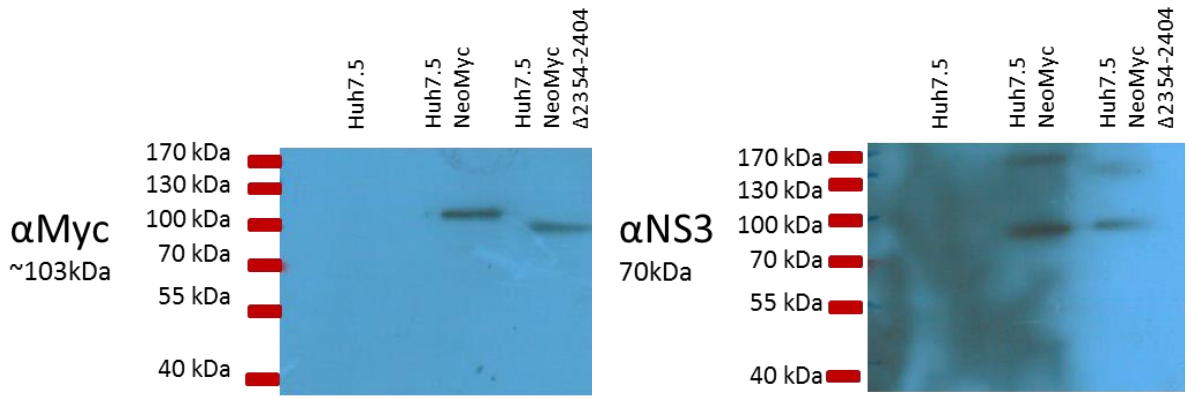

Figure 5-6 **Expression of MycNS5A and NS3 by Huh7.5 NeoMyc and Huh7.5 NeomycΔ2354-2404 cell lines**. (A) Schematic of the pSGRJFH1NeoMyc replicon. (B) Expression of MycNS5A and NS3. Huh7.5 NeoMyc and Huh7.5 NeomycΔ2354-2404 cells were lysed in Ripa buffer + 2x complete protease inhibitor and the expression of MycNS5A and NS3 was determined by Western blot.

5.5 PRELIMINARY CLICK CHEMISTRY

Traditional pulse chase experiments are performed using radio-labelling, for example 35S methionine labelling, in which the pulse incorporates a radioisotope of methionine into cellular proteins. Labelled proteins can therefore be monitored by virtue of the radioactive decay of this isotype. This approach could have been used to monitor the turnover of NS5A, however radiolabelling by its very nature requires the use of open sources of radiation, which carries certain health and safety risks and controls. To avoid these, a pulse chase was developed that made use of click chemistry instead.

Click chemistry refers to a class of bioconjugation reactions, in which a substrate is bound to a specific biomolecule. First described by Sharpless in 2001, Click chemistry reactions are high yielding, wide in scope, create only byproducts that can be removed without chromatography, are stereospecific, simple to perform, and can be conducted in easily removable or benign solvents(Kolb et al., 2001). The earliest examples of such reactions were reported by Arthur Michael in 1893, and these were later further explored by, and took the name of, Rolf Huisgen. These early reactions however were slow, required high temperatures, and yielded multiple isomers.

Copper(I)-catalyzed azide-alkyne cycloaddition is the classical example of click chemistry. The addition of copper catalysis, discovered concurrently by the Sharpless and Meldal groups (Kolb et al., 2001, Tornoe et al., 2002), greatly enhances azide-alkyne cycloaddition reactions and reducing the activation barrier. In addition the copper(I) catalysed reaction only forms the 1,4-isomer, fulfilling the requirement for a click chemistry reaction to be specific. It is important to note that Copper(I) in the concentrations needed to facilitate azide-alkyne cycloaddition is cytotoxic and so it is commonly replaced by the use of copper(II) salts alongside a reducing agent such as sodium ascorbate.

The Sharpless group also developed a ruthenium catalysed reaction, analogous to copper(I)-catalyzed azide-alkyne cycloaddition. The reaction proceeds in a similar manner, however yields a 1,5-isomer instead.

Further work has also been conducted to develop a system without the need for a metal catalyst. One that has had success is the use of strained cycloactane, such as Strain-promoted azide-alkyne cycloaddition developed by the Bertozzi group (Agard et al., 2006). Instead of using a potentially toxic catalyst the alkyne is introduced into a strained difluorooctyne, forming an inherently unstable ring structure. This instability acts as the driving force behind the interaction of the alkyne and the azide. These, however, are considerably slower than

copper catalysed reactions, but have been used successfully to detect azide groups in living systems (Agard et al., 2006, Codelli et al., 2008, Gordon et al., 2012).

In this work copper(I)-catalyzed azide-alkyne cycloaddition was used as a form of isotypic labelling to allow a pulse chase experiment to be performed. During the pulse azido-homo-alanine (L-AHA) is incorporated into protein in place of methionine. This carries an azide group that is open to cycloaddition. After the chase this allows a copper catalysed cycloaddition reaction to be performed, forming a stable linkage between the azide group and the alkyne. The alkyne in this instance, Acetylene-PEG4-Biotin (AP4B), can be identified subsequently due to the presence of a biotin group, that can detected by Western blot using Streptavadin HRP. Tris(3-hydroxypropyltriazolylmethyl)amine (THPTA) serves to bind free Copper(I), limiting its bioavailability and preventing denaturing of proteins.

Prior to the pulse chase being performed, preliminary experiments were undertaken to establish the most effective way to proceed. To test the click chemistry procedure naïve Huh7.5 cells and Huh7.5 cells transfected with pSGRJFH1*neoMyc(DHFRClover@2442) replicons were labelled with L-azidohomoalanine (L-AHA) and immediately lysed in click lysis buffer. To act as a negative control lysate from unlabelled Huh7.5 cells were also included. Labelling was detecting by western blot using streptavidin-HRP to detect biotinylation (Figure 5-7). Biotinylated protein was evident in both labelled samples, but absent in unlabelled cells, confirming the specificity and functionality of the click chemistry reaction.

In addition to testing the click chemistry protocol it was important to test the pull down protocol. Initial attempts at pull down were made using commercially available magnetic beads that could be loaded with a primary antibody of choice. Lysates from labelled Huh7.5 and Huh7.5 NeoMyc(DHFRclover@2442) cells were used in a pull down using beads loaded with a monoclonal mouse anti-myc antibody, and success monitored by blotting for Myc. Initial attempts using the recommended amount of antibody (1 µg/100 µl lysate) proved inefficient; although pulldown was evident, the majority of the protein remained unbound (Figure 5-8).

In an attempt to improve the pulldown, 100 µl of labelled lysate was exposed to either 1 or 2 µg of antibody for 2 hours, as opposed to the 1 hour incubation that had been previously used, and pull down success was once again determined by western blot (Figure 5-9). Pull down was evident in both samples, and although pulldown efficiency improved with an increased amount of antibody on the beads the majority of NS5A remained in the unbound fraction.

As an alternative Streptavadin-agarose beads were tested. A complication of using this approach was, however, that to prevent free Acetylene-PEG_4-Biotin interfering with binding, labelled lysates first had to be subjected to an additional methanol precipitation step before being re-suspended in a SDS free buffer. To optimise the streptavidin-agarose bead pulldown 100 µl of purified lysate from the Huh7.5 NeoΔ2354-2404 cells was exposed to between 10 and 1.25 µl of streptavidin-agarose beads in a 50% slurry for 30 minutes, and the pull down performed. The products from the pulldown were then run on a 10% acrylamide gel and a Western blot performed to detect both biotinylated protein and myc (Figure 5-10). The results from the streptavidin-HRP blot showed that 5 µl of bead slurry was sufficient to pull down essentially all biotinylated protein in the samples. Binding appeared to be specific, as although 5 µl of beads also allowed the maximum amount of myc-tagged NS5A to be pulled-down, a large propotion of NS5A remained unbound, as would be expected given that much of this protein would be expected to be unlabelled after a 4 hour pulse of L-AHA.

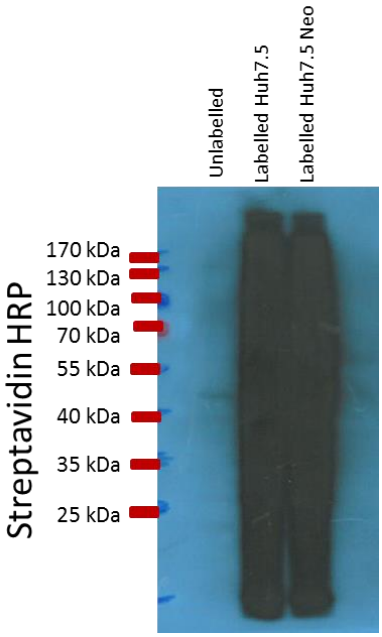

Figure 5-7 **Labelling of Huh7.5 and Huh7.5 JFH1*Neo(DHFRclover@2442) Myc cells with L-AHA.** Naïve Huh7.5 cells and Huh7.5 neoMyc were incubated in media lacking methionine but supplemented with L-AHA for 4 hours. These were then lysed in click lysis buffer and biotinylated by click chemistry. Biotinylation of L-AHA was detected by western blot using Streptavidin-HRP.

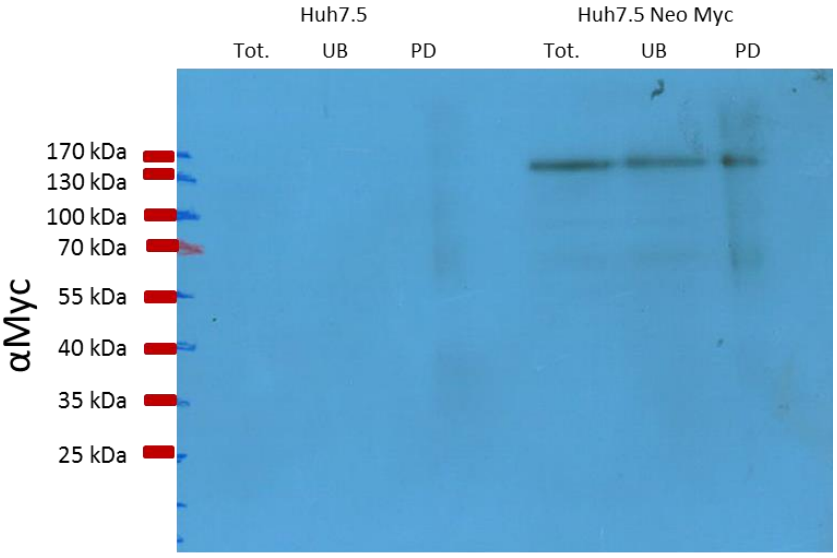

Figure 5-8 **Pull down assay using Myc Antibody at the recommended concentration**. Naïve Huh7.5 cells and Huh7.5 NeoMyc were lysed in click lysis buffer. 100 µl of each protein sample was exposed to 50 µl of SureBeadTM pre-loaded with 1 µg of Mouse αMyc antibody, and incubated for 1 hour. The beads were boiled in 40 µl of 1xSDS PAGE loading buffer to elute the protein. Samples included a total fraction (Tot.) collected prior to pulldown, an unbound fraction (UB) collected from protein samples exposed to the beads but had not bound, and a pulled down fraction (PD) collection from the elution. Pulldown efficiency was detected by western blotting using the mouse αMyc antibody.

A

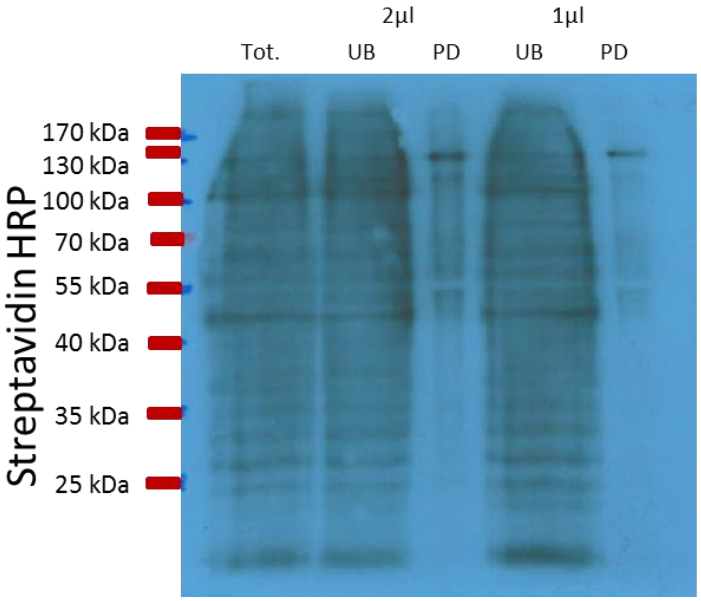

B

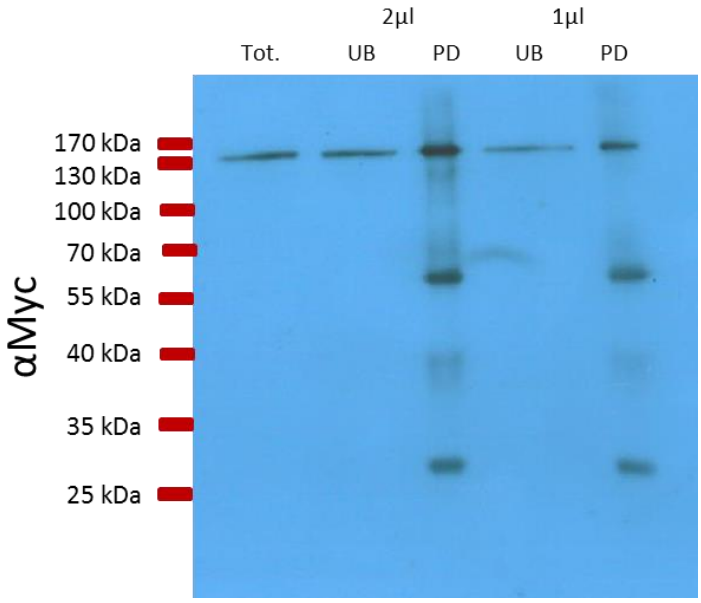

Figure 5-9 **Pulldown using αMyc.** Naïve Huh7.5 cells and Huh7.5 NeoMyc cells were incubated in media lacking methionine but supplemented with L-AHA for 4 hours. These were then lysed in click lysis buffer and biotinylated by click chemistry and Biotinylation of L-AHA was detected by western blot using Streptavadin-HRP (A). 100 µl of each protein sample was exposed to 50 µl of SureBead™ pre-loaded with 0.5 µg of Mouse αMyc antibody and incubated for 2 hours. The beads were boiled in 40 µl of 1xSDS PAGE loading buffer to elute the protein. Samples included a total fraction (Tot.) collected prior to pulldown, an unbound fraction (UB) collected from protein samples exposed to the beads but had not bound, and a pulled down fraction (PD) collection from the elution. Pulldown efficiency was detected by western blot using mouse αMyc (B).

A

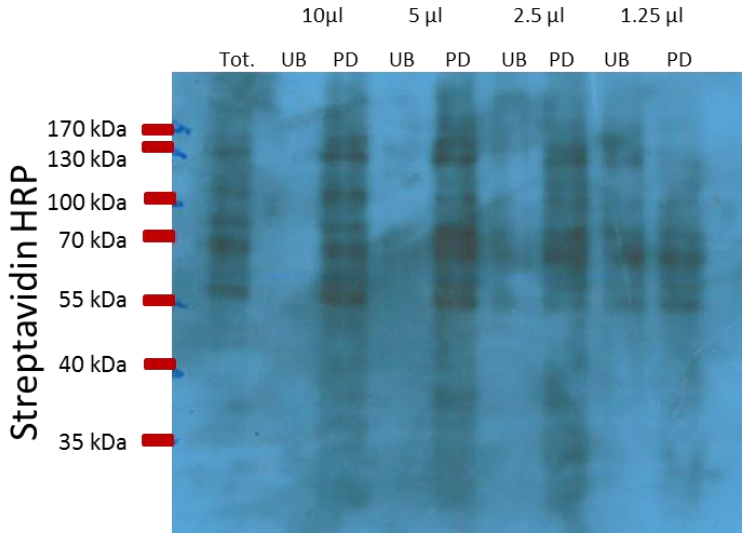

B

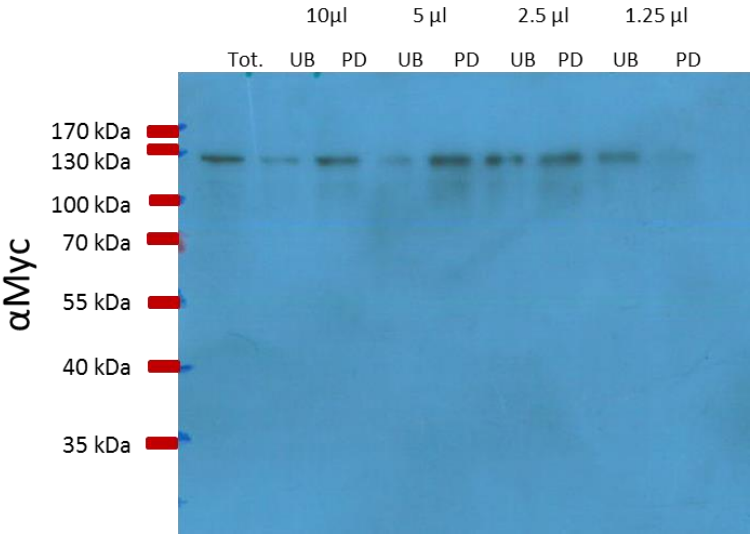

Figure 5-10 **Optimising pull down of biotinylated protein using streptavidin agarose beads**. Huh7.5 NeoMyc Cells were incubated in media lacking methionine but supplemented with L-AHA for 4 hours. These were then lysed in click lysis buffer and biotinylated by click chemistry. 100 µl of purified sample was exposed to between 10 and 1.25 µl of streptavidin agarose beads in a 50% slurry for 1 hour. The beads were boiled in 40 µl of 1xSDS PAGE loading buffer to elute the protein. Samples included a total fraction (Tot.) collected prior to pulldown, an unbound fraction (UB) collected from protein samples exposed to the beads but had not bound, and a pulled down fraction (PD) collection from the elution. Pulldown efficiency was detected by western blot using streptavidin HRP (A) and αMyc (B).

5.6 PULSE CHASE

To visualise the impact of domain III truncation on protein stability in both a stable and unstable state a pulse chase was performed using Huh7.5 NeoMyc and Huh7.5 NeoMycΔ2354-2404 cells. A uniform number of cells were labelled with L-AHA and incubated in the presence of TMP for 0/2/4/8 hours or in the absence of TMP for 0/1/2/3 hours. Samples were lysed in a buffer lacking SDS, and click chemistry performed to biotinylate the labelled protein. The difference in time was due to the expected rapid turnover of NS5A in the absence of TMP. The protein lysate was then purified by methanol precipitation before a pull down was performed using Streptavadin-agarose beads. The results were visualised by western blot using the mouse anti-myc monoclonal antibody (Figure 5-11). Blotting for GAPDH was included as a control as GAPDH has a half-life greater than 35 hours (Franch et al., 2001) and was therefore expected to be broadly invariant across all time points.

In contrast to the previous experiment truncated NS5A did not show increased sensitivity to TMP withdrawal. Indeed NS5A did not show any evidence of degradation over the course of the chase, both under conditions when it was stabilised by the presence of TMP, or when it was destabilised by TMP withdrawal. The results from the GAPDH blot indicated that variation between experimental groups due to biotinylation efficiency and processing was minimal

Of note, however, was the reduced level of NS5A produced by the Huh7.5 NeoMycΔ2354-2404 cells compared to the Huh7.5 NeoMyc cells. A similar pattern had been observed in previous Western blots with NS5A, and this data corroborates that observation, that truncation of domain III results in decreased NS5A abundance.

A

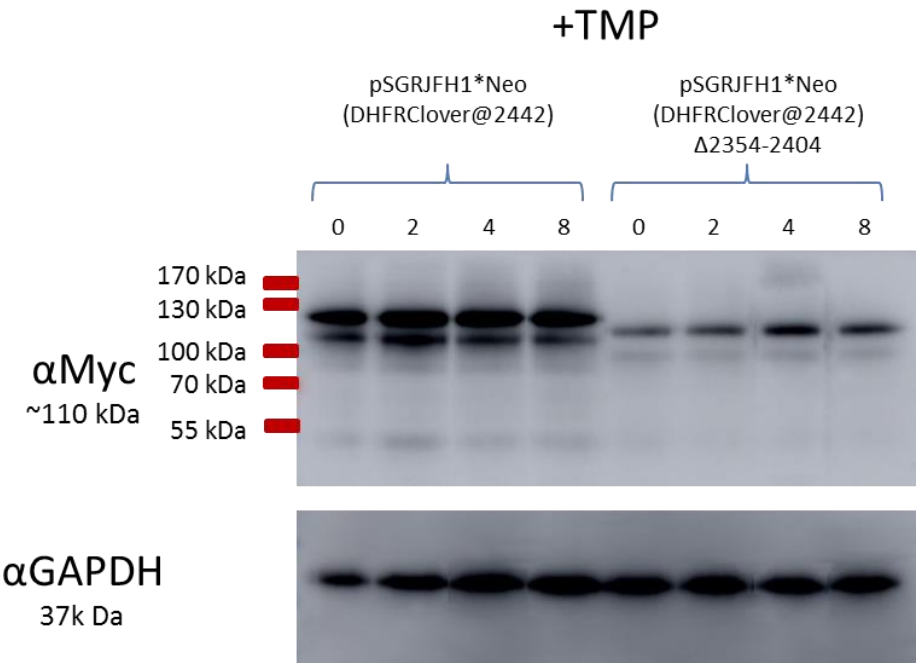

B

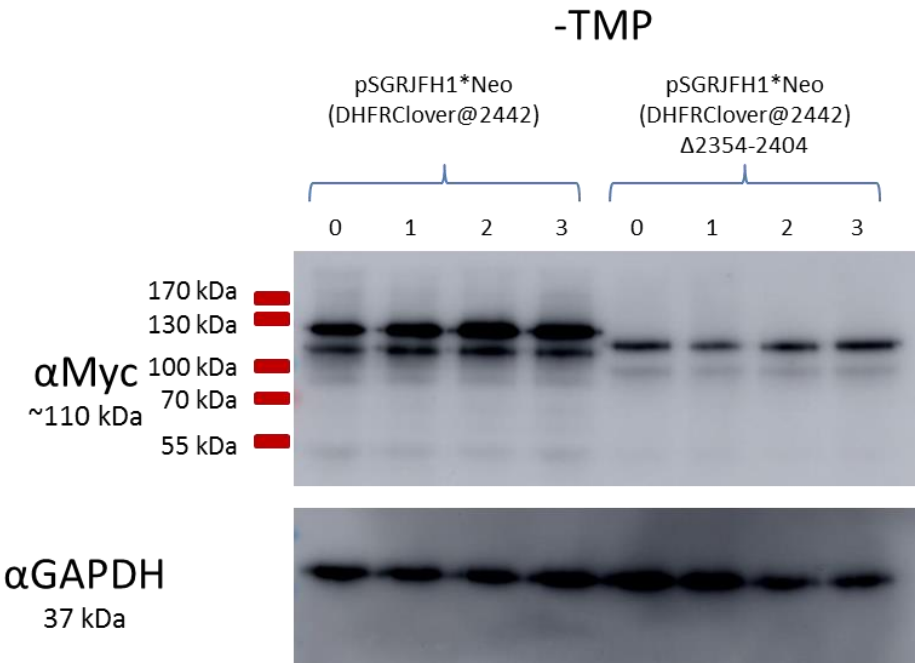

Figure 5-11 **Pulse chase of pSGRJFH1*neo(DHFRClover@2442)Myc and pSGRJFH1*neo(DHFRClover@2442)Δ2354-2404 Myc**. Huh7.5 NeoMyc and Huh7.5NeoMycΔ2354-2404 cells were incubated in media lacking methionine but supplemented with L-AHA and TMP for 4 hours, and then incubated in complete media +/- 10 µm TMP for between 0-8 hours if TMP supplemented or 0-4 hours if TMP starved. Cells were lysed in click lysis buffer and the protein biotinylated by click chemistry. The protein was then purified by methanol precipitation and a pulldown assay performed on 100 µl of purified sample using 5 µl of streptavidin agarose beads in a 50 % slurry for 1 hour. To elute the protein the beads were boiled in 40 µl of 1x SDS PAGE loading buffer. Abundance of NS5A at each time point was detected by western blot using mouse αmyc. Equal loading was checked by stripping and re-probing for GAPDH using mouse αGAPDH.

5.7 INVESTIGATING THE ROLE OF DOMAIN III ON INTERFERON SENSITIVITY USING TRANSIENT TRANSFECTION

IFNs are an important component of both the innate and adaptive immune responses. Released by virus infected cells, type I interferons stimulate an antiviral response in both infected and neighbouring cells. The end result of this is to induce the expression of anti-viral proteins and limit viral replication and spread. Due to the previous lack of specific anti-HCV therapies available, pegylated-IFNα was until recently an essential component of all anti-HCV treatments. Unfortunately the response rate to peg-IFN varies considerably between patients. It has recently been reported that TRIM22, a Tripartite-Motif protein is upregulated in HCV patients receiving IFNα therapy (Yang et al., 2016). This has been seen to result in polyubiquitination, and degradation of NS5A, suggesting a link between IFN therapy and NS5A stability. Investigations have also suggested that regions in NS5A domain III might be linked to IFN-based treatment outcomes, although it should be noted that there is a degree of controversy as to whether NS5A polymorphisms do indeed influence IFN treatment outcome. To look into the possibility that NS5A domain III promotes stability in the face of the IFN response, JFH1 replicons carrying either a full length domain III, or carrying the Δ2354-2404 deletion were introduced into Huh7.5 and incubated in the presence of IFNα ranging in concentration from 0.3 U/ml to 100 U/ml.

This was performed using replicon constructs lacking DHFR-clover. Although the DHFR-Clover cassette had proved invaluable during previous investigations, the artificial destabilisation resulting from DHFR unfolding has no equivalent during the real HCV life cycle (Iwamoto et al., 2010). As such further experimentation was needed that focused on the impact of NS5A domain III during biologically relevant destabilisation events. To eliminate the possibility of the DHFR-clover fusion partner confounding or masking these any such biologically relevant events, JFH1 replicons were generated that possessed either a full length or mutant domain III, but lacking the DHFR-clover cassette. To achieve this, the 2354-2404 deletion was introduced into pSGJFH1*luc (Appendix8.11).

To perform the assay Huh7.5 cells were transfected with either pSGRJFH1*luc or pSGRJFH1*Δ2354-2404 and incubated in the presence of between 0.3 U/ml and 100 U/ml IFNα, and a luciferase assay performed. The luciferase assay data showed that both replicons were indeed sensitive to IFN treatment, with both constructs exhibiting a steady decrease in replication with increasing concentration of IFN (Figure 5-12). However neither proved more sensitive than the other, suggesting that the status of domain III has no impact on the resistance to IFN, at least under transient replication assay conditions.

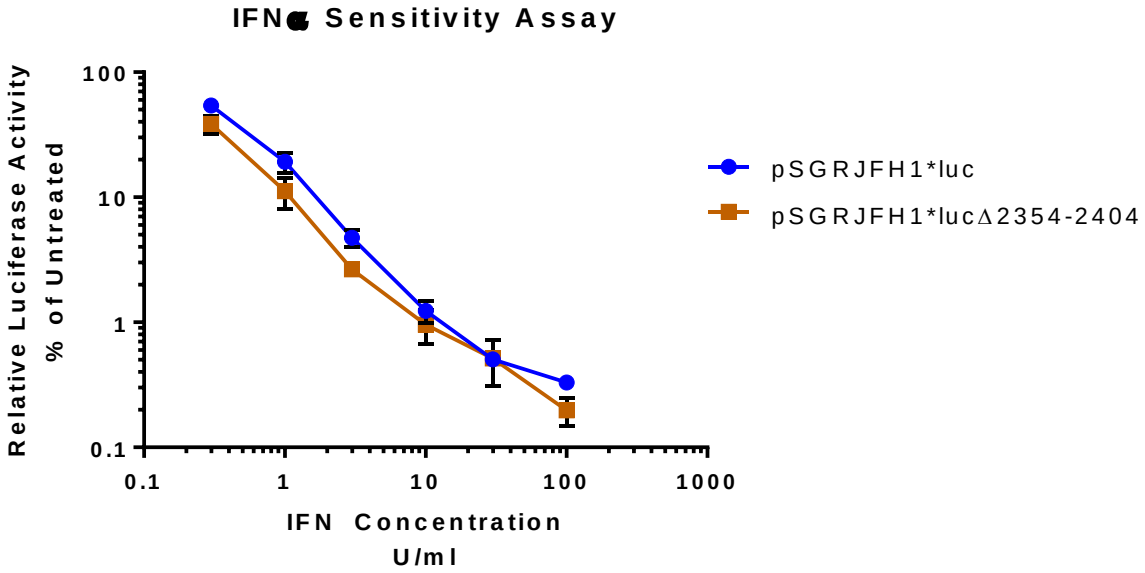

Figure 5-12 **Sensitivity of pSGRJFH1*luc and pSGRJFH1*lucΔ2354-2404 replicons to IFNα.** pSGRJFH1*luc and pSGRJFH1*lucΔ2354-2404 transcripts were electroporated into Huh7.5 cells. 4 hours post transfection cells were treated with IFNα at between 0.3 and 100 units/ml. The cells were then incubated for 48 hours before being lysed in 1 x Passive lysis buffer. These lysates were used in a luciferase assay to determine viral replication. Data represents the mean +/- Standard error of two assays.

5.8 GENERATION OF STABLY TRANSFECTED CELL LINES EXPRESSING PSGRJFH1*NEO AND PSGRJFH1*NEOΔ2354-2404

To extend the analysis to see whether domain III might be involved in interferon sensitivity, it was decided to look at the impact of IFN on cells stably carrying replicons expressing full length NS5A or NS5A with the Δ2354-2404 deletion. To generate a pSGRJFH1*neo plasmid carrying the Δ2354-2404 truncation an NPT gene was cloned into pSGRJFH1*luc Δ2354-2404 (Appendix 8.12).

Due to previous issues with the selection of stably transfected cell lines, transcripts of pSGRJFH1*neo, pSGRJFH1*neoΔ2354-2404, and pSGRJFH1*neoGND were electroporated into Huh7 cells, rather than Huh7.5. During earlier attempts to generate similar cell lines in Huh7.5 cells those transfected with full length replicons produced considerably fewer colonies than those transfected with the truncated replicon, and did not recover well post selection. Anecdotal evidence from work carried out by other lab personnel suggested that Huh7 cells produce a higher yield of colonies during selection than Huh7.5, at least for JFH1 based constructs. Huh7.5 cells were generated by curing Huh7 cells of HCV replicons, and are highly permissive to its replication (Blight et al., 2002). One hypothesis to explain the differences in colony production is that the Huh7.5 allow so much replication as to be overwhelmed, whereas the Huh7 cells support a more controlled replication.

After 48 hrs the transfected Huh7 cells were placed under G418 selection at 650 μg/ml to allow the emergence of resistant colonies. Colony formation in Huh7 cells transfected with pSGRJFH1*neo was markedly improved compared to cells transfected with similar replicons, although those cells transfected with pSGRJFH1*neoΔ2354-2404 still generated 3 times more colonies.

To confirm the presence of the replicons a Western blot was performed to detect NS3 (Figure 5-13).

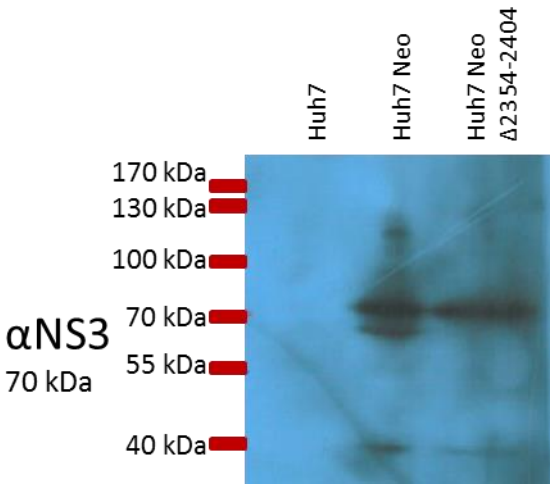

Figure 5-13 **Expression of NS3 by Huh7 Neo and Huh7 NeoΔ2354-2404 cell lines**. Huh7 Neo and Huh7 NeoΔ2354-2404 cells were lysed in Ripa buffer + 2x complete protease inhibitor and the expression of NS3 was determined by Western blot.

5.9 INVESTIGATING THE ROLE OF DOMAIN III ON INTERFERON SENSITIVITY USING STABLY TRANSFECTED CELL LINES.

To investigate the impact of domain III on interferon sensitivity 4 x 10^5 Huh7 cells stably transfected with either pSGRJFH1*neo or pSGRJFH1*neoΔ2354-2404 were incubated in the presence of 100, 75, 50, 25, or 0 units/ml IFNα for 5 days. These concentrations were selected to provide a dynamic range, based upon work in the Wakita group (Kato et al., 2005). A colony forming assay was then performed using 10^5, 10^4, or 10^3, transfected cells (Figure 5-14, Figure 5-15).

Both transformants demonstrated the ability to form colonies irrespective of interferon treatment. Neither demonstrated a dose dependent response to IFN, suggesting that the maximum doses of IFN used, or the duration of time for which it was applied, was insufficient to eliminate either of the replicons from the polyclonal cell population. However, those cells carrying the pSGRJFH1*neoΔ2354-2404 replicons yielded a great number of colonies compared to those cells carrying the full length replicon. The most likely explanation for this result is that replicons carrying the Δ2354-2404 truncation exhibit superior colony formation, particularly as earlier experimental results support such a conclusion, such as the during the generation of the Huh7.5NeoMyc cell lines. However, it also remains possible that this result is due to the pSGRJFH1*neo polyclonal cell line carrying a higher proportion of untransfected cells.

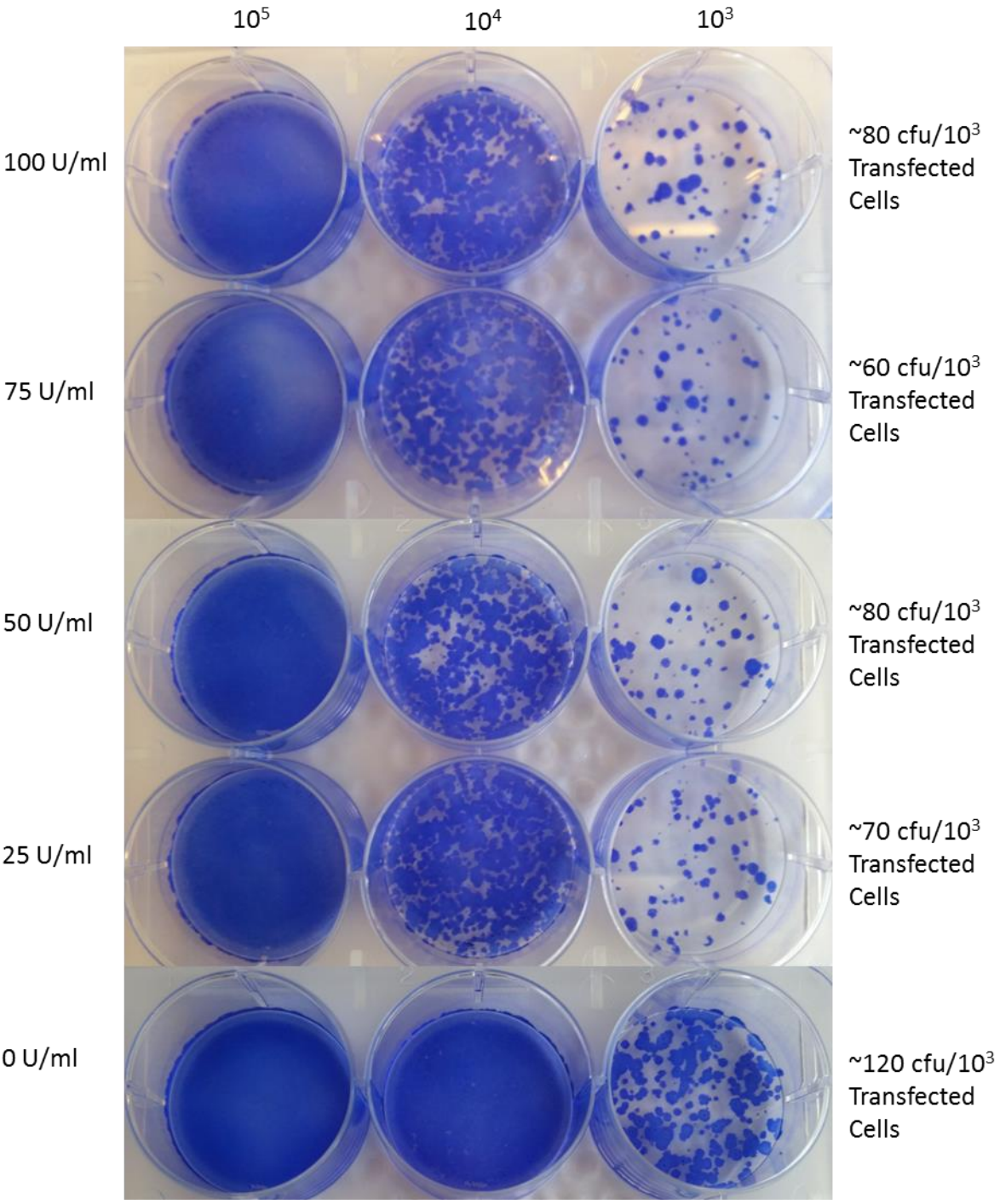

Figure 5-14 **Colony forming assay of Huh7 pSGRJFH1Neo cells treated with IFNα**. 4 x 10^5 cells were incubated in media supplemented with between 0-100 u/ml IFNα. After 5 days the cells were trypsinised and seeded at 10^5, 10^4, or 10^3 transfected cells per well, Each well was additionally seeded with naïve Huh7 cells to a total cell density of 2 x 10^5. These were incubated in media supplemented with 650 µg/ml G418 for 2 weeks. Colonies were stained with coomassie blue.

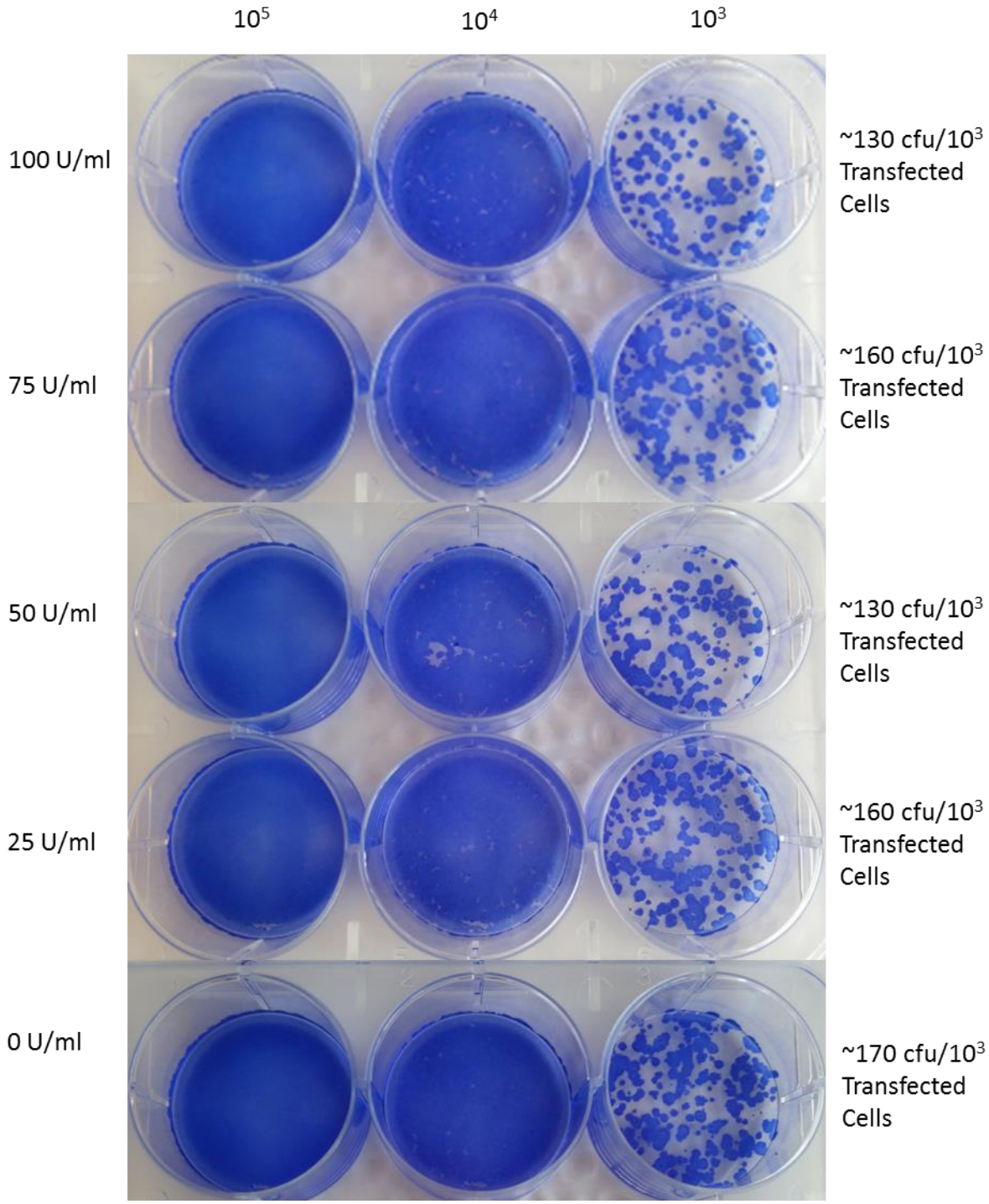

Figure 5-15 **Colony forming assay of Huh7.5 pSGRJFH1Neo*Δ2354-2404 cells treated with IFNα**. 4 x 10^5 cells were incubated in media supplemented with between 0-100 U/ml IFNα. After 5 days the cells were trypsinised and seeded at 10^5, 10^4, or 10^3 transfected cells per well, Each well was additionally seeded with naïve Huh7 cells to a total cell densitiy of 2 x 10^5. These were incubated in media supplemented with 650 µg/ml G418 for 2 weeks. Colonies were stained with coomassie blue.

5.10 INVESTIGATING THE IMPACT OF DOMAIN III ON ANTIGEN PRESENTATION

The proposed role of domain III in protein stability, although enigmatic, lent itself to several functions. One potential cellular function was protection of NS5A and possibly other viral proteins from antigen presentation. Detection of virus infected cells occurs through the Major Histocompatibility Complex (MHC), which presents both native and foreign peptide on the cell surface, and their subsequent detection by cells of the immune system. This process relies on processing of proteins by the proteasome to yield peptide fragments that can bind into the MHC class I groove. Given the findings of the thesis so far it was possible that domain III might reduce proteasomal processing of NS5A, and thereby delay detection of NS5A-containing peptides by the immune system.

In order to test this, an antigen presentation system was adapted from collaborators in the Ed James lab. This system relies on a mouse albumin epitope SL8 (SIINFEKL) which is presented on the cell surface by MHC class I complexes. Presentation is detected by co-culturing cells with a T-cell hybridoma called B3Z, which becomes activated upon detection of SL8. Activation triggers expression of the *lacZ* gene, leading to the production of β-galactosidase, which can be detected by the addition of chlorophenolred-β-D-galactopyranoside (CPRG). The idea was to introduce SL8 into NS5A of an HCV replicon, and monitor presentation, to determine whether or not domain III impacts on NS5A processing.

Preliminary work was focussed on whether or not SL8 could be presented if fused to NS5A. Previous work within the group had generated a series of JFH1 based bicistronic replicons, expressing a renilla luciferase Foot and Mouth disease virus (FMDV) 2A fusion product linked to other genes of interest in ORF1 and NS3-5B from JFH1 in ORF2 (Figure 5-16). The FMDV2A induces a co-translational ribosome skipping event, effectively cleaving itself from downstream proteins(Ryan and Drew, 1994). Additional coding regions contained within these replicons included a mouse MHC class I gene (H2K), a β-2 microglobulin gene (β2M), and an SL8 coding regions in various combinations. One replicon expressed SL8, H2K and β2M as a single fusion product downstream from Renilla-FMDV2A ORF1 and served as a positive antigen presentation control for the B3Z assay. Another only expressed H2K and β2M downstream from Renilla-FMDV2A, serving as a negative control. The final construct expressed H2K and β2M from ORF1 but also expressed SL8 fused to the end of NS5A-DHFR encoded by ORF2. In addition a pSGRJFH1*luc plasmid has been prepared also carrying the DHFRSL8 cassette.

While these constructs had been generated, the ability of SL8 expressed from ORF2 to be presented by H2K-β2M expressed from ORF1 had not been fully assessed. Therefore, transcripts of these replicon constructs, alongside pSGRJFH1*luc and pSGRJFH1*lucGND, were transfected into Huh7.5 cells by electroporation and incubated for 24 hours and an SL8 presentation assay performed (Figure 5-17).

Data from this experiment showed that only those B3Z cells co-cultures with cells carrying the control replicon, expressing H2K-β2M-SL8 fusion product from ORF 1, were activated. In contrast, the replicon expressing H2K-β2M from ORF1 and SL8 from NS5A-DHFR failed to generate a signal. Initially it was thought that the lack of signal might be due to insufficient levels of H2K-β2M presenting the SL8 peptide, as the MHC complex wasn't constrained to only present this peptide, unlike the situation with the positive control. However, on further discussion with the James group a further possibility was envisaged, that where the flexible linker fusing the H2K and β2M together prevent loading of downstream SL8 into the peptide binding groove by chaperones.

A

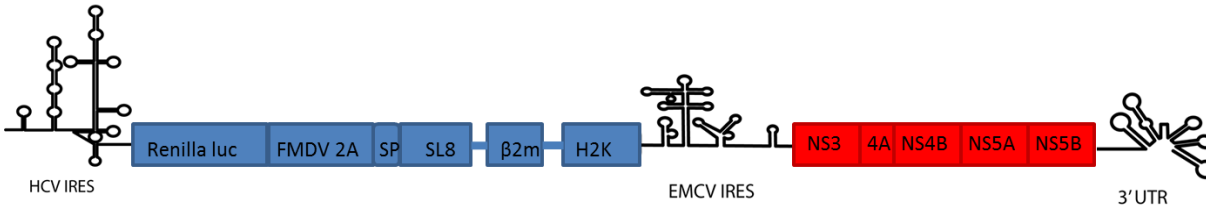

B

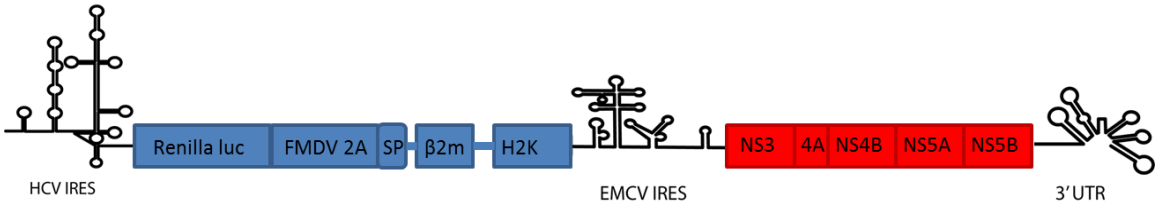

C

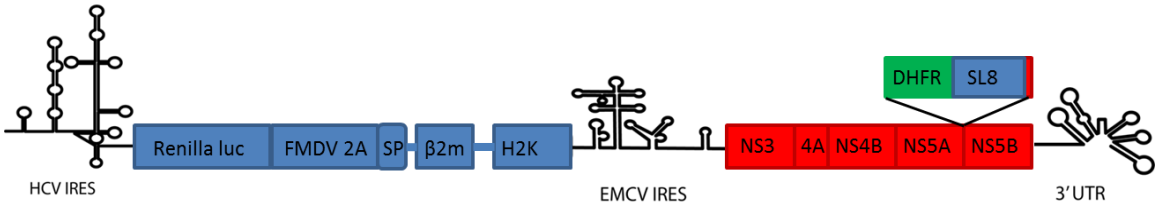

D

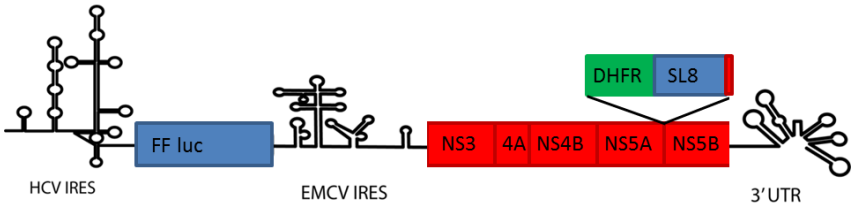

Figure 5-16 **Replicon constructs expressing H2k, β2M and SL8.** (A) pR2A-H2K-B2M-SL8-NS35B. (B) pR2a -H2K-β2m –NS35B. (C) pR2A-H2k-β2m –NS35B(DHFRSL8@2442). (D) pSGRJFH1*lucNS3-5B(DHFRsl8@2442).

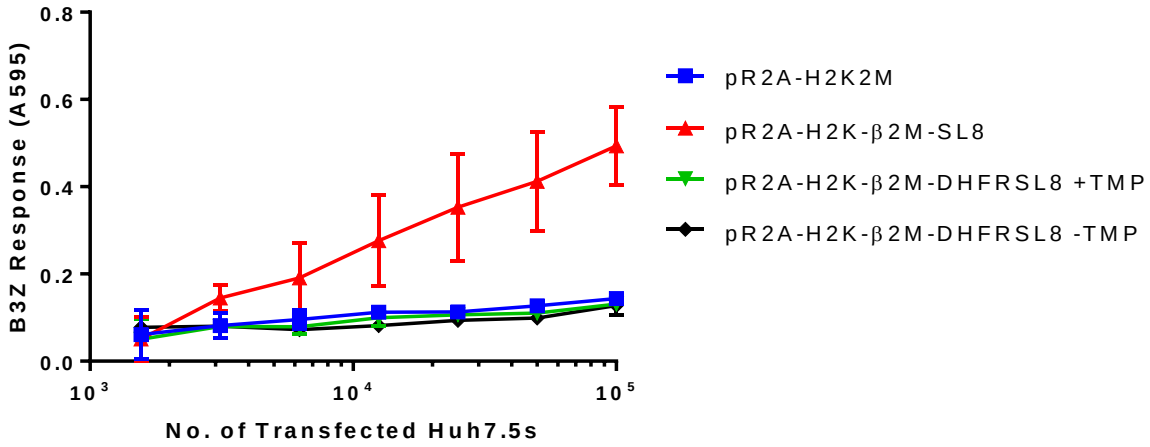

Figure 5-17 **B3Z assay of pR2A replicons.** Huh7.5 cells were transfected with pR2A replicons carrying SL8 in either ORF1, alongside H2K and β2M, or in ORF 2, within NS3-5B derived from JFH1.Post transfection a B3Z assay was performed using the transfected cells. B3Z cell activation was detected by addition of CPRG and measurement of the absorbance at 595 nm. Data represents the average of 2 assays.

To overcome the issue that the linker between the H2K and β2M might be preventing peptide loading, it was decided to express H2K alone, relying on endogenous human β2M to fulfil the role that the mouse β2M fusion partner had been playing up until this point. It was also decided to express H2K independently of the replicon to avoid difference in replicon replication introducing possible confounding issues with date interpretation. A pCDNA plasmid was therefore generated that expressed both H2K and a hygromycin resistance gene (Appendix 8.13).

Prior to the generation of stably transfected cell lines, the pCDNA-Hygro-H2K plasmid was tested by transient transfection to ensure that endogenous human β2M could indeed substitute for the mouse homolog and was present in sufficient levels. Huh7.5 cells were co-transfected with pCDNA-Hygro-H2K and pCDNA-SL8 (kindly donated by Dr Edd James), or pCDNA-Hygro-H2K and empty pCDNA, and a B3Z assay performed. In addition, cells were mock treated with PEI to ensure that transfection had no impact on B3Z cell activation (Figure 5-18). Those Huh7.5s transfected with both pCDNA-Hygro-H2K and pCDNA-SL8 caused slight activation of the B3Z cells suggesting that these were presenting SL8 and therefore that the pCDNA-Hygro-H2K plasmid was capable of expressing H2K. The level of activation was markedly lower than in typically observed when running a B3Z assay with SL8 antigen, however this was attributed to poor transfection efficiency.

Subsequently pCDNA-Hygro-H2K was transfected into Huh7.5 cells to generate a stable H2K expressing cell line, selection being performed using 100 μg/ml Hygromycin B gold (Melford). Four Huh7.5-pCDNA-Hygro-H2K cell lines were obtained of which three were monoclonal (Huh7.5 pCDNA-Hygro-H2K 1, 2, and 3) and one of which was polyclonal (Huh7.5 pCDNA-Hygro-H2K P). To determine the ability of the stably transfected cell lines to present SL8, each of the 4 cell lines was transfected with either empty pCDNA or pCDNA-SL8, and a B3Z assay performed (Figure 5-19).

All three of the monoclonal cells lines failed to present SL8, suggesting that they were not expressing H2K. On the other hand the Huh7.5-pCDNA-Hygro-H2K Poly cell line did show evidence of B3Z activation, and therefore H2K expression. Attempts to enrich the H2K positive population by FACS met with little success. During the initial flow cytometry analysis, using an αH2K antibody directly conjugated to FITC (kindly donated by Dr Edd James), no difference was observed between the Huh7.5-pCDNA-Hygro-H2K Poly cell line, and the naïve Huh7.5 control cells (data not shown). As such these cells were abandoned.

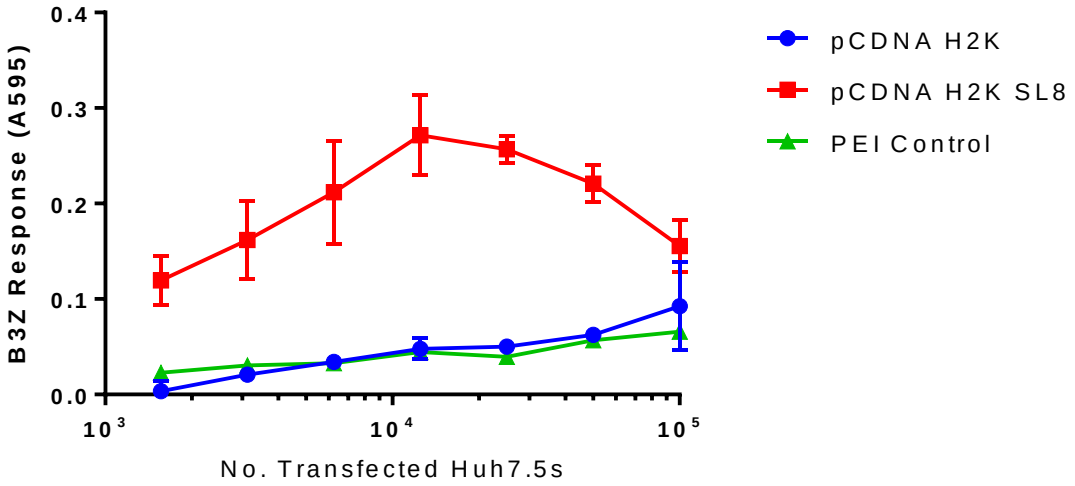

Figure 5-18 **B3Z assay using cells transiently transfected with pCDNA-Hygro-H2K**. Huh7.5 cells were transfected with pCDNA-Hygro-H2K alongside either pCDNA-SL8, or empty pCDNA. 48 hours Post transfection a B3Z assay was performed using the transfected cells. B3Z cell activation was detected by addition of CPRG and measurement of the absorbance at 595 nm. Data Represents the average of 2 assays.

A pCDNA

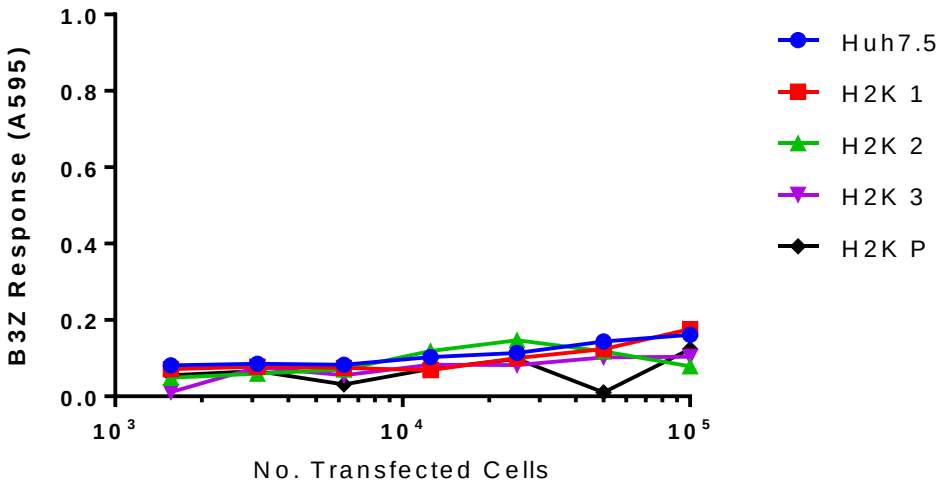

B pCDNA-SL8

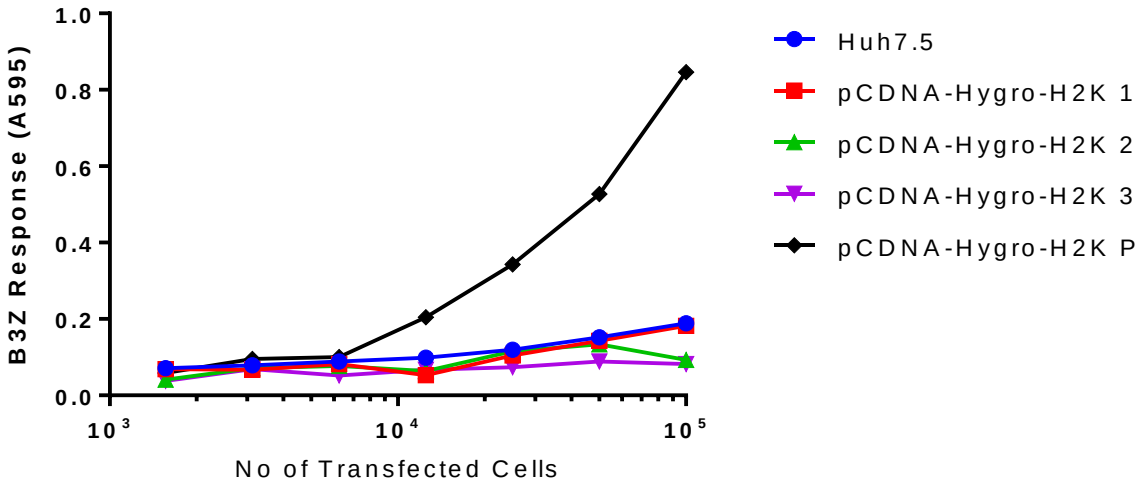

Figure 5-19 **B3Z assay with Huh7.5 cells stably transfected with pCDNA-Hygro-H2K**. Huh7.5 pCDNA-Hygro-H2K cells 1, 2, 3, and P, were transfected with either pCDNA-SL8 or empty pCDNA. 48 hours Post transfection a B3Z assay was performed using the transfected cells. B3Z cell activation was detected by addition of CPRG and measurement of the absorbance at 595 nm. Data represents the average of 2 assays.

5.11 GENERATION OF A H2K EXPRESSING CELL LINE

As attempts to stably transfect in a plasmid expressing both H2K and a selectable marker had failed to produce cells expressing sufficient H2K, it was decided to use lentivirus transduction to generate an H2K expressing Huh7.5 cell line. H2K from pCDNA-Hygro-H2K was therefore cloned into the GFP-expressing pLVTHM plasmid, generating pLVTHM-GFP-H2K (Appendix 8.14). The resulting plasmid was then transduced into naïve Huh7.5 cells by lentiviral transduction.

To determine the transduction efficiency the transduced cells were analysed by flow cytometry to determine the expression of GFP, and therefore H2K within this population (Figure 5-20). After gating the Huh7.5-H2K cell line appeared to form two distinct populations, with approximately 65% of the Huh7.5-H2K cells positive for GFP expression.

To confirm the ability of the Huh7.5-H2K cells to present SL8 the cells were transfected with either pCNDA-Hygro-H2K or pCDNA-SL8. To provide a positive control some cells were also transfected with equal amounts of both plasmids, while some were transfected with pCDNA expressing neither. The cells were incubated for 48 hours to allow expression, and a B3Z assay performed (Figure 5-21). Transfection with pCDNA-SL8 led to activation of the B3Z cells both alone and when co-transfected with H2K, confirming the presentation of SL8, and therefore the expression of H2K. Interestingly those cells transfected with pCDNA-SL8 alone demonstrated increased B3Z activation compared to the co-transfected cells, but more importantly showed enhanced activation of the B3Z cells compared to the polyclonal cell line expressing H2K derived by plasmid transfection.

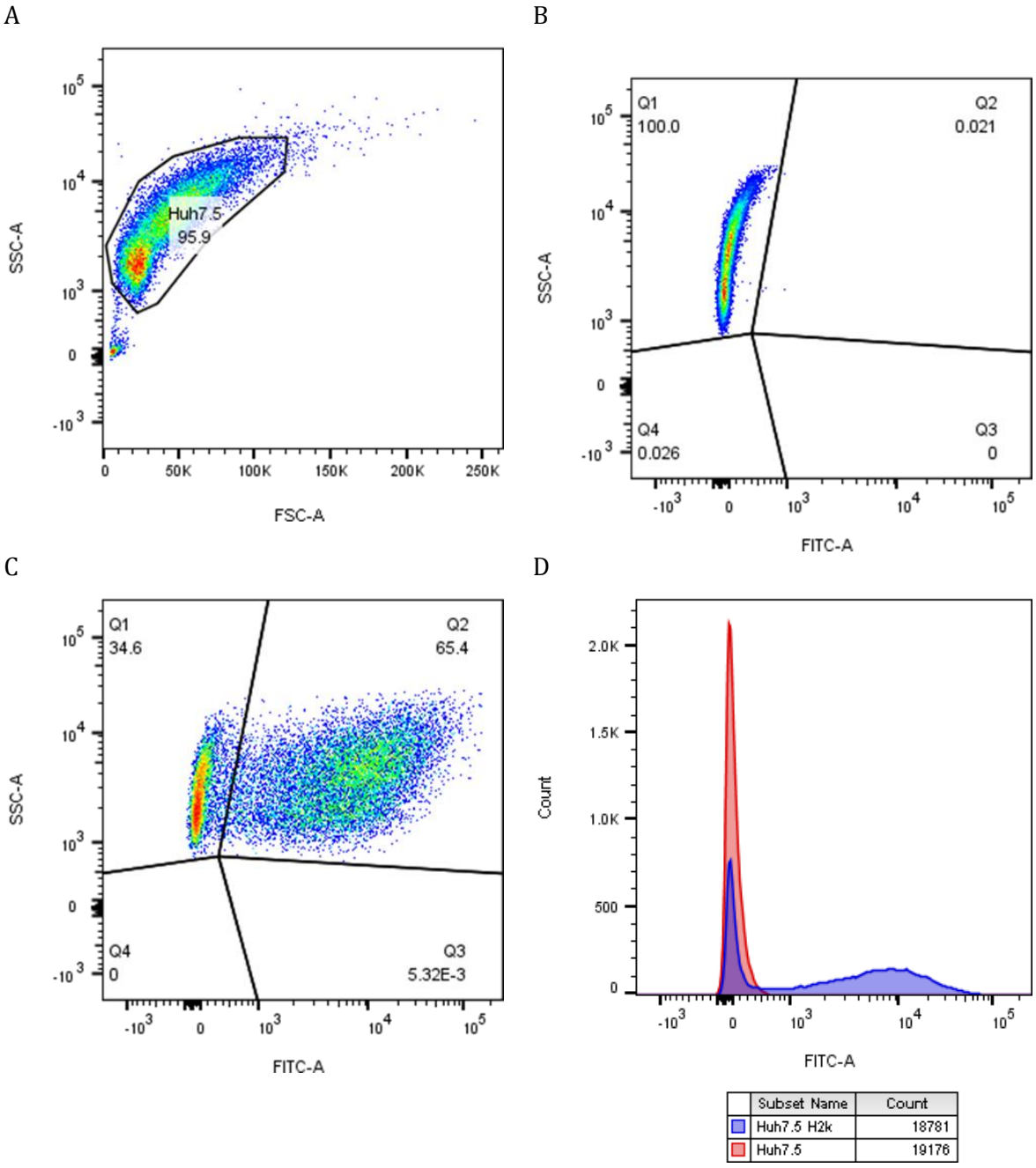

Figure 5-20 **Flow cytometry analysis of Huh7.5H2K cells.** (A) Gating of Huh7.5 cells excluding debris and outliers using forward scatter and side scatter. (B) Gating of Huh7.5 cells based upon side scatter and GFP expression. (C) Flow cytometry of Huh7.7H2K cells. (D) Shift in GFP expression between Huh7.5 cells and Huh7.5H2K cells.

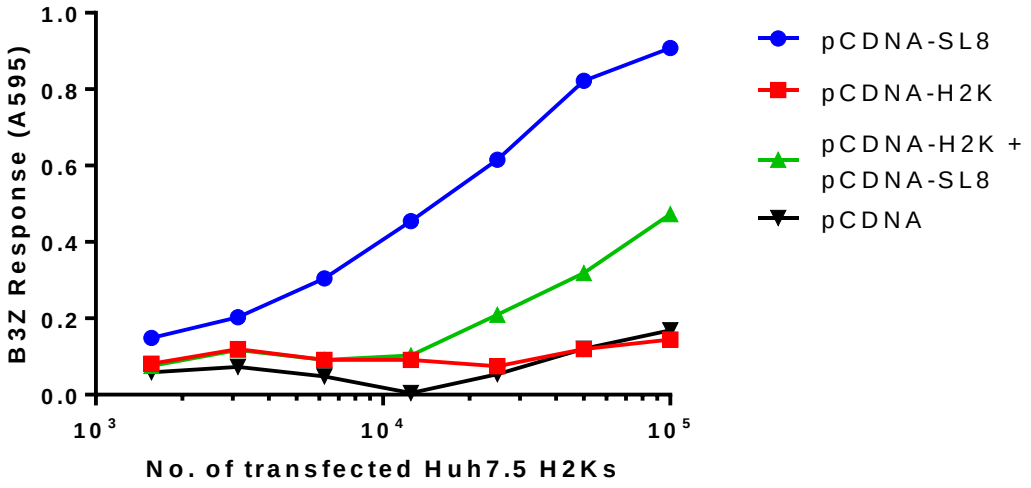

Figure 5-21 **B3Z assay using Huh7.5-H2K cells.** Huh7.5H2K cells were transfected with either pCDNA-Hygro-H2K, or pCDNA-SL8, or both. 48 hours post transfection a B3Z assay was performed using the transfected cells. B3Z cell activation was detected by addition of CPRG and measurement of the absorbance at 570 nm.

5.12 GENERATION OF PSGRJFH1*LUC REPLICONS EXPRESSING DHFRSL8

Alongside the generation of a Huh7.5 cell line expressing H2K, JFH1 replicons were generated that carried the DHFR-SL8 cassette in both a full length and Δ2354-2404 based vector. As pSGRJFH1*lucNS3-5B(DHFRsl8@2442) was already available the Δ2354-2404 deletion from pSGRJFH1*lucNS3-5B(DHFRclover@2442)Δ2354-2404 was cloned into it, generating pSGRJFH1*lucNS3-5B(DHFRSL8@2442)Δ2354-2404 (Appendix 8.15). However, even under stabilising conditions there is some variance in replication between full length pSGRJFH1*lucNS3-5B replicons and those carrying the Δ2354-2404 truncation, and therefore there was concern that this could have an impact on SL8 processing and detection beyond any direct impact that changes to NS5A might cause. As such the GND mutation was introduced into the NS5B of both pSGRJFH1*lucNS3-5B(DHFRSL8@2442) and pSGRJFH1*lucNS3-5B(DHFRSL8@2442)Δ2354-2404. Replicons from these constructs should not replicate, and so only that protein expressed from the translated RNA should be detected. To achieve this NS5A from both replicating plasmids, including the truncation and DHFRSL8 cassettes, was cloned into pSGRJFH1*lucGND(Appendix 8.15).

Prior to the presentation assay, transcripts of the four plasmids were electroporated into naïve Huh7.5 cells, and a replication assay performed in the presence or absence of 10 mM TMP (Figure 5-22). Each of the 4 replicons behaved as expected, with both GND carrying replicons dropping off rapidly, and the functional replicons showing a differential response to TMP. The replicon from pSGRJFH1*lucNS3-5B(DHFRSL8@2442) demonstrated robust replication in the presence of TMP, and showed evidence of recovery in its absence, whilst the replicon from pSGRJFH1*lucNS3-5B(DHFRSL8@2442)Δ2354-2404 only showed evidence of replication in the presence of TMP. The replication assay also showed there to be a slight difference in growth between the full length and truncated replicons even in the presence of TMP, consistent with earlier observations that the Δ2354-2404 does impact on replication in the presence of TMP.

A

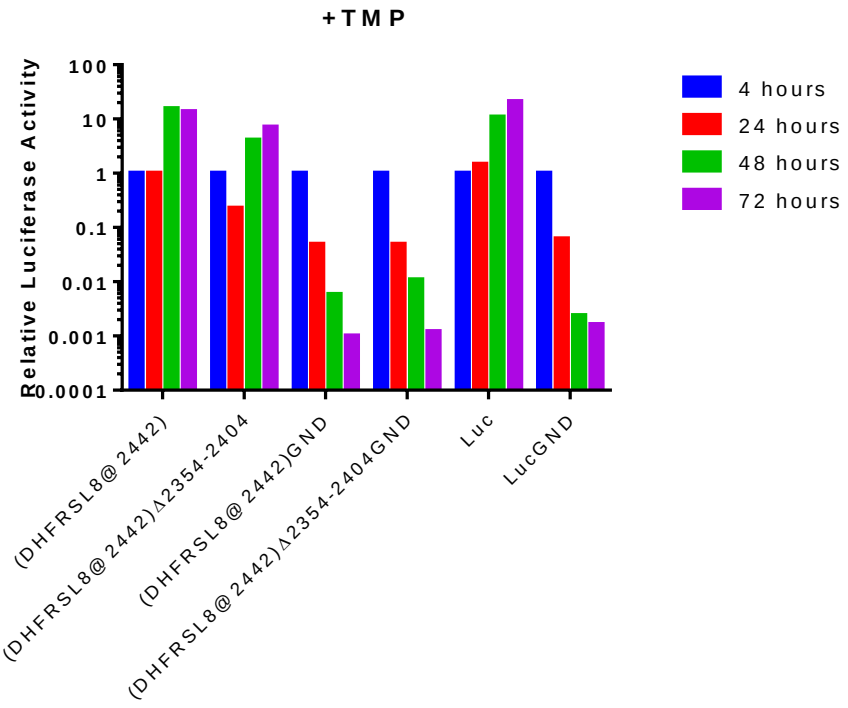

B

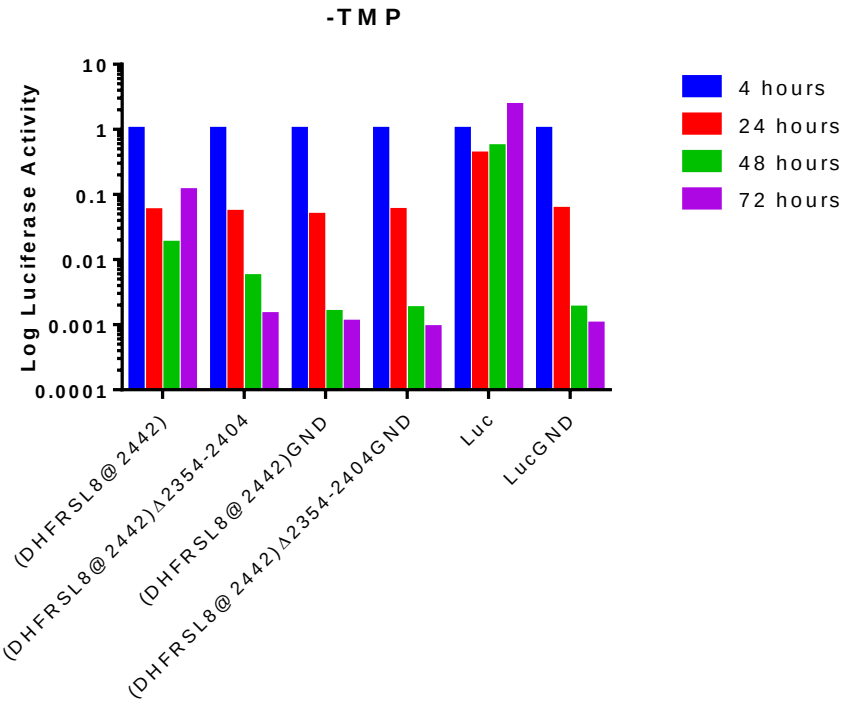

Figure 5-22 **pSGRJFH1 SL8 plasmid replication assay.** Huh7.5 cells were transfected with transcripts of pSGRJFH1*luc(DHFRSL8@2442), pSGRJFH1*luc(DHFRSL8@2442)Δ2354-2404, pSGRJFH1*luc(DHFRSL8@2442)GND, and pSGRJFH1*luc(DHFRSL8@2442)Δ2354-2404GND and incubated in the presence (A), or absence (B) of 10μM TMP. After 4, 24, 48, or 72 hours the cells were lysed in 1x Passive lysis buffer, and a luciferase assay performed. Data from a single assay.

5.13 SL8 PRESENTATION ASSAY

Having confirmed the functionality of all four SL8 replicons, they were electroporated into Huh7.5-H2K cells to assess presentation of the SL8 epitope embedded within the different NS5A-DHFR clover coding regions. Post electroporation the cells were immediately separated, half re-suspended in DMEM alone, and half re-suspended in DMEM supplemented with 10 μM TMP, and a B3Z assay performed (Figure 5-23). Although replication may impact presentation, the replicase functional pSGRJFH1*lucNS3-5B(DHFRSL8@2442) and pSGRJFH1*lucNS3-5B(DHFRSL8@2442)Δ2354-2404 were included to offset the possibility that the GND constructs did not yield sufficient protein for presentation. To ensure that the B3Z cells remained sensitive a positive control replicon was also included that expressed the H2K-SL8 fusion peptide.

Disappointingly SL8 presentation was only detectable in those transfected with the positive control. None of the cells electroporated replicon constructs containing SL8 in the NS5A coding region appeared capable of activating the B3Z cells.

A number of possibilities exist that could explain the failure of this experiment, however time constraints meant it was not possible to determine what the problem was, and therefore take this work further. The first possibility is that the Huh7.5-H2K cells may have stopped expressing H2K. No selectable marker was included in the lentiviral plasmid transduced into these cells, meaning there is nothing to ensure continued expression. This was a deliberate choice, to remove any factors that may negatively impact replication and antigen processing, however it leaves possibility for metabolic pressure to drive the cells to stop expressing H2K. To address this, the experiment was repeated in fresh Huh7.5-H2K cells that had been stored in liquid nitrogen since the preliminary experiments that had confirmed expression of H2K. This produced identical results.

As mentioned previously the Huh7.5-H2K cells exist in a mixed population in which only approximately 65% actually expressed H2K. Although this was deemed acceptable previously, the lack of B3Z activation may be due to insufficient H2K expression.

Alternatively the issue may be due to the replicons themselves. Although the preliminary replication assay had shown that the replicons were functioning as expected, there is the possibility that the replicons are not generating sufficient protein to be detected by the B3Z assay.

Finally it may be a mixture of any of the three. Electroporation results in considerable die off, and it is possible that, in combination with the relatively low level of H2K expression, this led to only a small population expressing both H2K and SL8.

A

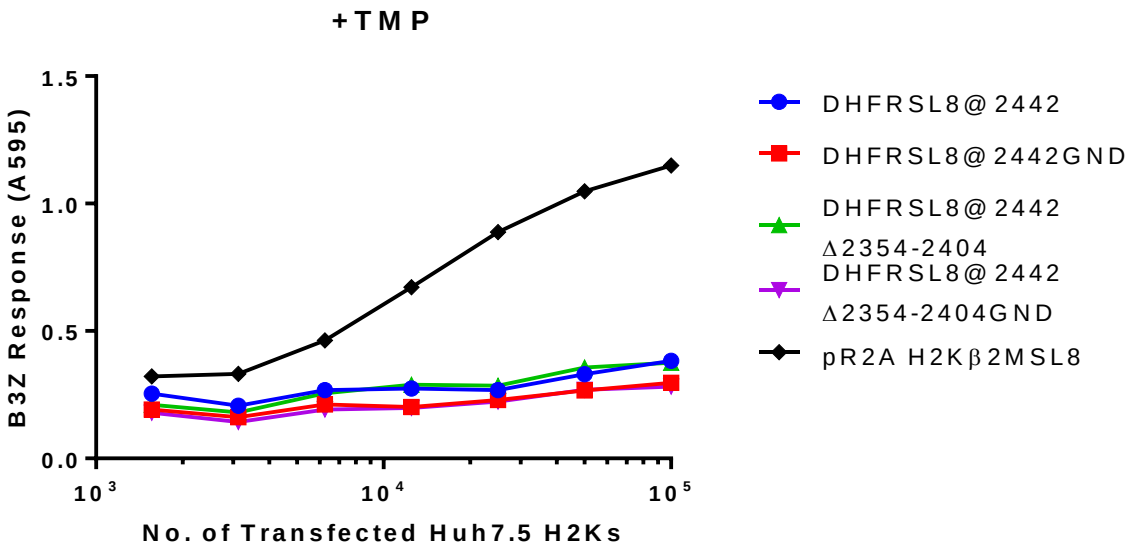

B

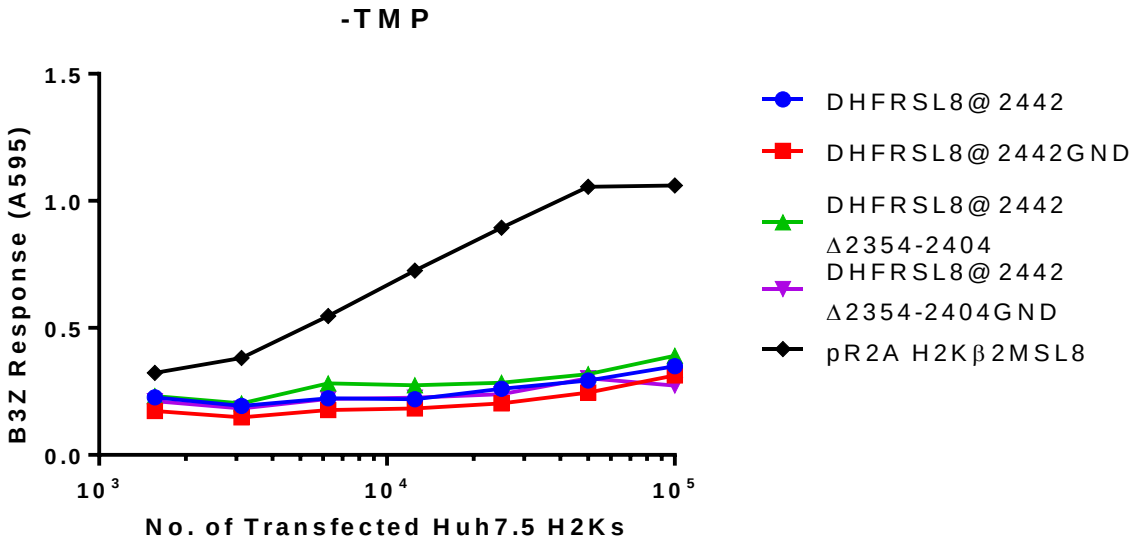

Figure 5-23 B**3Z assay of pSGRJFH1*luc(DHFRSL8@2442) replicons.** Huh7.5H2K cells were transfected with pSGRJFH1*luc(DHFRSL8@2442), pSGRJFH1*luc(DHFRSL8@2442)Δ2354-2404, pSGRJFH1*luc(DHFRSL8@2442)GND, pSGRJFH1*luc(DHFRSL8@2442)Δ2354-2404GND of pRSET2H2Kβ2MSL8 and a B3Z assay performed in either the presence (A) or absence (B) of 10 μM TMP . Data represents the average of 2 assays.

5.14 SUMMARY

Previous work has shown that an intact NS5A domain III was capable of rescuing replication when NS5A is targeted for degradation, however the benefit this has to the virus life cycle remains enigmatic. The work described in this chapter was therefore focused on determining this benefit.

The original observation that sparked this work, along with much of the subsequent work, involved destabilising the NS5A protein, either through the N-end rule or through the use of a destabilising domain. However, the impact of domain III on protein stability remained anecdotal; despite the clear ability of domain III to rescue replication during destabilisation there was no direct evidence linking domain III to protein stability. To determine the impact of domain III on NS5A stability, replicon carrying cells were treated with cycloheximide, chloroquine, and MG132, and the abundance of NS5A from the various mutant constructs monitored over time. The NS5A from both full length replicons, NeoDHFRClover@2394 and NeoDHFRClover@2442, appeared to be highly stable, showing little change over the 12 hour period. In contrast both the Δ2354-2404 and Δ2404-2435 truncated replicons demonstrated reduced stability, with each showing a clear drop in NS5A after 12 hours in the presence of cycloheximide. Interestingly the loss of stability in the Δ2354-2404 replicon could be rescued by the addition of either chloroquine or MG132, inhibiting the activity of the lysosomes and proteasome respectively, supporting a role for domain III in counteracting a cellular protein degradation pathway. Furthermore as both lysosomal and proteasomal degradation are in part regulated by ubiquitination, and that DHFR destabilisation is mediated by ubiquitin, it is likely that an interaction between domain III and ubiquitin is involved.

Although this work provided the first direct evidence that domain III has an impact on stability, and had highlighted two possible routes, attempts to repeat the work met with little success. The toxicity of the chemicals involved led to cell death and difficulties visualising the protein. As such an alternative was sought, through which NS5A stability could assessed in a more biologically relevant environment. This led to the generation of stably transfected cells lines carrying JFH1 replicons marked with a myc tag, which allowed pulse chase experiments to be performed. Disappointingly this work failed to show any difference in susceptibility to DHFR mediated degradation between full length NS5A and NS5A that carried the Δ2354-2404 truncation, with neither showing a drop off over the course of the experiment. It should be noted that this experiment was conducted over an 8 hour period, based upon the predicted half-life of NS5A of between 4-6 hours, however previous work with DHFR replicons had been conducted over a 72 hour period, with the impact of DHFR becoming apparent within 24 hours. This leaves the possibility that cells were given insufficient time

for DHFR to have a visible impact on NS5A. Alternatively, as there was only the opportunity to perform the pulse chase experiment once, due to time constraints, it is possible that residual levels of TMP in the –TMP group confounded the experiment. Further experiments are need where the time course used in the chase is extended and the cells are washed more extensively after the L-AHA pulse, perhaps with 5 minute intervals between washes to allow leeching of TMP from the cells and ensure its complete removal.

Despite not seeing a DHFR-mediated drop off in NS5A by pulse chase, there was a clear difference in the expression of NS5A in total, with the Δ2354-2404 replicon yielding considerably less protein than the full length. One possible explanation for this is that domain III may function earlier than previously thought, possibly immediately post translation. Typically unfolded proteins, similar to domains II and III will be identified by the cell and rapidly degraded by Endoplasmic reticulum associated degradation (ERAD). It may be that domain III allows NS5A to avoid being targeted by ERAD, thus increasing the level of NS5A in infected cells. Alternatively domain III may serve to protect NS5A during ER stress, a cellular condition triggered by a build-up of un-folded protein, in the ER lumen. During ER stress cells undergo metabolic changes to cope with the excess of unfolded proteins, including inhibition of translation, enhanced expression of chaperone proteins, and increased turnover of unfolded proteins by ERAD. Domain III may have therefore evolved to counter this response.

Although the role of domain III in promoting NS5A stability remains inconclusive, the impact of domain III on several virus host interactions was investigated. NS5A has long been associated with resistance to the IFN response, although the precise nature of this remains controversial. The potential involvement of domain III in interferon sensitivity was therefore tested by transfection of Huh7.5 cells with either a full length JFH1 replicon, or one carrying the Δ2354-2404 truncation, and treating the cells with varying concentrations of IFNα. In transiently transfected cells both replicons demonstrated sensitivity to IFN, although there was no difference in sensitivity between the two. This was further confirmed using stably transfected cells, which were treated with different concentrations of IFN. As before, neither truncated nor full length replicons demonstrated enhanced sensitivity to IFN than the either. Together these data suggest that the 2354-2415 region of domain III has little impact on IFN sensitivity, although given the artificial nature of using Huh7 cells to assess IFN sensitivity, there remains a possibility that domain III may yet be involved. Previous studies have shown that it is possible to get replicon-containing Huh7 cells to behave in a more 'hepatocyte-like' state(Bauhofer et al., 2012). Under such conditions the replicon becomes far more resistant to IFN treatment, and it would be interesting to see the impact of the Δ2354-2404 deletion under such circumstances.

In addition to IFN sensitivity domain III was tested for impact on antigen presentation. The potential role of domain III on protein stability and degradation may benefit the virus by limiting the generation of peptide fragments that can be presented on the cell surface by MHC, thus delaying detection of virally infected cell by the immune system. Testing of this involved the introduction of SL8 into NS5A, and transfection of these replicons into a cell line capable of presenting it. Unfortunately, although preliminary experiments had shown that the Huh7.5-H2K cells were capable of processing and presenting SL8 from a pCDNA plasmid, they did not appear capable of presenting SL8 when expressed from the context of an NS5A fusion protein.

6 DISCUSSION

This work stemmed from the initial observation that JFH1 replicons carrying a DHFR destabilising domain at different locations within NS5A domain III showed different levels of replication in the absence of TMP, but comparable levels in its presence. Given that the DHFR destabilisation domain has been reported to target conjoined proteins for proteasomal degradation via polyubiquitination (Iwamoto et al., 2010), the initial hypothesis was that an activity of domain III that protects NS5A against polyubiquitin-mediated degradation was being disrupted. As NS5A does not possess any known enzymatic activity and domain III is unstructured, a further implication of this hypothesis is that domain III is likely to mediate the effect through recruitment of a host cell protein or proteins. The aim of this study was therefore to test this hypothesis and establish whether this protective feature of domain III reflected an activity that might have an important role in other physiological settings.

USP19 was quickly identified as a potential candidate for domain III's binding partner responsible for this effect. Work in the Bartenschlager group has shown that USP19 is capable of associating with NS5A within domain III (Pichlmair et al., 2012). Furthermore this interaction would provide a clear mechanism for the process as USP19 is a de-ubiquitinase, capable of rescuing a variety of proteins from polyubiquinitation and subsequent degradation, particularly in the context of ER associated degradation (Hassink et al., 2009). Initial deletion work was consistent with involvement of USP19, as deletion of a region of NS5A domain III implicated in USP19 binding proved also to be the same deletion that made replicon replication most susceptible to TMP withdrawal. However, further investigation failed to support a role for USP19. Indeed knock down of the proteins by shRNAs was found to have no impact on the ability of HCV replicons carrying domain III deletions to recover under conditions where the NS5A-DHFR-Clover fusion product was destabilised through TMP withdrawal. At present it is not possible to rule out the possibility that residual levels of USP19 during these experiments were sufficient to provide complete protection to NS5A. However a more probable scenario is that other mechanisms are in play.

One early finding that perhaps indicated this best was the surprising observation that small 20 amino acid deletions across this same region of NS5A had little or no impact on the protein's ability to counter DHFR-mediated destabilisation. These observations argue against there being a single defined contact point between domain III and a host protein that counteracted DHFR-mediated destabilisation, but left open a number of alternative explanations.

The first was that the original hypothesis was incorrect, and that rather than modification of domain III inhibiting an activity that allows rescue from DHFR-mediated degradation, the differential response to TMP withdrawal demonstrated by the constructs was instead due to the scale of disruption to domain III. In this model the larger deletions and internal insertion of DHFRClover into domain III would have acted as cryptic degrons enhancing targeting of NS5A to the proteasome. This model makes the further assumption that proteasomal degradation only becomes the rate limiting step in replication once it reaches a certain threshold, and the impact of the modifications to domain III when TMP was still present was not sufficient for this to happen. In the case of the large scale deletion assay results this would make sense, with the largest deletion, Δ2354-2404, resulting in the greatest drop in replication, and the smallest deletion, Δ2325-2353 having no impact at all. This could also explain why the smaller deletions were tolerated, with these not being severe enough to warrant NS5A's degradation. However, further experimentation argued against this possibility, as replicons expressing an NS5A-DHFR-Clover fusion protein with a duplicated domain III, one of which was intact and one of which carried the Δ2354-2404 deletion, showed resistance to TMP withdrawal.

Whilst the data continues to point to domain III being actively involved in the protection of NS5A from DHFR-mediated degradation, a failure to identify responsible host cell proteins counteracting DHFR means that other possibilities have to be considered. A second possible explanation could relate to endogenous host cell protease activity. NS5A is well known to be the target of host cell proteases (Hidajat et al., 2004, Kalamvoki and Mavromara, 2004), with many target sites within domain III (Kalamvoki et al., 2006), and the differential response to TMP withdrawal demonstrated by the DHFR@2394 and DHFR@2442 constructs could in theory have been due to differential cleavage of the DHFR group away from those sections of NS5A (domains I and II) essential for replication. This explanation could then extend to the results from the large scale deletion replication assays if the same cleavage site was to fall between residues 2354 and 2394. However, arguing against such a model is the finding that none of the overlapping 20 amino acid deletions across the same area enhanced susceptibility to TMP withdrawal. Thus if the protease model is correct, multiple cleavage sites would have to exist in the region between residues 2354 and 2394. This seems unlikely given the relatively small region in question. Moreover analysis of the sequence between residues 2354-2394, using PROSPER (Song et al., 2012) identifies only a single calpain cleavage site after residue 2387 of limited cleavage potential.

A third possibility is that the differences in susceptibility to TMP are due to the nascent viral polyprotein's ability to form 'protective' high-ordered protein complexes that are more

resistant to degradation prior to the destabilising effect of DHFR becoming apparent. Certainly the stability of individual proteins in other settings is known to be influenced by whether they exist in isolation or in a complex (McShane et al., 2016). Furthermore, the minimum components of the replicase capable of supporting RNA replication through genetic complementation, and thus be able to engage in NS complex formation is NS3-5A, but the polyprotein can probably only start to fulfil this function once domain II (the last RNA replication essential domain of NS5A) has exited the ribosome. Thus the presence of an internal DHFR, or large deletion in domain III, shortens the time between when nascent NS3-5A is available to engage in RC activities and when the DHFR domain clears the ribosome. Some of the data collected in this study would support this mechanism; for example there is clear correlation between the size of deletion introduced into domain III, and the impact on replication. However, the data obtained with those constructs carrying two copies of domain III argues against such a model. In these experiments the duplicated Δ2354-2404 construct had a larger separation between domain II and the DHFR domain compared to the single intact domain III construct, yet the latter replicated more effectively.

The lack of complexity in domain III, including both the V5 hypervariable and the highly conserved sequence, could also suggest a fourth alternative mechanism, in which NS5A functions independently to protect itself. Low complexity is known to inhibit proteasomal degradation of proteins (Sharipo et al., 1998, Fishbain et al., 2015), by inhibiting the progression of the protein into the catalytically active 20S subunit. It is possible therefore that domain III inhibits degradation simply by stalling the proteasome. In this model the introduction of the DHFR-clover fusion peptide internally within domain III would therefore decrease the extent to which low complexity sequence separated replication essential regions of NS5A from its degron-linked partner complexity. Introduction of deletions would have the same effect, explaining the differential susceptibility to TMP withdrawal seen in these experiments. The resistance of the 2354-2404 scrambled replicon to destabilisation further supports this, as no additional amino acid complexity was introduced.

This model would however cast some doubt on whether the mapping experiments were identifying exactly the right region involved in protection against DHFR-mediated degradation. Use of the small scale deletions mapped the region of interest to between residues 2354-2415 in JFH1. However, analysis of domain III using the SEG algorithm (Wootton, 1994) predicts low complexity to residue 2428, which includes the majority of the sequence deleted in the Δ2415-2435 construct. It is therefore possible that these additional 13 residues contribute to stability, but that their loss is tolerable, due to reduced size of deletion relative to the region of interest. In support of this argument is the early observation

that both the 2354-2404 and 2404-2435 deletions had an impact on replication, whilst the smaller 20 amino acid deletions within this same region were much better tolerated.

A fifth and final model to explain the results would be that the deletions that have been introduced into domain III were not specific contact points for one or more host cell proteins that afforded protection against DHFR-mediated degradation, but instead were involved in providing the appropriate spacing between two separate contact sites within NS5A. The possibility that two separate functional sites might be needed for NS5A-host protein binding interaction is not without precedence; recruitment of p85 and β-catenin has been found to require sites in both domain I and domain III, such that loss of either the N or C termini inhibited recruitment of β-catenin completely (Milward et al., 2010). However, for this model to be correct, it would require one of the contact points to be contained within the final 6 residues of NS5A representing the NH_2 side of the NS5A/5B cleavage boundary. This region has been implicated in binding to host cell proteins, e.g. NAP1L1 (Cevik et al., 2017), and it would be interesting to see what impact knocking these down would have on replication using the DHFR constructs.

As yet it has not been possible to extend this work to include genotypes other than the genotype 2 (JFH1) strain. The NS5A domain III of genotype 2 strains of HCV contains an additional stretch of 20 amino acids not found in any other strain. This stretch represents residues 2406-2425, and as such is included in the region that has been mapped as being active in protecting NS5A during DHFR-mediated destabilisation. Additional there is considerable variation with domain III sequence between genotypes. This variation in size and sequence of domain III could suggest, therefore, that the protective ability is restricted to this one strain. However, there are several indicators that this may not be the case. Firstly, attempts made to generate equivalent genotype 1b (con1) replicons carrying DHFR-clover with or without deletions in domain III revealed that large scale disruption of domain III had such a detrimental effect on replication that often it was difficult to detect replication of these constructs. Secondly, though there is considerable variation within domain III, analysis of con1 shows it to have low complexity, similar to JFH1. Indeed similar analysis of the consensus sequence of domain III suggests that this low complexity is a common trait of domain III.

Clearly, more work needs to be done to resolve the various possible models that could account for the protective phenomenon observed here. What is obvious, however, is that while domain III might not be essential for RNA replication, its presence is required for efficient replication.

Disappointingly any role that domain III might play in stabilising NS5A could not be visualised directly. Cycloheximide based experiments generated variable results, and the single pulse chase experiment failed to see any difference between full length NS5A and NS5A carrying the Δ2354-2404 truncation. Despite this, the differential response that the DHFRClover replicons showed to TMP withdrawal still suggests that domain III plays a role in NS5A stability. The key question remains though, what is this role? Several experiments were undertaken to see whether it could include certain key aspects of HCV's interaction with the host cell.

One of these was how the virus responds to IFNα. The presence of the V3 hypervariable domain, previously shown to impact IFN sensitivity (Murphy et al., 2002, Duverlie et al., 1998), and the fact that NS5A is targeted for polyubiquitination by TRIM22 (Yang et al., 2016) and ISG12a (Xue et al., 2016), both of which are interferon stimulated genes, prompted examination into whether or not the domain III deletions altered the replicon's susceptibility to IFN. However, both transient and stable replicon experiments failed to identify any difference in IFN sensitivity between JFH1 replicons with a full length or truncated domain III. It should be noted however that the IFN work was limited to JFH1 replicons, and IFN sensitivity is the product of a variety of viral factors that include almost all HCV proteins (Kumthip and Maneekarn, 2015, Blindenbacher et al., 2003, Lin et al., 2006b, Taylor et al., 1999, Xu et al., 2009). It also remains possible that domain III could be involved in antagonising the block to virus particle production imposed on HCV by IFN. Therefore, it could be worthwhile undertaking future investigations using full length viral construct, particularly as the region of domain III involved in protecting against DHFR-mediated destabilisation is distinct from those believed to be involved in particle production (Ross-Thriepland and Harris, 2015, Appel et al., 2008, Hughes et al., 2009).

A second area explored that might be influenced by altered NS5A stability was antigen presentation. Previous investigators have found that the NS4B/5A precursor can inhibit the transport of MHC class I complexes to the cell membrane (Konan et al., 2003). Furthermore HCV is well documented to induce ER stress within infected cells (Tardif et al., 2002), which itself has a detrimental impact on antigen processing and presentation (Granados et al., 2009). It was therefore hypothesised that NS5A domain III might play a role in reducing presentation of its own, and maybe other NS protein epitopes on MHC class I molecules. However, it was not possible to either confirm or deny this due to the continued failure of the Huh7.5 derived cell lines to present the SL8 epitope when expressed from the HCV replicon. It seems unlikely however, that the failure to see SL8 presentation is due to the virus completely blocking presentation as it is well documented that CD8+ cells have a protective

role against HCV *in vivo* (Cooper et al., 1999). Moreover the protective nature of the HLA-B*27 allele, documented to promote HCV clearance, is believed to be mediated by efficient processing and presentation of HCV epitopes (Schmidt et al., 2012). In addition it has been reported that expression of HCV proteins does not interfere with MHC class I processing and presentation (Moradpour et al., 2001) so it would be expected that some presentation should still occur. More likely was that the Huh7.5 cells line expressing H2K were simply incapable of processing and presenting the SL8 from the replicons at sufficient levels to be detectable.

A third possibility that was not investigated was whether the protective role offered by domain III somehow related to the viruses ability to replicate in the face of ER stress. One of the more remarkable observations made in this study was that while deletions in domain III consistently reduced the replicative capacity of genotype 1 and 2a replicons in transient replication assays, this was not the case in stable colony formation assays. While deletion in domain III reduced colony formation in con1 replicons it enhanced colony formation in the JFH1 replicons. Replication of genotype 2 replicons is much more robust that genotype 1 replicons, and often cytopathic effects can be seen 48-72 hours after cells are transfected with these. One possibility therefore maybe that genotype 2a replicons expressing full length NS5A 'overcome' any suppressive effects that ER stress impose upon the cell, but in doing so the high levels of replication ultimately lead to cell death. In contrast replication of the equivalent constructs expressing NS5A with the domain III deletion is tempered in such a way to allow long term survival of both the cell and replicon. It would be interesting to see the effect of pre-imposed ER stress on replication of these various constructs under transient conditions.

6.1 FINAL THOUGHTS

This work has examined a novel activity within the HCV NS5A protein, specifically domain III, which I propose protects or stabilises the protein. Despite my best attempts however it was not possible to determine the molecular mechanism behind this activity, or what benefits it might provide the virus. It could be that by having two intrinsically disordered domains, features that normally destabilize proteins, selective pressure has resulted in domain III being able to counteract this. Perhaps a collateral consequence of a necessary interaction that NS5A undertakes with host cell signalling molecules exposes it to degradative processes, and that domain III has evolved in such a way to limit co-degradation. Alternatively as a virus capable of establishing a chronic infection, an ability to avoid immunity is likely to be important for HCV. Finally domain III may simply play a role in passively boosting protein stability to promote viral replication. Data presenting within this thesis would certainly

support this idea as both JFH1 and Con1 replicons demonstrate impaired replication upon truncation of this domain. HCV infection is known to trigger ER stress in infected cells, leading to reduced translation, enhanced expression of chaperon proteins and increased turnover of unfolded proteins. It is therefore possible that NS5A domain III has evolved in such a way as to protect itself during this response.

7 BIBLIOGRAPHY

ABE, H., OCHI, H., MAEKAWA, T., HAYES, C. N., TSUGE, M., MIKI, D., MITSUI, F., HIRAGA, N., IMAMURA, M., TAKAHASHI, S., OHISHI, W., ARIHIRO, K., KUBO, M., NAKAMURA, Y. & CHAYAMA, K. 2010. Common variation of IL28 affects gamma-GTP levels and inflammation of the liver in chronically infected hepatitis C virus patients. *J Hepatol,* 53**,** 439-43.

AGARD, N. J., BASKIN, J. M., PRESCHER, J. A., LO, A. & BERTOZZI, C. R. 2006. A Comparative Study of Bioorthogonal Reactions with Azides. *ACS Chemical Biology,* 1**,** 644-648.

AGNELLO, V., ABEL, G., ELFAHAL, M., KNIGHT, G. B. & ZHANG, Q. X. 1999. Hepatitis C virus and other flaviviridae viruses enter cells via low density lipoprotein receptor. *Proc Natl Acad Sci U S A,* 96**,** 12766-71.

AIT-GOUGHOULTE, M., HOURIOUX, C., PATIENT, R., TRASSARD, S., BRAND, D. & ROINGEARD, P. 2006. Core protein cleavage by signal peptide peptidase is required for hepatitis C virus-like particle assembly. *J Gen Virol,* 87**,** 855-60.

AIZAKI, H., SAITO, S., OGINO, T., MIYAJIMA, N., HARADA, T., MATSUURA, Y., MIYAMURA, T. & KOHASE, M. 2000. Suppression of interferon-induced antiviral activity in cells expressing hepatitis C virus proteins. *J Interferon Cytokine Res,* 20**,** 1111-20.

ALTUN, M., ZHAO, B., VELASCO, K., LIU, H., HASSINK, G., PASCHKE, J., PEREIRA, T. & LINDSTEN, K. 2012. Ubiquitin-specific protease 19 (USP19) regulates hypoxia-inducible factor 1alpha (HIF-1alpha) during hypoxia. *J Biol Chem,* 287**,** 1962-9.

AMPUERO, J., DEL CAMPO, J. A., ROJAS, L., CALLEJA, J. L., CABEZAS, J., LENS, S., CRESPO, J., FORNS, X., ANDRADE, R. J., FERNANDEZ, I., BUTI, M., MILLAN, R. & ROMERO-GOMEZ, M. 2015. Role of ITPA and SLC28A2 genes in the prediction of anaemia associated with protease inhibitor plus ribavirin and peginterferon in hepatitis C treatment. *J Clin Virol,* 68**,** 56-60.

APPEL, N., PIETSCHMANN, T. & BARTENSCHLAGER, R. 2005. Mutational analysis of hepatitis C virus nonstructural protein 5A: potential role of differential phosphorylation in RNA replication and identification of a genetically flexible domain. *J Virol,* 79**,** 3187-94.

APPEL, N., ZAYAS, M., MILLER, S., KRIJNSE-LOCKER, J., SCHALLER, T., FRIEBE, P., KALLIS, S., ENGEL, U. & BARTENSCHLAGER, R. 2008. Essential role of domain III of nonstructural protein 5A for hepatitis C virus infectious particle assembly. *PLoS Pathog,* 4**,** e1000035.

APPLEBY, T. C., PERRY, J. K., MURAKAMI, E., BARAUSKAS, O., FENG, J., CHO, A., FOX, D., 3RD, WETMORE, D. R., MCGRATH, M. E., RAY, A. S., SOFIA, M. J., SWAMINATHAN, S. & EDWARDS, T. E. 2015. Viral replication. Structural basis for RNA replication by the hepatitis C virus polymerase. *Science,* 347**,** 771-5.

ARNAUD, N., DABO, S., MAILLARD, P., BUDKOWSKA, A., KALLIAMPAKOU, K. I., MAVROMARA, P., GARCIN, D., HUGON, J., GATIGNOL, A., AKAZAWA, D., WAKITA, T. & MEURS, E. F. 2010. Hepatitis C virus controls interferon production through PKR activation. *PLoS One,* 5**,** e10575.

ARUMUGASWAMI, V., REMENYI, R., KANAGAVEL, V., SUE, E. Y., NGOC HO, T., LIU, C., FONTANES, V., DASGUPTA, A. & SUN, R. 2008. High-resolution functional profiling of hepatitis C virus genome. *PLoS Pathog,* 4**,** e1000182.

ASABE, S. I., TANJI, Y., SATOH, S., KANEKO, T., KIMURA, K. & SHIMOTOHNO, K. 1997. The N-terminal region of hepatitis C virus-encoded NS5A is important for NS4A-dependent phosphorylation. *J Virol,* 71**,** 790-6.

AUFDERHEIDE, A., UNVERDORBEN, P., BAUMEISTER, W. & FORSTER, F. 2015. Structural disorder and its role in proteasomal degradation. *FEBS Lett,* 589**,** 2552-60.

BADILLO, A., RECEVEUR-BRECHOT, V., SARRAZIN, S., CANTRELLE, F. X., DELOLME, F., FOGERON, M. L., MOLLE, J., MONTSERRET, R., BOCKMANN, A., BARTENSCHLAGER, R., LOHMANN, V., LIPPENS, G., RICARD-BLUM, S., HANOULLE, X. & PENIN, F. 2017. Overall Structural Model of NS5A Protein from Hepatitis C Virus and Modulation by Mutations Confering Resistance of Virus Replication to Cyclosporin A. *Biochemistry,* 56**,** 3029-3048.

BANASZYNSKI, L. A., CHEN, L. C., MAYNARD-SMITH, L. A., OOI, A. G. & WANDLESS, T. J. 2006. A rapid, reversible, and tunable method to regulate protein function in living cells using synthetic small molecules. *Cell,* 126**,** 995-1004.

BARBA, G., HARPER, F., HARADA, T., KOHARA, M., GOULINET, S., MATSUURA, Y., EDER, G., SCHAFF, Z., CHAPMAN, M. J., MIYAMURA, T. & BRECHOT, C. 1997. Hepatitis C virus core protein shows a

cytoplasmic localization and associates to cellular lipid storage droplets. *Proc Natl Acad Sci U S A,* 94**,** 1200-5.

BARTENSCHLAGER, R., AHLBORN-LAAKE, L., MOUS, J. & JACOBSEN, H. 1994. Kinetic and structural analyses of hepatitis C virus polyprotein processing. *J Virol,* 68**,** 5045-55.

BARTENSCHLAGER, R., PENIN, F., LOHMANN, V. & ANDRE, P. 2011. Assembly of infectious hepatitis C virus particles. *Trends Microbiol,* 19**,** 95-103.

BARTOSCH, B. & COSSET, F. L. 2006. Cell entry of hepatitis C virus. *Virology,* 348**,** 1-12.

BARTOSCH, B., VITELLI, A., GRANIER, C., GOUJON, C., DUBUISSON, J., PASCALE, S., SCARSELLI, E., CORTESE, R., NICOSIA, A. & COSSET, F. L. 2003. Cell entry of hepatitis C virus requires a set of co-receptors that include the CD81 tetraspanin and the SR-B1 scavenger receptor. *J Biol Chem,* 278**,** 41624-30.

BAUHOFER, O., RUGGIERI, A., SCHMID, B., SCHIRMACHER, P. & BARTENSCHLAGER, R. 2012. Persistence of HCV in quiescent hepatic cells under conditions of an interferon-induced antiviral response. *Gastroenterology,* 143**,** 429-38.e8.

BEHRENS, S. E., TOMEI, L. & DE FRANCESCO, R. 1996. Identification and properties of the RNA-dependent RNA polymerase of hepatitis C virus. *EMBO J,* 15**,** 12-22.

BELEMA, M. & MEANWELL, N. A. 2014. Discovery of Daclatasvir, a Pan-Genotypic Hepatitis C Virus NS5A Replication Complex Inhibitor with Potent Clinical Effect. *Journal of Medicinal Chemistry,* 57**,** 5057-5071.

BELON, C. A. & FRICK, D. N. 2009. Helicase inhibitors as specifically targeted antiviral therapy for hepatitis C. *Future Virol,* 4**,** 277-293.

BERAN, R. K., SEREBROV, V. & PYLE, A. M. 2007. The serine protease domain of hepatitis C viral NS3 activates RNA helicase activity by promoting the binding of RNA substrate. *J Biol Chem,* 282**,** 34913-20.

BISWAS, A., TREADAWAY, J. & TELLINGHUISEN, T. L. 2016. Interaction between Nonstructural Proteins NS4B and NS5A Is Essential for Proper NS5A Localization and Hepatitis C Virus RNA Replication. *J Virol,* 90**,** 7205-18.

BLANCHARD, E., BELOUZARD, S., GOUESLAIN, L., WAKITA, T., DUBUISSON, J., WYCHOWSKI, C. & ROUILLE, Y. 2006. Hepatitis C virus entry depends on clathrin-mediated endocytosis. *J Virol,* 80**,** 6964-72.

BLIGHT, K. J., KOLYKHALOV, A. A. & RICE, C. M. 2000. Efficient initiation of HCV RNA replication in cell culture. *Science,* 290**,** 1972-4.

BLIGHT, K. J., MCKEATING, J. A. & RICE, C. M. 2002. Highly permissive cell lines for subgenomic and genomic hepatitis C virus RNA replication. *J Virol,* 76**,** 13001-14.

BLINDENBACHER, A., DUONG, F. H., HUNZIKER, L., STUTVOET, S. T., WANG, X., TERRACCIANO, L., MORADPOUR, D., BLUM, H. E., ALONZI, T., TRIPODI, M., LA MONICA, N. & HEIM, M. H. 2003. Expression of hepatitis c virus proteins inhibits interferon alpha signaling in the liver of transgenic mice. *Gastroenterology,* 124**,** 1465-75.

BOURLIERE, M., GORDON, S. C., FLAMM, S. L., COOPER, C. L., RAMJI, A., TONG, M., RAVENDHRAN, N., VIERLING, J. M., TRAN, T. T., PIANKO, S., BANSAL, M. B., DE LEDINGHEN, V., HYLAND, R. H., STAMM, L. M., DVORY-SOBOL, H., SVAROVSKAIA, E., ZHANG, J., HUANG, K. C., SUBRAMANIAN, G. M., BRAINARD, D. M., MCHUTCHISON, J. G., VERNA, E. C., BUGGISCH, P., LANDIS, C. S., YOUNES, Z. H., CURRY, M. P., STRASSER, S. I., SCHIFF, E. R., REDDY, K. R., MANNS, M. P., KOWDLEY, K. V. & ZEUZEM, S. 2017. Sofosbuvir, Velpatasvir, and Voxilaprevir for Previously Treated HCV Infection. *N Engl J Med,* 376**,** 2134-2146.

BRASS, V., BIECK, E., MONTSERRET, R., WOLK, B., HELLINGS, J. A., BLUM, H. E., PENIN, F. & MORADPOUR, D. 2002. An amino-terminal amphipathic alpha-helix mediates membrane association of the hepatitis C virus nonstructural protein 5A. *J Biol Chem,* 277**,** 8130-9.

BRASS, V., PAL, Z., SAPAY, N., DELEAGE, G., BLUM, H. E., PENIN, F. & MORADPOUR, D. 2007. Conserved determinants for membrane association of nonstructural protein 5A from hepatitis C virus and related viruses. *J Virol,* 81**,** 2745-57.

BRESSANELLI, S., TOMEI, L., REY, F. A. & DE FRANCESCO, R. 2002. Structural analysis of the hepatitis C virus RNA polymerase in complex with ribonucleotides. *J Virol,* 76**,** 3482-92.

BUCKWOLD, V. E., BEER, B. E. & DONIS, R. O. 2003. Bovine viral diarrhea virus as a surrogate model of hepatitis C virus for the evaluation of antiviral agents. *Antiviral Research,* 60**,** 1-15.

CAMBORDE, L., PLANCHAIS, S., TOURNIER, V., JAKUBIEC, A., DRUGEON, G., LACASSAGNE, E., PFLIEGER, S., CHENON, M. & JUPIN, I. 2010. The ubiquitin-proteasome system regulates the accumulation of Turnip yellow mosaic virus RNA-dependent RNA polymerase during viral infection. *Plant Cell,* 22**,** 3142-52.

CARRERE-KREMER, S., MONTPELLIER-PALA, C., COCQUEREL, L., WYCHOWSKI, C., PENIN, F. & DUBUISSON, J. 2002. Subcellular localization and topology of the p7 polypeptide of hepatitis C virus. *J Virol,* 76**,** 3720-30.

CATANESE, M. T., URYU, K., KOPP, M., EDWARDS, T. J., ANDRUS, L., RICE, W. J., SILVESTRY, M., KUHN, R. J. & RICE, C. M. 2013. Ultrastructural analysis of hepatitis C virus particles. *Proc Natl Acad Sci U S A,* 110**,** 9505-10.

CEVIK, R. E., CESAREC, M., DA SILVA FILIPE, A., LICASTRO, D., MCLAUCHLAN, J. & MARCELLO, A. 2017. Hepatitis C virus NS5A targets the nucleosome assembly protein NAP1L1 to control the innate cellular response. *J Virol*.

CHAN, D. P., SUN, H. Y., WONG, H. T., LEE, S. S. & HUNG, C. C. 2016. Sexually acquired hepatitis C virus infection: a review. *Int J Infect Dis,* 49**,** 47-58.

CHANG, J., GUO, J. T., JIANG, D., GUO, H., TAYLOR, J. M. & BLOCK, T. M. 2008. Liver-specific microRNA miR-122 enhances the replication of hepatitis C virus in nonhepatic cells. *J Virol,* 82**,** 8215-23.

CHANG, K. S., JIANG, J., CAI, Z. & LUO, G. 2007. Human apolipoprotein e is required for infectivity and production of hepatitis C virus in cell culture. *J Virol,* 81**,** 13783-93.

CHANG, L. & KARIN, M. 2001. Mammalian MAP kinase signalling cascades. *Nature,* 410**,** 37-40.

CHEN, S. H. & TAN, S. L. 2005. Discovery of small-molecule inhibitors of HCV NS3-4A protease as potential therapeutic agents against HCV infection. *Curr Med Chem,* 12**,** 2317-42.

CHENON, M., CAMBORDE, L., CHEMINANT, S. & JUPIN, I. 2012. A viral deubiquitylating enzyme targets viral RNA-dependent RNA polymerase and affects viral infectivity. *EMBO J,* 31**,** 741-53.

CHERRY, A. L., DENNIS, C. A., BARON, A., EISELE, L. E., THOMMES, P. A. & JAEGER, J. 2015. Hydrophobic and charged residues in the C-terminal arm of hepatitis C virus RNA-dependent RNA polymerase regulate initiation and elongation. *J Virol,* 89**,** 2052-63.

CICERO, D. O., BARBATO, G., KOCH, U., INGALLINELLA, P., BIANCHI, E., NARDI, M. C., STEINKUHLER, C., CORTESE, R., MATASSA, V., DE FRANCESCO, R., PESSI, A. & BAZZO, R. 1999. Structural characterization of the interactions of optimized product inhibitors with the N-terminal proteinase domain of the hepatitis C virus (HCV) NS3 protein by NMR and modelling studies. *J Mol Biol,* 289**,** 385-96.

CLACKSON, T., YANG, W., ROZAMUS, L. W., HATADA, M., AMARA, J. F., ROLLINS, C. T., STEVENSON, L. F., MAGARI, S. R., WOOD, S. A., COURAGE, N. L., LU, X., CERASOLI, F., JR., GILMAN, M. & HOLT, D. A. 1998. Redesigning an FKBP-ligand interface to generate chemical dimerizers with novel specificity. *Proc Natl Acad Sci U S A,* 95**,** 10437-42.

COCQUEREL, L., KUO, C. C., DUBUISSON, J. & LEVY, S. 2003. CD81-dependent binding of hepatitis C virus E1E2 heterodimers. *J Virol,* 77**,** 10677-83.

CODELLI, J. A., BASKIN, J. M., AGARD, N. J. & BERTOZZI, C. R. 2008. Second-Generation Difluorinated Cyclooctynes for Copper-Free Click Chemistry. *Journal of the American Chemical Society,* 130**,** 11486-11493.

COOPER, S., ERICKSON, A. L., ADAMS, E. J., KANSOPON, J., WEINER, A. J., CHIEN, D. Y., HOUGHTON, M., PARHAM, P. & WALKER, C. M. 1999. Analysis of a successful immune response against hepatitis C virus. *Immunity,* 10**,** 439-49.

CORNBERG, M., RAZAVI, H. A., ALBERTI, A., BERNASCONI, E., BUTI, M., COOPER, C., DALGARD, O., DILLION, J. F., FLISIAK, R., FORNS, X., FRANKOVA, S., GOLDIS, A., GOULIS, I., HALOTA, W., HUNYADY, B., LAGGING, M., LARGEN, A., MAKARA, M., MANOLAKOPOULOS, S., MARCELLIN, P., MARINHO, R. T., POL, S., POYNARD, T., PUOTI, M., SAGALOVA, O., SIBBEL, S., SIMON, K., WALLACE, C., YOUNG, K., YURDAYDIN, C., ZUCKERMAN, E., NEGRO, F. & ZEUZEM, S. 2011. A systematic review of hepatitis C virus epidemiology in Europe, Canada and Israel. *Liver Int,* 31 Suppl 2**,** 30-60.

CRISTOFARI, G., IVANYI-NAGY, R., GABUS, C., BOULANT, S., LAVERGNE, J. P., PENIN, F. & DARLIX, J. L. 2004. The hepatitis C virus Core protein is a potent nucleic acid chaperone that directs dimerization of the viral (+) strand RNA in vitro. *Nucleic Acids Res,* 32**,** 2623-31.

DAFA-BERGER, A., KUZMINA, A., FASSLER, M., YITZHAK-ASRAF, H., SHEMER-AVNI, Y. & TAUBE, R. 2012. Modulation of hepatitis C virus release by the interferon-induced protein BST-2/tetherin. *Virology,* 428**,** 98-111.

DAHARI, H., FELIU, A., GARCIA-RETORTILLO, M., FORNS, X. & NEUMANN, A. U. 2005. Second hepatitis C replication compartment indicated by viral dynamics during liver transplantation. *J Hepatol,* 42**,** 491-8.

DATE, T., KATO, T., MIYAMOTO, M., ZHAO, Z., YASUI, K., MIZOKAMI, M. & WAKITA, T. 2004. Genotype 2a hepatitis C virus subgenomic replicon can replicate in HepG2 and IMY-N9 cells. *J Biol Chem,* 279**,** 22371-6.

DE CASTRO, E., SIGRIST, C. J., GATTIKER, A., BULLIARD, V., LANGENDIJK-GENEVAUX, P. S., GASTEIGER, E., BAIROCH, A. & HULO, N. 2006. ScanProsite: detection of PROSITE signature matches and ProRule-associated functional and structural residues in proteins. *Nucleic Acids Res,* 34**,** W362-5.

DE FRANCESCO, R., URBANI, A., NARDI, M. C., TOMEI, L., STEINKUHLER, C. & TRAMONTANO, A. 1996. A zinc binding site in viral serine proteinases. *Biochemistry,* 35**,** 13282-7.

DIAO, J., PANTUA, H., NGU, H., KOMUVES, L., DIEHL, L., SCHAEFER, G. & KAPADIA, S. B. 2012. Hepatitis C virus induces epidermal growth factor receptor activation via CD81 binding for viral internalization and entry. *J Virol,* 86**,** 10935-49.

DING, Q., VON SCHAEWEN, M. & PLOSS, A. 2014. The impact of hepatitis C virus entry on viral tropism. *Cell host & microbe,* 16**,** 562-568.

DONAHUE, J. G., MUÑOZ, A., NESS, P. M., BROWN, D. E., YAWN, D. H., MCALLISTER, H. A., REITZ, B. A. & NELSON, K. E. 1992. The Declining Risk of Post-Transfusion Hepatitis C Virus Infection. *New England Journal of Medicine,* 327**,** 369-373.

DROZDETSKIY, A., COLE, C., PROCTER, J. & BARTON, G. J. 2015. JPred4: a protein secondary structure prediction server. *Nucleic Acids Res,* 43**,** W389-94.

DUBUISSON, J., HSU, H. H., CHEUNG, R. C., GREENBERG, H. B., RUSSELL, D. G. & RICE, C. M. 1994. Formation and intracellular localization of hepatitis C virus envelope glycoprotein complexes expressed by recombinant vaccinia and Sindbis viruses. *J Virol,* 68**,** 6147-60.

DUJARDIN, M., MADAN, V., MONTSERRET, R., AHUJA, P., HUVENT, I., LAUNAY, H., LEROY, A., BARTENSCHLAGER, R., PENIN, F., LIPPENS, G. & HANOULLE, X. 2015. A Proline-Tryptophan Turn in the Intrinsically Disordered Domain 2 of NS5A Protein Is Essential for Hepatitis C Virus RNA Replication. *J Biol Chem,* 290**,** 19104-20.

DUMOULIN, F. L., VON DEM BUSSCHE, A., LI, J., KHAMZINA, L., WANDS, J. R., SAUERBRUCH, T. & SPENGLER, U. 2003. Hepatitis C Virus NS2 Protein Inhibits Gene Expression from Different Cellular and Viral Promoters in Hepatic and Nonhepatic Cell Lines. *Virology,* 305**,** 260-266.

DUVERLIE, G., KHORSI, H., CASTELAIN, S., JAILLON, O., IZOPET, J., LUNEL, F., EB, F., PENIN, F. & WYCHOWSKI, C. 1998. Sequence analysis of the NS5A protein of European hepatitis C virus 1b isolates and relation to interferon sensitivity. *J Gen Virol,* 79 (Pt 6)**,** 1373-81.

EGGER, D., WOLK, B., GOSERT, R., BIANCHI, L., BLUM, H. E., MORADPOUR, D. & BIENZ, K. 2002. Expression of hepatitis C virus proteins induces distinct membrane alterations including a candidate viral replication complex. *J Virol,* 76**,** 5974-84.

EL-HAGE, N. & LUO, G. 2003. Replication of hepatitis C virus RNA occurs in a membrane-bound replication complex containing nonstructural viral proteins and RNA. *J Gen Virol,* 84**,** 2761-9.

ELAZAR, M., CHEONG, K. H., LIU, P., GREENBERG, H. B., RICE, C. M. & GLENN, J. S. 2003. Amphipathic helix-dependent localization of NS5A mediates hepatitis C virus RNA replication. *J Virol,* 77**,** 6055-61.

ELGHARABLY, A., GOMAA, A. I., CROSSEY, M. M. E., NORSWORTHY, P. J., WAKED, I. & TAYLOR-ROBINSON, S. D. 2017. Hepatitis C in Egypt – past, present, and future. *International Journal of General Medicine,* 10**,** 1-6.

ENOMOTO, N., SAKUMA, I., ASAHINA, Y., KUROSAKI, M., MURAKAMI, T., YAMAMOTO, C., OGURA, Y., IZUMI, N., MARUMO, F. & SATO, C. 1996. Mutations in the nonstructural protein 5A gene and response to interferon in patients with chronic hepatitis C virus 1b infection. *N Engl J Med,* 334**,** 77-81.

ERDTMANN, L., FRANCK, N., LERAT, H., LE SEYEC, J., GILOT, D., CANNIE, I., GRIPON, P., HIBNER, U. & GUGUEN-GUILLOUZO, C. 2003. The hepatitis C virus NS2 protein is an inhibitor of CIDE-B-induced apoptosis. *J Biol Chem,* 278**,** 18256-64.

EVANS, M. J., RICE, C. M. & GOFF, S. P. 2004. Phosphorylation of hepatitis C virus nonstructural protein 5A modulates its protein interactions and viral RNA replication. *Proceedings of the National Academy of Sciences of the United States of America,* 101**,** 13038-13043.

EVANS, M. J., VON HAHN, T., TSCHERNE, D. M., SYDER, A. J., PANIS, M., WOLK, B., HATZIIOANNOU, T., MCKEATING, J. A., BIENIASZ, P. D. & RICE, C. M. 2007. Claudin-1 is a hepatitis C virus co-receptor required for a late step in entry. *Nature,* 446**,** 801-5.

EYRE, N. S., FICHES, G. N., ALOIA, A. L., HELBIG, K. J., MCCARTNEY, E. M., MCERLEAN, C. S., LI, K., AGGARWAL, A., TURVILLE, S. G. & BEARD, M. R. 2014. Dynamic imaging of the hepatitis C virus NS5A protein during a productive infection. *J Virol,* 88**,** 3636-52.

FALSON, P., BARTOSCH, B., ALSALEH, K., TEWS, B. A., LOQUET, A., CICZORA, Y., RIVA, L., MONTIGNY, C., MONTPELLIER, C., DUVERLIE, G., PECHEUR, E. I., LE MAIRE, M., COSSET, F. L., DUBUISSON, J. & PENIN, F. 2015. Hepatitis C Virus Envelope Glycoprotein E1 Forms Trimers at the Surface of the Virion. *J Virol,* 89**,** 10333-46.

FDA. 2015. *HARVONI® (ledipasvir and sofosbuvir) tablets* [Online]. Available: https://www.accessdata.fda.gov/drugsatfda_docs/label/2015/205834s001lbl.pdf [Accessed 2017].

FDA. 2016. *Daklinza (daclatasvir) tablets* [Online]. PDA. Available: https://www.accessdata.fda.gov/drugsatfda_docs/label/2016/206843s004lbl.pdf [Accessed 12/09/2017 2017].

FEUERSTEIN, S., SOLYOM, Z., ALADAG, A., FAVIER, A., SCHWARTEN, M., HOFFMANN, S., WILLBOLD, D. & BRUTSCHER, B. 2012. Transient structure and SH3 interaction sites in an intrinsically disordered fragment of the hepatitis C virus protein NS5A. *J Mol Biol,* 420**,** 310-23.

FINN, R. D., ATTWOOD, T. K., BABBITT, P. C., BATEMAN, A., BORK, P., BRIDGE, A. J., CHANG, H. Y., DOSZTANYI, Z., EL-GEBALI, S., FRASER, M., GOUGH, J., HAFT, D., HOLLIDAY, G. L., HUANG, H., HUANG, X., LETUNIC, I., LOPEZ, R., LU, S., MARCHLER-BAUER, A., MI, H., MISTRY, J., NATALE, D. A., NECCI, M., NUKA, G., ORENGO, C. A., PARK, Y., PESSEAT, S., PIOVESAN, D., POTTER, S. C., RAWLINGS, N. D., REDASCHI, N., RICHARDSON, L., RIVOIRE, C., SANGRADOR-VEGAS, A., SIGRIST, C., SILLITOE, I., SMITHERS, B., SQUIZZATO, S., SUTTON, G., THANKI, N., THOMAS, P. D., TOSATTO, S. C., WU, C. H., XENARIOS, I., YEH, L. S., YOUNG, S. Y. & MITCHELL, A. L. 2017. InterPro in 2017-beyond protein family and domain annotations. *Nucleic Acids Res,* 45**,** D190-d199.

FISHBAIN, S., INOBE, T., ISRAELI, E., CHAVALI, S., YU, H., KAGO, G., BABU, M. M. & MATOUSCHEK, A. 2015. Sequence composition of disordered regions fine-tunes protein half-life. *Nat Struct Mol Biol,* 22**,** 214-21.

FISHMAN, S. L., MURRAY, J. M., ENG, F. J., WALEWSKI, J. L., MORGELLO, S. & BRANCH, A. D. 2008. Molecular and bioinformatic evidence of hepatitis C virus evolution in brain. *J Infect Dis,* 197**,** 597-607.

FLETCHER, N. F. & MCKEATING, J. A. 2012. Hepatitis C virus and the brain. *J Viral Hepat,* 19**,** 301-6.

FORTON, D. M., KARAYIANNIS, P., MAHMUD, N., TAYLOR-ROBINSON, S. D. & THOMAS, H. C. 2004. Identification of unique hepatitis C virus quasispecies in the central nervous system and comparative analysis of internal translational efficiency of brain, liver, and serum variants. *J Virol,* 78**,** 5170-83.

FRANCH, H. A., SOOPARB, S., DU, J. & BROWN, N. S. 2001. A mechanism regulating proteolysis of specific proteins during renal tubular cell growth. *J Biol Chem,* 276**,** 19126-31.

FRASER, C. S. & DOUDNA, J. A. 2007. Structural and mechanistic insights into hepatitis C viral translation initiation. *Nat Rev Microbiol,* 5**,** 29-38.

FRENTZEN, A., ANGGAKUSUMA, GURLEVIK, E., HUEGING, K., KNOCKE, S., GINKEL, C., BROWN, R. J., HEIM, M., DILL, M. T., KROGER, A., KALINKE, U., KADERALI, L., KUEHNEL, F. & PIETSCHMANN, T. 2014. Cell entry, efficient RNA replication, and production of infectious hepatitis C virus progeny in mouse liver-derived cells. *Hepatology,* 59**,** 78-88.

FRICK, D. N., RYPMA, R. S., LAM, A. M. & GU, B. 2004. The nonstructural protein 3 protease/helicase requires an intact protease domain to unwind duplex RNA efficiently. *J Biol Chem,* 279**,** 1269-80.

FRIDELL, R. A., QIU, D., WANG, C., VALERA, L. & GAO, M. 2010. Resistance analysis of the hepatitis C virus NS5A inhibitor BMS-790052 in an in vitro replicon system. *Antimicrob Agents Chemother,* 54**,** 3641-50.

FRIEBE, P. & BARTENSCHLAGER, R. 2009. Role of RNA structures in genome terminal sequences of the hepatitis C virus for replication and assembly. *J Virol,* 83**,** 11989-95.

FRIEBE, P., LOHMANN, V., KRIEGER, N. & BARTENSCHLAGER, R. 2001. Sequences in the 5' nontranslated region of hepatitis C virus required for RNA replication. *J Virol,* 75**,** 12047-57.

GALE, M. J., JR., KORTH, M. J. & KATZE, M. G. 1998. Repression of the PKR protein kinase by the hepatitis C virus NS5A protein: a potential mechanism of interferon resistance. *Clin Diagn Virol,* 10**,** 157-62.

GALE, M. J., JR., KORTH, M. J., TANG, N. M., TAN, S. L., HOPKINS, D. A., DEVER, T. E., POLYAK, S. J., GRETCH, D. R. & KATZE, M. G. 1997. Evidence that hepatitis C virus resistance to interferon is mediated through repression of the PKR protein kinase by the nonstructural 5A protein. *Virology,* 230**,** 217-27.

GANNAGE, M., DORMANN, D., ALBRECHT, R., DENGJEL, J., TOROSSI, T., RAMER, P. C., LEE, M., STROWIG, T., ARREY, F., CONENELLO, G., PYPAERT, M., ANDERSEN, J., GARCIA-SASTRE, A. & MUNZ, C. 2009. Matrix protein 2 of influenza A virus blocks autophagosome fusion with lysosomes. *Cell Host Microbe,* 6**,** 367-80.

GARAIGORTA, U. & CHISARI, F. V. 2009. Hepatitis C virus blocks interferon effector function by inducing protein kinase R phosphorylation. *Cell Host Microbe,* 6**,** 513-22.

GE, D., FELLAY, J., THOMPSON, A. J., SIMON, J. S., SHIANNA, K. V., URBAN, T. J., HEINZEN, E. L., QIU, P., BERTELSEN, A. H., MUIR, A. J., SULKOWSKI, M., MCHUTCHISON, J. G. & GOLDSTEIN, D. B. 2009. Genetic variation in IL28B predicts hepatitis C treatment-induced viral clearance. *Nature,* 461**,** 399-401.

GENTILE, I., BORGIA, F., BUONOMO, A. R., CASTALDO, G. & BORGIA, G. 2013. A novel promising therapeutic option against hepatitis C virus: an oral nucleotide NS5B polymerase inhibitor sofosbuvir. *Curr Med Chem,* 20**,** 3733-42.

GENTILE, I., BUONOMO, A. R. & BORGIA, G. 2014. Dasabuvir: A Non-Nucleoside Inhibitor of NS5B for the Treatment of Hepatitis C Virus Infection. *Rev Recent Clin Trials,* 9**,** 115-23.

GENTILE, I., VIOLA, C., BORGIA, F., CASTALDO, G. & BORGIA, G. 2009. Telaprevir: a promising protease inhibitor for the treatment of hepatitis C virus infection. *Curr Med Chem,* 16**,** 1115-21.

GENTZSCH, J., BROHM, C., STEINMANN, E., FRIESLAND, M., MENZEL, N., VIEYRES, G., PERIN, P. M., FRENTZEN, A., KADERALI, L. & PIETSCHMANN, T. 2013. Hepatitis C Virus p7 is Critical for Capsid Assembly and Envelopment. *PLOS Pathogens,* 9**,** e1003355.

GHOSH, A. K., MAJUMDER, M., STEELE, R., MEYER, K., RAY, R. & RAY, R. B. 2000. Hepatitis C virus NS5A protein protects against TNF-alpha mediated apoptotic cell death. *Virus Res,* 67**,** 173-8.

GHOSH, A. K., STEELE, R., MEYER, K., RAY, R. & RAY, R. B. 1999. Hepatitis C virus NS5A protein modulates cell cycle regulatory genes and promotes cell growth. *J Gen Virol,* 80 (Pt 5)**,** 1179-83.

GIBB, D. M., GOODALL, R. L., DUNN, D. T., HEALY, M., NEAVE, P., CAFFERKEY, M. & BUTLER, K. 2000. Mother-to-child transmission of hepatitis C virus: evidence for preventable peripartum transmission. *Lancet,* 356**,** 904-7.

GOFFARD, A., CALLENS, N., BARTOSCH, B., WYCHOWSKI, C., COSSET, F.-L., MONTPELLIER, C. & DUBUISSON, J. 2005. Role of N-Linked Glycans in the Functions of Hepatitis C Virus Envelope Glycoproteins. *Journal of Virology,* 79**,** 8400-8409.

GOMAA, A., ALLAM, N., ELSHARKAWY, A., EL KASSAS, M. & WAKED, I. 2017. Hepatitis C infection in Egypt: prevalence, impact and management strategies. *Hepat Med,* 9**,** 17-25.

GOMES, R. G., ISKEN, O., TAUTZ, N., MCLAUCHLAN, J. & MCCORMICK, C. J. 2016. Polyprotein-Driven Formation of Two Interdependent Sets of Complexes Supporting Hepatitis C Virus Genome Replication. *J Virol,* 90**,** 2868-83.

GONDA, D. K., BACHMAIR, A., WUNNING, I., TOBIAS, J. W., LANE, W. S. & VARSHAVSKY, A. 1989. Universality and structure of the N-end rule. *J Biol Chem,* 264**,** 16700-12.

GONG, G. Z., CAO, J., JIANG, Y. F., ZHOU, Y. & LIU, B. 2007. Hepatitis C virus non-structural 5A abrogates signal transducer and activator of transcription-1 nuclear translocation induced by IFN-alpha through dephosphorylation. *World J Gastroenterol,* 13**,** 4080-4.

GONG, G. Z., LAI, L. Y., JIANG, Y. F., HE, Y. & SU, X. S. 2003. HCV replication in PBMC and its influence on interferon therapy. *World J Gastroenterol,* 9**,** 291-4.

GORDON, C. G., MACKEY, J. L., JEWETT, J. C., SLETTEN, E. M., HOUK, K. N. & BERTOZZI, C. R. 2012. Reactivity of Biarylazacyclooctynones in Copper-Free Click Chemistry. *Journal of the American Chemical Society,* 134**,** 9199-9208.

GOSERT, R., EGGER, D., LOHMANN, V., BARTENSCHLAGER, R., BLUM, H. E., BIENZ, K. & MORADPOUR, D. 2003. Identification of the hepatitis C virus RNA replication complex in Huh-7 cells harboring subgenomic replicons. *J Virol,* 77**,** 5487-92.

GOTTWEIN, J. M., SCHEEL, T. K., CALLENDRET, B., LI, Y. P., ECCLESTON, H. B., ENGLE, R. E., GOVINDARAJAN, S., SATTERFIELD, W., PURCELL, R. H., WALKER, C. M. & BUKH, J. 2010. Novel infectious cDNA clones of hepatitis C virus genotype 3a (strain S52) and 4a (strain ED43): genetic analyses and in vivo pathogenesis studies. *J Virol,* 84**,** 5277-93.

GOUTTENOIRE, J., MONTSERRET, R., PAUL, D., CASTILLO, R., MEISTER, S., BARTENSCHLAGER, R., PENIN, F. & MORADPOUR, D. 2014. Aminoterminal amphipathic alpha-helix AH1 of hepatitis C virus nonstructural protein 4B possesses a dual role in RNA replication and virus production. *PLoS Pathog,* 10**,** e1004501.

GRAKOUI, A., MCCOURT, D. W., WYCHOWSKI, C., FEINSTONE, S. M. & RICE, C. M. 1993. A second hepatitis C virus-encoded proteinase. *Proc Natl Acad Sci U S A,* 90**,** 10583-7.

GRANADOS, D. P., TANGUAY, P. L., HARDY, M. P., CARON, E., DE VERTEUIL, D., MELOCHE, S. & PERREAULT, C. 2009. ER stress affects processing of MHC class I-associated peptides. *BMC Immunol,* 10**,** 10.

GRIFFIN, S. D., BEALES, L. P., CLARKE, D. S., WORSFOLD, O., EVANS, S. D., JAEGER, J., HARRIS, M. P. & ROWLANDS, D. J. 2003. The p7 protein of hepatitis C virus forms an ion channel that is blocked by the antiviral drug, Amantadine. *FEBS Lett,* 535**,** 34-8.

GROSS, C. T. & MCGINNIS, W. 1996. DEAF-1, a novel protein that binds an essential region in a Deformed response element. *Embo j,* 15**,** 1961-70.

GU, Z., SHI, W., ZHANG, L., HU, Z. & XU, C. 2017. USP19 suppresses cellular type I interferon signaling by targeting TRAF3 for deubiquitination. *Future Microbiol,* 12**,** 767-779.

HALLER, O., KOCHS, G. & WEBER, F. 2006. The interferon response circuit: induction and suppression by pathogenic viruses. *Virology,* 344**,** 119-30.

HAN, J. Q. & BARTON, D. J. 2002. Activation and evasion of the antiviral 2'-5' oligoadenylate synthetase/ribonuclease L pathway by hepatitis C virus mRNA. *Rna,* 8**,** 512-25.

HANOULLE, X., BADILLO, A., VERDEGEM, D., PENIN, F. & LIPPENS, G. 2010. The domain 2 of the HCV NS5A protein is intrinsically unstructured. *Protein Pept Lett,* 17**,** 1012-8.

HANOULLE, X., VERDEGEM, D., BADILLO, A., WIERUSZESKI, J. M., PENIN, F. & LIPPENS, G. 2009. Domain 3 of non-structural protein 5A from hepatitis C virus is natively unfolded. *Biochem Biophys Res Commun,* 381**,** 634-8.

HARAK, C., MEYRATH, M., ROMERO-BREY, I., SCHENK, C., GONDEAU, C., SCHULT, P., ESSER-NOBIS, K., SAEED, M., NEDDERMANN, P., SCHNITZLER, P., GOTTHARDT, D., PEREZ-DEL-PULGAR, S., NEUMANN-HAEFELIN, C., THIMME, R., MEULEMAN, P., VONDRAN, F. W. R., DE FRANCESCO, R., RICE, C. M., BARTENSCHLAGER, R. & LOHMANN, V. 2016. Tuning a cellular lipid kinase activity adapts hepatitis C virus to replication in cell culture. *Nature Microbiology,* 2**,** 16247.

HASSINK, G. C., ZHAO, B., SOMPALLAE, R., ALTUN, M., GASTALDELLO, S., ZININ, N. V., MASUCCI, M. G. & LINDSTEN, K. 2009. The ER-resident ubiquitin-specific protease 19 participates in the UPR and rescues ERAD substrates. *EMBO Rep,* 10**,** 755-61.

HE, Y., NAKAO, H., TAN, S. L., POLYAK, S. J., NEDDERMANN, P., VIJAYSRI, S., JACOBS, B. L. & KATZE, M. G. 2002. Subversion of cell signaling pathways by hepatitis C virus nonstructural 5A protein via interaction with Grb2 and P85 phosphatidylinositol 3-kinase. *J Virol,* 76**,** 9207-17.

HE, Y., STASCHKE, K. A. & TAN, S. L. 2006. HCV NS5A: A Multifunctional Regulator of Cellular Pathways and Virus Replication. *In:* TAN, S. L. (ed.) *Hepatitis C Viruses: Genomes and Molecular Biology.* Norfolk (UK): Horizon Bioscience

Horizon Bioscience.

HE, Y., TAN, S. L., TAREEN, S. U., VIJAYSRI, S., LANGLAND, J. O., JACOBS, B. L. & KATZE, M. G. 2001. Regulation of mRNA translation and cellular signaling by hepatitis C virus nonstructural protein NS5A. *J Virol,* 75**,** 5090-8.

HE, Y., WENG, L., LI, R., LI, L., TOYODA, T. & ZHONG, J. 2012. The N-terminal helix alpha(0) of hepatitis C virus NS3 protein dictates the subcellular localization and stability of NS3/NS4A complex. *Virology,* 422**,** 214-23.

HEIM, M. H., MORADPOUR, D. & BLUM, H. E. 1999. Expression of hepatitis C virus proteins inhibits signal transduction through the Jak-STAT pathway. *J Virol,* 73**,** 8469-75.

HEO, Y. A. & DEEKS, E. D. 2018. Sofosbuvir/Velpatasvir/Voxilaprevir: A Review in Chronic Hepatitis C. *Drugs,* 78**,** 577-587.

HEROD, M. R., JONES, D. M., MCLAUCHLAN, J. & MCCORMICK, C. J. 2012. Increasing rate of cleavage at boundary between non-structural proteins 4B and 5A inhibits replication of hepatitis C virus. *J Biol Chem,* 287**,** 568-80.

HERZER, K., FALK, C. S., ENCKE, J., EICHHORST, S. T., ULSENHEIMER, A., SELIGER, B. & KRAMMER, P. H. 2003. Upregulation of major histocompatibility complex class I on liver cells by hepatitis C virus core protein via p53 and TAP1 impairs natural killer cell cytotoxicity. *J Virol,* 77**,** 8299-309.

HIDAJAT, R., NAGANO-FUJII, M., DENG, L. & HOTTA, H. 2004. Cleavage of the hepatitis C virus NS5A protein by caspase-3 in the interferon sensitivity-determining region in a sequence-dependent manner. *Kobe J Med Sci,* 50**,** 153-66.

HIJIKATA, M., KATO, N., OOTSUYAMA, Y., NAKAGAWA, M. & SHIMOTOHNO, K. 1991. Gene mapping of the putative structural region of the hepatitis C virus genome by in vitro processing analysis. *Proc Natl Acad Sci U S A,* 88**,** 5547-51.

HIJIKATA, M., OHTA, Y. & MISHIRO, S. 2000. Identification of a single nucleotide polymorphism in the MxA gene promoter (G/T at nt -88) correlated with the response of hepatitis C patients to interferon. *Intervirology,* 43**,** 124-7.

HONG, Z., CAMERON, C. E., WALKER, M. P., CASTRO, C., YAO, N., LAU, J. Y. & ZHONG, W. 2001. A novel mechanism to ensure terminal initiation by hepatitis C virus NS5B polymerase. *Virology,* 285**,** 6-11.

HOPE, R. G. & MCLAUCHLAN, J. 2000. Sequence motifs required for lipid droplet association and protein stability are unique to the hepatitis C virus core protein. *The Journal of general virology,* 81**,** 1913-1925.

HOURIOUX, C., AIT-GOUGHOULTE, M., PATIENT, R., FOUQUENET, D., ARCANGER-DOUDET, F., BRAND, D., MARTIN, A. & ROINGEARD, P. 2007. Core protein domains involved in hepatitis C virus-like particle assembly and budding at the endoplasmic reticulum membrane. *Cell Microbiol,* 9**,** 1014-27.

HOYT, M. A., ZICH, J., TAKEUCHI, J., ZHANG, M., GOVAERTS, C. & COFFINO, P. 2006. Glycine-alanine repeats impair proper substrate unfolding by the proteasome. *Embo j,* 25**,** 1720-9.

HUANG, H., SUN, F., OWEN, D. M., LI, W., CHEN, Y., GALE, M., JR. & YE, J. 2007. Hepatitis C virus production by human hepatocytes dependent on assembly and secretion of very low-density lipoproteins. *Proc Natl Acad Sci U S A,* 104**,** 5848-53.

HUANG, L., HWANG, J., SHARMA, S. D., HARGITTAI, M. R., CHEN, Y., ARNOLD, J. J., RANEY, K. D. & CAMERON, C. E. 2005. Hepatitis C virus nonstructural protein 5A (NS5A) is an RNA-binding protein. *J Biol Chem,* 280**,** 36417-28.

HUEGING, K., DOEPKE, M., VIEYRES, G., BANKWITZ, D., FRENTZEN, A., DOERRBECKER, J., GUMZ, F., HAID, S., WOLK, B., KADERALI, L. & PIETSCHMANN, T. 2014. Apolipoprotein E codetermines tissue tropism of hepatitis C virus and is crucial for viral cell-to-cell transmission by contributing to a postenvelopment step of assembly. *J Virol,* 88**,** 1433-46.

HUGHES, M., GRIFFIN, S. & HARRIS, M. 2009. Domain III of NS5A contributes to both RNA replication and assembly of hepatitis C virus particles. *J Gen Virol,* 90**,** 1329-34.

HÜGLE, T., FEHRMANN, F., BIECK, E., KOHARA, M., KRÄUSSLICH, H.-G., RICE, C. M., BLUM, H. E. & MORADPOUR, D. 2001. The Hepatitis C Virus Nonstructural Protein 4B Is an Integral Endoplasmic Reticulum Membrane Protein. *Virology,* 284**,** 70-81.

HWANG, J., HUANG, L., CORDEK, D. G., VAUGHAN, R., REYNOLDS, S. L., KIHARA, G., RANEY, K. D., KAO, C. C. & CAMERON, C. E. 2010. Hepatitis C virus nonstructural protein 5A: biochemical characterization of a novel structural class of RNA-binding proteins. *J Virol,* 84**,** 12480-91.

IGLOI, Z., KAZLAUSKAS, A., SAKSELA, K., MACDONALD, A., MANKOURI, J. & HARRIS, M. 2015. Hepatitis C virus NS5A protein blocks epidermal growth factor receptor degradation via a proline motif-dependent interaction. *J Gen Virol,* 96**,** 2133-44.

IVASHKIV, L. B. & DONLIN, L. T. 2014. Regulation of type I interferon responses. *Nat Rev Immunol,* 14**,** 36-49.

IWAMOTO, M., BJORKLUND, T., LUNDBERG, C., KIRIK, D. & WANDLESS, T. J. 2010. A general chemical method to regulate protein stability in the mammalian central nervous system. *Chem Biol,* 17**,** 981-8.

JIRASKO, V., MONTSERRET, R., LEE, J. Y., GOUTTENOIRE, J., MORADPOUR, D., PENIN, F. & BARTENSCHLAGER, R. 2010. Structural and functional studies of nonstructural protein 2 of the hepatitis C virus reveal its key role as organizer of virion assembly. *PLoS Pathog,* 6**,** e1001233.

JONES, C. T., MURRAY, C. L., EASTMAN, D. K., TASSELLO, J. & RICE, C. M. 2007a. Hepatitis C virus p7 and NS2 proteins are essential for production of infectious virus. *J Virol,* 81**,** 8374-83.

JONES, D. M., GRETTON, S. N., MCLAUCHLAN, J. & TARGETT-ADAMS, P. 2007b. Mobility analysis of an NS5A-GFP fusion protein in cells actively replicating hepatitis C virus subgenomic RNA. *J Gen Virol,* 88**,** 470-5.

JOPLING, C. L., SCHUTZ, S. & SARNOW, P. 2008. Position-dependent function for a tandem microRNA miR-122-binding site located in the hepatitis C virus RNA genome. *Cell Host Microbe,* 4**,** 77-85.

JOPLING, C. L., YI, M., LANCASTER, A. M., LEMON, S. M. & SARNOW, P. 2005. Modulation of hepatitis C virus RNA abundance by a liver-specific MicroRNA. *Science,* 309**,** 1577-81.

JOYCE, M. A., WALTERS, K. A., LAMB, S. E., YEH, M. M., ZHU, L. F., KNETEMAN, N., DOYLE, J. S., KATZE, M. G. & TYRRELL, D. L. 2009. HCV induces oxidative and ER stress, and sensitizes infected cells to apoptosis in SCID/Alb-uPA mice. *PLoS Pathog,* 5**,** e1000291.

JU, X., YAN, Y., LIU, Q., LI, N., SHENG, M., ZHANG, L., LI, X., LIANG, Z., HUANG, F., LIU, K., ZHAO, Y., ZHANG, Y., ZOU, Z., DU, J., ZHONG, Y., ZHOU, H., YANG, P., LU, H., TIAN, M., LI, D., ZHANG, J., JIN, N. & JIANG, C. 2015. Neuraminidase of Influenza A Virus Binds Lysosome-Associated Membrane Proteins Directly and Induces Lysosome Rupture. *J Virol,* 89**,** 10347-58.

KALAMVOKI, M., GEORGOPOULOU, U. & MAVROMARA, P. 2006. The NS5A protein of the hepatitis C virus genotype 1a is cleaved by caspases to produce C-terminal-truncated forms of the protein that reside mainly in the cytosol. *J Biol Chem,* 281**,** 13449-62.

KALAMVOKI, M. & MAVROMARA, P. 2004. Calcium-dependent calpain proteases are implicated in processing of the hepatitis C virus NS5A protein. *J Virol,* 78**,** 11865-78.
KANEKO, T., TANJI, Y., SATOH, S., HIJIKATA, M., ASABE, S., KIMURA, K. & SHIMOTOHNO, K. 1994. Production of two phosphoproteins from the NS5A region of the hepatitis C viral genome. *Biochem Biophys Res Commun,* 205**,** 320-6.
KANG, W., SUNG, P. S., PARK, S. H., YOON, S., CHANG, D. Y., KIM, S., HAN, K. H., KIM, J. K., REHERMANN, B., CHWAE, Y. J. & SHIN, E. C. 2014. Hepatitis C virus attenuates interferon-induced major histocompatibility complex class I expression and decreases CD8+ T cell effector functions. *Gastroenterology,* 146**,** 1351-60.e1-4.
KATO, T., DATE, T., MIYAMOTO, M., SUGIYAMA, M., TANAKA, Y., ORITO, E., OHNO, T., SUGIHARA, K., HASEGAWA, I., FUJIWARA, K., ITO, K., OZASA, A., MIZOKAMI, M. & WAKITA, T. 2005. Detection of anti-hepatitis C virus effects of interferon and ribavirin by a sensitive replicon system. *J Clin Microbiol,* 43**,** 5679-84.
KATO, T., FURUSAKA, A., MIYAMOTO, M., DATE, T., YASUI, K., HIRAMOTO, J., NAGAYAMA, K., TANAKA, T. & WAKITA, T. 2001. Sequence analysis of hepatitis C virus isolated from a fulminant hepatitis patient. *J Med Virol,* 64**,** 334-9.
KIEFT, J. S., ZHOU, K., JUBIN, R. & DOUDNA, J. A. 2001. Mechanism of ribosome recruitment by hepatitis C IRES RNA. *RNA,* 7**,** 194-206.
KIM, J. H., PARK, S. M., PARK, J. H., KEUM, S. J. & JANG, S. K. 2011. eIF2A mediates translation of hepatitis C viral mRNA under stress conditions. *Embo j,* 30**,** 2454-64.
KIM, S. J., SYED, G. H., KHAN, M., CHIU, W. W., SOHAIL, M. A., GISH, R. G. & SIDDIQUI, A. 2014. Hepatitis C virus triggers mitochondrial fission and attenuates apoptosis to promote viral persistence. *Proc Natl Acad Sci U S A,* 111**,** 6413-8.
KIM, S. J., SYED, G. H. & SIDDIQUI, A. 2013. Hepatitis C virus induces the mitochondrial translocation of Parkin and subsequent mitophagy. *PLoS Pathog,* 9**,** e1003285.
KIM, Y. K., KIM, C. S., LEE, S. H. & JANG, S. K. 2002. Domains I and II in the 5' nontranslated region of the HCV genome are required for RNA replication. *Biochem Biophys Res Commun,* 290**,** 105-12.
KLEIN, K. C., DELLOS, S. R. & LINGAPPA, J. R. 2005. Identification of residues in the hepatitis C virus core protein that are critical for capsid assembly in a cell-free system. *J Virol,* 79**,** 6814-26.
KLEIN, K. C., POLYAK, S. J. & LINGAPPA, J. R. 2004. Unique features of hepatitis C virus capsid formation revealed by de novo cell-free assembly. *J Virol,* 78**,** 9257-69.
KNAPP, S., YEE, L. J., FRODSHAM, A. J., HENNIG, B. J., HELLIER, S., ZHANG, L., WRIGHT, M., CHIARAMONTE, M., GRAVES, M., THOMAS, H. C., HILL, A. V. & THURSZ, M. R. 2003. Polymorphisms in interferon-induced genes and the outcome of hepatitis C virus infection: roles of MxA, OAS-1 and PKR. *Genes Immun,* 4**,** 411-9.
KOLB, H. C., FINN, M. G. & SHARPLESS, K. B. 2001. Click Chemistry: Diverse Chemical Function from a Few Good Reactions. *Angew Chem Int Ed Engl,* 40**,** 2004-2021.
KOLYKHALOV, A. A., MIHALIK, K., FEINSTONE, S. M. & RICE, C. M. 2000. Hepatitis C virus-encoded enzymatic activities and conserved RNA elements in the 3' nontranslated region are essential for virus replication in vivo. *J Virol,* 74**,** 2046-51.
KONAN, K. V., GIDDINGS, T. H., JR., IKEDA, M., LI, K., LEMON, S. M. & KIRKEGAARD, K. 2003. Nonstructural protein precursor NS4A/B from hepatitis C virus alters function and ultrastructure of host secretory apparatus. *J Virol,* 77**,** 7843-55.
KOUYOUMJIAN, S. P., CHEMAITELLY, H. & ABU-RADDAD, L. J. 2018. Characterizing hepatitis C virus epidemiology in Egypt: systematic reviews, meta-analyses, and meta-regressions. *Sci Rep,* 8**,** 1661.
KRAFT, C., PETER, M. & HOFMANN, K. 2010. Selective autophagy: ubiquitin-mediated recognition and beyond. *Nat Cell Biol,* 12**,** 836-41.
KRAVTSOVA-IVANTSIV, Y. & CIECHANOVER, A. 2012. Non-canonical ubiquitin-based signals for proteasomal degradation. *J Cell Sci,* 125**,** 539-48.
KRIEGER, N., LOHMANN, V. & BARTENSCHLAGER, R. 2001. Enhancement of hepatitis C virus RNA replication by cell culture-adaptive mutations. *J Virol,* 75**,** 4614-24.
KUMTHIP, K., CHUSRI, P., JILG, N., ZHAO, L., FUSCO, D. N., ZHAO, H., GOTO, K., CHENG, D., SCHAEFER, E. A., ZHANG, L., PANTIP, C., THONGSAWAT, S., O'BRIEN, A., PENG, L. F., MANEEKARN, N., CHUNG, R. T. & LIN, W. 2012. Hepatitis C virus NS5A disrupts STAT1 phosphorylation and suppresses type I interferon signaling. *J Virol,* 86**,** 8581-91.
KUMTHIP, K. & MANEEKARN, N. 2015. The role of HCV proteins on treatment outcomes. *Virol J,* 12**,** 217.

KWONG, A. D., KAUFFMAN, R. S., HURTER, P. & MUELLER, P. 2011. Discovery and development of telaprevir: an NS3-4A protease inhibitor for treating genotype 1 chronic hepatitis C virus. *Nat Biotechnol,* 29**,** 993-1003.

LAI, M. M. C. & WARE, C. F. 2000. Hepatitis C Virus Core Protein: Possible Roles in Viral Pathogenesis. *In:* HAGEDORN, C. H. & RICE, C. M. (eds.) *The Hepatitis C Viruses.* Berlin, Heidelberg: Springer Berlin Heidelberg.

LAM, A. M. & FRICK, D. N. 2006. Hepatitis C virus subgenomic replicon requires an active NS3 RNA helicase. *J Virol,* 80**,** 404-11.

LAM, A. M., MURAKAMI, E., ESPIRITU, C., STEUER, H. M., NIU, C., KEILMAN, M., BAO, H., ZENNOU, V., BOURNE, N., JULANDER, J. G., MORREY, J. D., SMEE, D. F., FRICK, D. N., HECK, J. A., WANG, P., NAGARATHNAM, D., ROSS, B. S., SOFIA, M. J., OTTO, M. J. & FURMAN, P. A. 2010. PSI-7851, a pronucleotide of beta-D-2'-deoxy-2'-fluoro-2'-C-methyluridine monophosphate, is a potent and pan-genotype inhibitor of hepatitis C virus replication. *Antimicrob Agents Chemother,* 54**,** 3187-96.

LAMBERT, S. M., LANGLEY, D. R., GARNETT, J. A., ANGELL, R., HEDGETHORNE, K., MEANWELL, N. A. & MATTHEWS, S. J. 2014. The crystal structure of NS5A domain 1 from genotype 1a reveals new clues to the mechanism of action for dimeric HCV inhibitors. *Protein Sci,* 23**,** 723-34.

LAN, K. H., LAN, K. L., LEE, W. P., SHEU, M. L., CHEN, M. Y., LEE, Y. L., YEN, S. H., CHANG, F. Y. & LEE, S. D. 2007. HCV NS5A inhibits interferon-alpha signaling through suppression of STAT1 phosphorylation in hepatocyte-derived cell lines. *J Hepatol,* 46**,** 759-67.

LAN, K. H., SHEU, M. L., HWANG, S. J., YEN, S. H., CHEN, S. Y., WU, J. C., WANG, Y. J., KATO, N., OMATA, M., CHANG, F. Y. & LEE, S. D. 2002. HCV NS5A interacts with p53 and inhibits p53-mediated apoptosis. *Oncogene,* 21**,** 4801-11.

LAVANCHY, D. 2011. Evolving epidemiology of hepatitis C virus. *Clin Microbiol Infect,* 17**,** 107-15.

LAVIE, M., GOFFARD, A. & DUBUISSON, J. 2007. Assembly of a functional HCV glycoprotein heterodimer. *Curr Issues Mol Biol,* 9**,** 71-86.

LAWITZ, E. J., O'RIORDAN, W. D., ASATRYAN, A., FREILICH, B. L., BOX, T. D., OVERCASH, J. S., LOVELL, S., NG, T. I., LIU, W., CAMPBELL, A., LIN, C. W., YAO, B. & KORT, J. 2015. Potent Antiviral Activities of the Direct-Acting Antivirals ABT-493 and ABT-530 with Three-Day Monotherapy for Hepatitis C Virus Genotype 1 Infection. *Antimicrob Agents Chemother,* 60**,** 1546-55.

LEE, C., MA, H., HANG, J. Q., LEVEQUE, V., SKLAN, E. H., ELAZAR, M., KLUMPP, K. & GLENN, J. S. 2011. The hepatitis C virus NS5A inhibitor (BMS-790052) alters the subcellular localization of the NS5A non-structural viral protein. *Virology,* 414**,** 10-8.

LEMM, J. A., O'BOYLE, D., LIU, M., NOWER, P. T., COLONNO, R., DESHPANDE, M. S., SNYDER, L. B., MARTIN, S. W., ST. LAURENT, D. R., SERRANO-WU, M. H., ROMINE, J. L., MEANWELL, N. A. & GAO, M. 2010. Identification of Hepatitis C Virus NS5A Inhibitors. *Journal of Virology,* 84**,** 482-491.

LERAT, H., RUMIN, S., HABERSETZER, F., BERBY, F., TRABAUD, M. A., TREPO, C. & INCHAUSPE, G. 1998. In vivo tropism of hepatitis C virus genomic sequences in hematopoietic cells: influence of viral load, viral genotype, and cell phenotype. *Blood,* 91**,** 3841-9.

LEVITSKAYA, J., SHARIPO, A., LEONCHIKS, A., CIECHANOVER, A. & MASUCCI, M. G. 1997. Inhibition of ubiquitin/proteasome-dependent protein degradation by the Gly-Ala repeat domain of the Epstein-Barr virus nuclear antigen 1. *Proc Natl Acad Sci U S A,* 94**,** 12616-21.

LEVY, D. E., MARIÉ, I. J. & DURBIN, J. E. 2011. Induction and Function of Type I and III Interferon in Response to Viral Infection. *Current opinion in virology,* 1**,** 476-486.

LI, K., FOY, E., FERREON, J. C., NAKAMURA, M., FERREON, A. C., IKEDA, M., RAY, S. C., GALE, M., JR. & LEMON, S. M. 2005. Immune evasion by hepatitis C virus NS3/4A protease-mediated cleavage of the Toll-like receptor 3 adaptor protein TRIF. *Proc Natl Acad Sci U S A,* 102**,** 2992-7.

LI, Y. P., RAMIREZ, S., MIKKELSEN, L. & BUKH, J. 2015. Efficient infectious cell culture systems of the hepatitis C virus (HCV) prototype strains HCV-1 and H77. *J Virol,* 89**,** 811-23.

LIANG, Y., YE, H., KANG, C. B. & YOON, H. S. 2007. Domain 2 of nonstructural protein 5A (NS5A) of hepatitis C virus is natively unfolded. *Biochemistry,* 46**,** 11550-8.

LIESA, M., PALACIN, M. & ZORZANO, A. 2009. Mitochondrial dynamics in mammalian health and disease. *Physiol Rev,* 89**,** 799-845.

LIN, C., KWONG, A. D. & PERNI, R. B. 2006a. Discovery and development of VX-950, a novel, covalent, and reversible inhibitor of hepatitis C virus NS3.4A serine protease. *Infect Disord Drug Targets,* 6**,** 3-16.

LIN, C., LINDENBACH, B. D., PRAGAI, B. M., MCCOURT, D. W. & RICE, C. M. 1994a. Processing in the hepatitis C virus E2-NS2 region: identification of p7 and two distinct E2-specific products with different C termini. *J Virol,* 68**,** 5063-73.

LIN, C., PRAGAI, B. M., GRAKOUI, A., XU, J. & RICE, C. M. 1994b. Hepatitis C virus NS3 serine proteinase: trans-cleavage requirements and processing kinetics. *J Virol,* 68**,** 8147-57.
LIN, L. T., NOYCE, R. S., PHAM, T. N., WILSON, J. A., SISSON, G. R., MICHALAK, T. I., MOSSMAN, K. L. & RICHARDSON, C. D. 2010. Replication of subgenomic hepatitis C virus replicons in mouse fibroblasts is facilitated by deletion of interferon regulatory factor 3 and expression of liver-specific microRNA 122. *J Virol,* 84**,** 9170-80.
LIN, W., KIM, S. S., YEUNG, E., KAMEGAYA, Y., BLACKARD, J. T., KIM, K. A., HOLTZMAN, M. J. & CHUNG, R. T. 2006b. Hepatitis C virus core protein blocks interferon signaling by interaction with the STAT1 SH2 domain. *J Virol,* 80**,** 9226-35.
LINDENBACH, B. D. 2013. Virion assembly and release. *Curr Top Microbiol Immunol,* 369**,** 199-218.
LINDENBACH, B. D., EVANS, M. J., SYDER, A. J., WOLK, B., TELLINGHUISEN, T. L., LIU, C. C., MARUYAMA, T., HYNES, R. O., BURTON, D. R., MCKEATING, J. A. & RICE, C. M. 2005. Complete replication of hepatitis C virus in cell culture. *Science,* 309**,** 623-6.
LINDENBACH, B. D., PRAGAI, B. M., MONTSERRET, R., BERAN, R. K., PYLE, A. M., PENIN, F. & RICE, C. M. 2007. The C terminus of hepatitis C virus NS4A encodes an electrostatic switch that regulates NS5A hyperphosphorylation and viral replication. *J Virol,* 81**,** 8905-18.
LINK, J. O., TAYLOR, J. G., XU, L., MITCHELL, M., GUO, H., LIU, H., KATO, D., KIRSCHBERG, T., SUN, J., SQUIRES, N., PARRISH, J., KELLER, T., YANG, Z.-Y., YANG, C., MATLES, M., WANG, Y., WANG, K., CHENG, G., TIAN, Y., MOGALIAN, E., MONDOU, E., CORNPROPST, M., PERRY, J. & DESAI, M. C. 2014. Discovery of Ledipasvir (GS-5885): A Potent, Once-Daily Oral NS5A Inhibitor for the Treatment of Hepatitis C Virus Infection. *Journal of Medicinal Chemistry,* 57**,** 2033-2046.
LIU, Q., BHAT, R. A., PRINCE, A. M. & ZHANG, P. 1999. The hepatitis C virus NS2 protein generated by NS2-3 autocleavage is required for NS5A phosphorylation. *Biochem Biophys Res Commun,* 254**,** 572-7.
LOHMANN, V., HOFFMANN, S., HERIAN, U., PENIN, F. & BARTENSCHLAGER, R. 2003. Viral and cellular determinants of hepatitis C virus RNA replication in cell culture. *J Virol,* 77**,** 3007-19.
LOHMANN, V., KORNER, F., DOBIERZEWSKA, A. & BARTENSCHLAGER, R. 2001. Mutations in hepatitis C virus RNAs conferring cell culture adaptation. *J Virol,* 75**,** 1437-49.
LOHMANN, V., KORNER, F., HERIAN, U. & BARTENSCHLAGER, R. 1997. Biochemical properties of hepatitis C virus NS5B RNA-dependent RNA polymerase and identification of amino acid sequence motifs essential for enzymatic activity. *J Virol,* 71**,** 8416-28.
LOHMANN, V., KORNER, F., KOCH, J., HERIAN, U., THEILMANN, L. & BARTENSCHLAGER, R. 1999. Replication of subgenomic hepatitis C virus RNAs in a hepatoma cell line. *Science,* 285**,** 110-3.
LORENZ, I. C., MARCOTRIGIANO, J., DENTZER, T. G. & RICE, C. M. 2006. Structure of the catalytic domain of the hepatitis C virus NS2-3 protease. *Nature,* 442**,** 831-5.
LOVE, R. A., BRODSKY, O., HICKEY, M. J., WELLS, P. A. & CRONIN, C. N. 2009. Crystal structure of a novel dimeric form of NS5A domain I protein from hepatitis C virus. *J Virol,* 83**,** 4395-403.
LU, Y., ADEGOKE, O. A., NEPVEU, A., NAKAYAMA, K. I., BEDARD, N., CHENG, D., PENG, J. & WING, S. S. 2009. USP19 deubiquitinating enzyme supports cell proliferation by stabilizing KPC1, a ubiquitin ligase for p27Kip1. *Mol Cell Biol,* 29**,** 547-58.
LUKAVSKY, P. J. 2009. Structure and function of HCV IRES domains. *Virus Res,* 139**,** 166-71.
LUNDIN, M., MONNE, M., WIDELL, A., VON HEIJNE, G. & PERSSON, M. A. 2003. Topology of the membrane-associated hepatitis C virus protein NS4B. *J Virol,* 77**,** 5428-38.
LUO, G., HAMATAKE, R. K., MATHIS, D. M., RACELA, J., RIGAT, K. L., LEMM, J. & COLONNO, R. J. 2000. De novo initiation of RNA synthesis by the RNA-dependent RNA polymerase (NS5B) of hepatitis C virus. *J Virol,* 74**,** 851-63.
LUPBERGER, J., DUONG, F. H., FOFANA, I., ZONA, L., XIAO, F., THUMANN, C., DURAND, S. C., PESSAUX, P., ZEISEL, M. B., HEIM, M. H. & BAUMERT, T. F. 2013. Epidermal growth factor receptor signaling impairs the antiviral activity of interferon-alpha. *Hepatology,* 58**,** 1225-35.
LUPBERGER, J., ZEISEL, M. B., XIAO, F., THUMANN, C., FOFANA, I., ZONA, L., DAVIS, C., MEE, C. J., TUREK, M., GORKE, S., ROYER, C., FISCHER, B., ZAHID, M. N., LAVILLETTE, D., FRESQUET, J., COSSET, F. L., ROTHENBERG, S. M., PIETSCHMANN, T., PATEL, A. H., PESSAUX, P., DOFFOEL, M., RAFFELSBERGER, W., POCH, O., MCKEATING, J. A., BRINO, L. & BAUMERT, T. F. 2011. EGFR and EphA2 are host factors for hepatitis C virus entry and possible targets for antiviral therapy. *Nat Med,* 17**,** 589-95.
MA, H., JIANG, W. R., ROBLEDO, N., LEVEQUE, V., ALI, S., LARA-JAIME, T., MASJEDIZADEH, M., SMITH, D. B., CAMMACK, N., KLUMPP, K. & SYMONS, J. 2007. Characterization of the metabolic activation of hepatitis C virus nucleoside inhibitor beta-D-2'-Deoxy-2'-fluoro-2'-C-methylcytidine (PSI-6130) and identification of a novel active 5'-triphosphate species. *J Biol Chem,* 282**,** 29812-20.

MACDONALD, A., CHAN, J. K. & HARRIS, M. 2005. Perturbation of epidermal growth factor receptor complex formation and Ras signalling in cells harbouring the hepatitis C virus subgenomic replicon. *J Gen Virol,* 86**,** 1027-33.

MACDONALD, A., CROWDER, K., STREET, A., MCCORMICK, C. & HARRIS, M. 2004. The hepatitis C virus NS5A protein binds to members of the Src family of tyrosine kinases and regulates kinase activity. *J Gen Virol,* 85**,** 721-9.

MACDONALD, A. & HARRIS, M. 2004. Hepatitis C virus NS5A: tales of a promiscuous protein. *J Gen Virol,* 85**,** 2485-502.

MACHLIN, E. S., SARNOW, P. & SAGAN, S. M. 2011. Masking the 5' terminal nucleotides of the hepatitis C virus genome by an unconventional microRNA-target RNA complex. *Proc Natl Acad Sci U S A,* 108**,** 3193-8.

MAJUMDER, M., GHOSH, A. K., STEELE, R., RAY, R. & RAY, R. B. 2001. Hepatitis C virus NS5A physically associates with p53 and regulates p21/waf1 gene expression in a p53-dependent manner. *J Virol,* 75**,** 1401-7.

MAJUMDER, M., GHOSH, A. K., STEELE, R., ZHOU, X. Y., PHILLIPS, N. J., RAY, R. & RAY, R. B. 2002. Hepatitis C virus NS5A protein impairs TNF-mediated hepatic apoptosis, but not by an anti-FAS antibody, in transgenic mice. *Virology,* 294**,** 94-105.

MALATHI, K., SAITO, T., CROCHET, N., BARTON, D. J., GALE, M., JR. & SILVERMAN, R. H. 2010. RNase L releases a small RNA from HCV RNA that refolds into a potent PAMP. *Rna,* 16**,** 2108-19.

MALCOLM, B. A., LIU, R., LAHSER, F., AGRAWAL, S., BELANGER, B., BUTKIEWICZ, N., CHASE, R., GHEYAS, F., HART, A., HESK, D., INGRAVALLO, P., JIANG, C., KONG, R., LU, J., PICHARDO, J., PRONGAY, A., SKELTON, A., TONG, X., VENKATRAMAN, S., XIA, E., GIRIJAVALLABHAN, V. & NJOROGE, F. G. 2006. SCH 503034, a mechanism-based inhibitor of hepatitis C virus NS3 protease, suppresses polyprotein maturation and enhances the antiviral activity of alpha interferon in replicon cells. *Antimicrob Agents Chemother,* 50**,** 1013-20.

MANNS, M. P., WEDEMEYER, H. & CORNBERG, M. 2006. Treating viral hepatitis C: efficacy, side effects, and complications. *Gut,* 55**,** 1350-9.

MARCHLER-BAUER, A., ZHENG, C., CHITSAZ, F., DERBYSHIRE, M. K., GEER, L. Y., GEER, R. C., GONZALES, N. R., GWADZ, M., HURWITZ, D. I., LANCZYCKI, C. J., LU, F., LU, S., MARCHLER, G. H., SONG, J. S., THANKI, N., YAMASHITA, R. A., ZHANG, D. & BRYANT, S. H. 2013. CDD: conserved domains and protein three-dimensional structure. *Nucleic Acids Res,* 41**,** D348-52.

MASAKI, T., SUZUKI, R., MURAKAMI, K., AIZAKI, H., ISHII, K., MURAYAMA, A., DATE, T., MATSUURA, Y., MIYAMURA, T., WAKITA, T. & SUZUKI, T. 2008. Interaction of hepatitis C virus nonstructural protein 5A with core protein is critical for the production of infectious virus particles. *J Virol,* 82**,** 7964-76.

MATSUYAMA, N., MISHIRO, S., SUGIMOTO, M., FURUICHI, Y., HASHIMOTO, M., HIJIKATA, M. & OHTA, Y. 2003. The dinucleotide microsatellite polymorphism of the IFNAR1 gene promoter correlates with responsiveness of hepatitis C patients to interferon. *Hepatol Res,* 25**,** 221-225.

MATTHEWS, D. A., BOLIN, J. T., BURRIDGE, J. M., FILMAN, D. J., VOLZ, K. W. & KRAUT, J. 1985. Dihydrofolate reductase. The stereochemistry of inhibitor selectivity. *J Biol Chem,* 260**,** 392-9.

MCCORMICK, C. J., MAUCOURANT, S., GRIFFIN, S., ROWLANDS, D. J. & HARRIS, M. 2006. Tagging of NS5A expressed from a functional hepatitis C virus replicon. *J Gen Virol,* 87**,** 635-40.

MCCOWN, M. F., RAJYAGURU, S., LE POGAM, S., ALI, S., JIANG, W. R., KANG, H., SYMONS, J., CAMMACK, N. & NAJERA, I. 2008. The hepatitis C virus replicon presents a higher barrier to resistance to nucleoside analogs than to nonnucleoside polymerase or protease inhibitors. *Antimicrob Agents Chemother,* 52**,** 1604-12.

MCLAUCHLAN 2000. Properties of the hepatitis C virus core protein: a structural protein that modulates cellular processes. *Journal of Viral Hepatitis,* 7**,** 2-14.

MCLAUCHLAN, J., LEMBERG, M. K., HOPE, G. & MARTOGLIO, B. 2002. Intramembrane proteolysis promotes trafficking of hepatitis C virus core protein to lipid droplets. *Embo j,* 21**,** 3980-8.

MCSHANE, E., SIN, C., ZAUBER, H., WELLS, J. N., DONNELLY, N., WANG, X., HOU, J., CHEN, W., STORCHOVA, Z., MARSH, J. A., VALLERIANI, A. & SELBACH, M. 2016. Kinetic Analysis of Protein Stability Reveals Age-Dependent Degradation. *Cell,* 167**,** 803-815.e21.

MEI, Y., HAHN, A. A., HU, S. & YANG, X. 2011. The USP19 deubiquitinase regulates the stability of c-IAP1 and c-IAP2. *J Biol Chem,* 286**,** 35380-7.

MESSINA, J. P., HUMPHREYS, I., FLAXMAN, A., BROWN, A., COOKE, G. S., PYBUS, O. G. & BARNES, E. 2015. Global distribution and prevalence of hepatitis C virus genotypes. *Hepatology,* 61**,** 77-87.

METZ, P., DAZERT, E., RUGGIERI, A., MAZUR, J., KADERALI, L., KAUL, A., ZEUGE, U., WINDISCH, M. P., TRIPPLER, M., LOHMANN, V., BINDER, M., FRESE, M. & BARTENSCHLAGER, R. 2012. Identification of type I and type II interferon-induced effectors controlling hepatitis C virus replication. *Hepatology,* 56**,** 2082-93.

METZ, P., REUTER, A., BENDER, S. & BARTENSCHLAGER, R. 2013. Interferon-stimulated genes and their role in controlling hepatitis C virus. *J Hepatol,* 59**,** 1331-41.

MEUNIER, J. C., FOURNILLIER, A., CHOUKHI, A., CAHOUR, A., COCQUEREL, L., DUBUISSON, J. & WYCHOWSKI, C. 1999. Analysis of the glycosylation sites of hepatitis C virus (HCV) glycoprotein E1 and the influence of E1 glycans on the formation of the HCV glycoprotein complex. *Journal of General Virology,* 80**,** 887-896.

MILLER, R. H. & PURCELL, R. H. 1990. Hepatitis C virus shares amino acid sequence similarity with pestiviruses and flaviviruses as well as members of two plant virus supergroups. *Proc Natl Acad Sci U S A,* 87**,** 2057-61.

MILWARD, A., MANKOURI, J. & HARRIS, M. 2010. Hepatitis C virus NS5A protein interacts with beta-catenin and stimulates its transcriptional activity in a phosphoinositide-3 kinase-dependent fashion. *J Gen Virol,* 91**,** 373-81.

MIYANARI, Y., ATSUZAWA, K., USUDA, N., WATASHI, K., HISHIKI, T., ZAYAS, M., BARTENSCHLAGER, R., WAKITA, T., HIJIKATA, M. & SHIMOTOHNO, K. 2007. The lipid droplet is an important organelle for hepatitis C virus production. *Nat Cell Biol,* 9**,** 1089-97.

MIYAZAKI, Y., IMOTO, H., CHEN, L. C. & WANDLESS, T. J. 2012. Destabilizing domains derived from the human estrogen receptor. *J Am Chem Soc,* 134**,** 3942-5.

MIZUSHIMA, H., HIJIKATA, M., ASABE, S., HIROTA, M., KIMURA, K. & SHIMOTOHNO, K. 1994. Two hepatitis C virus glycoprotein E2 products with different C termini. *J Virol,* 68**,** 6215-22.

MOHAMOUD, Y. A., MUMTAZ, G. R., RIOME, S., MILLER, D. & ABU-RADDAD, L. J. 2013. The epidemiology of hepatitis C virus in Egypt: a systematic review and data synthesis. *BMC Infect Dis,* 13**,** 288.

MONAZAHIAN, M., BOHME, I., BONK, S., KOCH, A., SCHOLZ, C., GRETHE, S. & THOMSSEN, R. 1999. Low density lipoprotein receptor as a candidate receptor for hepatitis C virus. *J Med Virol,* 57**,** 223-9.

MORADPOUR, D., ENGLERT, C., WAKITA, T. & WANDS, J. R. 1996. Characterization of cell lines allowing tightly regulated expression of hepatitis C virus core protein. *Virology,* 222**,** 51-63.

MORADPOUR, D., EVANS, M. J., GOSERT, R., YUAN, Z., BLUM, H. E., GOFF, S. P., LINDENBACH, B. D. & RICE, C. M. 2004. Insertion of green fluorescent protein into nonstructural protein 5A allows direct visualization of functional hepatitis C virus replication complexes. *J Virol,* 78**,** 7400-9.

MORADPOUR, D., GRABSCHEID, B., KAMMER, A. R., SCHMIDTKE, G., GROETTRUP, M., BLUM, H. E. & CERNY, A. 2001. Expression of hepatitis C virus proteins does not interfere with major histocompatibility complex class I processing and presentation in vitro. *Hepatology,* 33**,** 1282-7.

MORIYA, K., FUJIE, H., SHINTANI, Y., YOTSUYANAGI, H., TSUTSUMI, T., ISHIBASHI, K., MATSUURA, Y., KIMURA, S., MIYAMURA, T. & KOIKE, K. 1998. The core protein of hepatitis C virus induces hepatocellular carcinoma in transgenic mice. *Nat Med,* 4**,** 1065-7.

MOTTOLA, G., CARDINALI, G., CECCACCI, A., TROZZI, C., BARTHOLOMEW, L., TORRISI, M. R., PEDRAZZINI, E., BONATTI, S. & MIGLIACCIO, G. 2002. Hepatitis C virus nonstructural proteins are localized in a modified endoplasmic reticulum of cells expressing viral subgenomic replicons. *Virology,* 293**,** 31-43.

MURAKAMI, T., ENOMOTO, N., KUROSAKI, M., IZUMI, N., MARUMO, F. & SATO, C. 1999. Mutations in nonstructural protein 5A gene and response to interferon in hepatitis C virus genotype 2 infection. *Hepatology,* 30**,** 1045-53.

MURPHY, D. G., SABLON, E., CHAMBERLAND, J., FOURNIER, E., DANDAVINO, R. & TREMBLAY, C. L. 2015. Hepatitis C virus genotype 7, a new genotype originating from central Africa. *J Clin Microbiol,* 53**,** 967-72.

MURPHY, M. D., ROSEN, H. R., MAROUSEK, G. I. & CHOU, S. 2002. Analysis of sequence configurations of the ISDR, PKR-binding domain, and V3 region as predictors of response to induction interferon-alpha and ribavirin therapy in chronic hepatitis C infection. *Dig Dis Sci,* 47**,** 1195-205.

NALDINI, L., BLOMER, U., GALLAY, P., ORY, D., MULLIGAN, R., GAGE, F. H., VERMA, I. M. & TRONO, D. 1996. In vivo gene delivery and stable transduction of nondividing cells by a lentiviral vector. *Science,* 272**,** 263-7.

NARAYANA, S. K., HELBIG, K. J., MCCARTNEY, E. M., EYRE, N. S., BULL, R. A., ELTAHLA, A., LLOYD, A. R. & BEARD, M. R. 2015. The Interferon-induced Transmembrane Proteins, IFITM1, IFITM2, and IFITM3 Inhibit Hepatitis C Virus Entry. *J Biol Chem,* 290**,** 25946-59.

NAVARRO, R., CHEN, L. C., RAKHIT, R. & WANDLESS, T. J. 2016. A Novel Destabilizing Domain Based on a Small-Molecule Dependent Fluorophore. *ACS Chem Biol,* 11**,** 2101-4.

NEDDERMANN, P., CLEMENTI, A. & DE FRANCESCO, R. 1999. Hyperphosphorylation of the hepatitis C virus NS5A protein requires an active NS3 protease, NS4A, NS4B, and NS5A encoded on the same polyprotein. *J Virol,* 73**,** 9984-91.

NICE 2018. Glecaprevir–pibrentasvir for treating chronic hepatitis C (TA499). National Institute for Health and Care Excellence.

NOUSBAUM, J., POLYAK, S. J., RAY, S. C., SULLIVAN, D. G., LARSON, A. M., CARITHERS, R. L., JR. & GRETCH, D. R. 2000. Prospective characterization of full-length hepatitis C virus NS5A quasispecies during induction and combination antiviral therapy. *J Virol,* 74**,** 9028-38.

OP DE BEECK, A., MONTSERRET, R., DUVET, S., COCQUEREL, L., CACAN, R., BARBEROT, B., LE MAIRE, M., PENIN, F. & DUBUISSON, J. 2000. The Transmembrane Domains of Hepatitis C Virus Envelope Glycoproteins E1 and E2 Play a Major Role in Heterodimerization. *Journal of Biological Chemistry,* 275**,** 31428-31437.

PAGNI, M., IOANNIDIS, V., CERUTTI, L., ZAHN-ZABAL, M., JONGENEEL, C. V., HAU, J., MARTIN, O., KUZNETSOV, D. & FALQUET, L. 2007. MyHits: improvements to an interactive resource for analyzing protein sequences. *Nucleic Acids Res,* 35**,** W433-7.

PARK, K. J., CHOI, S. H., CHOI, D. H., PARK, J. M., YIE, S. W., LEE, S. Y. & HWANG, S. B. 2003. Hepatitis C virus NS5A protein modulates c-Jun N-terminal kinase through interaction with tumor necrosis factor receptor-associated factor 2. *J Biol Chem,* 278**,** 30711-8.

PARK, K. J., CHOI, S. H., LEE, S. Y., HWANG, S. B. & LAI, M. M. 2002. Nonstructural 5A protein of hepatitis C virus modulates tumor necrosis factor alpha-stimulated nuclear factor kappa B activation. *J Biol Chem,* 277**,** 13122-8.

PATERSON, M., LAXTON, C. D., THOMAS, H. C., ACKRILL, A. M. & FOSTER, G. R. 1999. Hepatitis C virus NS5A protein inhibits interferon antiviral activity, but the effects do not correlate with clinical response. *Gastroenterology,* 117**,** 1187-97.

PAUL, D., HOPPE, S., SAHER, G., KRIJNSE-LOCKER, J. & BARTENSCHLAGER, R. 2013. Morphological and biochemical characterization of the membranous hepatitis C virus replication compartment. *J Virol,* 87**,** 10612-27.

PAVLOVIC, D., NEVILLE, D. C., ARGAUD, O., BLUMBERG, B., DWEK, R. A., FISCHER, W. B. & ZITZMANN, N. 2003. The hepatitis C virus p7 protein forms an ion channel that is inhibited by long-alkyl-chain iminosugar derivatives. *Proc Natl Acad Sci U S A,* 100**,** 6104-8.

PENIN, F., BRASS, V., APPEL, N., RAMBOARINA, S., MONTSERRET, R., FICHEUX, D., BLUM, H. E., BARTENSCHLAGER, R. & MORADPOUR, D. 2004a. Structure and function of the membrane anchor domain of hepatitis C virus nonstructural protein 5A. *J Biol Chem,* 279**,** 40835-43.

PENIN, F., DUBUISSON, J., REY, F. A., MORADPOUR, D. & PAWLOTSKY, J. M. 2004b. Structural biology of hepatitis C virus. *Hepatology,* 39**,** 5-19.

PETRACCA, R., FALUGI, F., GALLI, G., NORAIS, N., ROSA, D., CAMPAGNOLI, S., BURGIO, V., DI STASIO, E., GIARDINA, B., HOUGHTON, M., ABRIGNANI, S. & GRANDI, G. 2000. Structure-function analysis of hepatitis C virus envelope-CD81 binding. *J Virol,* 74**,** 4824-30.

PETRUZZIELLO, A., MARIGLIANO, S., LOQUERCIO, G., COZZOLINO, A. & CACCIAPUOTI, C. 2016. Global epidemiology of hepatitis C virus infection: An up-date of the distribution and circulation of hepatitis C virus genotypes. *World J Gastroenterol,* 22**,** 7824-40.

PFLUGHEBER, J., FREDERICKSEN, B., SUMPTER, R., JR., WANG, C., WARE, F., SODORA, D. L. & GALE, M., JR. 2002. Regulation of PKR and IRF-1 during hepatitis C virus RNA replication. *Proc Natl Acad Sci U S A,* 99**,** 4650-5.

PHAN, T., BERAN, R. K., PETERS, C., LORENZ, I. C. & LINDENBACH, B. D. 2009. Hepatitis C virus NS2 protein contributes to virus particle assembly via opposing epistatic interactions with the E1-E2 glycoprotein and NS3-NS4A enzyme complexes. *J Virol,* 83**,** 8379-95.

PICCININNI, S., VARAKLIOTI, A., NARDELLI, M., DAVE, B., RANEY, K. D. & MCCARTHY, J. E. 2002. Modulation of the hepatitis C virus RNA-dependent RNA polymerase activity by the non-structural (NS) 3 helicase and the NS4B membrane protein. *J Biol Chem,* 277**,** 45670-9.

PICCOLI, C., SCRIMA, R., QUARATO, G., D'APRILE, A., RIPOLI, M., LECCE, L., BOFFOLI, D., MORADPOUR, D. & CAPITANIO, N. 2007. Hepatitis C virus protein expression causes calcium-mediated mitochondrial bioenergetic dysfunction and nitro-oxidative stress. *Hepatology,* 46**,** 58-65.

PICHLMAIR, A., KANDASAMY, K., ALVISI, G., MULHERN, O., SACCO, R., HABJAN, M., BINDER, M., STEFANOVIC, A., EBERLE, C. A., GONCALVES, A., BURCKSTUMMER, T., MULLER, A. C., FAUSTER, A.,

HOLZE, C., LINDSTEN, K., GOODBOURN, S., KOCHS, G., WEBER, F., BARTENSCHLAGER, R., BOWIE, A. G., BENNETT, K. L., COLINGE, J. & SUPERTI-FURGA, G. 2012. Viral immune modulators perturb the human molecular network by common and unique strategies. *Nature,* 487**,** 486-U101.

PIETSCHMANN, T., KAUL, A., KOUTSOUDAKIS, G., SHAVINSKAYA, A., KALLIS, S., STEINMANN, E., ABID, K., NEGRO, F., DREUX, M., COSSET, F. L. & BARTENSCHLAGER, R. 2006. Construction and characterization of infectious intragenotypic and intergenotypic hepatitis C virus chimeras. *Proc Natl Acad Sci U S A,* 103**,** 7408-13.

PILERI, P., UEMATSU, Y., CAMPAGNOLI, S., GALLI, G., FALUGI, F., PETRACCA, R., WEINER, A. J., HOUGHTON, M., ROSA, D., GRANDI, G. & ABRIGNANI, S. 1998. Binding of hepatitis C virus to CD81. *Science,* 282**,** 938-41.

PLOSS, A., EVANS, M. J., GAYSINSKAYA, V. A., PANIS, M., YOU, H., DE JONG, Y. P. & RICE, C. M. 2009. Human occludin is a hepatitis C virus entry factor required for infection of mouse cells. *Nature,* 457**,** 882-6.

POLYAK, S. J., KHABAR, K. S., PASCHAL, D. M., EZELLE, H. J., DUVERLIE, G., BARBER, G. N., LEVY, D. E., MUKAIDA, N. & GRETCH, D. R. 2001. Hepatitis C virus nonstructural 5A protein induces interleukin-8, leading to partial inhibition of the interferon-induced antiviral response. *J Virol,* 75**,** 6095-106.

POPESCU, C. I., CALLENS, N., TRINEL, D., ROINGEARD, P., MORADPOUR, D., DESCAMPS, V., DUVERLIE, G., PENIN, F., HELIOT, L., ROUILLE, Y. & DUBUISSON, J. 2011. NS2 protein of hepatitis C virus interacts with structural and non-structural proteins towards virus assembly. *PLoS Pathog,* 7**,** e1001278.

POWERS, K. A., RIBEIRO, R. M., PATEL, K., PIANKO, S., NYBERG, L., POCKROS, P., CONRAD, A. J., MCHUTCHISON, J. & PERELSON, A. S. 2006. Kinetics of hepatitis C virus reinfection after liver transplantation. *Liver Transpl,* 12**,** 207-16.

PREMKUMAR, A., WILSON, L., EWART, G. D. & GAGE, P. W. 2004. Cation-selective ion channels formed by p7 of hepatitis C virus are blocked by hexamethylene amiloride. *FEBS Lett,* 557**,** 99-103.

QUEZADA, E. M. & KANE, C. M. 2009. The Hepatitis C Virus NS5A Stimulates NS5B During In Vitro RNA Synthesis in a Template Specific Manner. *Open Biochem J,* 3**,** 39-48.

RADKOWSKI, M., WILKINSON, J., NOWICKI, M., ADAIR, D., VARGAS, H., INGUI, C., RAKELA, J. & LASKUS, T. 2002. Search for hepatitis C virus negative-strand RNA sequences and analysis of viral sequences in the central nervous system: evidence of replication. *J Virol,* 76**,** 600-8.

RAMIREZ, S., LI, Y. P., JENSEN, S. B., PEDERSEN, J., GOTTWEIN, J. M. & BUKH, J. 2014. Highly efficient infectious cell culture of three hepatitis C virus genotype 2b strains and sensitivity to lead protease, nonstructural protein 5A, and polymerase inhibitors. *Hepatology,* 59**,** 395-407.

RAYCHOUDHURI, A., SHRIVASTAVA, S., STEELE, R., KIM, H., RAY, R. & RAY, R. B. 2011. ISG56 and IFITM1 proteins inhibit hepatitis C virus replication. *J Virol,* 85**,** 12881-9.

REESINK, H. W., ZEUZEM, S., WEEGINK, C. J., FORESTIER, N., VAN VLIET, A., VAN DE WETERING DE ROOIJ, J., MCNAIR, L., PURDY, S., KAUFFMAN, R., ALAM, J. & JANSEN, P. L. 2006. Rapid decline of viral RNA in hepatitis C patients treated with VX-950: a phase Ib, placebo-controlled, randomized study. *Gastroenterology,* 131**,** 997-1002.

REISS, S., REBHAN, I., BACKES, P., ROMERO-BREY, I., ERFLE, H., MATULA, P., KADERALI, L., POENISCH, M., BLANKENBURG, H., HIET, M. S., LONGERICH, T., DIEHL, S., RAMIREZ, F., BALLA, T., ROHR, K., KAUL, A., BUHLER, S., PEPPERKOK, R., LENGAUER, T., ALBRECHT, M., EILS, R., SCHIRMACHER, P., LOHMANN, V. & BARTENSCHLAGER, R. 2011. Recruitment and activation of a lipid kinase by hepatitis C virus NS5A is essential for integrity of the membranous replication compartment. *Cell Host Microbe,* 9**,** 32-45.

REMENYI, R., QI, H., SU, S. Y., CHEN, Z., WU, N. C., ARUMUGASWAMI, V., TRUONG, S., CHU, V., STOKELMAN, T., LO, H. H., OLSON, C. A., WU, T. T., CHEN, S. H., LIN, C. Y. & SUN, R. 2014. A comprehensive functional map of the hepatitis C virus genome provides a resource for probing viral proteins. *MBio,* 5**,** e01469-14.

RIJNBRAND, R., BREDENBEEK, P., VAN DER STRAATEN, T., WHETTER, L., INCHAUSPE, G., LEMON, S. & SPAAN, W. 1995. Almost the entire 5' non-translated region of hepatitis C virus is required for cap-independent translation. *FEBS Lett,* 365**,** 115-9.

ROBERTS, A. P., LEWIS, A. P. & JOPLING, C. L. 2011. miR-122 activates hepatitis C virus translation by a specialized mechanism requiring particular RNA components. *Nucleic Acids Res,* 39**,** 7716-29.

ROCK, K. L. & GOLDBERG, A. L. 1999. DEGRADATION OF CELL PROTEINS AND THE GENERATION OF MHC CLASS I-PRESENTED PEPTIDES. *Annual Review of Immunology,* 17**,** 739-779.

ROMERO-BREY, I., MERZ, A., CHIRAMEL, A., LEE, J. Y., CHLANDA, P., HASELMAN, U., SANTARELLA-MELLWIG, R., HABERMANN, A., HOPPE, S., KALLIS, S., WALTHER, P., ANTONY, C., KRIJNSE-LOCKER, J. &

BARTENSCHLAGER, R. 2012. Three-dimensional architecture and biogenesis of membrane structures associated with hepatitis C virus replication. *PLoS Pathog,* 8**,** e1003056.
ROSS-THRIEPLAND, D., AMAKO, Y. & HARRIS, M. 2013. The C terminus of NS5A domain II is a key determinant of hepatitis C virus genome replication, but is not required for virion assembly and release. *J Gen Virol,* 94**,** 1009-18.
ROSS-THRIEPLAND, D. & HARRIS, M. 2014. Insights into the complexity and functionality of hepatitis C virus NS5A phosphorylation. *J Virol,* 88**,** 1421-32.
ROSS-THRIEPLAND, D. & HARRIS, M. 2015. Hepatitis C virus NS5A: enigmatic but still promiscuous 10 years on! *J Gen Virol,* 96**,** 727-38.
RYAN, M. D. & DREW, J. 1994. Foot-and-mouth disease virus 2A oligopeptide mediated cleavage of an artificial polyprotein. *Embo j,* 13**,** 928-33.
SADASIVAN, B., LEHNER, P. J., ORTMANN, B., SPIES, T. & CRESSWELL, P. 1996. Roles for Calreticulin and a Novel Glycoprotein, Tapasin, in the Interaction of MHC Class I Molecules with TAP. *Immunity,* 5**,** 103-114.
SAEED, M., ANDREO, U., CHUNG, H. Y., ESPIRITU, C., BRANCH, A. D., SILVA, J. M. & RICE, C. M. 2015. SEC14L2 enables pan-genotype HCV replication in cell culture. *Nature,* 524**,** 471-5.
SAINZ, B., JR., BARRETTO, N., MARTIN, D. N., HIRAGA, N., IMAMURA, M., HUSSAIN, S., MARSH, K. A., YU, X., CHAYAMA, K., ALREFAI, W. A. & UPRICHARD, S. L. 2012. Identification of the Niemann-Pick C1-like 1 cholesterol absorption receptor as a new hepatitis C virus entry factor. *Nat Med,* 18**,** 281-5.
SAITO, T., OWEN, D. M., JIANG, F., MARCOTRIGIANO, J. & GALE, M., JR. 2008. Innate immunity induced by composition-dependent RIG-I recognition of hepatitis C virus RNA. *Nature,* 454**,** 523-7.
SAKAI, A., CLAIRE, M. S., FAULK, K., GOVINDARAJAN, S., EMERSON, S. U., PURCELL, R. H. & BUKH, J. 2003. The p7 polypeptide of hepatitis C virus is critical for infectivity and contains functionally important genotype-specific sequences. *Proc Natl Acad Sci U S A,* 100**,** 11646-51.
SARRAZIN, C., KIEFFER, T. L., BARTELS, D., HANZELKA, B., MUH, U., WELKER, M., WINCHERINGER, D., ZHOU, Y., CHU, H. M., LIN, C., WEEGINK, C., REESINK, H., ZEUZEM, S. & KWONG, A. D. 2007. Dynamic hepatitis C virus genotypic and phenotypic changes in patients treated with the protease inhibitor telaprevir. *Gastroenterology,* 132**,** 1767-77.
SCARSELLI, E., ANSUINI, H., CERINO, R., ROCCASECCA, R. M., ACALI, S., FILOCAMO, G., TRABONI, C., NICOSIA, A., CORTESE, R. & VITELLI, A. 2002. The human scavenger receptor class B type I is a novel candidate receptor for the hepatitis C virus. *Embo j,* 21**,** 5017-25.
SCHMIDT-MENDE, J., BIECK, E., HUGLE, T., PENIN, F., RICE, C. M., BLUM, H. E. & MORADPOUR, D. 2001. Determinants for membrane association of the hepatitis C virus RNA-dependent RNA polymerase. *J Biol Chem,* 276**,** 44052-63.
SCHMIDT, J., IVERSEN, A. K., TENZER, S., GOSTICK, E., PRICE, D. A., LOHMANN, V., DISTLER, U., BOWNESS, P., SCHILD, H., BLUM, H. E., KLENERMAN, P., NEUMANN-HAEFELIN, C. & THIMME, R. 2012. Rapid antigen processing and presentation of a protective and immunodominant HLA-B*27-restricted hepatitis C virus-specific CD8+ T-cell epitope. *PLoS Pathog,* 8**,** e1003042.
SCHNELL, G., LOO, Y. M., MARCOTRIGIANO, J. & GALE, M., JR. 2012. Uridine composition of the poly-U/UC tract of HCV RNA defines non-self recognition by RIG-I. *PLoS Pathog,* 8**,** e1002839.
SCHREGEL, V., JACOBI, S., PENIN, F. & TAUTZ, N. 2009. Hepatitis C virus NS2 is a protease stimulated by cofactor domains in NS3. *Proc Natl Acad Sci U S A,* 106**,** 5342-7.
SCHREIBER, J., MCNALLY, J., CHODAVARAPU, K., SVAROVSKAIA, E. & MORENO, C. 2016. Treatment of a patient with genotype 7 hepatitis C virus infection with sofosbuvir and velpatasvir. *Hepatology,* 64**,** 983-5.
SELVARAJAH, S. & BUSCH, M. P. 2012. TRANSFUSION-TRANSMISSION OF HCV, A LONG BUT SUCCESSFUL ROAD MAP TO SAFETY. *Antiviral therapy,* 17**,** 1423-1429.
SHANMUGAM, S. & YI, M. 2013. Efficiency of E2-p7 processing modulates production of infectious hepatitis C virus. *J Virol,* 87**,** 11255-66.
SHARIPO, A., IMREH, M., LEONCHIKS, A., IMREH, S. & MASUCCI, M. G. 1998. A minimal glycine-alanine repeat prevents the interaction of ubiquitinated I kappaB alpha with the proteasome: a new mechanism for selective inhibition of proteolysis. *Nat Med,* 4**,** 939-44.
SHARMA, N. R., MATEU, G., DREUX, M., GRAKOUI, A., COSSET, F. L. & MELIKYAN, G. B. 2011. Hepatitis C virus is primed by CD81 protein for low pH-dependent fusion. *J Biol Chem,* 286**,** 30361-76.
SHETTY, S., KIM, S., SHIMAKAMI, T., LEMON, S. M. & MIHAILESCU, M. R. 2010. Hepatitis C virus genomic RNA dimerization is mediated via a kissing complex intermediate. *Rna,* 16**,** 913-25.

SHI, G., ANDO, T., SUZUKI, R., MATSUDA, M., NAKASHIMA, K., ITO, M., OMATSU, T., OBA, M., OCHIAI, H., KATO, T., MIZUTANI, T., SAWASAKI, T., WAKITA, T. & SUZUKI, T. 2016. Involvement of the 3' Untranslated Region in Encapsidation of the Hepatitis C Virus. *PLOS Pathogens,* 12**,** e1005441.

SHIMAKAMI, T., HIJIKATA, M., LUO, H., MA, Y. Y., KANEKO, S., SHIMOTOHNO, K. & MURAKAMI, S. 2004. Effect of Interaction between Hepatitis C Virus NS5A and NS5B on Hepatitis C Virus RNA Replication with the Hepatitis C Virus Replicon. *J Virol,* 78**,** 2738-48.

SHIMOIKE, T., MCKENNA, S. A., LINDHOUT, D. A. & PUGLISI, J. D. 2009. Translational insensitivity to potent activation of PKR by HCV IRES RNA. *Antiviral Res,* 83**,** 228-37.

SHIROTA, Y., LUO, H., QIN, W., KANEKO, S., YAMASHITA, T., KOBAYASHI, K. & MURAKAMI, S. 2002. Hepatitis C virus (HCV) NS5A binds RNA-dependent RNA polymerase (RdRP) NS5B and modulates RNA-dependent RNA polymerase activity. *J Biol Chem,* 277**,** 11149-55.

SIMISTER, P., SCHMITT, M., GEITMANN, M., WICHT, O., DANIELSON, U. H., KLEIN, R., BRESSANELLI, S. & LOHMANN, V. 2009. Structural and functional analysis of hepatitis C virus strain JFH1 polymerase. *J Virol,* 83**,** 11926-39.

SIMMONDS, P., ALBERTI, A., ALTER, H. J., BONINO, F., BRADLEY, D. W., BRECHOT, C., BROUWER, J. T., CHAN, S. W., CHAYAMA, K., CHEN, D. S. & ET AL. 1994. A proposed system for the nomenclature of hepatitis C viral genotypes. *Hepatology,* 19**,** 1321-4.

SIU, G. K. Y., ZHOU, F., YU, M. K., ZHANG, L., WANG, T., LIANG, Y., CHEN, Y., CHAN, H. C. & YU, S. 2016. Hepatitis C virus NS5A protein cooperates with phosphatidylinositol 4-kinase IIIα to induce mitochondrial fragmentation. *Scientific Reports,* 6**,** 23464.

SKLAN, E. H. & GLENN, J. S. 2006. HCV NS4B: From Obscurity to Central Stage. *In:* TAN, S. L. (ed.) *Hepatitis C Viruses: Genomes and Molecular Biology.* Norfolk (UK): Horizon Bioscience

Horizon Bioscience.

SMITH, D. B., BUKH, J., KUIKEN, C., MUERHOFF, A. S., RICE, C. M., STAPLETON, J. T. & SIMMONDS, P. 2014. Expanded classification of hepatitis C virus into 7 genotypes and 67 subtypes: updated criteria and genotype assignment web resource. *Hepatology,* 59**,** 318-27.

SOBOLESKI, M. R., OAKS, J. & HALFORD, W. P. 2005. Green fluorescent protein is a quantitative reporter of gene expression in individual eukaryotic cells. *Faseb j,* 19**,** 440-2.

SONG, J., FUJII, M., WANG, F., ITOH, M. & HOTTA, H. 1999. The NS5A protein of hepatitis C virus partially inhibits the antiviral activity of interferon. *J Gen Virol,* 80 (Pt 4)**,** 879-86.

SONG, J., TAN, H., PERRY, A. J., AKUTSU, T., WEBB, G. I., WHISSTOCK, J. C. & PIKE, R. N. 2012. PROSPER: an integrated feature-based tool for predicting protease substrate cleavage sites. *PLoS One,* 7**,** e50300.

SPAHN, C. M., KIEFT, J. S., GRASSUCCI, R. A., PENCZEK, P. A., ZHOU, K., DOUDNA, J. A. & FRANK, J. 2001. Hepatitis C virus IRES RNA-induced changes in the conformation of the 40s ribosomal subunit. *Science,* 291**,** 1959-62.

STEINKUHLER, C., BIASIOL, G., BRUNETTI, M., URBANI, A., KOCH, U., CORTESE, R., PESSI, A. & DE FRANCESCO, R. 1998. Product inhibition of the hepatitis C virus NS3 protease. *Biochemistry,* 37**,** 8899-905.

STREET, A., MACDONALD, A., CROWDER, K. & HARRIS, M. 2004. The Hepatitis C virus NS5A protein activates a phosphoinositide 3-kinase-dependent survival signaling cascade. *J Biol Chem,* 279**,** 12232-41.

SUEN, D. F., NORRIS, K. L. & YOULE, R. J. 2008. Mitochondrial dynamics and apoptosis. *Genes Dev,* 22**,** 1577-90.

SUH, W. K., COHEN-DOYLE, M. F., FRUH, K., WANG, K., PETERSON, P. A. & WILLIAMS, D. B. 1994. Interaction of MHC class I molecules with the transporter associated with antigen processing. *Science,* 264**,** 1322-6.

SUMPTER, R., JR., LOO, Y. M., FOY, E., LI, K., YONEYAMA, M., FUJITA, T., LEMON, S. M. & GALE, M., JR. 2005. Regulating intracellular antiviral defense and permissiveness to hepatitis C virus RNA replication through a cellular RNA helicase, RIG-I. *J Virol,* 79**,** 2689-99.

SUPPIAH, V., MOLDOVAN, M., AHLENSTIEL, G., BERG, T., WELTMAN, M., ABATE, M. L., BASSENDINE, M., SPENGLER, U., DORE, G. J., POWELL, E., RIORDAN, S., SHERIDAN, D., SMEDILE, A., FRAGOMELI, V., MULLER, T., BAHLO, M., STEWART, G. J., BOOTH, D. R. & GEORGE, J. 2009. IL28B is associated with response to chronic hepatitis C interferon-alpha and ribavirin therapy. *Nat Genet,* 41**,** 1100-4.

SWAIN, M. G., LAI, M. Y., SHIFFMAN, M. L., COOKSLEY, W. G., ZEUZEM, S., DIETERICH, D. T., ABERGEL, A., PESSOA, M. G., LIN, A., TIETZ, A., CONNELL, E. V. & DIAGO, M. 2010. A sustained virologic response is durable in patients with chronic hepatitis C treated with peginterferon alfa-2a and ribavirin. *Gastroenterology,* 139**,** 1593-601.

TAN, S. L. & KATZE, M. G. 2001. How hepatitis C virus counteracts the interferon response: the jury is still out on NS5A. *Virology,* 284**,** 1-12.

TAN, S. L., NAKAO, H., HE, Y., VIJAYSRI, S., NEDDERMANN, P., JACOBS, B. L., MAYER, B. J. & KATZE, M. G. 1999. NS5A, a nonstructural protein of hepatitis C virus, binds growth factor receptor-bound protein 2 adaptor protein in a Src homology 3 domain/ligand-dependent manner and perturbs mitogenic signaling. *Proc Natl Acad Sci U S A,* 96**,** 5533-8.

TANAKA, Y., NISHIDA, N., SUGIYAMA, M., KUROSAKI, M., MATSUURA, K., SAKAMOTO, N., NAKAGAWA, M., KORENAGA, M., HINO, K., HIGE, S., ITO, Y., MITA, E., TANAKA, E., MOCHIDA, S., MURAWAKI, Y., HONDA, M., SAKAI, A., HIASA, Y., NISHIGUCHI, S., KOIKE, A., SAKAIDA, I., IMAMURA, M., ITO, K., YANO, K., MASAKI, N., SUGAUCHI, F., IZUMI, N., TOKUNAGA, K. & MIZOKAMI, M. 2009. Genome-wide association of IL28B with response to pegylated interferon-alpha and ribavirin therapy for chronic hepatitis C. *Nat Genet,* 41**,** 1105-9.

TARDIF, K. D., MORI, K. & SIDDIQUI, A. 2002. Hepatitis C Virus Subgenomic Replicons Induce Endoplasmic Reticulum Stress Activating an Intracellular Signaling Pathway. *J Virol,* 76**,** 7453-9.

TARDIF, K. D. & SIDDIQUI, A. 2003. Cell surface expression of major histocompatibility complex class I molecules is reduced in hepatitis C virus subgenomic replicon-expressing cells. *J Virol,* 77**,** 11644-50.

TARGETT-ADAMS, P. & MCLAUCHLAN, J. 2005. Development and characterization of a transient-replication assay for the genotype 2a hepatitis C virus subgenomic replicon. *J Gen Virol,* 86**,** 3075-80.

TAYLOR, D. R., SHI, S. T., ROMANO, P. R., BARBER, G. N. & LAI, M. M. 1999. Inhibition of the interferon-inducible protein kinase PKR by HCV E2 protein. *Science,* 285**,** 107-10.

TE, H. S., RANDALL, G. & JENSEN, D. M. 2007. Mechanism of action of ribavirin in the treatment of chronic hepatitis C. *Gastroenterol Hepatol (N Y),* 3**,** 218-25.

TELLINGHUISEN, T. L., FOSS, K. L., TREADAWAY, J. C. & RICE, C. M. 2008. Identification of residues required for RNA replication in domains II and III of the hepatitis C virus NS5A protein. *J Virol,* 82**,** 1073-83.

TELLINGHUISEN, T. L., MARCOTRIGIANO, J., GORBALENYA, A. E. & RICE, C. M. 2004. The NS5A protein of hepatitis C virus is a zinc metalloprotein. *J Biol Chem,* 279**,** 48576-87.

TELLINGHUISEN, T. L., MARCOTRIGIANO, J. & RICE, C. M. 2005. Structure of the zinc-binding domain of an essential component of the hepatitis C virus replicase. *Nature,* 435**,** 374-9.

THIBAULT, P. A., HUYS, A., AMADOR-CANIZARES, Y., GAILIUS, J. E., PINEL, D. E. & WILSON, J. A. 2015. Regulation of Hepatitis C Virus Genome Replication by Xrn1 and MicroRNA-122 Binding to Individual Sites in the 5' Untranslated Region. *J Virol,* 89**,** 6294-311.

THOMSSEN, R., BONK, S., PROPFE, C., HEERMANN, K. H., KOCHEL, H. G. & UY, A. 1992. Association of hepatitis C virus in human sera with beta-lipoprotein. *Med Microbiol Immunol,* 181**,** 293-300.

THOMSSEN, R., BONK, S. & THIELE, A. 1993. Density heterogeneities of hepatitis C virus in human sera due to the binding of beta-lipoproteins and immunoglobulins. *Med Microbiol Immunol,* 182**,** 329-34.

TOKUMOTO, Y., HIASA, Y., HORIIKE, N., MICHITAKA, K., MATSUURA, B., CHUNG, R. T. & ONJI, M. 2007. Hepatitis C virus expression and interferon antiviral action is dependent on PKR expression. *J Med Virol,* 79**,** 1120-7.

TORNOE, C. W., CHRISTENSEN, C. & MELDAL, M. 2002. Peptidotriazoles on solid phase: [1,2,3]-triazoles by regiospecific copper(i)-catalyzed 1,3-dipolar cycloadditions of terminal alkynes to azides. *J Org Chem,* 67**,** 3057-64.

TSUKADA, H., OCHI, H., MAEKAWA, T., ABE, H., FUJIMOTO, Y., TSUGE, M., TAKAHASHI, H., KUMADA, H., KAMATANI, N., NAKAMURA, Y. & CHAYAMA, K. 2009. A polymorphism in MAPKAPK3 affects response to interferon therapy for chronic hepatitis C. *Gastroenterology,* 136**,** 1796-805.e6.

TSUKIYAMA-KOHARA, K., IIZUKA, N., KOHARA, M. & NOMOTO, A. 1992. Internal ribosome entry site within hepatitis C virus RNA. *J Virol,* 66**,** 1476-83.

VAN DE WEIJER, M. L., LUTEIJN, R. D. & WIERTZ, E. J. H. J. 2015. Viral immune evasion: Lessons in MHC class I antigen presentation. *Seminars in Immunology,* 27**,** 125-137.

VARGAS, H. E., LASKUS, T., RADKOWSKI, M., WILKINSON, J., BALAN, V., DOUGLAS, D. D., HARRISON, M. E., MULLIGAN, D. C., OLDEN, K., ADAIR, D. & RAKELA, J. 2002. Detection of hepatitis C virus sequences in brain tissue obtained in recurrent hepatitis C after liver transplantation. *Liver Transpl,* 8**,** 1014-9.

VERDEGEM, D., BADILLO, A., WIERUSZESKI, J. M., LANDRIEU, I., LEROY, A., BARTENSCHLAGER, R., PENIN, F., LIPPENS, G. & HANOULLE, X. 2011. Domain 3 of NS5A protein from the hepatitis C virus has intrinsic alpha-helical propensity and is a substrate of cyclophilin A. *J Biol Chem,* 286**,** 20441-54.

VYAS, J. M., VAN DER VEEN, A. G. & PLOEGH, H. L. 2008. The known unknowns of antigen processing and presentation. *Nature reviews. Immunology,* 8**,** 607-618.

W.H.O. 2017. *Hepatitis C Fact Sheet* [Online]. Available: http://www.who.int/mediacentre/factsheets/fs164/en/ [Accessed 24/07 2017].
WAKITA, T., PIETSCHMANN, T., KATO, T., DATE, T., MIYAMOTO, M., ZHAO, Z., MURTHY, K., HABERMANN, A., KRAUSSLICH, H. G., MIZOKAMI, M., BARTENSCHLAGER, R. & LIANG, T. J. 2005. Production of infectious hepatitis C virus in tissue culture from a cloned viral genome. *Nat Med,* 11**,** 791-6.
WANG, C., PFLUGHEBER, J., SUMPTER, R., JR., SODORA, D. L., HUI, D., SEN, G. C. & GALE, M., JR. 2003. Alpha interferon induces distinct translational control programs to suppress hepatitis C virus RNA replication. *J Virol,* 77**,** 3898-912.
WANG, W., LAHSER, F. C., YI, M., WRIGHT-MINOGUE, J., XIA, E., WEBER, P. C., LEMON, S. M. & MALCOLM, B. A. 2004. Conserved C-terminal threonine of hepatitis C virus NS3 regulates autoproteolysis and prevents product inhibition. *J Virol,* 78**,** 700-9.
WEBSTER, D. P., KLENERMAN, P. & DUSHEIKO, G. M. 2015. Lancet Seminar – Hepatitis C. *Lancet (London, England),* 385**,** 1124-1135.
WILKINS, C., WOODWARD, J., LAU, D. T., BARNES, A., JOYCE, M., MCFARLANE, N., MCKEATING, J. A., TYRRELL, D. L. & GALE, M., JR. 2013. IFITM1 is a tight junction protein that inhibits hepatitis C virus entry. *Hepatology,* 57**,** 461-9.
WING, S. S. 2013. Deubiquitinases in skeletal muscle atrophy. *Int J Biochem Cell Biol,* 45**,** 2130-5.
WOLK, B., BUCHELE, B., MORADPOUR, D. & RICE, C. M. 2008. A dynamic view of hepatitis C virus replication complexes. *J Virol,* 82**,** 10519-31.
WOOTTON, J. C. 1994. Non-globular domains in protein sequences: automated segmentation using complexity measures. *Comput Chem,* 18**,** 269-85.
WOZNIAK, A. L., GRIFFIN, S., ROWLANDS, D., HARRIS, M., YI, M., LEMON, S. M. & WEINMAN, S. A. 2010. Intracellular proton conductance of the hepatitis C virus p7 protein and its contribution to infectious virus production. *PLoS Pathog,* 6**,** e1001087.
WRIGHT, P. E. & DYSON, H. J. 1999. Intrinsically unstructured proteins: re-assessing the protein structure-function paradigm. *J Mol Biol,* 293**,** 321-31.
WRIGHT, P. E. & DYSON, H. J. 2009. Linking folding and binding. *Curr Opin Struct Biol,* 19**,** 31-8.
WU, S. C., CHANG, S. C., WU, H. Y., LIAO, P. J. & CHANG, M. F. 2008. Hepatitis C virus NS5A protein down-regulates the expression of spindle gene Aspm through PKR-p38 signaling pathway. *J Biol Chem,* 283**,** 29396-404.
XIE, Z., XIAO, Z. & WANG, F. 2017. Hepatitis C Virus Nonstructural 5A Protein (HCV-NS5A) Inhibits Hepatocyte Apoptosis through the NF-kappab/miR-503/bcl-2 Pathway. *Mol Cells,* 40**,** 202-210.
XU, J., LIU, S., XU, Y., TIEN, P. & GAO, G. 2009. Identification of the nonstructural protein 4B of hepatitis C virus as a factor that inhibits the antiviral activity of interferon-alpha. *Virus Res,* 141**,** 55-62.
XUE, B., YANG, D., WANG, J., XU, Y., WANG, X., QIN, Y., TIAN, R., CHEN, S., XIE, Q., LIU, N. & ZHU, H. 2016. ISG12a Restricts Hepatitis C Virus Infection through the Ubiquitination-Dependent Degradation Pathway. *J Virol,* 90**,** 6832-45.
YAMANE, D., MCGIVERN, D. R., WAUTHIER, E., YI, M., MADDEN, V. J., WELSCH, C., ANTES, I., WEN, Y., CHUGH, P. E., MCGEE, C. E., WIDMAN, D. G., MISUMI, I., BANDYOPADHYAY, S., KIM, S., SHIMAKAMI, T., OIKAWA, T., WHITMIRE, J. K., HEISE, M. T., DITTMER, D. P., KAO, C. C., PITSON, S. M., MERRILL JR, A. H., REID, L. M. & LEMON, S. M. 2014. Regulation of the hepatitis C virus RNA replicase by endogenous lipid peroxidation. *Nat Med,* 20**,** 927-935.
YAMASHITA, T., KANEKO, S., SHIROTA, Y., QIN, W., NOMURA, T., KOBAYASHI, K. & MURAKAMI, S. 1998. RNA-dependent RNA polymerase activity of the soluble recombinant hepatitis C virus NS5B protein truncated at the C-terminal region. *J Biol Chem,* 273**,** 15479-86.
YAN, B. S., TAM, M. H. & SYU, W. J. 1998. Self-association of the C-terminal domain of the hepatitis-C virus core protein. *Eur J Biochem,* 258**,** 100-6.
YANG, C., ZHAO, X., SUN, D., YANG, L., CHONG, C., PAN, Y., CHI, X., GAO, Y., WANG, M., SHI, X., SUN, H., LV, J., GAO, Y., ZHONG, J., NIU, J. & SUN, B. 2016. Interferon alpha (IFNalpha)-induced TRIM22 interrupts HCV replication by ubiquitinating NS5A. *Cell Mol Immunol,* 13**,** 94-102.
YAO, L., DONG, H., ZHU, H., NELSON, D., LIU, C., LAMBIASE, L. & LI, X. 2011. Identification of the IFITM3 gene as an inhibitor of hepatitis C viral translation in a stable STAT1 cell line. *J Viral Hepat,* 18**,** e523-9.
YI, M., MA, Y., YATES, J. & LEMON, S. M. 2007. Compensatory mutations in E1, p7, NS2, and NS3 enhance yields of cell culture-infectious intergenotypic chimeric hepatitis C virus. *J Virol,* 81**,** 629-38.
ZAYAS, M., LONG, G., MADAN, V. & BARTENSCHLAGER, R. 2016. Coordination of Hepatitis C Virus Assembly by Distinct Regulatory Regions in Nonstructural Protein 5A. *PLoS Pathog,* 12**,** e1005376.

ZEUZEM, S., FOSTER, G. R., WANG, S., ASATRYAN, A., GANE, E., FELD, J. J., ASSELAH, T., BOURLIERE, M., RUANE, P. J., WEDEMEYER, H., POL, S., FLISIAK, R., POORDAD, F., CHUANG, W. L., STEDMAN, C. A., FLAMM, S., KWO, P., DORE, G. J., SEPULVEDA-ARZOLA, G., ROBERTS, S. K., SOTO-MALAVE, R., KAITA, K., PUOTI, M., VIERLING, J., TAM, E., VARGAS, H. E., BRUCK, R., FUSTER, F., PAIK, S. W., FELIZARTA, F., KORT, J., FU, B., LIU, R., NG, T. I., PILOT-MATIAS, T., LIN, C. W., TRINH, R. & MENSA, F. J. 2018. Glecaprevir-Pibrentasvir for 8 or 12 Weeks in HCV Genotype 1 or 3 Infection. *N Engl J Med,* 378**,** 354-369.

ZHANG, C., CAI, Z., KIM, Y. C., KUMAR, R., YUAN, F., SHI, P. Y., KAO, C. & LUO, G. 2005. Stimulation of hepatitis C virus (HCV) nonstructural protein 3 (NS3) helicase activity by the NS3 protease domain and by HCV RNA-dependent RNA polymerase. *J Virol,* 79**,** 8687-97.

ZHANG, M. & COFFINO, P. 2004. Repeat sequence of Epstein-Barr virus-encoded nuclear antigen 1 protein interrupts proteasome substrate processing. *J Biol Chem,* 279**,** 8635-41.

ZHANG, Y. L., GUO, Y. J., BIN, L. & SUN, S. H. 2009. Hepatitis C virus single-stranded RNA induces innate immunity via Toll-like receptor 7. *J Hepatol,* 51**,** 29-38.

ZHONG, J., GASTAMINZA, P., CHENG, G., KAPADIA, S., KATO, T., BURTON, D. R., WIELAND, S. F., UPRICHARD, S. L., WAKITA, T. & CHISARI, F. V. 2005. Robust hepatitis C virus infection in vitro. *Proc Natl Acad Sci U S A,* 102**,** 9294-9.

ZHONG, W., USS, A. S., FERRARI, E., LAU, J. Y. & HONG, Z. 2000. De novo initiation of RNA synthesis by hepatitis C virus nonstructural protein 5B polymerase. *J Virol,* 74**,** 2017-22.

8 APPENDIX

8.1 PRODUCTION OF 20AA DELETION REPLICONS

Seven overlapping 20 amino acid deletions were introduced into NS5A, spanning residues 2354 and 2435 within the JFH1 polyprotein. These deletions were introduced into a pSGRJFH1*lucNS3-5B(DHFRClover@2442) template, by two-step PCR, using primer pairs described in Table 8-1, (Figure 8-1). Deletion carrying fragments were then cloned into the pSGRJFH1*lucNS3-5B(DHFRClover@2442) vector using either *Cpo*I and *BamHI*(Δ2385,Δ2395,Δ2405,Δ2415) or *Mlu*I and *Bam*HI(Δ2354,Δ2365,Δ2375), (Figure 8-1). Post ligation, plasmids were screened for the presence of the desired insert by restriction digestion with the same enzymes used for cloning, and the insert region further verified by sequencing.

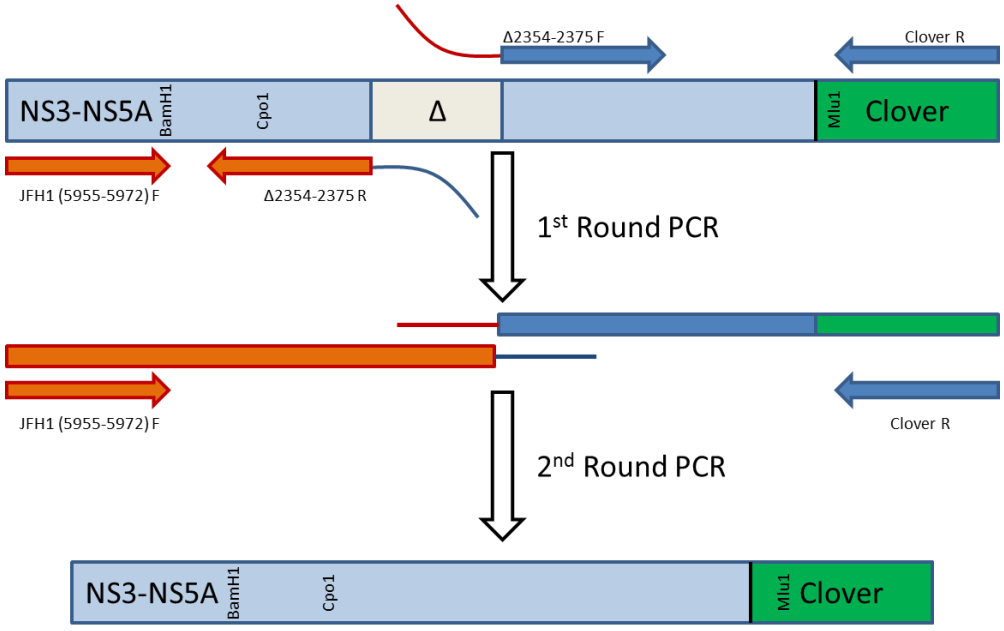

Figure 8-1 **Strategy to Generate pSGRJFH1*lucNS35B(DHFR-Clover@2442) replicons containing 20 Amino Acid deletions**. A two step PCR reaction was used to generate templates for cloning into the parental vector via *Bam*HI + *Mlu*I or *Cpo*I + *Mlu*I restriction sites (The Cpo1 site was chosen to minimise the size of fragment introduced and thereby limit the chance of mutation, however this site was removed in the Δ2354-2374, Δ2365-2385, and Δ2375-2395 constructs, necessitating the use of *MluI*). Δ primers anneal on either side of the deletion boundaries, and carry a 10 nucleotide tail complementary to the other side of the deletion boundary. Together with the flanking primers these generate 2 overlapping PCR products lacking the deleted fragment. A second PCR reaction, using these products as a template, yields the final PCR product for cloning.

Primer Name	Primer Sequence (5'-3')
Δ2354-2374 F	GACCTTTGGCCCGACGTCCCCTGGTGAGCC
Δ2354-2374 R	GGGACGTCGGGCCAAAGGTCTTGATGGCCAG
Δ2365-2384 F	CAGGCTCGTCCGAGACAGGTTCCGCCTCCTC
Δ2365-2384 R	GAACCTGTCTCGGACGAGCCTGCATCACCGC
Δ2375-2394 F	GAATCCGGCGGTCTCGAGGGGGAGCCTGGAGATC
Δ2375-2394 R	CCCCCTCGAGACCGCCGGATTCGGCGGCGC
Δ2385-2404 F	GGCCCCCTCAGAGTCTGATCAGGTAGAGC
Δ2385-2404 R	GATCAGACTCTGAGGGGGCCGGCTCACCAG
Δ2395-2414 F	CTATGCCCCCACCCCAGGGCGGTGGAGTAGC
Δ2395-2414 R	CGCCCTGGGGTGGGGGCATAGAGGAGGCGG
Δ2405-2424 F	GATCCGGACCTGGGCTCGGGGTCTTGGTCTAC
Δ2405-2424 R	GACCCCGAGCCCAGGTCCGGATCTCCAGGCTC
Δ2415-2435 F	CTTCAACCTCCCGACGATACCACCGTGTCCTG
Δ2415-2435 R	GTGGTATCGTCGGGAGGTTGAAGCTCTACCTG
JFH1 5955-5972 F	TCATGTCTGGCGAGAAGC
Clover R	TCCAGCTCGACCAGGATG

Table 8-1 **Primers used to introduce 20 amino acid deletions into pSGRJFH1*lucNS3-5B(DHFRClover@2442)**

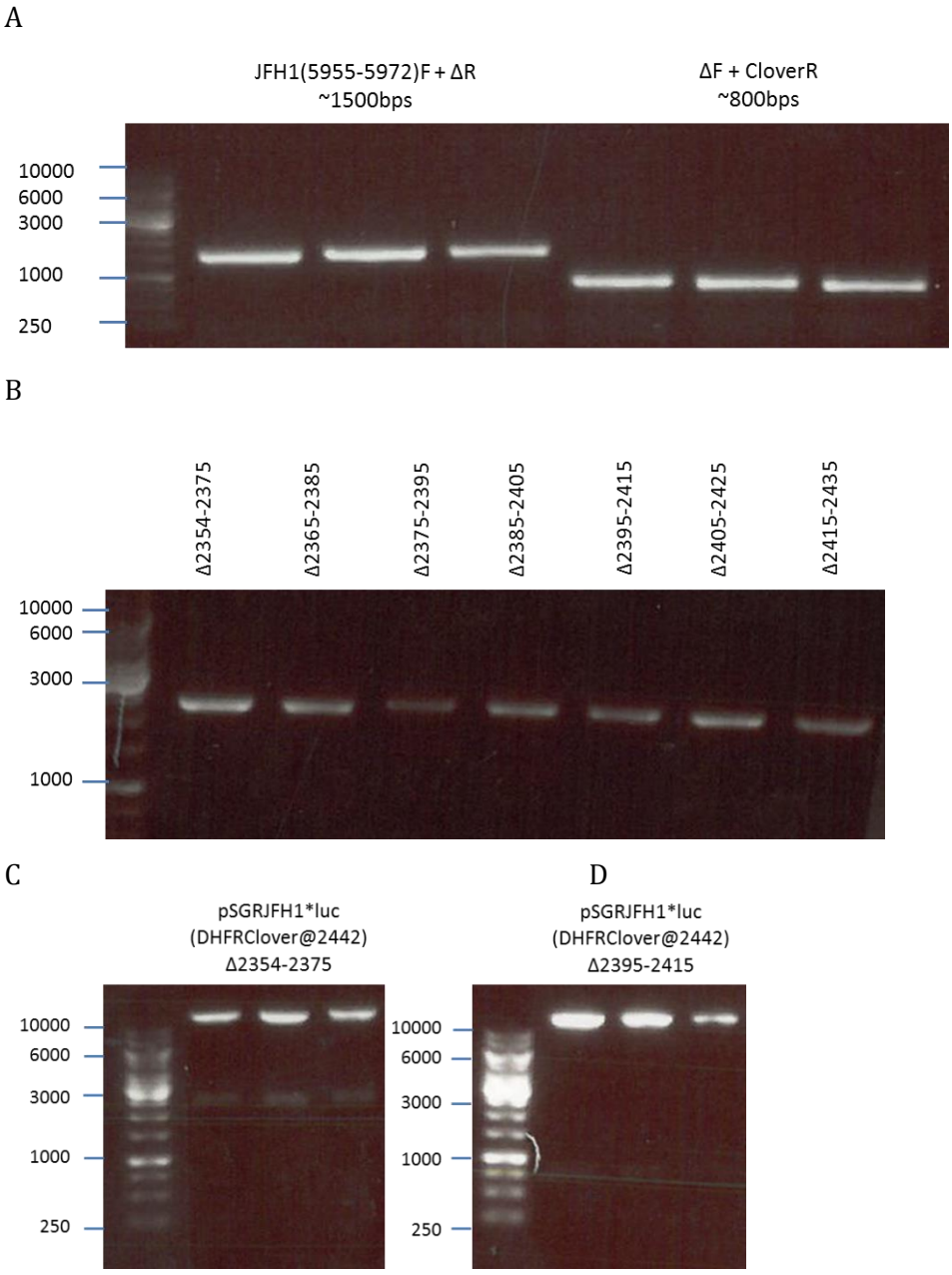

Figure 8-2 **Production of pSGRJFH1*lucNS35B(DHFR-clover@2442) replicons containing 20 amino acid deletions**. (A) Representative 1st round PCR products. Shown are the products of the Δ2354-2375, Δ2365-2385, and Δ2375-2395 upstream (~1500 bp) and downstream (~800 bp) reactions. (B) All 2nd round 2300 bp PCR products containing the appropriate 60 bp deletion prior to restriction digestion and cloning into pSGRJFH1(DHFR-clover@2442). (C, D) Confirmation of insertion by restriction digestion on ligated plasmid with either *Bam*HI and *Mlu*I(Δ2354,Δ2365,Δ2375) (C) or *Cpo*I and *Mlu*I(Δ2385,Δ2395,Δ2405, Δ2415) (D). Clones were considered positive if they yielded a ~2300 bp or ~800 bp fragment respectively.

8.2 INTRODUCING THE 2354-2400 DELETION INTO PFK5.1 CON1

The equivalent of the Δ2354-2404 deletion was introduced into genotype 1b strain, Con1 (accession number AJ238799(Lohmann et al., 1999)). Based on an alignment of 20 strains, representing genotypes 1-6, the equivalent deletion was considered to represent residues 2354-2400 of the Con1 sequence (Figure 8-3). This was introduced into pFK5.1 by 2 step PCR using the Con1 Δ2354-2400 F and R primers, in conjunction with the flanking Con1 MfeI R and Con1 XhoI F primers respectively (Table 8-2) (Figure 8-4). The 2nd round PCR product was then cloned into a pFK5.1 Neo Con1 base using an upstream *Xho*I site and a downstream *Mfe*I site to give pFK5.1Con1neoΔ2354-2400. The presence of the insert was confirmed by digestion with *Xho*I and *Mfe*I, whilst the fidelity of the PCR was confirmed by sequencing.

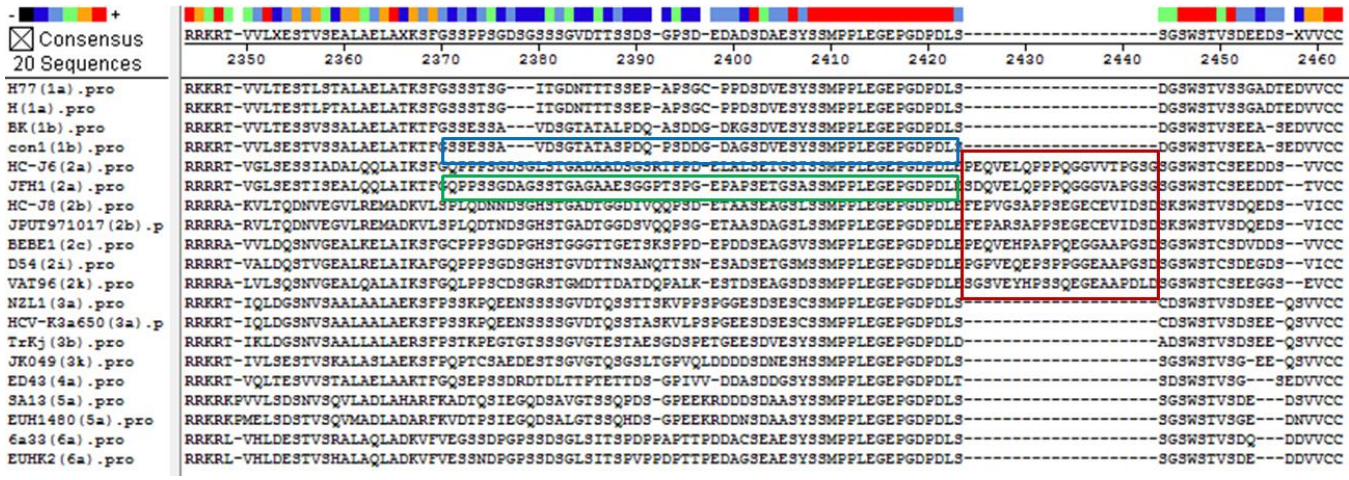

Figure 8-3 **Sequence Alignment of NS5A domain III.** The green box represents the Δ2354-2404 truncation in JFH1 whilst the Blue box represents the equivalent Δ2354-2400 truncation in con1. The red box indicates the 20 additional amino acids present in genotype 2 isolates.

Primer Name	Primer Sequence (5'-3')
Con1 XhoI F	CTTTCGAGCCGCTCCAAGCG
Con1 MfeI R	CGCAACACCTTAAATAAACC
Con1 Δ2354-2400 F	GACCTTCGGCCTCAGCGACGGGTCTTGGTC
Con1 Δ2354-2400 R	CCCGTCGCTGAGGCCGAAGGTCTCTGTGGCGAG

Table 8-2 **Primers used to introduce the 2354-2404 equivalent deletion into pFK5.1 Con1.**

A

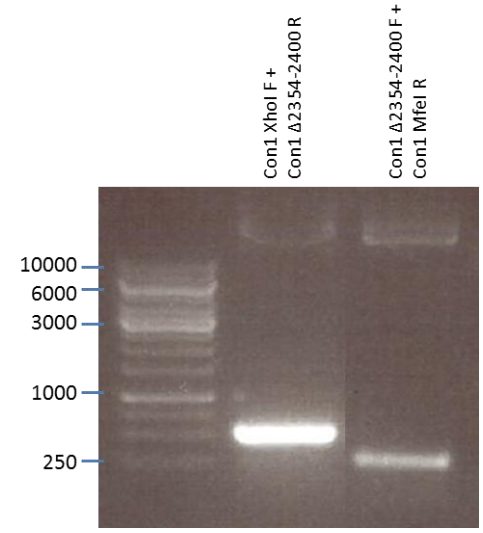

B

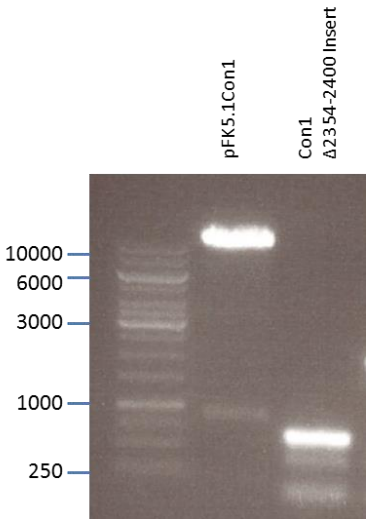

C

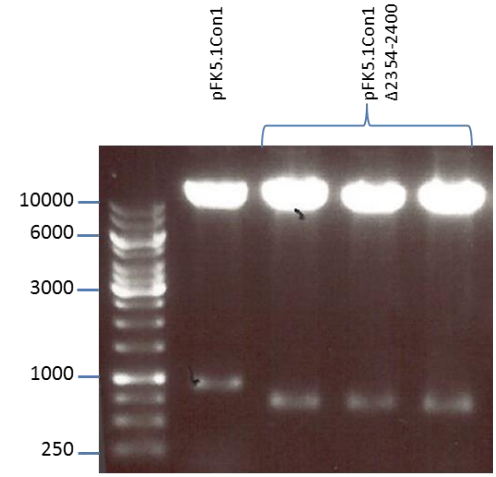

Figure 8-4 **Introduction of the Δ2354-2400 truncation into pFK5.1Con1**. (A)NS5A carrying the Δ2354-2400 truncation was PCR amplified from pFK5.1Con1 using Con1-XhoI-F and Con1Δ2354-2400R and Con1Δ2354-2400F and Con1-MfeI-R. (B) The truncation fragment (~730 bp) was then cloned into pFK5.1Con1 using *Xho*I and *Mfe*I.
(C) To confirm the presence of the insertion pFK5.1Con1Δ2354-2404 clones were re-digested with *Xho*I and *Mfe*I. Clones which yielded a ~730 bp fragment were considered positive.

8.3 CLONING OF MUTANT DOMAIN III INTO PFK5.1CON1LUC CONSTRUCTS WITH EITHER A WILD TYPE OF DESTABILISING NS4B/5A BOUNDARY

Constructs carrying either a wild type or destabilising NS4B/5A boundary alongside either a full length or truncated NS5A domain III were generated by cloning the NS5A, from pFK5.1Con1neo and pFK5.1Con1neoΔ2354-2400, into pFK5.1Con1luc and pFK5.1Con1lucSV/QGG vectors(Herod et al., 2012) using *Spe*I and *Xho*I (Figure 8-5). Success of cloning was determined by re-digestion with the same restriction enzymes.

A

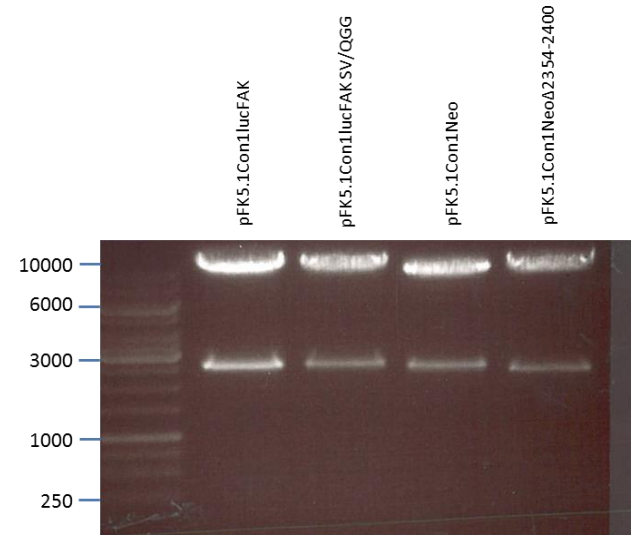

B

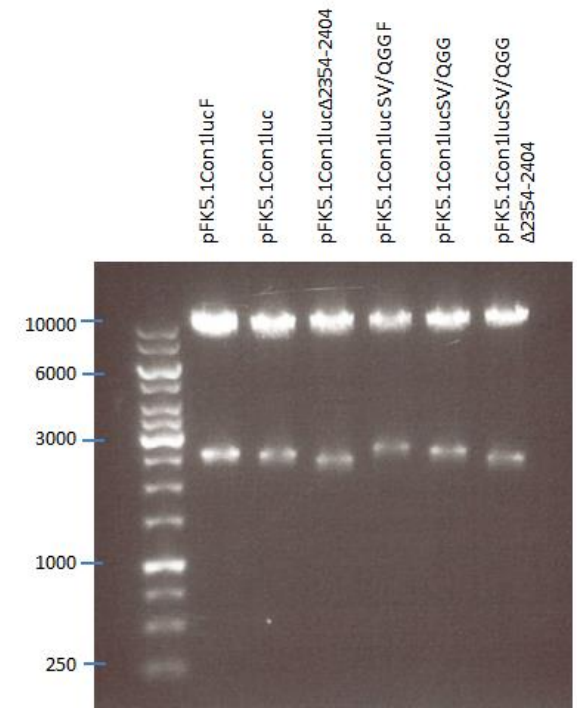

C

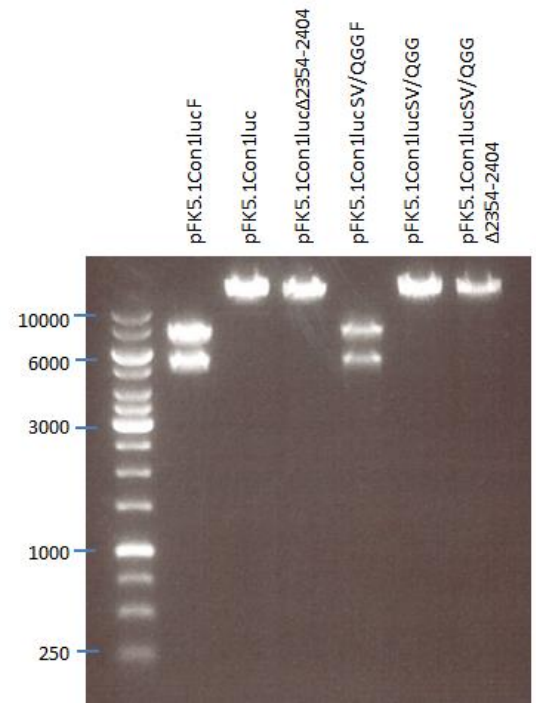

Figure 8-5 **Generation of pFK5.1Con1luc replicons carrying either a wildtype or destabilising NS4B/5A boundary, and either a full length or truncated NS5A domain III**. (A) NS5A (~3.5 kb), from both pFK5.1Con1neo and pFK5.1Con1neoΔ2354-2400 was cloned into pFK5.1Con1luc and pFK5.1Con1LucSV/QGG vectors (~9.5 kb) carrying either a wild type or mutant boundary using *Spe*I and *Xho*I. (B) To confirm the success of the cloning, clones were re-digested with *Spe*I and *Xho*I. (C) To confirm the absence of a Flag tag, present in the parental vectors but absent in the desired construct, clones were digested with *Cla*I. Clones carrying the unwanted flag tag were cut twice, while successful clones will only cut once. Both parental vectors were included as controls.

8.4 GENERATION OF PFK5.1CON1 CONSTRUCTS CARRYING EITHER A FULL LENGTH OR TRUNCATED NS5A DOMAIN III IN A NEO RESISTANT BACKBONE

To generate Neo resistant pFK5.1Con1 constructs carrying either a full length or truncated NS5A domain III, the DHFR-clover insert was introduced into pFK5.1Neo by multistep PCR using primers describe in Table 8-3 (Figure 8-6). The DHFR-clover insert was amplified from pSGRJFH1*lucNS3-5B (DHFRClover@2442) using Con1 5A-DHFR F and Con1 DHFR-5B R, while complementary upstream and downstream Con1 fragments were generated using Con1 XhoI F and Con1 5A-DHFR R, and Con1 MfeI R and Con1 DHFR-5B F, respectively. These were then combined in a final PCR reaction to generate the final PCR product, which was cloned into pFK5.1Neo using *Xho*I and *Mfe*I to form pFK5.1Con1neo(DHFRclover@2419). The presence of the insert was verified by restriction digestion, and the lack of unwanted mutation verified by sequencing.

A construct containing both the 2354-2400 deletion and the DHFR-clover insert was also generated by repeating the deletion PCR reaction, described in section 8.2, using the pFK5.1Con1neo(DHFRclover@2419) as the template. The resulting plasmid was named pFK5.1Con1neo(DHFRclover@2419)Δ2354-2400.

Primer Name	Primer Sequence (5'-3')
Con1 XhoI F	CTTTCGAGCCGCTCCAAGCG
Con1 MfeI R	CGCAACACCTTAAATAAACC
Con1 Δ2354-2400 F	GACCTTCGGCCTCAGCGACGGGTCTTGGTC
Con1 Δ2354-2400 R	CCCGTCGCTGAGGCCGAAGGTCTCTGTGGCGAG
Con1 5A-DHFR F	GGACGTCGTCTCCTGCCCCGAGAACTTGTAC
Con1 5A-DHFR R	CTCGGGGCAGGAGACGACGTCCTCACTAGC
Con1 DHFR-5B F	AGCGCTGAAGATGTGGTGTGTTGTTCGATGTCCTACACATGGAC
Con1 DHFR-5B R	ACAACACACCACATCTTCAGCGCTAGCGCTCTTGTACAGCTCGTC

Table 8-3 **Primers used to introduce the DHFR-Clover cassette into pFK5.1 Con1**.

A

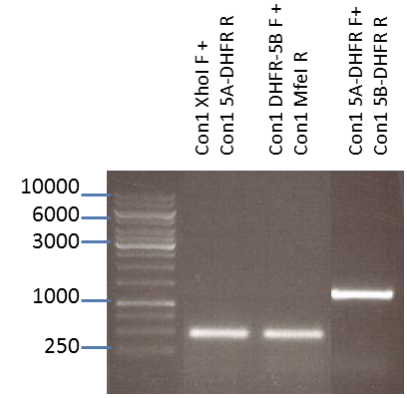
Con1 XhoI F +
Con1 5A-DHFR R
Con1 DHFR-5B F +
Con1 MfeI R
Con1 5A-DHFR F+
Con1 5B-DHFR R
10000
6000
3000
1000
250

B

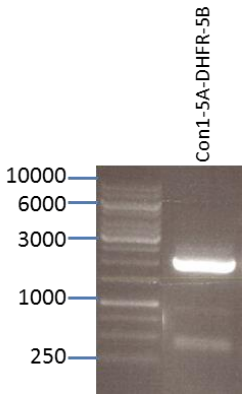
Con1-5A-DHFR-5B
10000
6000
3000
1000
250

C

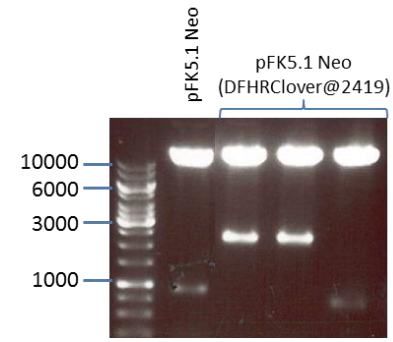
pFK5.1 Neo
pFK5.1 Neo
(DFHRClover@2419)
10000
6000
3000
1000

D

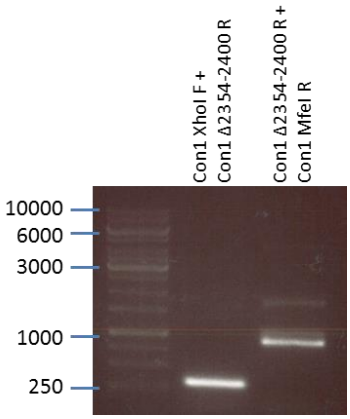
Con1 XhoI F +
Con1 Δ2354-2400 R
Con1 Δ2354-2400 R +
Con1 MfeI R
10000
6000
3000
1000
250

E

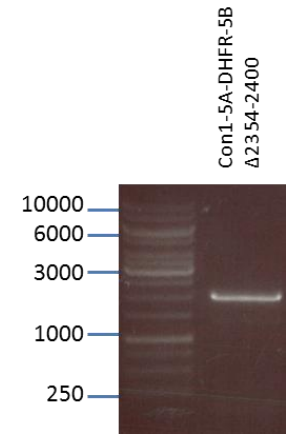
Con1-5A-DHFR-5B
Δ2354-2400
10000
6000
3000
1000
250

F

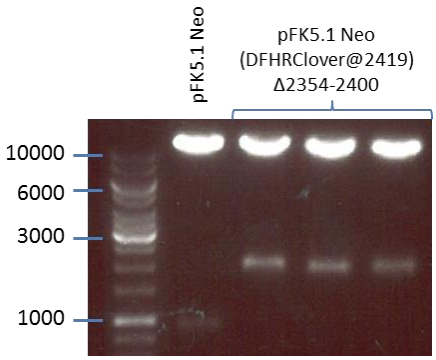
pFK5.1 Neo
pFK5.1 Neo
(DFHRClover@2419)
Δ2354-2400
10000
6000
3000
1000

Figure 8-6 **Generation of pFK5.1Con1neo replicons carrying the DHFR-Clover cassette at 2419**. (A) The DHFR-Clover cassette was PCR amplified from pSGRJFH1*lucNS3-5B(DHFRClover@2442) using Con1 5A-DHFR F and Con1 DHFR-5B R, while complementary upstream and downstream Con1 fragments were generated using Con1 XhoI F and Con1 5A-DHFR R, and Con1 MfeI R and Con1 DHFR-5B F**.** (B) The 3 products from the 1st round PCR were combined and amplified together using Con1 XhoI F and Con1 MfeI R and the DHFR-Clover insert fragment (~2.2 kb) cloned into pFK5.1Neo using *Xho*I and *Mfe*I. (C) To confirm the presence of the insertion pFK5.1Con1 Neo(DHFRClover@2419) clones were re-digested with *Xho*I and *Mfe*I. Clones which yielded a ~2.2 kb fragment were considered positive. (D)NS5A carrying The Δ2354-2400 truncation was PCR amplified from pFK5.1Con1neo(DHFRClover@2419) using Con1-XhoI-F and Con1Δ2354-2400R and Con1Δ2354-2400F and Con1-MfeI-R. (E) The 3 products from the 1st round PCR were combined and 'stitched' together by PCR using Con1 XhoI F and Con1 MfeI R and the truncation fragment (~2 kb) was then cloned into pFK5.1Con1neo(DHFRClover@2419) using *Xho*I and *Mfe*I. (F) To confirm the presence of the insertion pFK5.1Con1neo(DHFRClover@2419)Δ2354-2404 clones were re-digested with *Xho*I and *Mfe*I. Clones which yielded a ~2 kb fragment were considered positive.

8.5 GENERATION OF PCDNA PLASMID EXPRESSING V5-USP19

An N-terminal V5 tagged USP19 expressing plasmid was generated by cloning V5-USP19 from an in-house pCRBlunt construct, itself generated by others in the lab from a USP19 expression vector (Addgene), into pCDN3.1 using *Eco*RI restriction sites present at both ends of the desired gene. The resulting pCDNA3.1-V5-USP19 was then transfected into STBL2 *E. coli*, before the presence and orientation of the plasmid was confirmed by digestion with *Bgl*II (Figure 8-7).

Name	BglII	CCC	Sense	Loop	Antisense	TTTTT	MluI	HindIII
shUSP19 1	AGATCT	CCC	GCATGATTGGTGGCCACTACA	CGAA	TGTAGTGGCCACCAATCATGC	TTTTT	ACGCGT	AAGCTT
shUSP19 2	AGATCT	CCC	GCTGCCCAGCTACGATCTATA	CGAA	TATAGATCGTAGCTGGGCAGC	TTTTT	ACGCGT	AAGCTT
shUSP19 3	AGATCT	CCC	GCATTCAGAACAAGCCCTACA	CGAA	TGTAGGGCTTGTTCTGAATGC	TTTTT	ACGCGT	AAGCTT
shUSP19 4	AGATCT	CCC	GCCTGCCAAATGTTCTCATCG	CGAA	CGATGAGAACATTTGGCAGGC	TTTTT	ACGCGT	AAGCTT
shUSP19 5	AGATCT	CCC	GCGGCACAAGATGAGGAATGA	CGAA	TCATTCCTCATCTTGTGCCGC	TTTTT	ACGCGT	AAGCTT

Table 8-4 **USP19 shRNA oligonucleotides designed in Invitrogen Block-iT**. Each contains a unique Sense-Loop-Antisense sequence bordered by uniform CCC and TTTTT spacer sequences. *BglII*, *MluI* and *HindIII* restriction sites are included to allow versatile cloning.

A

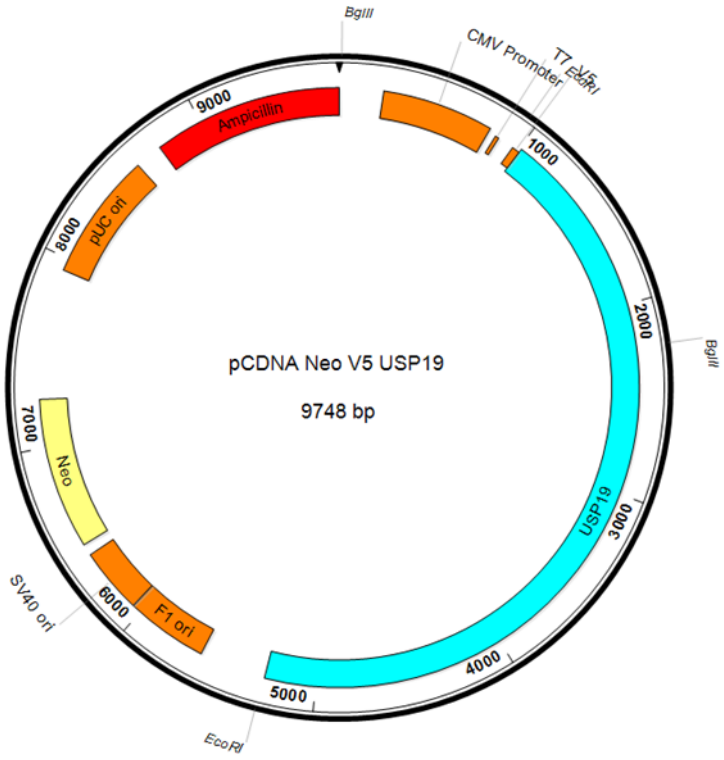

B

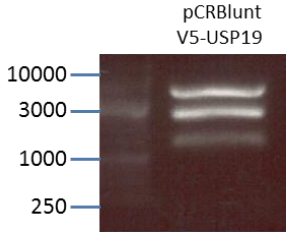

C

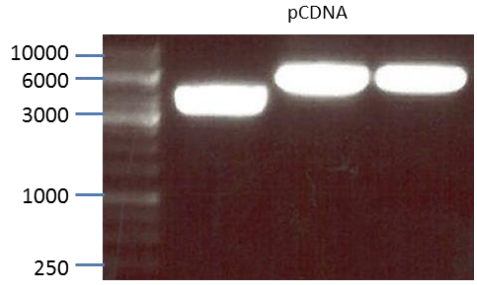

D

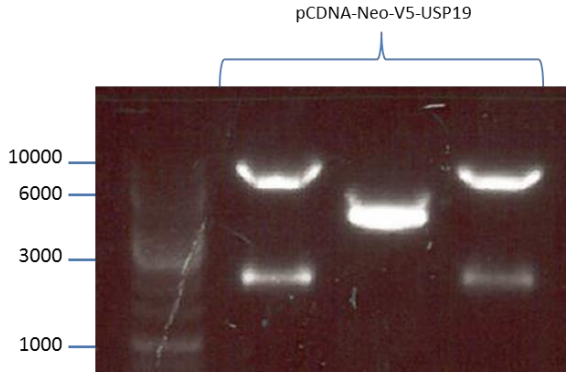

Figure 8-7 **Generation of pCDNA3.1-V5-USP19 (A).** A V5-Tagged USP19 gene from pCRBlunt was cloned into pCDNA3.1. To differentiate between the V5-USP19 fragment and a digestion product of similar size pCRBlunt was also digested with *Dra*I (B) and the 4320 bp fragment cloned into pCDNA (C). To detect the presence and orientation of the insertion, clones of pCDNA-Neo-V5-USP19 were digested with

*Bgl*II (D). Plasmids containing the insert in the correct orientation yielded a 2.2 kb band.

8.6 GENERATION OF REPLICON CONSTRUCTS CARRYING 2 COPIES OF DOMAIN III

Replicon constructs were generated that carried two copies of NS5A domain III. To limit the possibility of recombination the sequence encoding the second copy of domain III was derived from a synthetic, divergent replicase (DVR), which has 100% amino acid similarity to JFH1, but only 66% nucleotide similarity(Accession Number KR140016 (Gomes et al., 2016)). The first step in making the duplicated domain III constructs was to introduce the 2354-2404 deletion into this DVR sequence. This was achieved using a two-step PCR similar to that previously described (Figure 8-8A). Primers Δ2354-2404DVRF and Δ2354-2404DVRR were used with DVR/JFH1-LCS2.2R and DVR/JFH1-LCS2.1F to generate overlapping DVR fragments, which were subsequently used as the template in a second round PCR using DVR/JFH1-LCS2.1F and DVR/JFH1-LCS2.2R. Concurrently DVR/JFH1-LCS2.1F and DVR/JFH1-LCS2.2R were also used to generate an intact domain III from the DVR NS5A coding region (Figure 8-8B). Using pSGRJFH1*luc(DHFRClover@2442) and pSGRJFH1*luc(DHFRClover@2442)Δ2354-2404 additional PCR reactions were performed to produce compatible products designed to flank the DVR-based DNA and which shared overlapping regions of homology with them (Figure 8-8C,D) A final PCR reaction using JFH1 flanking primers was used to amplify all DNAs together and the resultant products were cloned into a pSGRJFH1*luc(DHFRClover@2442) vector using either *Bam*HI and *Mlu*I restriction sites. The presence of insert was confirmed by restriction digest using the same enzyme pair, and all positive clones sequenced across the PCR-generated inserts to establish the lack of any other unwanted mutations.

The resulting constructs are referred to as pSGRJFH1*lucWT/WT(DHFRClover@2442), pSGRJFH1*lucWT/Δ(DHFRClover@2442), pSGRJFH1*lucΔ/WT(DHFRClover@2442) and pSGRJFH1*lucΔ/Δ(DHFRClover@2442), depending on whether the DVR/JFH1 domain III is full length (WT) or carries the 2354-2404 deletion (Δ).

Primer Name	Primer Sequence (5'-3')
DVR/JFH1-LCS2.1F	GTTGCTGGTTGTGCTCTGCCCCCTCCAAAGAAAG
DVR/JFH1-LCS2.1R	GGGGCAGAGCACAACCAGCAACGGTGGGCG
DVR/JFH1-LCS2.2F	CGTCAGTTGCCCTGCTCTCCCACCTCCCAAGAAG
DVR/JFH1-LCS2.2F	GTGGGAGAGCAGGGCAACTGACGGTAGTGTCATC
Δ2354-2404DVRF	GACATTCGGGCTGGAAAGCGACCAGGTGGAAC
Δ2354-2404DVRR	GGTCGCTTTCCAGCCCGAATGTCTTAATAGCCAG
JFH1(5430-5450)F	CGTTGCGCCGGATAAGGAGG
JFH1(7803-7784)R	GAGGCGCTCTTTGATGTTGT

Table 8-5 **Primers used to introduce NS5A Domain III from DVR into pSGRJFH1*lucNS3-5B(DHFRClover@2442)**

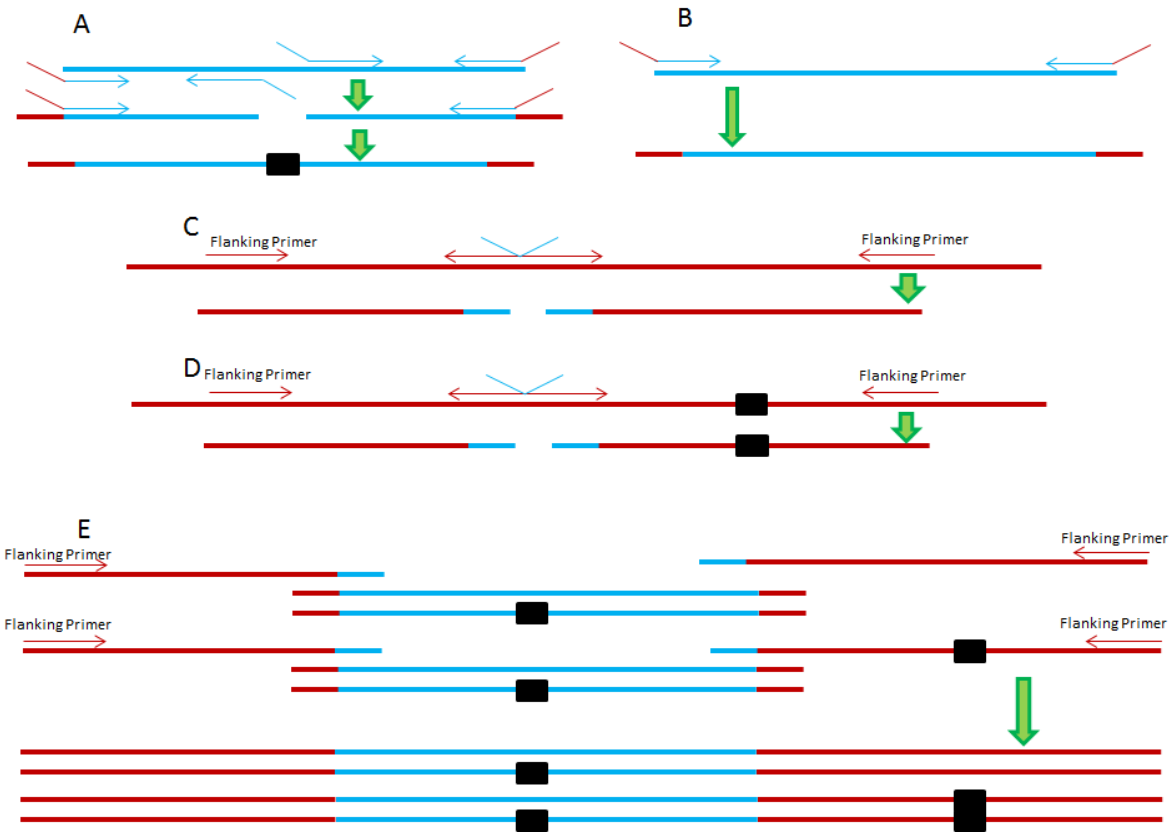

Figure 8-8 **Introducing a second NS5A domain III into pSGRJFH1*lucNS35B(DHFR-Clover@2442).** (A) Introduction of the 2354-2404 deletion into DVR domain III NS5A sequence using a 2-step PCR reaction where flanking primers' 3' ends were complementary to JFH1 NS5A LCS2/domain III boundary sequence. (B) Amplification of intact DVR domain III using the same flanking primers used in A. (C,D) Generation of JFH1 derived PCR products straddling the LCS2/domain III boundary with overhangs complementary to the domain III DVR inserts amplified in A and B. (E) Fusion of products generated in A or B with those produced in C and subsequent cloning into pSGRJFH1*lucNS35B(DHFR-Clover@2442 to generate constructs with a second DVR domain III in NS5A such that either the original domain III, the DVR domain III, or both, carry the 2354-2404 deletion. Blue – DVR derived sequence. Red – JFH1 derived sequence. Black box – 2354-2404 deletion.

A

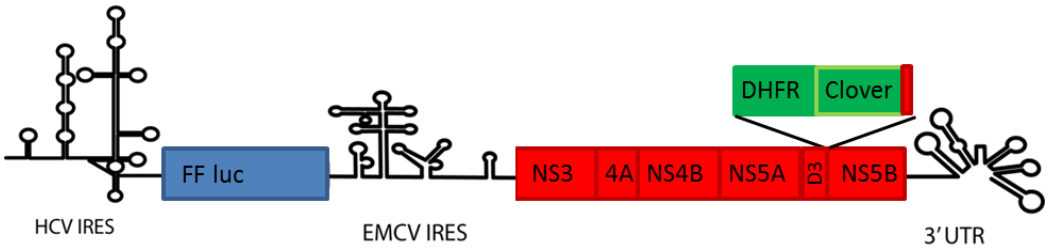
DHFR
Clover
FF luc
NS3
4A
NS4B
NS5A
D3
NS5B
HCV IRES
EMCV IRES
3'UTR

B

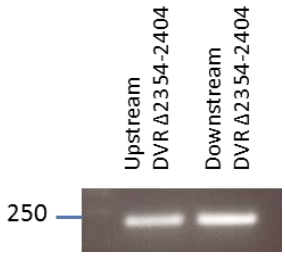
Upstream DVR Δ2354-2404
Downstream DVR Δ2354-2404
250

C

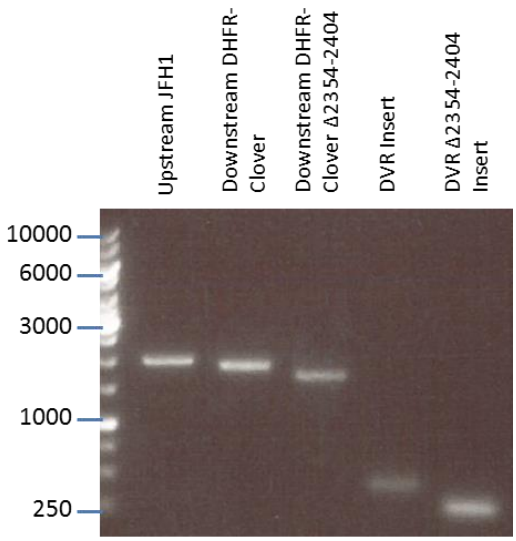
Upstream JFH1
Downstream DHFR-Clover
Downstream DHFR-Clover Δ2354-2404
DVR Insert
DVR Δ2354-2404 Insert
10000
6000
3000
1000
250

D

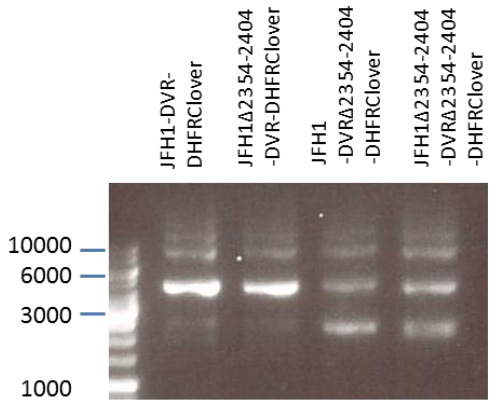
JFH1-DVR-DHFRClover
JFH1Δ2354-2404 -DVR-DHFRClover
JFH1 -DVRΔ2354-2404 -DHFRClover
JFH1Δ2354-2404 -DVRΔ2354-2404 -DHFRClover
10000
6000
3000
1000

E

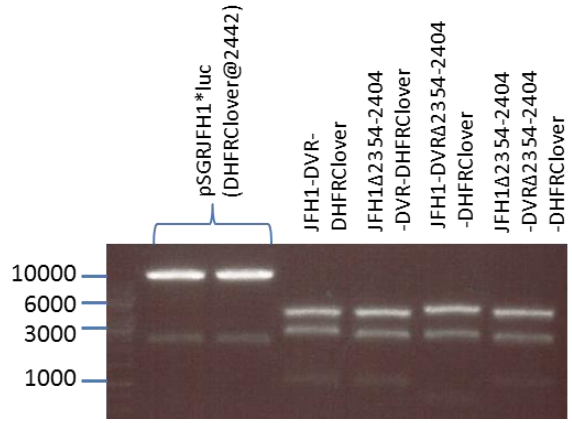

F

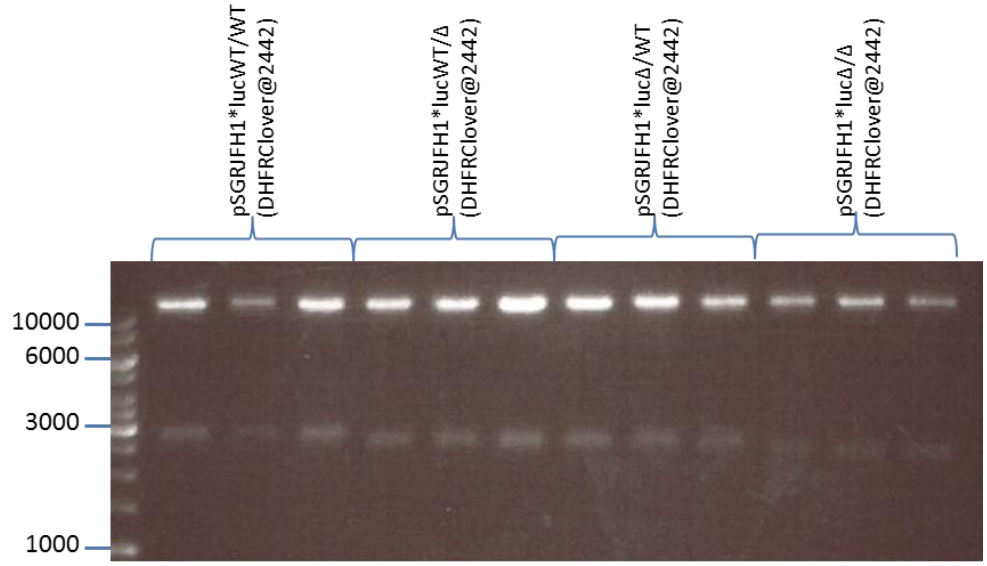

Figure 8-9 **Generation of pSGRJFH1*luc constructs carrying two fused copies of NS5A domain III as described in Figure 8-8**. (A) Schematic of the pSGRJFH1*lucWT/WT(DHFRClover@2442) construct (B) Sequence upstream and downstream of the Δ2354-2404 region of DVR NS5A was PCR amplified to have JFH1 compatible overhangs. (C) DVR and JFH1 NS5A fragments with cohesive compatible overhangs were PCR amplified, including the 'stitching' together of the 2 DVRΔ2354-2404 fragments. (D) The 1st Round PCR products from (C) were 'stitched' together using flanking JFH1 primers and the 4 kb band cloned first into PCRBlunt and then pSGRJFH1*luc(DHFRClover@2442) using *Bam*HI and *Mlu*I (E). (F) Recovered clones were tested for the presence of fused Domain III sequences by restriction digestion with *Bam*HI and *Mlu*I. Those clones which released a ~2.5 kb fragment were considered successful.

8.7 SCRAMBLING NS5A DOMAIN III

Replicon constructs that carried a scrambled domain III were produced by PCR. Scrambled sequence was amplified from the purchased string using primers NS5A Scramble F and Scramble NS5A DHFR R, whilst compatible upstream and downstream sequences were amplified from a pSGRJFH1*lucNS3-5B(DHFRClover@2442) template. To generate the upstream fragment JFH1(5430-5450)F and NS5A Scramble R primers were used, and to generate the downstream fragment Scramble NS5A DHFR F and 5' Clover R primers were used. The complete PCR product was generated in a final PCR reaction in which the products from the initial 3 reactions were combined to act as template, using the JFH1(5430-5450)F and 5' Clover R primers. This final product was then cloned into pSGRJFH1*lucNS3-5B(DHFRClover@2442) using *Bam*HI and *Mlu*I restriction sites. Due to the similarity in size, success of cloning was checked by digestion with *Mlu*I and *Rsr*II; an *Rsr*II site present in NS5A domain III was disrupted within the scramble such that only those plasmids carrying the unscrambled sequence would be cut by both enzymes, liberating a 720bp fragment. Additionally positive clones were sequenced to ensure the lack of any unwanted mutations.

Invitrogen String Sequence
agagcaccatatcagaagccctccagcaactggccatcaagacctttggcATGAGCGAGAGCAGCGCCACATCTG GCGGACCTGGCGAAGAACCTGCCGATGCTCCTCCTGGACCTGCCTCTGGACCTACAGAGGGACC TGGCAGCGGAGATCAGTCTGGCGAGACAGCCCCTTCTACCCCTGGCGCCTCTCCTGATTCTctgga Gtctgatcaggtagagcttcaacctccacctcagggcggtggagt

Table 8-6 **Nucleotide sequence of the of the Scrambled NS5A sequence**. The amino acid sequence of residues 2354-2404 of JFH1 NS5A was randomised and then reverse transcribed for human expression using the Invitrogen GeneArt Portal. A DNA string was then procured carrying this (Upper case) flanked by 50 bp bordering sequences (lower case)

Primer Name	Primer Sequence (5'-3-)
JFH1 5430-5450 F	CGTTGCGCCGGATAAGGAGG
Clover R	TCCAGCTCGACCAGGATG
NS5A Scramble F	GACCTTTGGCATGAGCGAGAGCAGCGCCAC
N55A Scramble R	CTCTCGCTCATGCCAAAGGTCTTGATGGCCAG
Scramble NS5A DHFR F	CTCCTGATTCTCTGGAGTCTGATCAGGTAGAG
Scramble NS5A DHFR R	CAGACTCCAGAGAATCAGGAGAGGCGCCAG

Table 8-7 **Primers used to introduce a scrambled NS5A domain III sequence into pSGRJFH1*lucNS3-5B(DHFRClover@2442).**

A

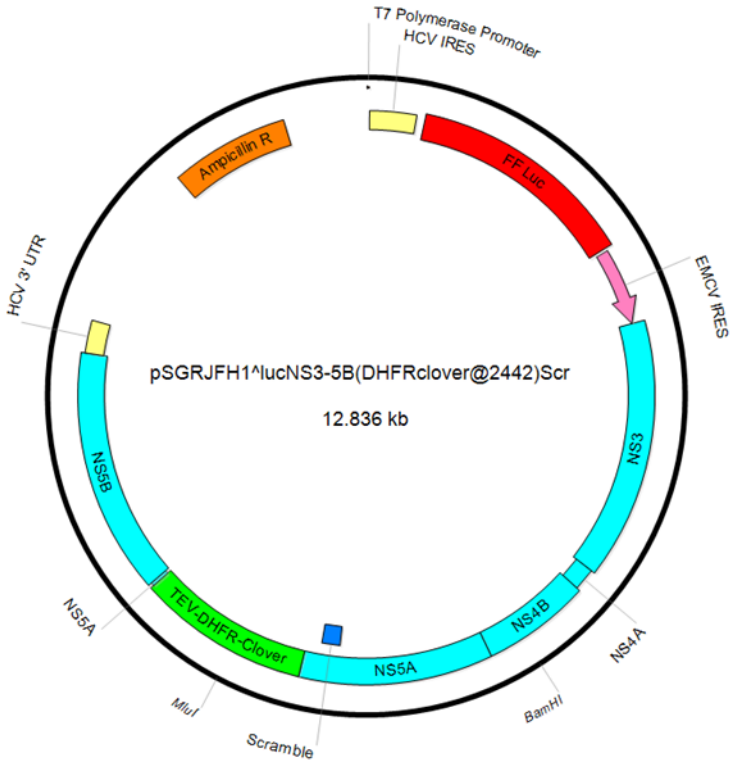
T7 Polymerase Promoter
HCV IRES
FF Luc
EMCV IRES
NS3
NS4A
NS4B
NS5A
TEV-DHFR-Clover
NS5B
HCV 3' UTR
Ampicillin R
pSGRJFH1^lucNS3-5B(DHFRclover@2442)Scr
12.836 kb
NS5A
MluI
Scramble
BamHI

B

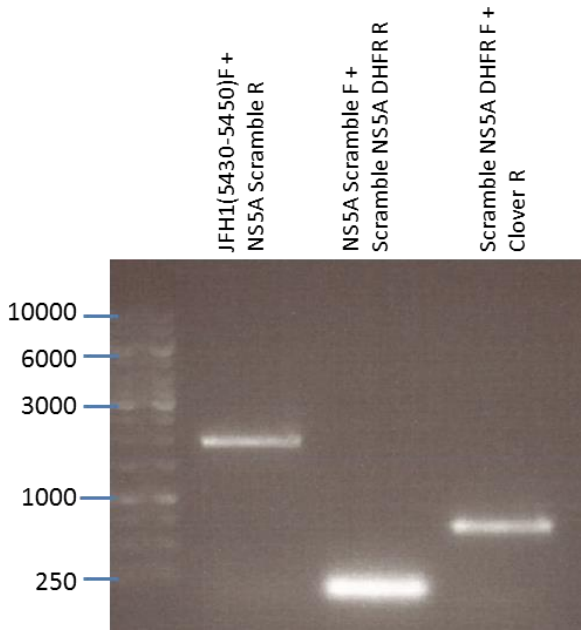
JFH1(5430-5450)F + NS5A Scramble R
NS5A Scramble F + Scramble NS5A DHFR R
Scramble NS5A DHFR F + Clover R
10000
6000
3000
1000
250

C

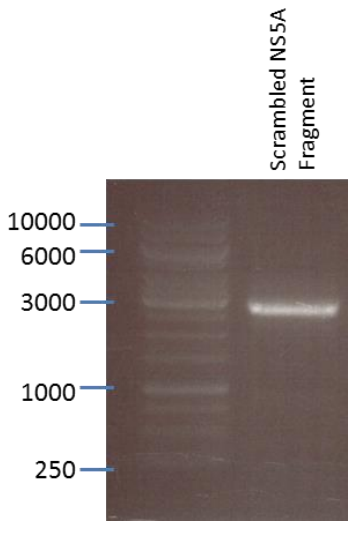
Scrambled NS5A Fragment
10000
6000
3000
1000
250

D

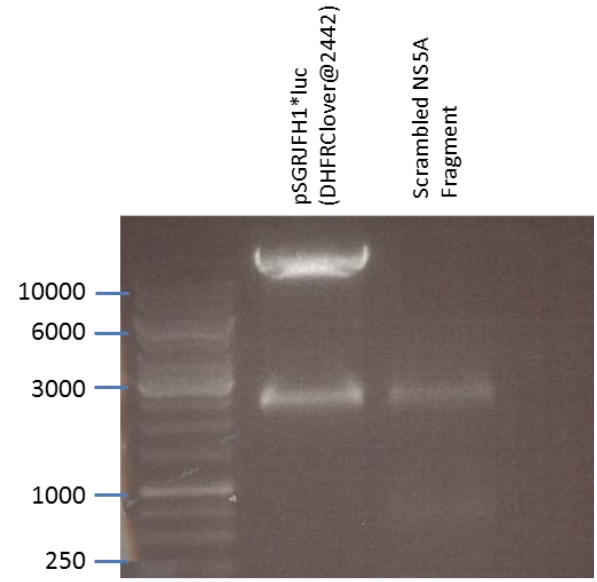

E

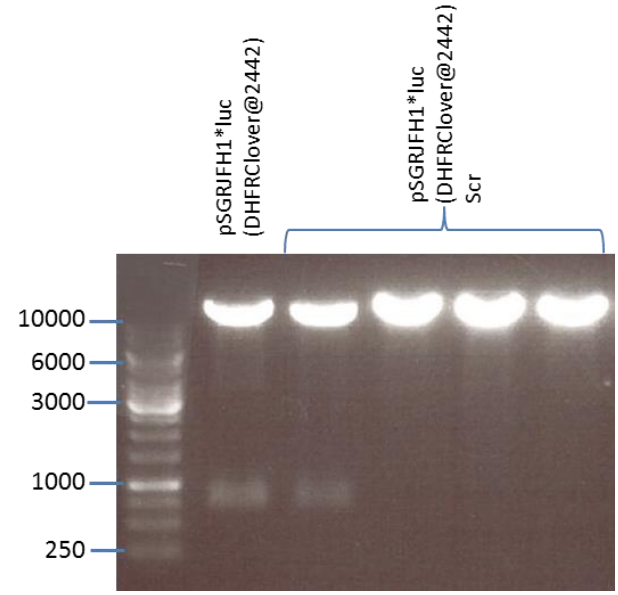

Figure 8-10 **Generation of pSGRJFH1*lucNS3-5B(DHFRClover@2442)Scr (A).** (A) Schematic of the pSGRJFH1*lucNS3-5B(DHFRClover@2442)Scr contruct (B) Sequences upstream and downstream of the 2354-2404 region of NS5A, alongside the 2354-2404 scrambled sequence, were PCR amplified to have compatible overhangs. (C) Products from the 1st round of PCR were purified by gel extraction and combined to act as template in the final round PCR, yielding a ~3 kb fragment carrying the scrambled sequence. (D) Both the scrambled sequence and pSGRJFH1*lucNS3-5B(DHFRClover@2442) were digested with *Bam*HI and *Mlu*I to generate DNAs that were gel extracted and used in a ligation reaction. (E) Recovered clones were tested for the presence of unscrambled sequence by restriction digestion with *Mlu*i and *Rsr*II, alongside a pSGRJFH1*lucNS3-5B(DHFRClover@2442) control (lane 2). Clones that released a 720 bp fragment contained unscrambled sequence.

8.8 GENERATION OF JFH1 REPLICONS WITH MUTANT NS3

Generation of JFH1 replicons with mutant NS3 was achieved by multi step PCR using primers in Table 8-8 (Figure 8-11). In the first round ubiquitin followed by the amino acid of interest was amplified using EMCV-Ubi F and one of, Ubi-NS3-Ala R Ubi-NS3-Tyr R or Ubi-NS3-Gln R. Meanwhile compatible primers Ubi-NS3-Ala F, Ubi-NS3-Tyr F, and Ubi-NS3-Gln F, were used in conjunction with JFHI(4569-4549) R to PCR amplify the N-terminus of NS3 including a unique *Spe*I site. Additionally EMCV-PmeI F and EMCV-Ubi R were used to amplify a fragment of EMCV IRES from pSGRJFH1*luc carrying a unique *Pme*I site. Each reaction generated a fragment with compatible overhangs as shown in Figure 8-11B. A final PCR reaction was performed in which the products of the 3 first round PCR reactions were combined to 'stitch' them together and generate the full length fragments carrying Ubiquitin and the desired amino acid between the EMCV IRES and the N-terminus of NS3. These fragments were then cloned into either pSGRJFH1*luc or pSGRJFH1*lucΔ2354-2404 using *Pme*I and *Spe*I restriction sites. To detect the presence of any unwanted mutations, each plasmid was sequenced across the PCR derived sequence.

The plasmids derived were referred to as pSGRJFH1*lucUbiAla, pSGRJFH1*lucUbiTyr, pSGRJFH1*lucUbiGln, pSGRJFH1*lucUbiAla Δ2354-2404, pSGRJFH1*lucUbiTyr Δ2354-2404, and pSGRJFH1*lucUbiGln Δ2354-2404.

Primer Name	Primer Sequence (5'-3-)
EMCV-Ubi F	CGATGATACCATGCAGATCTTCGTGAAGAC
EMCV-Ubi R	GAAGATCTGCATGGTATCATCGTGTTTTTC
Ubi-NS3-Ala F	CTCCGCGGTGGTGCAGCTCCCATCACTGCTTATGC
Ubi-NS3-Ala R	GTGATGGGAGCTGCACCACCGCGGAGACGCAGCAC
Ubi-NS3-Gln F	CTCCGCGGTGGTCAAGCTCCCATCACTGCTTATGC
Ubi-NS3-Gln R	GTGATGGGAGCTTGACCACCGCGGAGACGCAGCAC
Ubi-NS3-Tyr F	CTCCGCGGTGGTTATGCTCCCATCACTGCTTATGC
Ubi-NS3-Tyr R	GTGATGGGAGCATAACCACCGCGGAGACGCAGCAC
EMCV Pme1	CTCGACGCAAGAAAAATCAG
JFH1(4569-4549)R	CCGCCGCGAGCTCGTCACAC

Table 8-8 **Primers used in the generation of JFH1 replicon constructs carrying mutated NS3.**

A

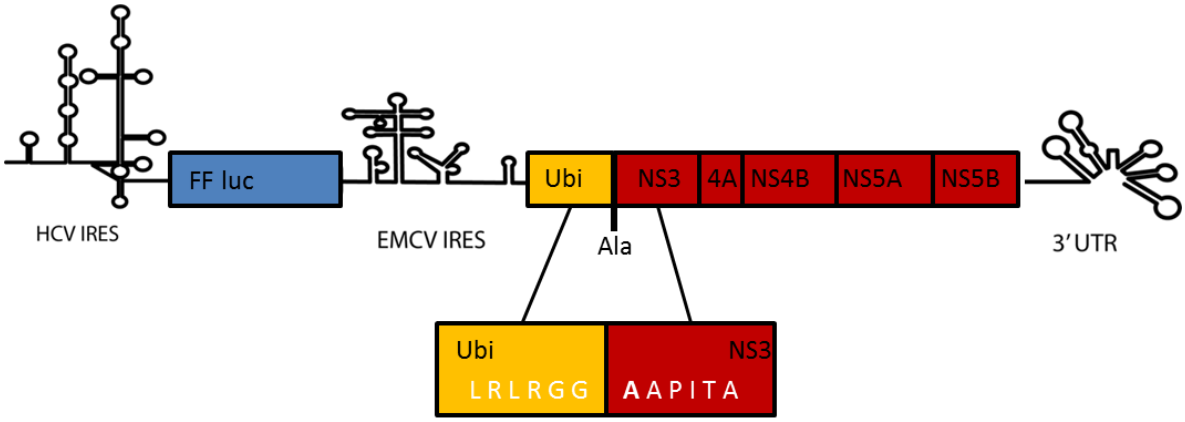
FF luc
HCV IRES
EMCV IRES
Ubi
NS3
4A
NS4B
NS5A
NS5B
Ala
3'UTR
Ubi
LRLRGG
NS3
AAPITA

B

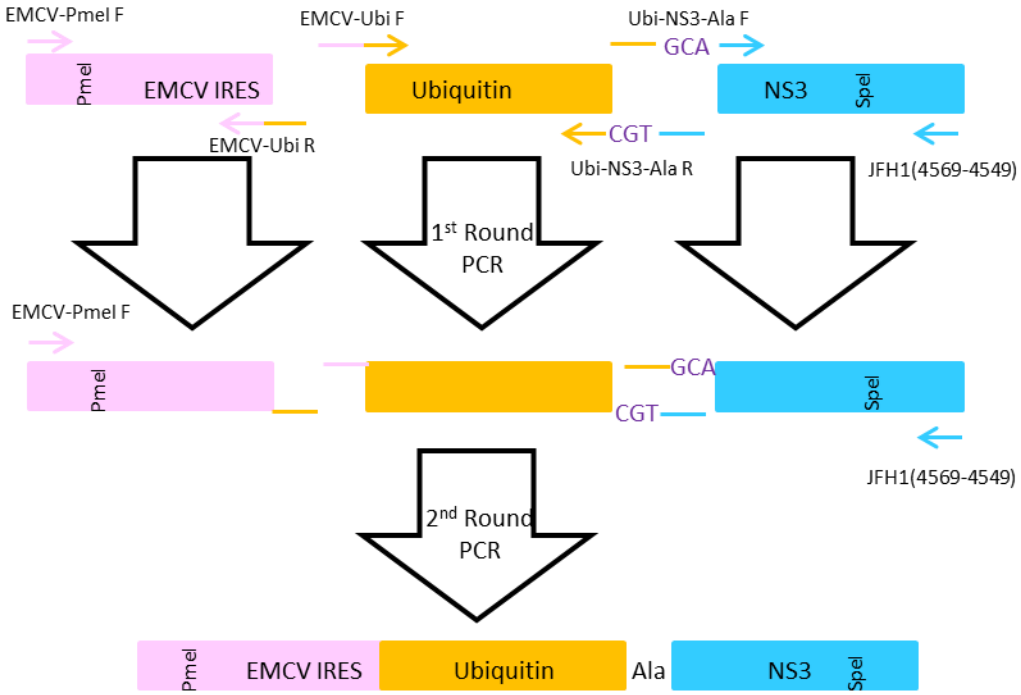
EMCV-Pmel F
EMCV-Ubi F
Ubi-NS3-Ala F
GCA
PmeI
EMCV IRES
Ubiquitin
NS3
SpeI
CGT
EMCV-Ubi R
Ubi-NS3-Ala R
JFH1(4569-4549)
1st Round PCR
EMCV-Pmel F
PmeI
GCA
CGT
SpeI
JFH1(4569-4549)
2nd Round PCR
PmeI
EMCV IRES
Ubiquitin
Ala
NS3
SpeI

C

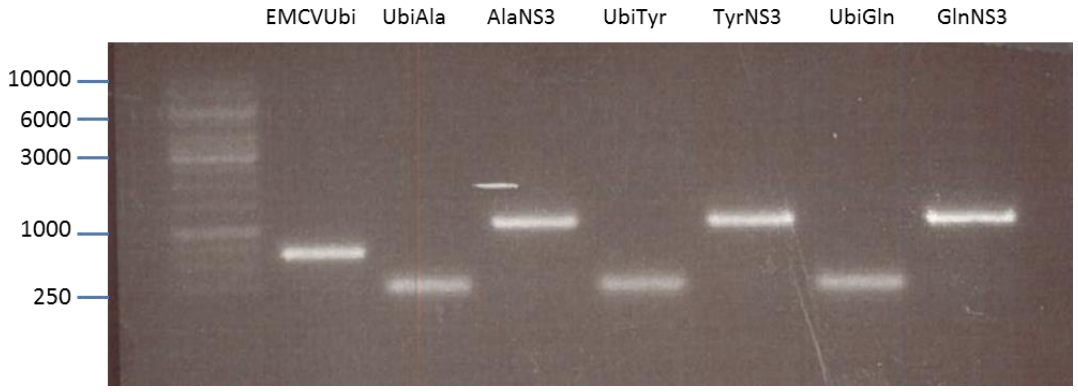
EMCVUbi
UbiAla
AlaNS3
UbiTyr
TyrNS3
UbiGln
GlnNS3
10000
6000
3000
1000
250

D

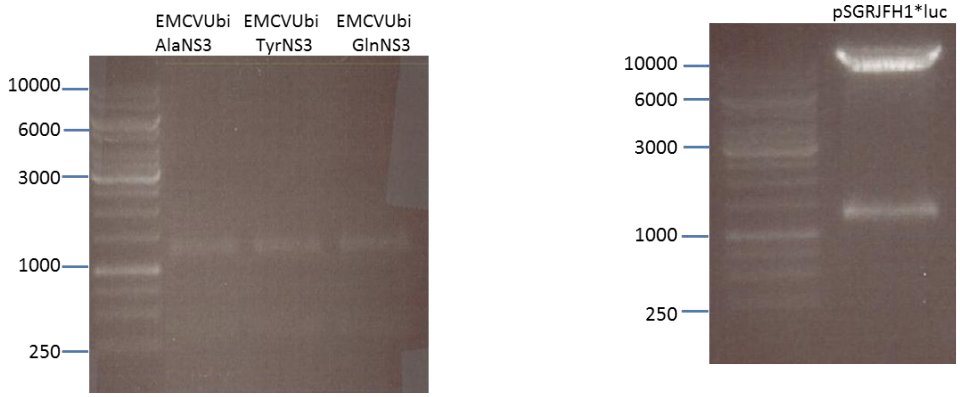

E

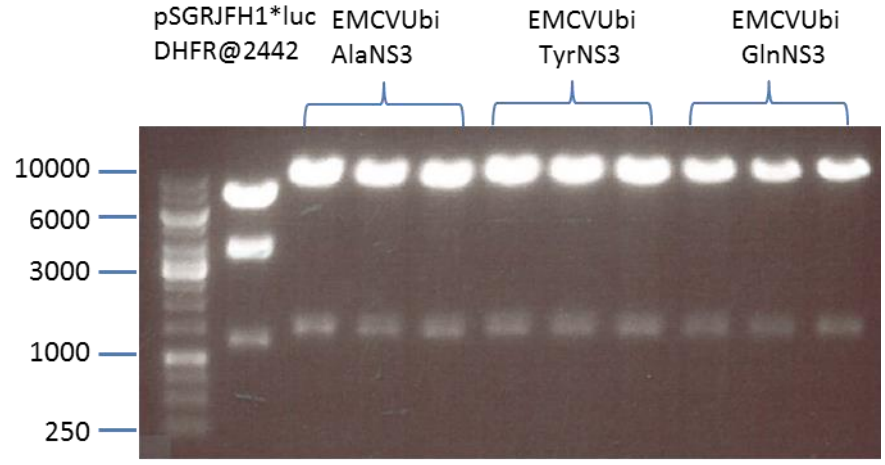

Figure 8-11**Generation of pSGRJFH1*luc NS3 mutants.** (A) Schematic of pSGRJFH1*lucUbiAla. (B) Multi-step PCR strategy used in the generation the replicon construct with Ala positioned on the NH2 terminus of NS3 (Comparable strategies were used for constructs with Tyr and Gln on the end of NS3). (C) PCR was used to amplify sequences from the EMCV IRES, Ubiquitin, and NS3, all with compatible, cohesive, overhangs. These were visualised on a 0.7% agarose gel and then purified by gel extraction. (D) Products from the 1st round of PCR reactions were combined and used as templates in the 2nd round reactions. These were purified and digested with *Pme*I and *Spe*I alongside pSGRJFH1*luc. (E) Colonies were screened for successful insertion by digestion with *Pme*I and *Spe*I. Clones that released a 1.5 kb fragment were considered successful.

8.9 GENERATION OF G418 RESISTANT REPLICON CONSTRUCTS

The neomycin resistance gene NPTII from pSGRJFH1Neo(Wakita et al., 2005) was cloned into the pSGRJFH1*, pSGRJFH1*NS3-5B(DHFRclover@2394), pSGRJFH1*NS3-5B(DHFRclover@2442), pSGRJFH1*NS3-5B(DHFRclover@2442)Δ2328-2353, pSGRJFH1*NS3-5B(DHFRclover@2442)Δ2354-2404, and pSGRJFH1*NS3-5B(DHFRclover@2442)Δ2404-2435 constructs via *Age*I and *Spe*I restriction sites (Figure 8-12), replacing the original Firefly luciferase reporter gene in these constructs. Success of the cloning was confirmed by re-digesting with the same restriction enzymes.

A

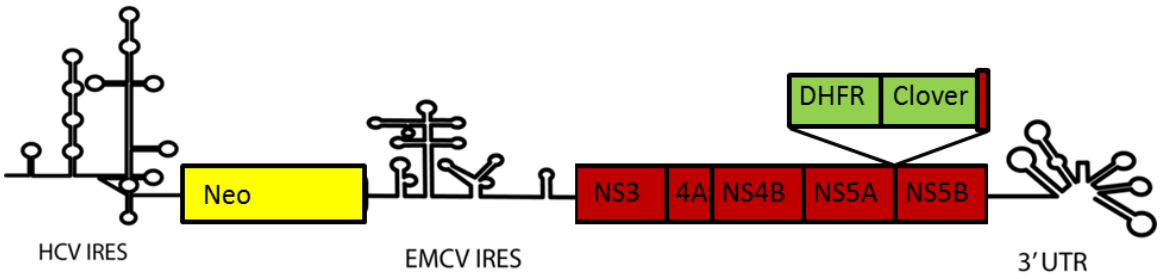

B

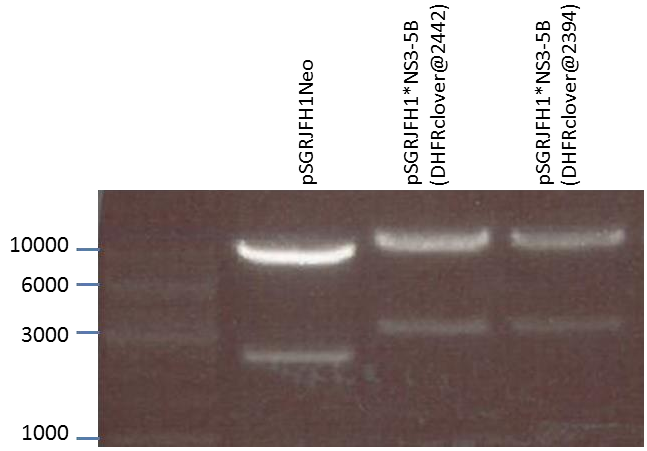

C

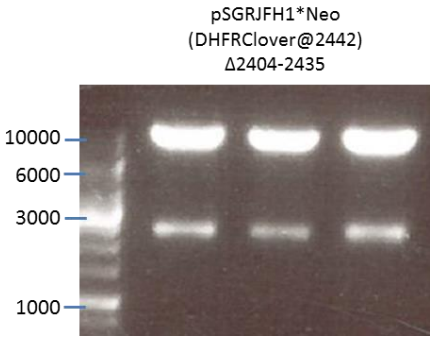

Figure 8-12 **Cloning of Neo resistance marker into pSGRJFH1 replicon vectors**. (A) Schematic of the pSGRJFH1*neoNS3-5B(DHFRClover@2442) replicon. (B) *Age*1 and *Spe*1 were used to clone the neo resistance gene (~2.3 kb) from pSGRJFH1 neo into pSGRJFH1*NS3-5B(DHFRClover@2394), pSGRJFH1*NS3-5B(DHFRClover@2442), pSGRJFH1*NS3-5B(DHFRClover@2442)Δ2328-2353, pSGRJFH1*NS3-5B(DHFRClover@2442)Δ2354-2404, and pSGRJFH1*NS3-5B(DHFRClover@2442)Δ2404-2435. (C) To confirm the presence of the insert, pSGRJFH1*neo(DHFRClover) clones were re-digested with *Age*I and *Spe*I, with positive clones yielding a ~2.3 kb band.

8.10 GENERATION OF PSGJFH1 REPLICON CONSTRUCTS CARRYING A MYC TAG WITHIN NS5A DOMAIN II

The Myc tag was introduced into both pSGRJFH1*neoNS3-5B(DHFRClover@2442) and pSGRJFH1*neoNS3-5B(DHFRClover@2442)Δ2354-2404 by 2 step PCR using primers in (Table 8-9). The first round of PCR used pairs of primers JFH1(5430-5450)F and MycNS5AR, and MycNS5AF and JFH1(8571-8551)R, to generate fragments each with compatible cohesive ends. A second round reaction using the flanking primers, JFH1(5430-5450)F and JFH1(8571-8551)R generated the full length fragment carrying the Myc insertion. This was then cloned into pSGRJFH1*neoNS3-5B(DHFRClover@2442) using unique *Bam*HI and *Rsr*II sites, and pSGRJFH1*neoNS3-5B(DHFRClover@2442)Δ2354-2404 using unique *Bam*HI and *Mlu*I sites (the use of *Mlu*I instead of *Rsr*II being due to the former site being absent within the truncated protein of this latter construct). Presence of the insert was determined by re-digestion and sequencing.

Primer Name	Primer Sequence (5'-3-)
JFH1 5430-5450 F	CGTTGCGCCGGATAAGGAGG
JFH1 7555-7536 R	CTCCAGGTCCGGATCTCCAG
Myc NS5A F	GAAGCTCATCTCAGAAGAGGATCTGGGGTTTCCACGGGCCTTACCG
Myc NS5A R	CCTCTTCTGAGATGAGCTTCTGTTCGCTCCTGGGGAGCATGCAC

Table 8-9 **Primers used to introduce the Myc tag into pSGRJFH1*neo**

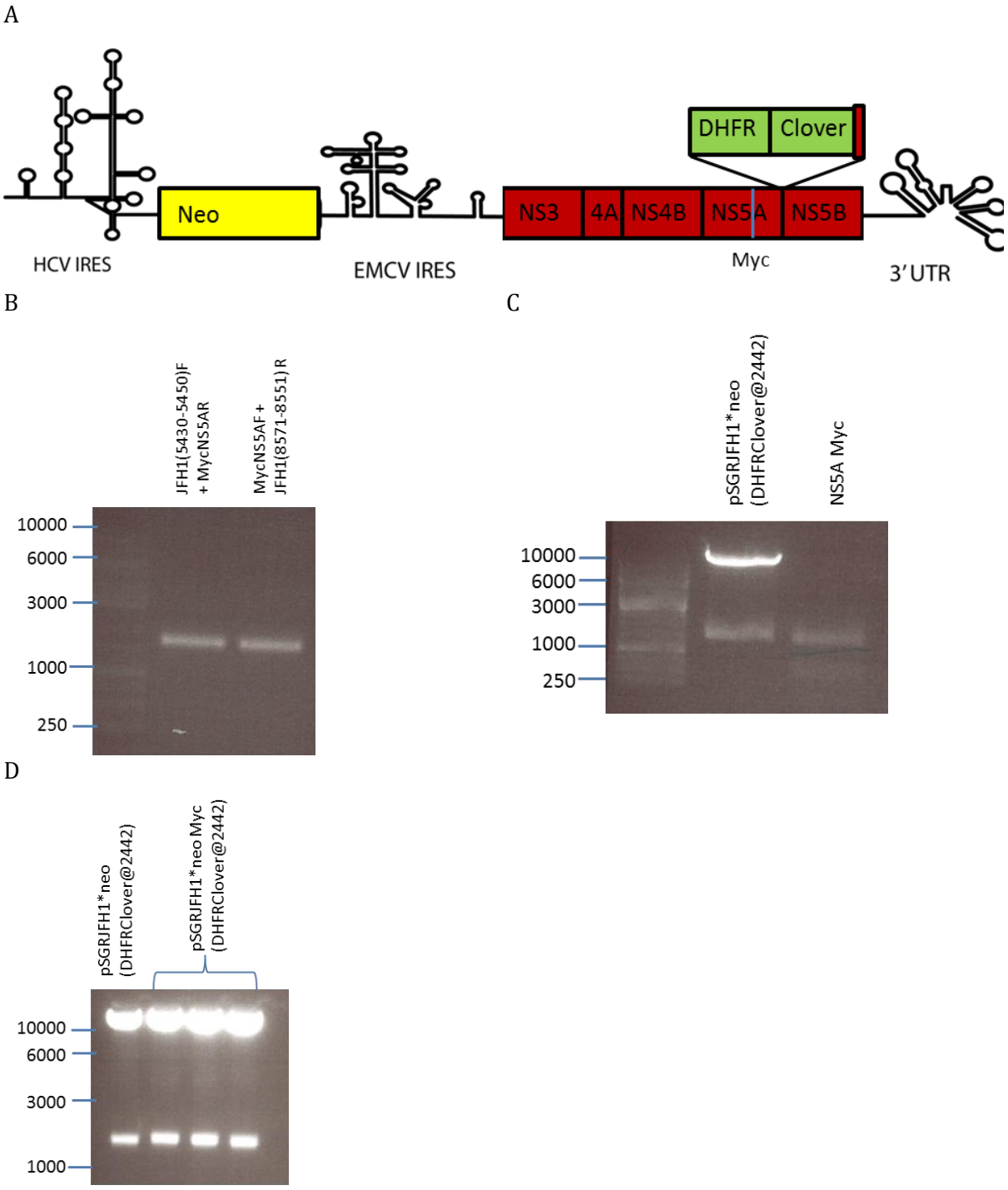

Figure 8-13 **Introduction of a Myc tag into pSGRJFH1*neo(DHFRclover@2442)Myc**. (A) Schematic of the pSGRJFH1*neo(DHFRclover@2442)Myc replicon. (B) First round PCR products amplified from pSGRJFH1*neo(DHFRCLover)@2442 using JFH15430-5450F and MycNS5AR or MycNS5AF and JFH1 8571-8551R. (C) *Bam*HI and *Rsr*II digestion of pSGRJFH1*neo(DHFRclover@2442) and a second round PCR production amplified from the 1st round PCR products using flanking primers JFH1(5430-5450)F and JFH18571-8551)R. (D) Confirmation of the insertion by *Bam*HI and *Rsr*II.

8.11 GENERATION PSGRJFH1 REPLICON CONSTRUCTS LACKING THE DHFR DOMAIN

JFH1 replicons were generated that possessed either a full length or mutant domain III, but lacking the DHFR-clover cassette. To achieve this, the 2354-2404 deletion was introduced into pSGJFH1*luc by 2-step PCR, using the primers in Table 8-10 (Figure 8-14). The resulting plasmid, pSGRJFH1*luc Δ2354-2404, was subsequently transformed into STBL2 *E. coli*, and the presence and fidelity of the insert confirmed by re-digestion and sequencing respectively.

Primer Name	Primer Sequence (5'-3-)
Δ2354-2404 F	GACCTTTGGCCTGGAGTCTGATCAGGTAG
Δ2354-2404 R	CAGACTCCAGGCCAAAGGTCTTGATGGCC
JFH1 5430-5450 F	CGTTGCGCCGGATAAGGAGG
JFH1 9477-9457 R	CAGTTAGCTATGGAGTGTACC

Table 8-10 **Primers used to introduce the Δ2354-2404 deletion into pSGRJFH1*luc.**

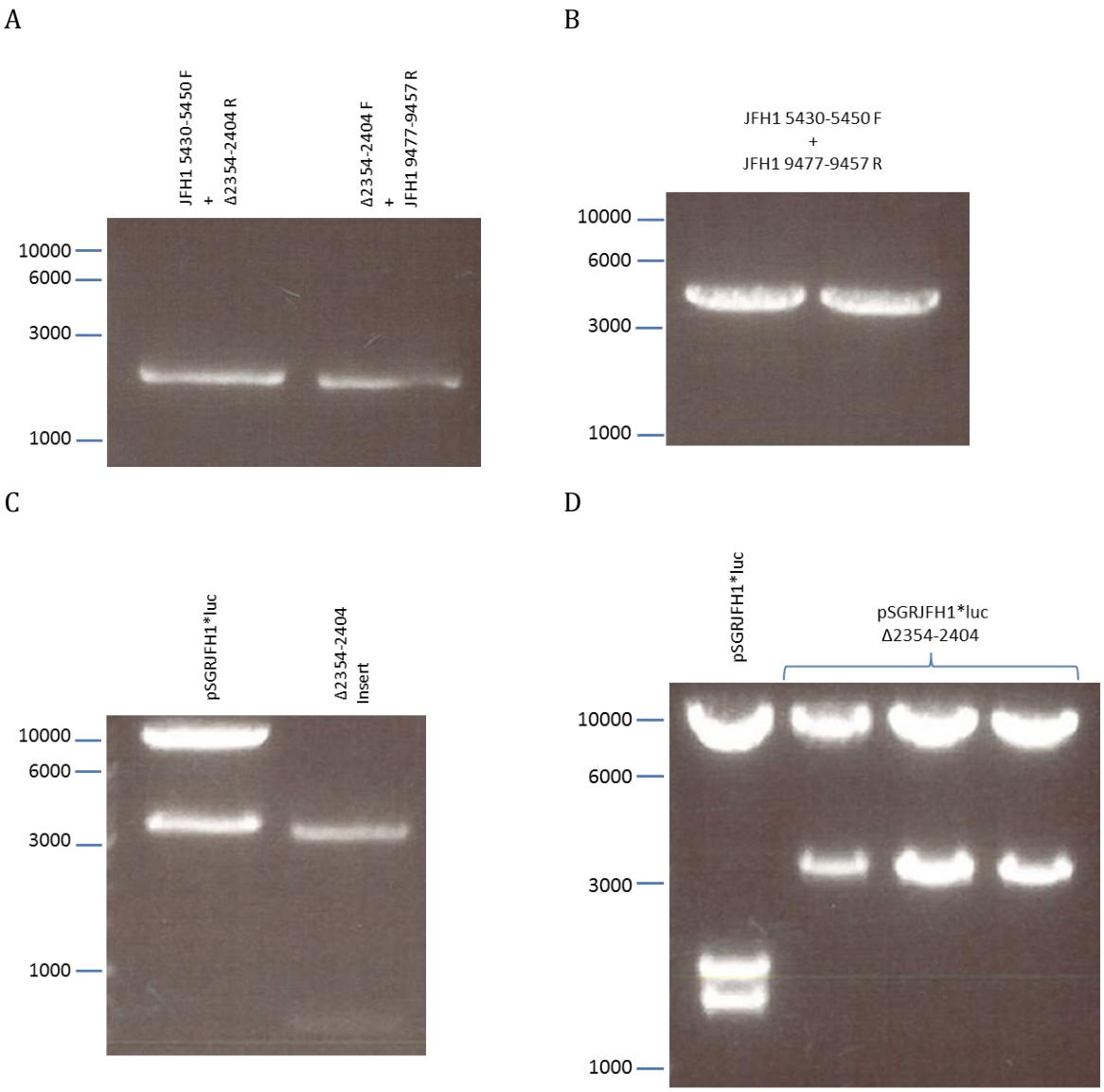

Figure 8-14 **Generation of pSGRJFH1*lucΔ2354-2404 by 2-step PCR.** (A) 1^{sT} round PCR products amplified from pSGRJFH1*luc using JFH1 5430-5450F and Δ2354-2404 R and Δ2354-2404 F and JFH1 9477-9457 R. (B) A second round PCR was used to 'stitch' together the products from (A) to generate a fragment carrying the Δ2354-2404 truncation. (C) This was cloned into pSGRJFH1*luc using *Bam*HI and *Eco*RV. (D) To check for the presence of the Δ2354-2404 insert clones of pSGRJFH1*lucΔ2354-2404 were digested with B*am*HI, *Eco*RV, and *Rsr*II. Clones were considered positive if they released a single ~3 kb fragment, rather than 2 smaller fragments, resulting from internal digestion of this fragment by *Eco*RV (This restriction site being found within the 2354-2404 coding regions).

8.12 GENERATION OF PSGRJFH1NEO CONSTRUCTS LACKING THE DHFR CLOVER CASSETTE.

To generate a pSGRJFH1*neo plasmid carrying the Δ2354-2404 truncation, an NPT gene was cloned into pSGRJFH1*luc Δ2354-2404 using *Age*I and *Spe*I (Figure 8-15). The success of the cloning was determined by re-digesting positive clones with *Age*I and *Spe*I, with successfully clones yielding a 2.2 kb fragment. The pSGRJFH1*neo construct was already available and so no cloning was required to make this.

A

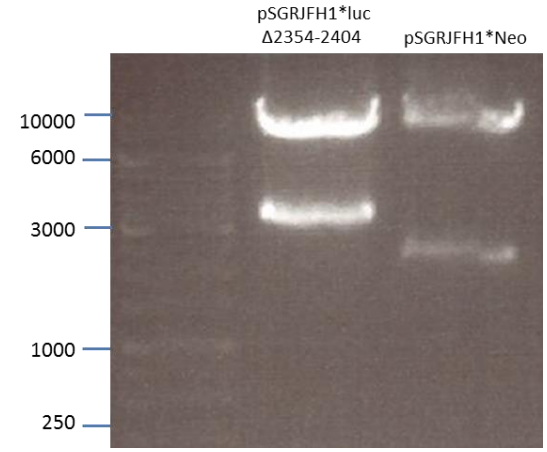

B

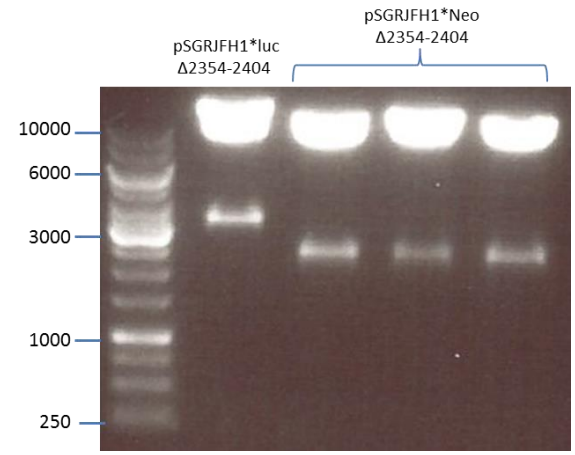

Figure 8-15 **Cloning of Neo Phosphotransferase into pSGRJFH1*lucΔ2354-2404**. A DNA fragment carrying NPT from pSGRJFH1*neo (~2.3 kb) was cloned into pSGRJFH1*Δ2354-2404 using *Age*I and *Spe*I (A), with success of cloning determined by redigestion of the resulting clones with *Age*I, and *Spe*I (B). Clones were considered positivie if they realeased a ~2.3 kb fragment.

8.13 CLONING H2K INTO PCDNA-HYGRO

To generate a pCDNA plasmid capable of expressing mouse MHC class I, H2K from a plasmid kindly donated by Dr Edd James was PCR amplified using HindIII-H2K-F and XhoI-H2K-R, and the resulting fragment cloned into pCDNA-Hygro (Addgene) using *Hind*III and *Xho*I restriction sites. The resulting plasmid, pCDNA-Hygro-H2K was then re-digested to confirm the presence of the insert (Figure 8-16).

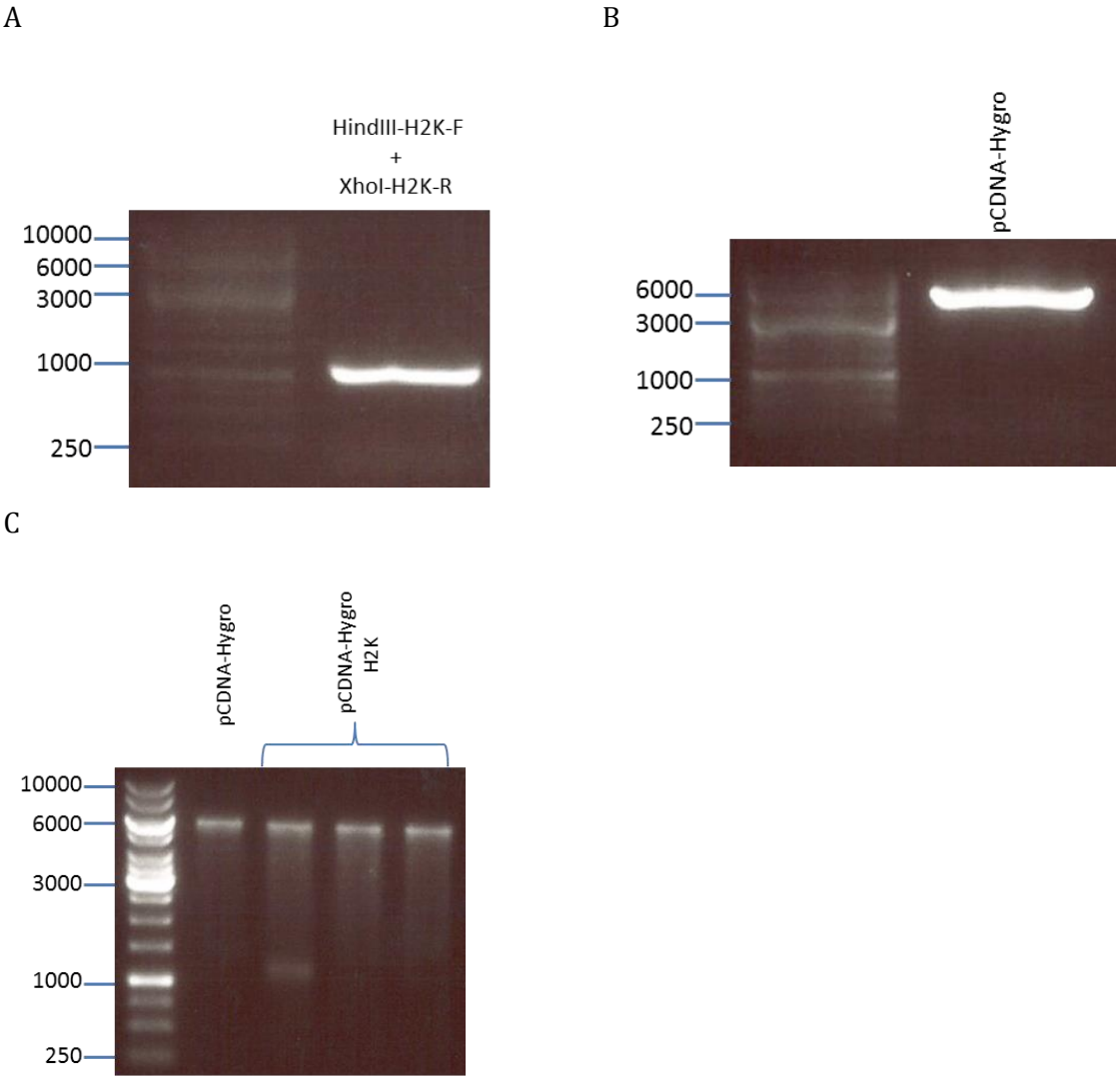

Figure 8-16 **Cloning of H2K into pCDNA-Hygro.** (A) H2K was PCR amplified from a plasmid kindly donated by Dr Edd James, using HindIII-H2K-F and XhoI-H2K-R (~1.1 kB), and cloned into pCDNA-Hygro (B), using *Hind*III and *XHo*I. To confirm the presence of the H2K insert pCDNA-Hygro-H2K clones were redigested with *Hind*III and *XHo*I (C). Clones were considered positive if they yielded a 1.1 kb fragment.

8.14 GENERATION OF A PLVTH-H2K

Lentiviral transduction was performed to generate an H2K expressing Huh7.5 cell line, however this relied on the generation of a lentiviral plasmid carrying H2K. To allow this, PCR was performed using *Eco*RI-CMV F and H2K-*Mlu*I R primers(Table 8-11) to amplify the CMV promoter and H2K gene from pCDNA-Hygro-H2K, and this was cloned into the GFP-encoding pLVTHM plasmid using the *Eco*RI and *Mlu*I restriction sites flanking the PCR product (Figure 8-17).

Primer Name	Primer Sequence (5'-3-)
EcoRI-CMV-H2K F	TGGACGAATTCACATTGATTATTGACTAG
MluI-H2K-R	ATGGACACGCGTTCACGCTAGAGAATGAGGGTC

Table 8-11 **Primers used to introduce a CMV promoter and H2K into pLVTHM**.

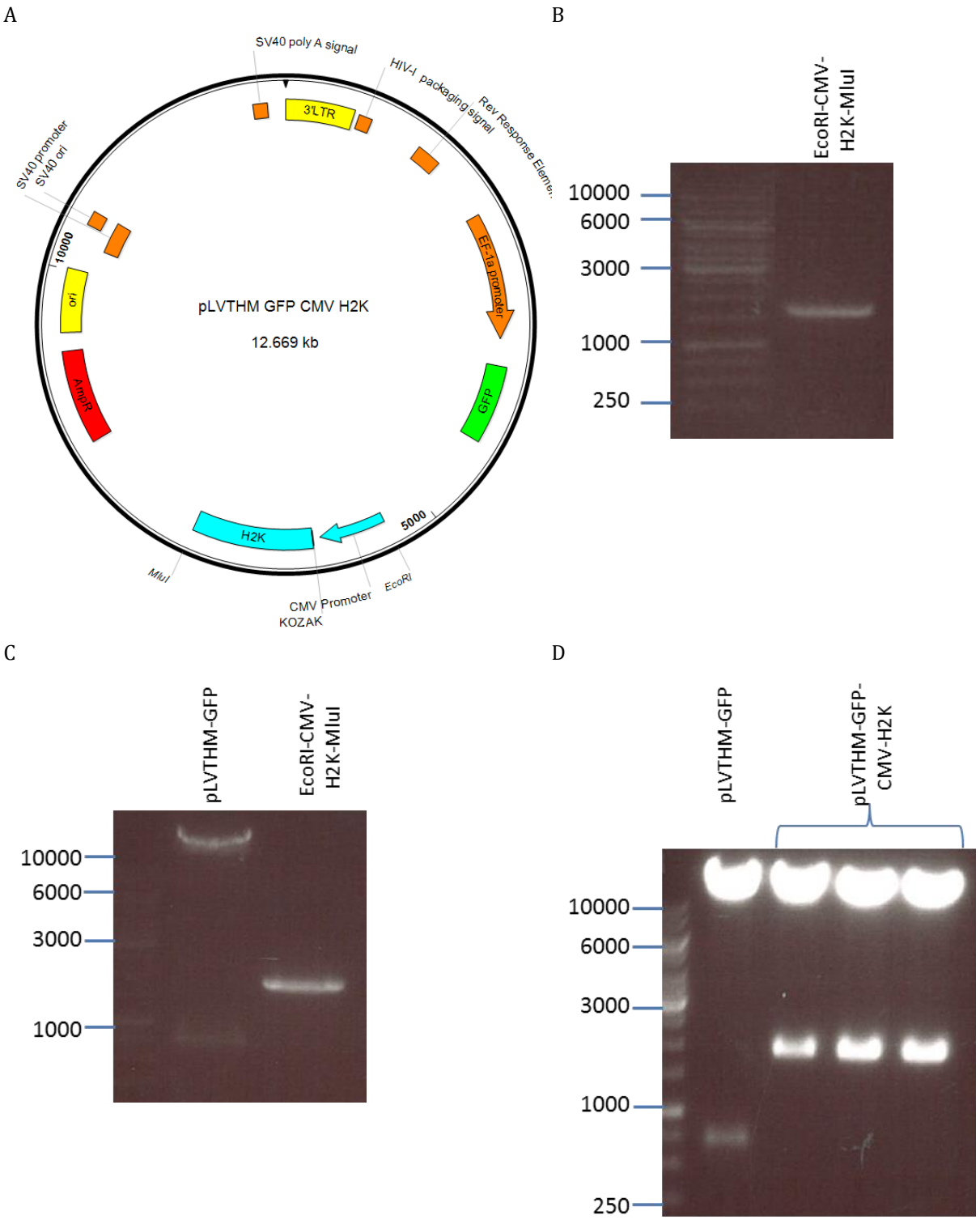

Figure 8-17 **Introduction of H2K into pLVTHM-GFP to generate pLVTHM-GFP-CMV-H2K (A).** H2K, alongside a CMV promoter and KOZAK sequence, was PCR amplified from pCDNA-Hygro-H2K using EcoRI-CMV-H2K-F and MluI-H2K-R (~1.8 kb) (B). This was then cloned into pLVTHM-GFP using *Eco*RI and *Mlu*I (C). To confirm the presenct of the CMV-H2K insert, pLVTHM-GFP-CMV-H2K clones were redigested with *Eco*RI and *Mlu*I (D). Clones were considered positive if they release a 1.8 kb fragment.

8.15 GENERATION OF PSGRJFH1*LUC REPLICONS EXPRESSING DHFRSL8

Alongside the generation of a Huh7.5 cell line expressing H2K, JFH1 replicons were generated that carried the DHFR-SL8 cassette in both a full length and Δ2354-2404 based vector. As pSGRJFH1*lucNS3-5B(DHFRSL8@2442) was already available the Δ2354-2404 deletion from pSGRJFH1*lucNS3-5B(DHFRclover@2442)Δ2354-2404 was cloned into it using unique *Bam*HI and *Mlu*I, generating pSGRJFH1*lucNS3-5B(DHFRSL8@2442)Δ2354-2404 (Figure 8-18).

Even under stabilising conditions there is some variance in replication between full length pSGRJFH1*lucNS3-5B replicons, and those carrying the Δ2354-2404 truncation, and there was concern that this could have an impact on SL8 processing and detection beyond any direct impact that changes to NS5A might cause. As such the GND mutation was introduced into the NS5B of both pSGRJFH1*lucNS3-5B(DHFRSL8@2442) and pSGRJFH1*lucNS3-5B(DHFRSL8@2442)Δ2354-2404. Replicons from these constructs should not replicate, and so only that protein expressed from the translated RNA should be detected. To achieve this NS5A from both replicating plasmids, including the truncation and DHFRSL8 cassettes, was cloned into pSGRJFH1*lucGND using unique *Bam*HI and *Hpa*I sites (Figure 8-18). The presence of the GND mutation in both constructs was confirmed by sequencing.

A

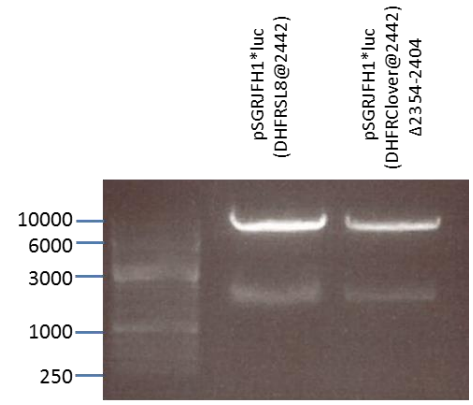
pSGRJFH1*luc (DHFRSL8@2442)
pSGRJFH1*luc (DHFRClover@2442) Δ2354-2404
10000
6000
3000
1000
250

B

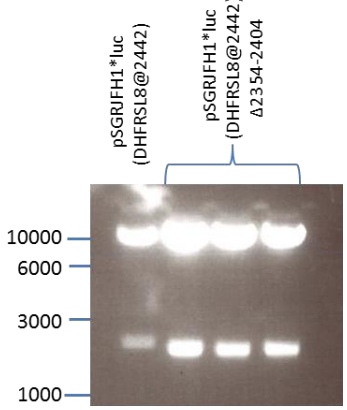
pSGRJFH1*luc (DHFRSL8@2442)
pSGRJFH1*luc (DHFRSL8@2442) Δ2354-2404
10000
6000
3000
1000

C

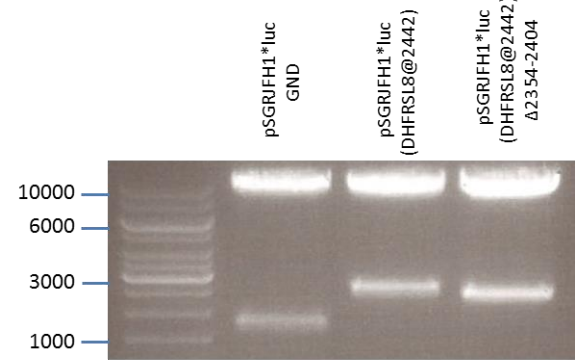
pSGRJFH1*luc GND
pSGRJFH1*luc (DHFRSL8@2442)
pSGRJFH1*luc (DHFRSL8@2442) Δ2354-2404
10000
6000
3000
1000

D

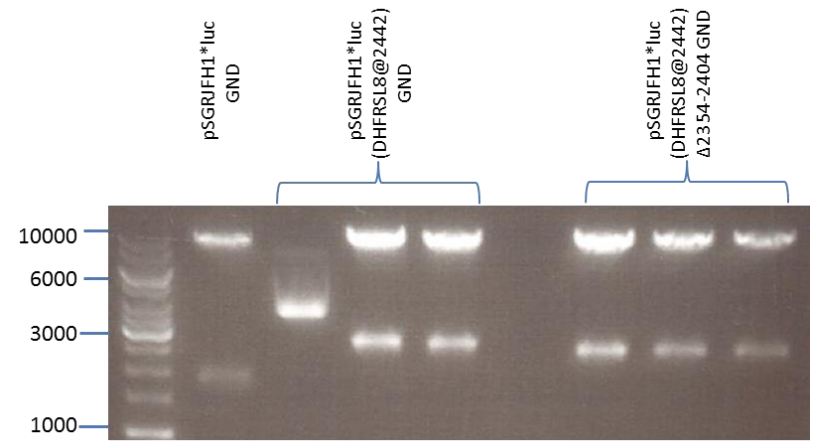
pSGRJFH1*luc GND
pSGRJFH1*luc (DHFRSL8@2442) GND
pSGRJFH1*luc (DHFRSL8@2442) Δ2354-2404 GND
10000
6000
3000
1000

E

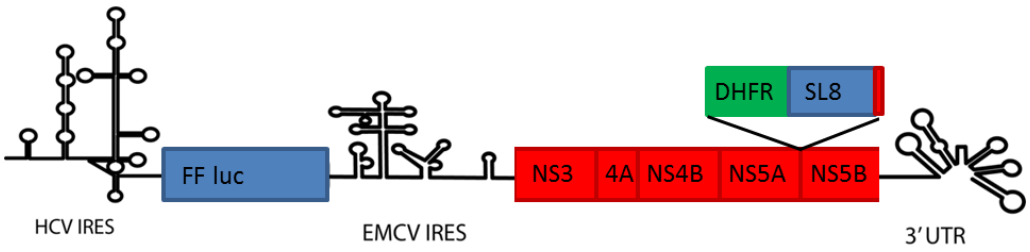

Figure 8-18 **Generation of pSGRJFH1 plasmids carrying the DHFRSL8 Cassette**. The Δ2354-2404 truncation (~2.2 kb) was introduced into pSGRJFH1*luc(DHFRSL8@2442) using *Bam*HI and *Mlu*I restriction sites (A). Success of the ligation was confirmed by re-digestion of pSGRJFH1*luc(DHFRSL8@2442)Δ2354-2404 clones with *Bam*HI and *Mlu*I (B). Due to the similarity in size between the 2.2 kb Δ2354-2404 fragment and the parental control the presence of the truncation was confirmed by sequencing.
The NS5B GND mutation was introduced into both pSGRJFH1*luc(DHFRSL8@2442) and pSGRJFH1*luc(DHFRSL8@2442)Δ2354-2404, by cloning NS5A (~2.6 kb)from these into pSGRJFH1*lucGND using *Bam*HI and *Hpa*I (C). Cloning success was confirmed by re-digestion of the resulting plasmid using *Bam*HI and *Hpa*I (D) with positive clones releasing a 2.6 kb fragment. (E) Schematic of the replicon encoded by pSGRJFH1*luc(DHFRSL8@2442).